Technische Universität Berlin,
Fakultät II für Mathematik und Naturwissenschaften,
Institut für Mathematik

Discrete Transparent Boundary Conditions for Multiband Effective Mass Approximations

Diplomarbeit
in Technomathematik

vorgelegt von
Dirk Klindworth
am 15. September 2009

Gutachter

Priv.-Doz. Dr. Matthias Ehrhardt
Prof. Dr. Andreas Unterreiter

Abstract

This diploma thesis is concerned with the derivation and numerical testing of *discrete transparent boundary conditions* (DTBCs) for *multiband effective mass approximations* (MEMAs). MEMAs are used to model electronic states in semiconductor nanostructures. This thesis is focused on the stationary case and comprises MEMAs such as the scalar Schrödinger equation, as a representative of single-band effective mass approximations, the two-band Kane-model and systems of $\mathbf{k} \cdot \mathbf{p}$-Schrödinger equations.

An analysis of the continuous problem is given and *transparent boundary conditions* (TBCs) are introduced. The discretization of the differential equations is done with the help of finite difference schemes. A fully discrete approach is used in order to develop DTBCs that are completely reflection-free. The analytical and discrete dispersion relations are analyzed in depth and the limitations of the numerical computations are shown.

The results of earlier works on DTBCs for the scalar Schrödinger equation are extended by alternative finite difference schemes. Existence and uniqueness of the numerical solutions are shown. The introduced schemes and their corresponding DTBCs are tested on numerical examples such as the single barrier potential and the tunneling effect at the double barrier potential.

The two-band *Kane-model* and the two-band $\mathbf{k} \cdot \mathbf{p}$-model with inter-band coupling are introduced as particular examples of MEMAs. DTBCs for the general d-band $\mathbf{k} \cdot \mathbf{p}$-model are derived and the numerical results are tested on a quantum well nanostructure.

Zusammenfassung

Die vorliegende Diplomarbeit beschäftigt sich mit der Herleitung von diskreten transparenten Randbedingungen für Effektive-Massen-Approximationen von Multiband-Systemen. Effektive-Massen-Approximationen finden Anwendung in der Berechnung der elektrischen Zustände in Halbleitern. Der Fokus dieser Arbeit liegt dabei auf dem stationären Fall. Es werden Modelle wie die skalare Schrödinger Gleichung, das Zwei-Band Kane-Modell sowie Multiband-$\mathbf{k} \cdot \mathbf{p}$-Modelle behandelt.

Zunächst werden die Modelle auf kontinuierlicher Ebene untersucht und anschließend transparente Randbedingungen hergeleitet. Die Diskretisierung der Modelle erfolgt mit Hilfe des Finite-Differenzen-Verfahrens. Auf Grundlage der diskreten Lösungen im Außenraum werden diskrete transparente Randbedingungen hergeleitet. Dieser sogenannte diskrete Ansatz verspricht reflektionsfreie Randbindungen, während eine ad-hoc Diskretisierung der transparenten Randbedingungen zu fehlerhaften Reflektionen an den künstlichen Rändern führen kann. Die diskreten Dispersionsrelationen der verschiedenen Modelle werden mit der analytischen Dispersionrelation verglichen und es werden daran die Grenzen der numerischen Schemata aufgezeigt.

Die Ergebnisse früherer Arbeiten zu diskreten transparenten Randbedingungen für die skalare Schrödinger Gleichung werden durch alternative Finite-Differenzen-Verfahren ergänzt. Für jedes dieser Verfahren wird die Existenz und Eindeutigkeit der numerischen Lösung gezeigt. Die eingeführten skalaren Schemata werden an einer einfachen Potentialbarriere sowie am Tunneleffekt der Doppelbarriere numerisch getestet.

Das Zwei-Band Kane-Modell sowie das Zwei-Band $\mathbf{k} \cdot \mathbf{p}$-Modell mit Interband-Kopplung werden als Beispiele von Multiband-Systemen eingeführt und auf kontinuierlichem sowie diskretem Niveau untersucht. Abschließend wird das allgemeine $\mathbf{k} \cdot \mathbf{p}$-Modell mit d Bändern analysiert und die zugehörigen diskreten transparenten Randbedingungen hergeleitet. Für das Acht-Band $\mathbf{k} \cdot \mathbf{p}$-Modell wird ein physikalisch realistisches Beispiel einer Quantum-Well-Struktur behandelt und die numerischen Ergebnisse mit den analytischen verglichen.

Acknowledgements

It is a pleasure to thank those who supported me in numerous ways.

First, I would like to express my sincere gratitude to my supervisor, Priv.-Doz. Dr. Matthias Ehrhardt, for his professional guidance, support and for his high degree of confidence in me.

Special thanks go to Dr. Thomas Koprucki without whose assistance in quantum mechanics, effective mass approximations and $\mathbf{k} \cdot \mathbf{p}$-Schrödinger operators this diploma thesis would not have been possible.

Finally, I wish to express my gratitude to my parents and Vanessa for their support, understanding, endless patience and encouragement when it was mostly required.

Contents

Notation

Throughout this diploma thesis we will use bold lower-case characters for vectors and bold capital characters for matrices while scalars are denoted by non-bold characters. However, there are some exceptions to this rule due to physical conventions. First of all, we will adopt the physical notation of the vector of the envelope functions and denote it by $\mathbf{F}$. Moreover, in Chap. 5, we will introduce matrices denoted by the bold lower-case characters $\mathbf{m}$, $\mathbf{v}$ and $\mathbf{e}$.

Schrödinger Equation

Ψ	microscopic wave function
H	scalar Hamiltonian operator
$\mathbf{H}$	matrix-valued Hamiltonian operator
d	number of considered bands, class-A bands
F_n	envelope function of the nth band
$\mathbf{F}$	vector of the d envelope functions $F_1, \ldots, F_d$
$\hbar$	reduced Planck constant
m_0	free electron mass
m^*	effective electron mass
m_c	effective electron mass of the conduction band
$\mathbf{p}$	quantum mechanical momentum operator, $\mathbf{p} = -\mathrm{i}\hbar\nabla$,
p	quantum mechanical momentum operator in 1D, $p = -\mathrm{i}\hbar\frac{\mathrm{d}}{\mathrm{d}x}$,
E_c	band edge of the conduction band
E_v	band edge of the valence band
E_g	band gap, $E_\mathrm{g} = E_\mathrm{c} - E_\mathrm{v}$
E_0	middle of the band gap, $E_0 = \frac{1}{2}(E_\mathrm{c} + E_\mathrm{v})$
Δ_so	spin-orbit splitting, i.e. energetic difference of the light holes and the split-off bands
E	energy
E^e	energy of the electron
E^h	energy of the hole
V_eff	effective potential energy of the electron
$\mathbf{k}$	wave vector, $\mathbf{k} = (k_x, k_y, k_z)$
$\mathbf{k}_\|$	reduced wave vector, $\mathbf{k}_\| = (k_x, k_y)$
k	scalar wave vector in direction of growth, $k = k_z$
$\hat{k}$	propagation coefficient of the scalar wave vector, $\hat{k} = \mathrm{Re}\, k$
$\check{k}$	attenuation coefficient of the scalar wave vector, $\check{k} = \mathrm{Im}\, k$

Mathematical Symbols

i	imaginary unit, $\mathrm{i}^2 = -1$
$\mathbb{C}$	set of complex numbers
$\mathbb{R}$	set of real numbers
$\mathrm{i}\mathbb{R}$	set of purely imaginary numbers
$\mathbb{Z}$	set of integers
$\mathbb{N}$	set of integers ≥ 0

Mathematical Symbols (continued)

$C^k(a,b)$	space of all functions f defined in (a,b) with k continuous derivatives
$L^p(a,b)$	space of all Lebesgue measurable functions f defined in (a,b) such that $\|f\|_p = \left(\int_a^b \|f(x)\|^p dx\right)^{1/p} < \infty$
$W^{k,p}(0,L)$	Sobolev space, space of all functions defined in (a,b) whose weak derivatives up to k-th order are in $L^p(a,b)$
$\overline{z}$	complex conjugate of z
$\langle x,y\rangle$	scalar or dot product of x and y
$\operatorname{sign}(x)$	sign of x, $\operatorname{sign}(x) = \begin{cases} 1 & x>0 \\ 0 & x=0 \\ -1 & x<0 \end{cases}$
$\mathcal{O}(h^n)$	Landau-symbol
$\mathbf{v}^{\mathrm{T}}$	Transpose of the vector $\mathbf{v}$
$\mathbf{M}^{\mathrm{T}}$	Transpose of the matrix $\mathbf{M}$
$\mathbf{M}^{\mathrm{H}}$	Hermitian (transpose conjugate) of the matrix $\mathbf{M}$
$\operatorname{in}(\mathbf{M})$	inertia of the matrix $\mathbf{M}$

Grid Variables

J	number of spatial grid points
h	step size in the spatial variable, $h = 1/J$
j	index for the spatial step, $x_j = jh$

Abbreviations

BC	Boundary Condition
TBC	Transparent Boundary Condition
DTBC	Discrete Transparent Boundary Condition
ODE	Ordinary Differential Equation
PDE	Partial Differential Equation
BVP	Boundary Value Problem
EMA	Effective Mass Approximation
MEMA	Multiband Effective Mass Approximation

Chapter 1

Introduction

Partial differential equations (PDEs) arise in a wide field of physical problems and often they are posed on unbounded domains. In order to compute a numerical solution to these PDEs one requires a finite computational domain. Usually, this is done by introducing *artificial boundary conditions*. If the solution of the unbounded domain restricted to the computational domain equals the approximate solution when using the artificial boundary conditions, then these boundary conditions are called *transparent boundary conditions* (TBCs).

TBCs of time-dependent Schrödinger equations have been discussed extensively, see for example the review by Antoine et. al. [1]. It has been shown that a fully discrete approach in deriving these TBCs, yielding so-called *discrete transparent boundary conditions* (DTBCs), implies significant numerical advantages. On the other hand, an ad-hoc discretization of the continuous TBCs can result in unphysical reflections at the TBCs and may influence the stability of the numerical scheme, cf. [3], [38]. Moreover, this discrete approach was successfully applied to general Schrödinger-type equations, see [2], [16] and [17].

DTBCs for systems of time-dependent Schrödinger equations were developed in [44] and [46]. For stationary Schrödinger equations, however, DTBCs have only been developed in the scalar case, [4].

In this diploma thesis we will summarize the results of the stationary scalar case and extend it to some alternative discretizations in Chap. 2. After that, we will derive DTBCs for systems of stationary Schrödinger equations. The first multiband model we will introduce is the so-called two-band *Kane-model* in Chap. 3. In contrast to all other introduced models, the Kane-model does not contain the Laplace-operator. The two-band $\mathbf{k}\cdot\mathbf{p}$-model, we will discuss in Chap. 4, equals basically the two-band Kane-model with an added Laplace-operator. Finally, we will focus on the general d-band $\mathbf{k}\cdot\mathbf{p}$-model in Chap. 5.

Before we start with the single-band model, let us briefly note some properties of electronic states in semiconductors and their mathematical description.

1.1 Properties of Electronic States in Bulk Semiconductor Materials

The electronic states in bulk semiconductor materials are described by the wave function $\Psi(\mathbf{r},\mathbf{k})$ that depends on the real *space vector* $\mathbf{r}=(x,y,z)$ and parametrically depends on the *wave vector* $\mathbf{k}=(k_x,k_y,k_z)$. The wave function satisfies the one-particle Schrödinger equation on the so-called *atomistic scale*

$$-\frac{\hbar^2}{2m_0}\Delta\Psi(\mathbf{r},\mathbf{k})+V_{\text{eff}}(\mathbf{r})\Psi(\mathbf{r},\mathbf{k})=E\Psi(\mathbf{r},\mathbf{k}), \tag{1.1}$$

with the *reduced Planck constant* $\hbar$ and the *free electron mass* m_0, cf. [26]. $V_{\text{eff}}(\mathbf{r})$ denotes the *effective potential* experienced by the electron or hole at the position $\mathbf{r}$ and E is the energy of the electron or hole in the *energy eigenstate* $\Psi(\mathbf{r},\mathbf{k})=\Psi_E(\mathbf{r},\mathbf{k})$ that solves Eq. (1.1).

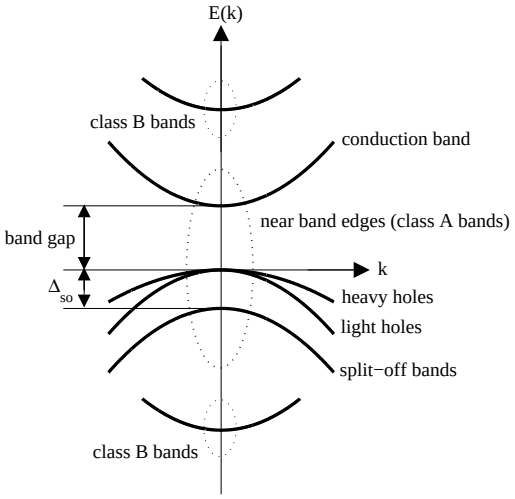

Figure 1.1: Schematic illustration of the band structure in a bulk semiconductor.

According to [11], the eigenstates can be expressed as *Bloch waves*

$$\Psi(\mathbf{r},\mathbf{k}) = e^{\mathrm{i}\mathbf{k}\cdot\mathbf{r}} u(\mathbf{r},\mathbf{k}), \tag{1.2}$$

with the periodic *Bloch function* $u(\mathbf{r},\mathbf{k})$. By applying the Bloch wave form (1.2) of the wave function to the one-particle Schrödinger equation (1.1) we get

$$-\frac{\hbar^2}{2m_0}\left(\Delta + 2\mathrm{i}\mathbf{k}\cdot\nabla - \mathbf{k}\cdot\mathbf{k}\right) u(\mathbf{r},\mathbf{k}) + V_{\text{eff}}(\mathbf{r}) u(\mathbf{r},\mathbf{k}) = E u(\mathbf{r},\mathbf{k}).$$

We use the *quantum mechanical momentum operator*

$$\mathbf{p} = -\mathrm{i}\hbar\nabla$$

and end up with the eigenvalue problem

$$\left(-\frac{\hbar^2}{2m_0}\Delta + \frac{\hbar}{m_0}\mathbf{k}\cdot\mathbf{p} + \frac{\hbar^2}{2m_0}\mathbf{k}\cdot\mathbf{k} + V(\mathbf{r})\right) u_n(\mathbf{r},\mathbf{k}) = E_n u_n(\mathbf{r},\mathbf{k}). \tag{1.3}$$

The eigenvalue curves $E_n = E_n(\mathbf{k})$, that correspond to the eigenfunctions $u_n(\mathbf{r},\mathbf{k})$ of the energy bands $n \in \mathbb{N}$, form the band structure of the semiconductor. If we set $\mathbf{k} = \mathbf{k}_0$ with $\mathbf{k}_0 = (0,0,0)$ the eigenvalue problem simplifies to

$$-\frac{\hbar^2}{2m_0}\Delta u_n^\Gamma(\mathbf{r}) + V_{\text{eff}}(\mathbf{r}) u_n^\Gamma(\mathbf{r}) = E_n^\Gamma u_n^\Gamma(\mathbf{r}), \tag{1.4}$$

with the so-called *zone center solutions* $u_n^\Gamma(\mathbf{r}) = u_n(\mathbf{r},\mathbf{k}_0)$ and the *zone center energies* $E_n^\Gamma = E_n(\mathbf{k}_0)$. Eq. (1.4) is significantly easier to solve than Eq. (1.1) since the Bloch functions u_n are periodic, cf. [43].

The set of all zone center solutions $u_m^\Gamma(\mathbf{r})$, $m \in \mathbb{N}$, forms a basis of the space of all Bloch functions $u_n(\mathbf{r},\mathbf{k})$ for $\mathbf{k} \neq \mathbf{0}$ and $n \in \mathbb{N}$. Hence, any Bloch function $u_n(\mathbf{r},\mathbf{k})$ can be expressed in terms of the zone center solutions u_m^Γ, $m \in \mathbb{N}$. For any energy band denoted by $n \in \mathbb{N}$ the Bloch function $u_n(\mathbf{r},\mathbf{k})$ takes the form

$$u_n(\mathbf{r},\mathbf{k}) = \sum_{m\in\mathbb{N}} c_m(\mathbf{k}) u_m^\Gamma(\mathbf{r}), \tag{1.5}$$

with some coefficients $c_m \in \mathbb{C}$, $m \in \mathbb{N}$. This procedure of describing the Bloch function $u_n(\mathbf{r}, \mathbf{k})$, that is an eigenfunction of Eq. (1.3), in terms of the zone center solutions $u_m^\Gamma(\mathbf{r})$, $m \in \mathbb{N}$, is known as $\mathbf{k} \cdot \mathbf{p}$-*method*.

The contribution of the zone center solutions u_m^Γ, $m \in \mathbb{N}$, to the sum in Eq. (1.5) decays proportionally to the difference of the energy $E_m = E_m(u_m^\Gamma)$ and the energy E_n, that corresponds to the Bloch function $u_n(\mathbf{r}, \mathbf{k})$. For the approximation of the d near band edge states, the so-called *class A bands*, we can restrict the sum in Eq. (1.5) to the first d near band edge zone center solutions and get the d-band representation of the Bloch function

$$u_n(\mathbf{r}, \mathbf{k}) \approx \sum_{m=1}^{d} c_m(\mathbf{k}) u_m^\Gamma(\mathbf{r}). \tag{1.6}$$

Fig. 1.1 shows a schematic illustration of the band structure in a bulk material. In this sketch the class A bands comprise by the lowest conduction band and the three top-most valence bands.

By applying the d-band representation of the Bloch function in Eq. (1.6) to the eigenvalue problem (1.3) we get an eigenvalue problem of the coefficient vector $\mathbf{c} = (c_1, \ldots, c_d)^{\mathrm{T}} \in \mathbb{C}^d$ given by

$$\mathbf{H}_{\mathrm{bulk}}(\mathbf{k})\mathbf{c}(\mathbf{k}) = E(\mathbf{k})\mathbf{c}(\mathbf{k}), \tag{1.7}$$

with the $d \times d$ bulk Hamiltonian $\mathbf{H}_{\mathrm{bulk}}(\mathbf{k})$. Note that this bulk Hamiltonian also includes the contribution of the class B bands as perturbations to the class A band contributions.

1.2 Semiconductor Nanostructures and Envelope Functions

In layered semiconductor nanostructures such as quantum wells and barriers the effective potential $V_{\mathrm{eff}}(\mathbf{r})$ changes from a periodic function to a superposition of an oscillatory part and a slowly-varying part, see Fig. 1.2. The oscillatory part corresponds to the microscopic effective potential of the semiconductor materials whereas the slowly-varying part is related to the composition of the semiconductor heterostructure of different bulk materials, see Fig. 1.2. According to Bastard and Burt, [7] and [12], the wave function also satisfies this property of a slowly and fast varying part. The slowly varying part is usually referred to as *envelope function*.

Burt and Foreman introduced a first rigorous approach, known as Burt-Foreman-approach, in order to extend the $\mathbf{k} \cdot \mathbf{p}$-method to heterostructures, cf. [12], [13], and [20]. Let us define the z-axis as direction of growth, i.e. perpendicular to the layered nanostructures. We introduce the reduced wave vector $\mathbf{k}_{||} = (k_x, k_y)$ as well as the in-plane space vector $\mathbf{r}_{||} = (x, y)$. According to the Burt-Foreman approach, we can replace the coefficients c_n in (1.6) by the envelope functions $F_n(z, \mathbf{k}_{||})$. Thus, the wave function Ψ can be expressed in the form

$$\Psi(\mathbf{r}, \mathbf{k}_{||}) = e^{\mathrm{i}\mathbf{k}_{||} \cdot \mathbf{r}_{||}} \sum_{n=1}^{d} F_n(z, \mathbf{k}_{||}) u_n^\Gamma(\mathbf{r}). \tag{1.8}$$

The so called *vector of the envelope functions* $\mathbf{F} = (F_1, \ldots, F_d) \in \mathbb{C}^d$ satisfies the stationary $\mathbf{k} \cdot \mathbf{p}$-Schrödinger equation

$$\mathbf{H}\left(\mathbf{k}_{||}, -\mathrm{i}\frac{\partial}{\partial z}\right)\mathbf{F}(z, \mathbf{k}_{||}) = E(\mathbf{k}_{||})\mathbf{F}(z, \mathbf{k}_{||}), \tag{1.9}$$

with the $\mathbf{k} \cdot \mathbf{p}$-Hamiltonian $\mathbf{H}$, cf. [12], [13] and [14]. This $\mathbf{k} \cdot \mathbf{p}$-Hamiltonian can also be derived from the bulk Hamiltonian as given in Eq. (1.7) by replacing k_z by $-\mathrm{i}\frac{\partial}{\partial z}$, [7]. Additionally, coupling effects near the material interface are taken into account. Fig. 1.2 illustrates the concept of the envelope function approximation in semiconductor heterostructures.

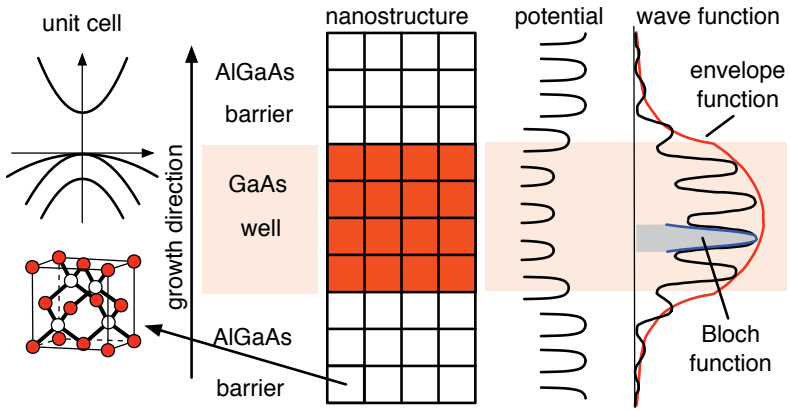

Figure 1.2: Illustration of the envelope function approximation (by courtesy of Th. Koprucki, [25]). The effective potential $V_{\text{eff}}(\mathbf{r})$ along the growth direction of a layered nanostructure consisting of a well and a barrier material is shown. Obviously, the potential can be split into fast and slowly-varying parts. Consequently, the wave function is a superposition of the fast-varying Bloch functions and the slowly-varying envelope function.

The $\mathbf{k}\cdot\mathbf{p}$-method together with the envelope function approximation is an established tool for modeling electronic states in semiconductor heterostructures. Basically, there exists a hierarchy of $\mathbf{k}\cdot\mathbf{p}$-models including 4, 6 and 8 bands respectively. From these $\mathbf{k}\cdot\mathbf{p}$-models one can derive simplified models such as the single-band model of the conduction band, we will discuss in Chap. 2, and the two-band Kane-model of the conduction band and the valence band in Chap. 3.

The single-band model is known as *effective mass approximation* (EMA), [6]. All multiband Hamiltonians $\mathbf{H}$ can be written in the form

$$\mathbf{H} = \mathbf{H}_{\text{intra}} + \mathbf{H}_{\text{inter}},$$

where $\mathbf{H}_{\text{intra}}$ is a diagonal operator that forms an EMA for every band and $\mathbf{H}_{\text{inter}}$ contains all inter-band couplings. Therefore, these multiband models are called *multiband effective mass approximations* (MEMAs).

1.3 Properties of the Solutions of Envelope Functions

In this thesis we will assume that the Hamiltonian $\mathbf{H}$ is constant outside the computational domain. In other words, the physical properties of semiconductor materials do not change outside the computational domain. We will drive elementary solutions of the vector of envelope functions in the exterior domain. Those solutions can generally be split into propagating and evanescent solutions as we will show later. We will consider traveling exterior solutions to enter the computational domain at an artificial boundary and analyze the vector of the envelope functions inside the computational domain and the vectors of the envelope functions that are reflected and transmitted at the artificial boundaries.

An important property we will use in order to derive the TBCs and the DTBCs is the continuity of the envelope functions and their derivatives if the material parameters are constant, see [24]. Since we assume that the physical properties do not change in the exterior domains, we can apply the continuity conditions to all incoming, reflected and transmitted envelope functions.

The approach to consider incoming, traveling envelope functions implies that the resulting envelope functions inside and outside the computational domain depend on the chosen norm and phase of the incoming envelope functions. Therefore, we shall define the norm of the vector

of incoming envelope functions to be unitary. Moreover, we have to consider that the phase of the resulting envelope functions might be shifted.

Finally, we will give some remarks on the notation in this thesis. In the single-band case, i.e. $d = 1$, the wave function Ψ is represented by the one-component vector of the envelope functions F. In this case we shall call the envelope function ψ and refer to it as the wave function of the single-band model. For multiband models, i.e. $d > 1$, we shall use the notation as introduced in this chapter.

According mathematical conventions, the direction of growth is called x instead of z and the wave vector k_z is denoted by k.

Chapter 2

Single-Band Effective Mass Approximations – The Schrödinger Equation

We start with the stationary linear Schrödinger equation for the wave function $\psi(x)$

$$H\psi = E\psi, \qquad x \in \mathbb{R}, \tag{2.1}$$

where E denotes the energy of the electron and H is the Hamiltonian operator that reads

$$H = -\frac{\hbar^2}{2m^*}\frac{\mathrm{d}^2}{\mathrm{d}x^2} + V(x), \tag{2.2}$$

with the reduced Planck constant $\hbar$, the effective mass m^* of the electron and the real-valued potential energy profile $V(x)$ of the electron at the position x.

A solution $\psi_E(x)$ of the stationary linear Schrödinger equation (2.1) is called an *energy eigenstate* with associated energy E.

We consider a semiconductor of length L connected to reservoirs at $x = 0$ and $x = L$. Let us assume that the potential $V(x)$ is constant in the reservoirs, i.e.

$$\begin{aligned} V(x) &= 0, \qquad x \leq 0, \\ V(x) &= V_L, \qquad x \geq L. \end{aligned}$$

The assumption $V(x) = 0$ for $x \leq 0$ means no loss of generality since we are free to set the energetic zero point. Similarly, the assumption that the left boundary is located at $x = 0$ is no loss of generality.

2.1 The Exterior Problem and the Quantum Mechanical Dispersion Relation

The *exterior problem* is concerned with the solution of the Schrödinger equation in the exterior domains. By assumption, the potential V is constant in these domains and given above. However, we will not use the particular values of the potential in the exterior domains. Instead let us continue with some constant potential V. The results stated can easily be transformed to the results in the exterior domains by setting $V \equiv 0$ and $V \equiv V_L$ respectively.

If V is constant, Eq. (2.1) is a second order ordinary differential equation (ODE) with constant coefficients that reads

$$-\frac{\hbar^2}{2m^*}\frac{\mathrm{d}^2}{\mathrm{d}x^2}\psi = (E - V)\,\psi, \qquad x \in \mathbb{R}. \tag{2.3}$$

As shown in the basic theory on ODEs, e.g. see [41], the solution of Eq. (2.3) takes the form

$$\psi(x) = \hat{\psi} e^{\kappa x}, \tag{2.4}$$

where $\hat{\psi} \in \mathbb{C}$ is an arbitrary constant and $\kappa = \kappa_{1,2} \in \mathbb{C}$ are the roots of the characteristic polynomial

$$\frac{\hbar^2}{2m^*}\kappa^2 + (E - V) = 0 \tag{2.5}$$

of Eq. (2.3). We will refer to $\hat{\psi}$ as the *amplitude* of the wave ψ.

Note that we can also write Eq. (2.4) in the form

$$\psi(x) = \hat{\psi} e^{\mathrm{i}kx}, \tag{2.6}$$

with the complex *wave vector*

$$k = \hat{k} + \mathrm{i}\check{k} = -\mathrm{i}\kappa,$$

where $\hat{k}$ is called *propagation coefficient* and $\check{k}$ denotes the *attenuation coefficient*. If the attenuation coefficient $\check{k}$ is zero, ψ is said to be *traveling*, while it is called *evanescent* otherwise.

With $k = -\mathrm{i}\kappa$ we can rewrite the characteristic polynomial (2.5) in the form

$$\frac{\hbar^2}{2m^*}k^2 = (E - V)\,.$$

If we assume that the energy E satisfies

$$E > V, \tag{2.7}$$

the wave vector k is real and takes the form

$$k = \pm\hat{k}, \tag{2.8}$$

with

$$\hat{k} = \sqrt{\frac{2m^*}{\hbar^2}(E - V)} > 0. \tag{2.9}$$

Note that the resulting waves of the form (2.6) are traveling. In classical physics the energy condition (2.7) is always fulfilled since there can only exist particles with an energy greater than the potential at that point. However, in quantum physics this is not the case and therefore, we shall, in general, not require the energy condition (2.7) to be fulfilled inside the computational domain.

As can be seen from the *quantum mechanical momentum operator* in 1D

$$p = -\mathrm{i}\hbar\frac{\mathrm{d}}{\mathrm{d}x},$$

the expectation value of the momentum p of the wave ψ of amplitude 1 is

$$\langle p\psi, \psi\rangle = \hbar k \,\langle \psi, \psi\rangle = \hbar k.$$

Hence, the expectation value of the momentum p is proportional to the wave vector k. This means that a positive wave vector corresponds to a positive momentum, i.e. a right-traveling wave, while a negative wave vector corresponds to a negative momentum, i.e. a left-traveling wave.

If the energy does not satisfy the condition (2.7), i.e.

$$E \leq V, \tag{2.10}$$

then the wave vector k is purely imaginary and takes the form

$$k_{1,2} = \pm \mathrm{i}\check{k}, \tag{2.11}$$

with

$$\check{k} = \sqrt{\frac{2m^*}{\hbar^2}(V - E)}. \tag{2.12}$$

This wave vector yields evanescent waves (2.6).

If we apply the solution (2.6) to Eq. (2.3) we obtain

$$\frac{\hbar^2 k^2}{2m^*}\hat{\psi} = (E - V)\,\hat{\psi}.$$

Since we can neglect the trivial solution $\psi \equiv 0$, the energy E satisfies the *quantum mechanical dispersion relation*

$$E = E(k) = V + \frac{\hbar^2 k^2}{2m^*}. \tag{2.13}$$

2.2 Transparent Boundary Conditions

In order to transform the Schrödinger equation (2.1) on the real line $x \in \mathbb{R}$ into an equivalent system posed on the bounded domain $(0, L)$ we introduce artificial boundary conditions at $x = 0$ and $x = L$. As described in Chap. 1, artificial boundary conditions that form a system whose solution equals the solution of the unbounded problem on the domain $(0, L)$ are called *transparent boundary conditions* (TBCs).

In order to derive these TBCs we consider a plain wave of amplitude 1 with positive momentum and coming from $-\infty$ that enters the computational domain from the left at $x = 0$

$$\psi^{\mathrm{in}} = e^{\mathrm{i}\hat{k}_0 x}, \qquad x < 0, \tag{2.14}$$

where $\hat{k}_0 > 0$ denotes the propagation coefficient (2.9) of the wave vector k in the left exterior domain $x \leq 0$, i.e. with $V \equiv 0$. The incoming wave (2.14) results in a reflected, left-traveling wave

$$\psi^{\mathrm{r}} = re^{-\mathrm{i}\hat{k}_0 x}, \qquad x < 0, \tag{2.15a}$$

with the reflection coefficient r, and a transmitted, right-traveling wave

$$\psi^{\mathrm{t}} = te^{\mathrm{i}\hat{k}_L x}, \qquad x > L, \tag{2.15b}$$

with the transmission coefficient t and the propagation coefficient $\check{k}_L > 0$ of the wave vector k in the right exterior domain $x \geq L$, i.e. with $V \equiv V_L$. The propagation coefficient $\hat{k}_L$ satisfies

$$\hat{k}_L = \sqrt{\hat{k}_0^2 - \frac{2m^* V_L}{\hbar^2}}.$$

Thus, the solution in the left exterior domain has the form

$$\psi = \psi^{\mathrm{in}} + \psi^{\mathrm{r}}, \qquad x < 0, \tag{2.16a}$$

and the solution in the right exterior domain is

$$\psi = \psi^{\mathrm{t}}, \qquad x > L. \tag{2.16b}$$

We know that the wave and its first derivative are continuous at the two boundaries, cf. [24]. Hence, we can eliminate the reflection and transmission coefficients by comparing Eq. (2.16a) and its first derivative at $x = 0$ as well as Eq. (2.16b) and its first derivative at $x = L$.

The resulting *boundary value problem* (BVP) reads

$$-\frac{\hbar^2}{2m^*}\psi_{xx} + V(x)\psi = E\psi, \qquad 0 < x < L, \tag{2.17a}$$

$$\psi_x(0) + \mathrm{i}k\psi(0) = 2\mathrm{i}\hat{k}_0, \tag{2.17b}$$

$$\psi_x(L) - \mathrm{i}\sqrt{\hat{k}_0^2 - \frac{2m^*V_L}{\hbar^2}}\psi(L) = 0. \tag{2.17c}$$

Theorem 2.1 (Proposition 2.3 in [8])**.** Let V be in $L^\infty(0,L)$ and real valued. Then the BVP (2.17) has a unique solution $\psi \in W^{2,\infty}(0,L)$.

2.3 The Standard Discretization

After stating the BVP (2.17) and showing that it has a unique solution, we want to derive techniques to solve it numerically and compute eigenstates for corresponding energies and potentials. First let us set $\hbar = m^* = 1$ for the remainder of this chapter. We will introduce *finite difference schemes* (FDS) to solve the BVP, using the uniform discretization $x_j = jh,\ j = 0,\ldots,J$ with $L = Jh$, of the computational domain $(0,L)$.

Definition 2.1. Let $\{x_j\}, j = 0,\ldots,J$, with the positive step size $h = x_j - x_{j-1}, \forall j = 1,\ldots,J$, be given and let $\{f_j\}$ be the discretization of $f : x \mapsto f(x)$ with the approximation $f(x_j) \approx f_j$. Then we define the standard finite difference quotient operators

$$\mathrm{D}_h^{\mathrm{fwd}} f_j := \frac{f_{j+1} - f_j}{h} \qquad \text{(first order forward)}$$

$$\mathrm{D}_h^{\mathrm{bwd}} f_j := \frac{f_j - f_{j-1}}{h} \qquad \text{(first order backward)}$$

$$\mathrm{D}_h^{\mathrm{cen}} f_j := \frac{f_{j+1} - f_{j-1}}{2h} \qquad \text{(second order centered)}$$

$$\mathrm{D}_h^{\mathrm{std}} f_j := \frac{f_{j-1} - 2f_j + f_{j+1}}{h^2} \qquad \text{(standard second order).}$$

By applying the standard second order finite difference quotient operator we get the *second order standard FDS*

$$-\frac{1}{2}\mathrm{D}_h^{\mathrm{std}}\psi_j + V_j\psi_j = E\psi_j, \qquad j = 1,\ldots,J-1, \tag{2.18}$$

for the Schrödinger equation (2.17) with $V_j = V(x_j)$ and the approximation $\psi_j \approx \psi(x_j)$, $j = 0,\ldots,J$. We can rewrite Eq. (2.18) in the form

$$-\psi_{j+1} + 2\left(1 - (E - V_j)h^2\right)\psi_j - \psi_{j-1} = 0, \qquad j = 1,\ldots,J-1. \tag{2.19}$$

This is a linear second order homogeneous difference equation with a spatially varying coefficient V_j.

Now let us analyze the *discrete exterior problem* of the standard FDS. We will continue with some constant potential V. The results of the exterior domains $x \le 0$ and $x \ge L$ can later be derived by inserting the respective value of the potential in the results stated.

If V is constant, Eq. (2.19) is a linear second order difference equation with constant coefficients and as shown in [28], Eq. (2.19) has a solution of the form

$$\psi_j = \hat{\psi}_h\alpha^j = \hat{\psi}_h e^{\ln(\alpha)j} = \hat{\psi}_h e^{(\ln|\alpha| + \mathrm{i}\arg(\alpha))j} = \hat{\psi}_h e^{\mathrm{i}k_h jh}, \tag{2.20}$$

with $\alpha \in \mathbb{C}$, cf. (2.6). We will call $\hat{\psi}_h$ the *discrete amplitude* of the discrete wave ψ_j and

$$k_h = -\mathrm{i}\frac{1}{h}\ln(\alpha) = \frac{1}{h}\left(\arg(\alpha) - \mathrm{i}\ln|\alpha|\right) \tag{2.21}$$

the *discrete wave vector*. By applying Eq. (2.20) to Eq. (2.19) we get

$$-\alpha^{j+1} + 2(1-(E-V)\,h^2)\alpha^j - \alpha^{j-1} = \alpha^{j-1}\left(\alpha^2 - 2\left(1-(E-V)\,h^2\right)\alpha + 1\right) = 0.$$

Since we neglect the trivial solution $\alpha = 0$, we have

$$\alpha^2 - 2\left(1-(E-V)\,h^2\right)\alpha + 1 = 0,$$

which implies

$$\left(\alpha - \left(1-(E-V)\,h^2\right)\right)^2 = (E-V)\,h^2\left((E-V)\,h^2 - 2\right). \tag{2.22}$$

If the energy E satisfies the energy condition (2.7), i.e.

$$E > V,$$

the right hand side of Eq. (2.22) is negative if the step size h satisfies

$$h < \sqrt{\frac{2}{E-V}}, \tag{2.23}$$

and hence, the roots of Eq. (2.22) are complex and read

$$\alpha_{1,2} = 1-(E-V)\,h^2 \pm \mathrm{i}\sqrt{(E-V)\,h^2\,(2-(E-V)\,h^2)}. \tag{2.24}$$

We find that

$$|\alpha_{1,2}| = \left(1-(E-V)\,h^2\right)^2 + (E-V)\,h^2\left(2-(E-V)\,h^2\right) = 1,$$

and thus, the discrete wave vector k_h is real and takes the form

$$k_h = \pm\hat{k}_h, \tag{2.25}$$

cf. (2.8), with the propagation coefficient

$$\hat{k}_h = \frac{1}{h}\arg(\alpha) = \frac{1}{h}\arccos\frac{\operatorname{Re}\alpha}{|\alpha|} = \frac{1}{h}\arccos\left(1-(E-V)\,h^2\right).$$

Note that we can neglect to add the term $n\frac{2\pi}{h}$, $n \in \mathbb{Z}$, to this formula since for any $n \neq 0$ this term diverges for $h \to 0$. On the other hand, we will see later that the discrete wave vector k_h as given in Eq. (2.25), i.e. with $n = 0$, tends to the analytical wave vector k for $h \to 0$.

The wave vector $k_h = \hat{k}_h$ corresponds to

$$\alpha_1 = 1-(E-V)\,h^2 + \mathrm{i}\sqrt{(E-V)\,h^2\,(2-(E-V)\,h^2)},$$

while $k_h = -\hat{k}_h$ is associated with

$$\alpha_2 = 1-(E-V)\,h^2 - \mathrm{i}\sqrt{(E-V)\,h^2\,(2-(E-V)\,h^2)}.$$

Hence, we get two traveling waves, $\psi_j = \alpha_1^j$ being right-traveling and $\psi_j = \alpha_2^j$ being left-traveling.

The case

$$h \geq \sqrt{\frac{2}{E-V}},$$

results in a nonnegative right hand side of Eq. (2.22) and thus, a complex conjugate pair of purely imaginary wave vectors that give evanescent waves. However, this case is numerically not applicable since it defines a lower bound for the step size h.

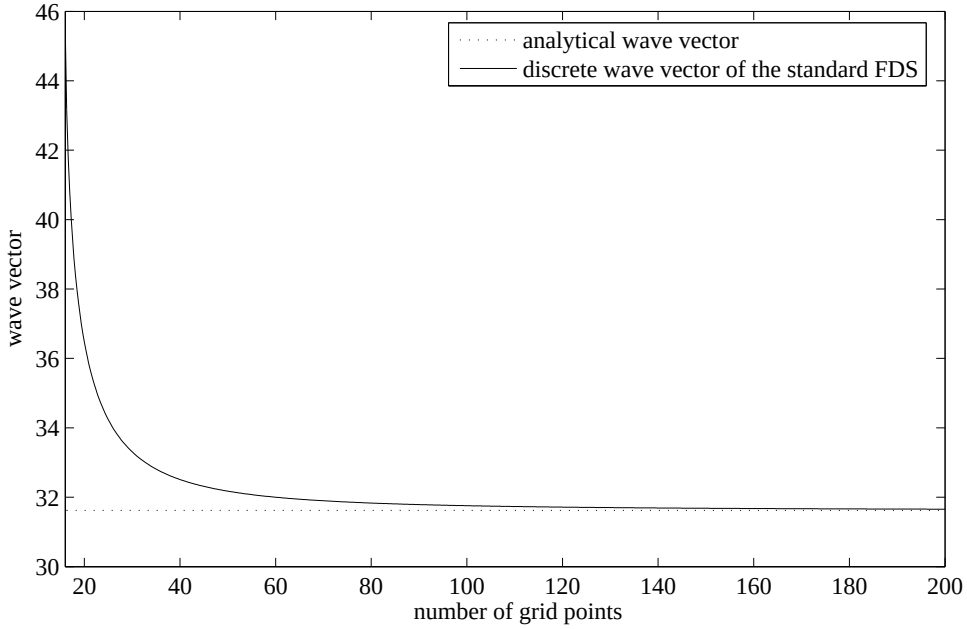

Figure 2.1: Analytical wave vector and discrete wave vector of the standard FDS against the number of grid points $J = 1/h$ for an energy $E = 500$ and a potential $V = 0$.

On the other hand, if the energy E does not satisfy the energy condition (2.7), i.e.

$$E \leq V,$$

the right hand side of Eq. (2.22) is also nonnegative, yielding a complex conjugate pair of purely imaginary wave vectors that give evanescent waves. Let us recall the TBCs we derived in Sec. 2.2. We considered an incoming wave, i.e. a traveling wave to enter the semiconductor at $x = 0$. Hence, the case $E \leq V$ is not applicable either for the exterior domains since it leads to evanescent waves only.

Now let us analyze the behavior of the discrete wave vector k_h of the standard FDS for $h \to 0$. Therefore, we use l'Hôpital's rule to get

$$\begin{aligned}
\lim_{h\to 0} k_h &= \pm \lim_{h\to 0} \hat{k}_h \\
&= \pm \lim_{h\to 0} \frac{1}{h} \arccos\left(1 - (E-V)\, h^2\right) \\
&= \pm \lim_{h\to 0} \frac{-2\,(E-V)\, h}{\sqrt{1 - \left(1 - (E-V)\, h^2\right)^2}} \\
&= \pm \lim_{h\to 0} \frac{2\,(E-V)}{\sqrt{2\,(E-V) - (E-V)^2\, h^2}} \\
&= \pm\sqrt{2\,(E-V)},
\end{aligned}$$

which equals the analytical wave vector (2.8) for $\hbar = m^* = 1$. Fig. 2.1 shows the discrete wave vector $\hat{k}_h$ of the standard FDS versus the number of grid points $J = 1/h$ compared to the analytical wave vector $\hat{k}$ for an energy $E = 500$ and a potential $V = 0$. Considering that the step size h has to satisfy Eq. (2.23), i.e. $h < 1/16$ in our example, the standard FDS overestimates the wave vector for any admissible step size h.

Note, that Eq. (2.25) defines the *discrete dispersion relation*. Finally, we will state this relation in the reciprocal form. To do this, we recall the wave representation of the form $\psi_j = \hat{\psi} e^{\mathrm{i}k_h jh}$ that implies

$$\psi_{j+1} e^{-\mathrm{i}kh} = \psi_j = \psi_{j-1} e^{\mathrm{i}kh}.$$

Applied to the difference equation (2.19), this gives

$$-e^{\mathrm{i}kh} + 2\left(1 - (E - V)\, h^2\right) - e^{-\mathrm{i}kh} = 0,$$

which leads to

$$E = E_h^{\mathrm{std}}(k_h) = V + \frac{1 - \cos k_h h}{h^2} = V + \frac{2}{h^2} \sin^2 \frac{k_h h}{2} = V + \frac{k_h^2 h}{2} + \mathcal{O}(h^2), \tag{2.26}$$

cf. the continuous dispersion relation (2.13).

2.4 Discretization of the Transparent Boundary Conditions

Let us now introduce a finite difference discretization of the two Robin-type TBCs (2.17b) and (2.17c). We apply the second order centered difference operator $\mathrm{D}_h^{\mathrm{cen}}$ to ψ_0 at the left boundary and ψ_J at the right boundary. Let $\hat{k}_0$ denote the analytical propagation coefficient of a right-traveling wave in the left exterior domain $x \leq 0$. Then the analytical propagation coefficient of a right-traveling wave in the right exterior domain is

$$\hat{k}_L = \sqrt{\hat{k}_0^2 - 2V_L}.$$

At the left boundary we have

$$\frac{\psi_1 - \psi_{-1}}{2h} + \mathrm{i}\hat{k}_0 \psi_0 = 2\mathrm{i}\hat{k}_0,$$

which implies

$$-\psi_{-1} + 2\mathrm{i}\hat{k}_0 h \psi_0 + \psi_1 = 4\mathrm{i}\hat{k}_0 h. \tag{2.27a}$$

On the other hand, discretizing the right TBC gives

$$\frac{\psi_{J+1} - \psi_{J-1}}{2h} = \mathrm{i}\sqrt{\hat{k}_0^2 - 2V_L}\,\psi_J,$$

that can be expressed in the form

$$\psi_{J-1} + 2\mathrm{i}\sqrt{\hat{k}_0^2 - 2V_L}\, h \psi_J - \psi_{J+1} = 0. \tag{2.27b}$$

The two ghost points ψ_{-1} and ψ_{J+1} in Eq. (2.27) can be eliminated by subtracting the FDS (2.19) of the Schrödinger equation (2.17a) at $j = 0$ and $j = J$. By using the identities $E = \hat{k}_0^2/2$ and $E - V_L = \hat{k}_L^2/2$ we get the two second order discretized TBCs

$$\left(\frac{1}{2}\hat{k}_0^2 h^2 - 1 + \mathrm{i}\hat{k}_0 h\right)\psi_0 + \psi_1 = 2\mathrm{i}\hat{k}_0 h \tag{2.28a}$$

and

$$\psi_{J-1} + \left(\frac{1}{2}\left(\hat{k}_0^2 - 2V_L\right) h^2 - 1 + \mathrm{i}\sqrt{\hat{k}_0^2 - 2V_L}\, h\right)\psi_J = 0. \tag{2.28b}$$

Before we show the existence and uniqueness of the solution of the described numerical scheme together with the discretized TBCs, we prove the discrete analogon of integration by parts.

Lemma 2.2. Let $\{x_j\}, j = 0, \ldots, J$, with the positive step size $h = x_j - x_{j-1}, \forall j = 1, \ldots, J$, be given. Let $\{f_j\}$ and $\{g_j\}$ be the discretization of $f : x \mapsto f(x)$ and $g : x \mapsto g(x)$ with the approximations $f(x_j) \approx f_j$ and $g(x_j) \approx g_j$. Then

$$\sum_{j=1}^{J-1} \left(\mathrm{D}_h^{\mathrm{fwd}} f_j\right) g_j = -\sum_{j=1}^{J-1} f_j \left(\mathrm{D}_h^{\mathrm{bwd}} g_j\right) - \frac{1}{h} f_1 g_0 + \frac{1}{h} f_j g_{J-1}.$$

Proof. The left hand side of the above equation can be written in the form

$$\sum_{j=1}^{J-1} \left(\mathrm{D}_h^{\mathrm{fwd}} f_j\right) g_j = \frac{1}{h} \sum_{j=1}^{J-1} (f_{j+1} - f_1) g_j = \frac{1}{h} \left(-f_1 g_1 + f_2 g_1 - \ldots - f_{J-1} g_{J-1} + f_J g_{J-1}\right).$$

By adding

$$0 = -\frac{1}{h} f_1 g_0 + \frac{1}{h} f_j g_{J-1} + \frac{1}{h} f_1 g_0 - \frac{1}{h} f_j g_{J-1},$$

we get

$$\begin{aligned}\sum_{j=1}^{J-1} \left(\mathrm{D}_h^{\mathrm{fwd}} f_j\right) g_j &= \frac{1}{h} \left(f_1 g_0 - f_1 g_1 + \ldots + f_{J-1} g_{J-2} - f_{J-1} g_{J-1}\right) - \frac{1}{h} f_1 g_0 + \frac{1}{h} f_j g_{J-1} \\ &= -\sum_{j=1}^{J-1} f_j \left(\mathrm{D}_h^{\mathrm{bwd}} g_j\right) - \frac{1}{h} f_1 g_0 + \frac{1}{h} f_j g_{J-1}.\end{aligned}$$

□

Existence and uniqueness of the solution of the numerical scheme together with the discretized TBCs is shown in

Theorem 2.3 (presented in [4] without proof)**.** Let $\{V_j\}, j = 0, \ldots, J$, and $E > \max\{0, V_L\}$ be given, and assume $h < \min\left\{\sqrt{\frac{2}{E}}, \sqrt{\frac{2}{E - V_L}}\right\}$. Then the discrete BVP (2.19) with the discretized TBCs (2.28) has a unique solution $\{\psi_j\}, j = 0, \ldots, J$.

Proof. In order to show that the discrete BVP (2.19) together with the discretized TBCs (2.28) has a unique solution we follow the ideas of the proof of Thm. 2.1 on a purely discrete level. To do this, we rewrite the discrete BVP (2.19) in the form

$$\mathrm{D}_h^{\mathrm{std}} \psi_j = -2 (E - V_j) \psi_j.$$

Moreover, we rewrite the discretized TBCs in the form

$$-\gamma_1 \psi_0 + \psi_1 = \eta_1$$

and

$$\psi_{J-1} - \gamma_2 \psi_J = \eta_2,$$

with

$$\begin{aligned}\gamma_1 &= 1 - \frac{1}{2} \hat{k}_0^2 h^2 - \mathrm{i} \hat{k}_0 h, \\ \gamma_2 &= 1 - \frac{1}{2} \left(\hat{k}_0^2 - 2V_L\right) h^2 - \mathrm{i} \sqrt{\hat{k}_0^2 - 2V_L}\, h,\end{aligned}$$

and

$$\begin{aligned}\eta_1 &= 2\mathrm{i} \hat{k}_0 h, \\ \eta_2 &= 0.\end{aligned}$$

The discrete BVP together with the discretized TBCs form a system of linear equations. If the coefficient matrix of this system is regular then the solution is unique. By showing that the homogeneous case of the TBCs, i.e. $\eta_1 = \eta_2 = 0$, implies that the discrete solution is zero at every grid point, we prove that the coefficient matrix is regular.

Now let us write the homogeneous, discretized TBCs in the form

$$h\mathrm{D}_h^{\mathrm{bwd}}\psi_1 = (\gamma_1 - 1)\,\psi_0,$$

and

$$h\mathrm{D}_h^{\mathrm{bwd}}\psi_J = \left(\gamma_2^{-1} - 1\right)\psi_{J-1}.$$

We sum up the discrete BVP for $j = 1, \ldots, J-1$, which gives

$$\sum_{j=1}^{J-1} \mathrm{D}_h^{\mathrm{std}}\psi_j = -2\sum_{j=1}^{J-1} (E - V_j)\,\psi_j.$$

By multiplying this equation by the complex conjugate $\bar{\psi}_j$ of ψ_j we get

$$-2\sum_{j=1}^{J-1} (E - V_j)\,|\psi_j|^2 = \sum_{j=1}^{J-1} \left(\mathrm{D}_h^{\mathrm{std}}\psi_j\right)\bar{\psi}_j.$$

Now we use Lem. 2.2 and the obvious property

$$\mathrm{D}_h^{\mathrm{std}} = \mathrm{D}_h^{\mathrm{bwd}}\mathrm{D}_h^{\mathrm{fwd}} = \mathrm{D}_h^{\mathrm{fwd}}\mathrm{D}_h^{\mathrm{bwd}},$$

to obtain

$$\begin{aligned}
-2\sum_{j=1}^{J-1} (E - V_j)\,|\psi_j|^2 &= \sum_{j=1}^{J-1} \left(\mathrm{D}_h^{\mathrm{fwd}}\left(\mathrm{D}_h^{\mathrm{bwd}}\psi_j\right)\right)\bar{\psi}_j \\
&= -\sum_{j=1}^{J-1} \left(\mathrm{D}_h^{\mathrm{bwd}}\psi_j\right)\left(\mathrm{D}_h^{\mathrm{bwd}}\bar{\psi}_j\right) - \frac{1}{h}\bar{\psi}_0\mathrm{D}_h^{\mathrm{bwd}}\psi_1 + \frac{1}{h}\bar{\psi}_{J-1}\mathrm{D}_h^{\mathrm{bwd}}\psi_J \\
&= -\sum_{j=1}^{J-1} \left|\mathrm{D}_h^{\mathrm{bwd}}\psi_j\right|^2 - \frac{1}{h}\bar{\psi}_0\mathrm{D}_h^{\mathrm{bwd}}\psi_1 + \frac{1}{h}\bar{\psi}_{J-1}\mathrm{D}_h^{\mathrm{bwd}}\psi_J.
\end{aligned}$$

At this point by apply the homogeneous, discretized TBCs. It yields

$$-2\sum_{j=1}^{J-1} (E - V_j)\,|\psi_j|^2 = -\sum_{j=1}^{J-1} \left|\mathrm{D}_h^{\mathrm{bwd}}\psi_j\right|^2 - \frac{1}{h^2}(\gamma_1 - 1)\,|\psi_0|^2 + \frac{1}{h}\left(\gamma_2^{-1} - 1\right)|\psi_{J-1}|^2.$$

By taking the imaginary part of this equation it reduces to

$$0 = -\operatorname{Im}\gamma_1\,|\psi_0|^2 + \operatorname{Im}\gamma_2^{-1}\,|\psi_{J-1}|^2.$$

Since

$$\operatorname{Im}\gamma_1 = -\hat{k}_0 h < 0,$$

and

$$\operatorname{Im}\gamma_2^{-1} = -\frac{1}{|\gamma_2|^2}\operatorname{Im}\gamma_2 = \frac{1}{|\gamma_2|^2}\sqrt{\hat{k}_0^2 - 2V_L}\,h > 0,$$

we end up with the equation

$$0 = \hat{k}_0 h\,|\psi_0|^2 + \frac{1}{|\gamma_2|^2}\sqrt{\hat{k}_0^2 - 2V_L}\,h\,|\psi_{J-1}|^2.$$

This implies that $|\psi_0|^2 = |\psi_{J-1}|^2 = 0$ and hence, $\psi_0 = \psi_{J-1} = 0$. By using the homogeneous, discrete TBCs we get $\psi_1 = 0$ and $\psi_J = 0$. Successively applying the discrete BVP gives $\psi_j = 0$ for $j = 0, \ldots, J$ and hence, the discrete solution vanishes at every grid point if the discretized TBCs are homogeneous. Thus, the coefficient matrix of the system of linear equations formed by the discrete BVP and the two discretized TBCs is regular and therefore, the discrete solution is unique. □

Let us recall the discrete waves in the exterior domains

$$\psi_j = e^{\mathrm{i}\hat{k}_{h,0}jh}, \qquad j \leq 0,$$

and

$$\psi_j = e^{\mathrm{i}\hat{k}_{h,L}jh}, \qquad j \geq J.$$

Suppose that they are solutions to the difference scheme in a small vicinity of the two boundaries, i.e. $j = 0, 1$ and $j = J-1, J$. Then they should also satisfy the discretized TBCs (2.28). However, at the left boundary we get

$$\begin{aligned}
2\mathrm{i}\hat{k}_0 h &= \left(Eh^2 - 1 + \mathrm{i}\hat{k}_0 h\right)\psi_0 + \psi_1 \\
&= \left(Eh^2 - 1 + \mathrm{i}\hat{k}_0 h\right) + e^{\mathrm{i}\hat{k}_{h,0}h} \\
&= \left(Eh^2 - 1 + \mathrm{i}\hat{k}_0 h\right) + \left(1 - Eh^2 + \mathrm{i}\sqrt{2Eh^2 - E^2h^4}\right) \\
&= \mathrm{i}\hat{k}_0 h + \mathrm{i}\hat{k}_0 h \underbrace{\sqrt{1 - \hat{k}_0^2 h^2/4}}_{\neq 1} \neq 2\mathrm{i}\hat{k}_0 h,
\end{aligned}$$

which is a contradiction. A similar contradiction can be found at the right boundary.

The reason is that the TBCs are based on the analytical solution as derived in Sec. 2.1. The wave vector of the analytical solution, see Eq. (2.8), however, is different from the discrete wave vector (2.25). Hence, the discretized TBCs model exterior domains whose physical properties (i.e. wave vector and dispersion relation) are discretization of the analytical properties. Inside the computational domain, however, we use the FDS (2.19) that implies a discrete wave vector and a discrete dispersion relation. In other words, a wave coming from $-\infty$ and entering the semiconductor at $x = 0$ is *refracted* at the boundary $x = 0$ as it comes from a media with the analytical dispersion relation and enters a media with the discrete dispersion relation. This leads to spurious oscillations in the numerical solutions as shown in the following example.

Let us set $V \equiv 0$, $L = 1$, $h = 1/100$ and $E = 500$. The analytical solution is given by

$$\psi(x) = e^{\mathrm{i}\hat{k}x},$$

with $\hat{k} = \sqrt{2E}$. Fig. 2.2(a) shows a comparison of the modulus of the analytical solution and the discrete solution. We observe that the modulus of the discrete solution oscillates, while the modulus of the analytical solution is constantly 1. These oscillations decrease for smaller step sizes but they do not vanish. The phase of the discrete solution also differs from the phase of the analytical solution, see Fig. 2.2(b). This error, however, is not related to the spurious oscillations of the modulus but can be explained with the difference between the analytical and discrete wave vector, see Fig. 2.1. Since the discrete wave vector is greater than the analytical wave vector, the wave length of the discrete solution is smaller than the wave length of the analytical solution.

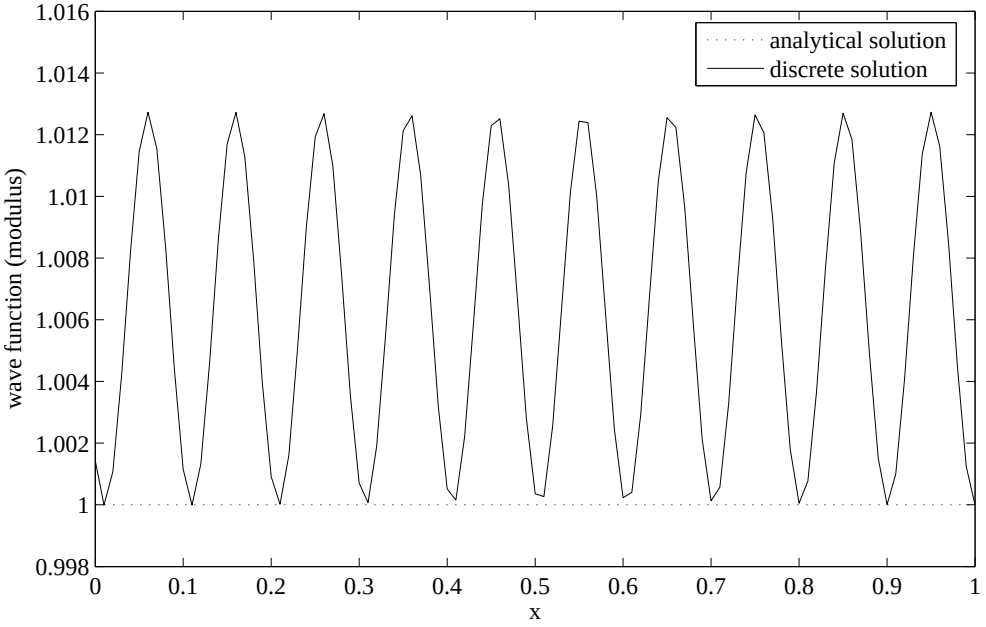

(a) Modulus of the analytical (dotted line) and discrete (solid line) solutions.

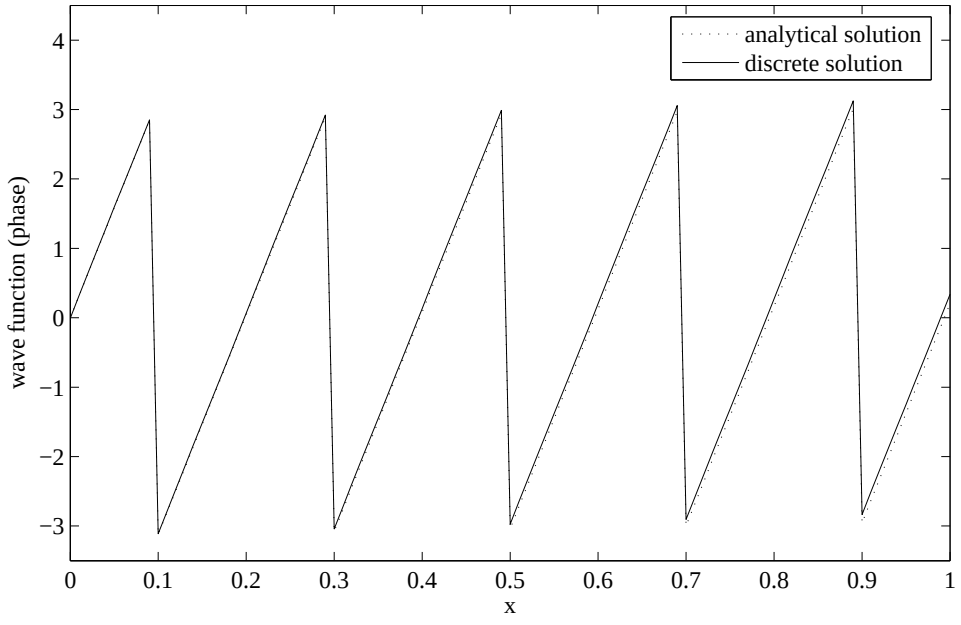

(b) Phases of the analytical (dotted line) and discrete (solid line) solutions.

Figure 2.2: Comparison of the analytical solution $\psi(x) = e^{\mathrm{i}\hat{k}x}$ and the discrete solution of the second order standard FDS using discretized TBCs for a step size $h = 1/100$, an energy $E = 500$ and a potential $V \equiv 0$.

2.5 Discrete Transparent Boundary Conditions

In this section we will derive the *discrete transparent boundary conditions* (DTBCs) of the single-band model. DTBCs are derived on a fully discrete level. This means that they are deduced with the help the discrete exterior solution as given in Eq. (2.20). We assume that the discrete exterior solution holds in a small vicinity of the two boundaries. Consequently, the refraction at the boundaries, resulting in spurious oscillations, vanishes completely.

Let us recall the right-traveling discrete wave $\psi_j = e^{\mathrm{i}\hat{k}_h jh}$ and the left-traveling discrete wave $\psi_j = e^{-\mathrm{i}\hat{k}_h jh}$ with discrete amplitude $\hat{\psi}_h = 1$. Let $\hat{k}_{h,0}$ denote the discrete wave vector in the left exterior domain $x \leq 0$, i.e. with $V \equiv 0$, and $\hat{k}_{h,L}$ the discrete wave vector in the right exterior domain $x \geq L$, i.e. with $V \equiv V_L$. We apply these discrete waves to the reflection and transmission conditions (2.16) and consider that they hold in a small vicinity of the two boundaries, i.e. $j = 0, 1$ and $j = J-1, J$ respectively. It yields

$$\psi_j = \psi_j^{\mathrm{in}} + \psi_j^{\mathrm{r}} = e^{\mathrm{i}\hat{k}_{h,0}x_j} + re^{-\mathrm{i}\hat{k}_{h,0}x_j}, \qquad j = 0, 1,$$

and

$$\psi_j = \psi_j^{\mathrm{t}} = te^{\mathrm{i}\hat{k}_{h,L}x_j}, \qquad j = J-1, J.$$

By eliminating the reflection and transmission coefficients we obtain the DTBCs

$$-\psi_0 e^{-\mathrm{i}\hat{k}_{h,0}h} + \psi_1 = 2\mathrm{i}\sin\hat{k}_{h,0}h, \tag{2.29a}$$

and

$$\psi_{J-1}e^{\mathrm{i}\hat{k}_{h,L}h} - \psi_J = 0, \tag{2.29b}$$

cf. the TBCs (2.17b) and (2.17c).

Let us recall the discretized TBCs (2.28). We expand the exponential function and the sine function in the left DTBC (2.29a). Keeping terms up to second order gives

$$-\left(1 - \mathrm{i}\hat{k}_{h,0}h - \frac{1}{2}\hat{k}_{h,0}^2h^2\right)\psi_0 + \psi_1 = 2\mathrm{i}\hat{k}_{h,0}h.$$

If we replace the discrete wave vector $\hat{k}_{h,0}$ by the analytical wave vector $\hat{k}_0$ the above equation becomes

$$\left(\frac{1}{2}\hat{k}_0^2h^2 - 1 + \mathrm{i}\hat{k}_0h\right)\psi_0 + \psi_1 = 2\mathrm{i}\hat{k}_0h,$$

which equals the left discretized TBC. Similarly, we can deduce the right discretized TBC from the right DTBC.

Now we can reformulate Thm. 2.3 for the DTBCs.

Theorem 2.4 (presented in [4] without proof)**.** Let $\{V_j\}, j = 0, \ldots, J$, and $E > \max\{0, V_L\}$ be given, and assume $h < \min\left\{\sqrt{\frac{2}{E}}, \sqrt{\frac{2}{E-V_L}}, \frac{\pi}{\hat{k}_{h,0}}, \frac{\pi}{\hat{k}_{h,L}}\right\}$. Then the discrete BVP (2.19) with the DTBCs (2.29) has a unique solution $\{\psi_j\}, j = 0, \ldots, J$.

Proof. We show that for the homogeneous DTBCs the discrete solution is zero at every grid point. Therefore, we write the homogeneous DTBCs in the form

$$h\mathrm{D}_h^{\mathrm{bwd}}\psi_1 = (\gamma_1 - 1)\,\psi_0$$

and

$$h\mathrm{D}_h^{\mathrm{bwd}}\psi_J = \left(\gamma_2^{-1} - 1\right)\psi_{J-1},$$

with

$$\gamma_1 = e^{-\mathrm{i}\hat{k}_{h,0}h}$$

and

$$\gamma_2 = e^{-\mathrm{i}\hat{k}_{h,L}h}.$$

Analogously to the proof of Thm. 2.3, we multiply the sum of the discrete BVP for $j = 1, \ldots, J-1$ by $\bar{\psi}_j$, apply Lem. 2.2 and take the imaginary part. This yields

$$0 = -\operatorname{Im}\gamma_1 \left|\psi_0\right|^2 + \operatorname{Im}\gamma_2^{-1} \left|\psi_{J-1}\right|^2,$$

with

$$\operatorname{Im}\gamma_1 = -\sin\hat{k}_{h,0}h < 0, \qquad h < \frac{\pi}{\hat{k}_{h,0}},$$

and

$$\operatorname{Im}\gamma_2^{-1} = -\frac{1}{\left|\gamma_2\right|^2}\operatorname{Im}\gamma_2 = \sin\hat{k}_{h,0}h > 0, \qquad h < \frac{\pi}{\hat{k}_{h,L}}.$$

Hence, we end up with the equation

$$0 = \sin\hat{k}_{h,0}h \left|\psi_0\right|^2 + \sin\hat{k}_{h,L}h \left|\psi_{J-1}\right|^2,$$

that implies $\left|\psi_0\right|^2 = \left|\psi_{J-1}\right|^2 = 0$. Thus, we have $\psi_0 = \psi_{J-1} = 0$ and by using the homogeneous DTBCs we get $\psi_1 = 0$ and $\psi_J = 0$. Successively applying the discrete BVP gives $\psi_j = 0$ for $j = 0, \ldots, J$, and hence, the discrete solution vanishes at every grid point if the DTBCs are homogeneous. This implies that the coefficient matrix of the system of linear equations formed by the discrete BVP and the two DTBCs is regular and therefore, the discrete solution is unique. □

In the remainder of this section we will show that the use of the DTBCs in fact does not lead to spurious oscillations of the modulus of the numerical solution. Again we set $V \equiv 0$, $L = 1$, $h = 1/100$ and $E = 500$. The analytical solution is given by

$$\psi(x) = e^{\mathrm{i}\hat{k}x},$$

with $\hat{k} = \sqrt{2E}$. The modulus of the analytical solution is 1. Fig. 2.3(a) shows that the modulus of the discrete solution coincides with the modulus of the analytical solution. As in the previous example when using discretized TBCs the phase of the discrete solution differs slightly from the phase of the analytical solution near the right boundary, see Fig. 2.3(b). This can also be seen in Fig. 2.3(a), where the wave length of the real part of the analytical solution is greater than the wave length of the real part of the discrete solution. Recall that this error is directly related with the difference of the analytical and discrete wave vector, see Fig. 2.1. Since the discrete wave vector is greater than the analytical wave vector the wave length of the discrete solution is smaller than the wave length of the analytical solution. Note that this error tends to zero for $h \to 0$.

2.6 Alternative Finite Difference Schemes

Before we will examine the numerical results of more advanced physical examples we will derive and compare alternative FDSs. Our aim is to improve the convergence of the scheme or to develop schemes that solve the problem exactly if certain conditions are fulfilled.

2.6.1 The Numerov Discretization

We start with the so-called *Numerov discretization*, see [33], [34], that is of higher order than the standard discretization.

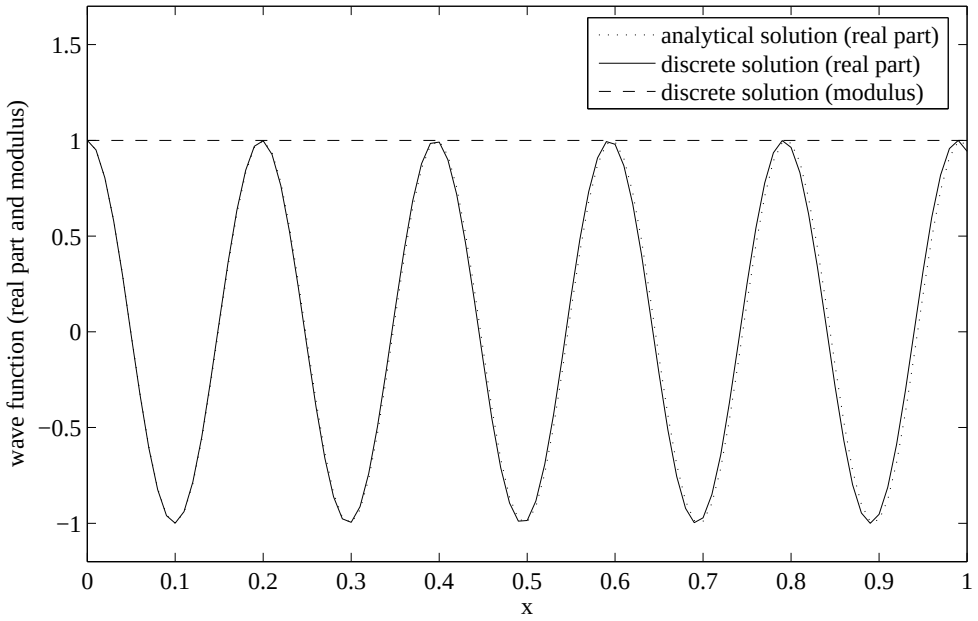

(a) Real parts of the analytical (dotted line) and discrete (solid line) solutions and modulus (dashed line) of the discrete solution, which coincides with the modulus of the analytical solution.

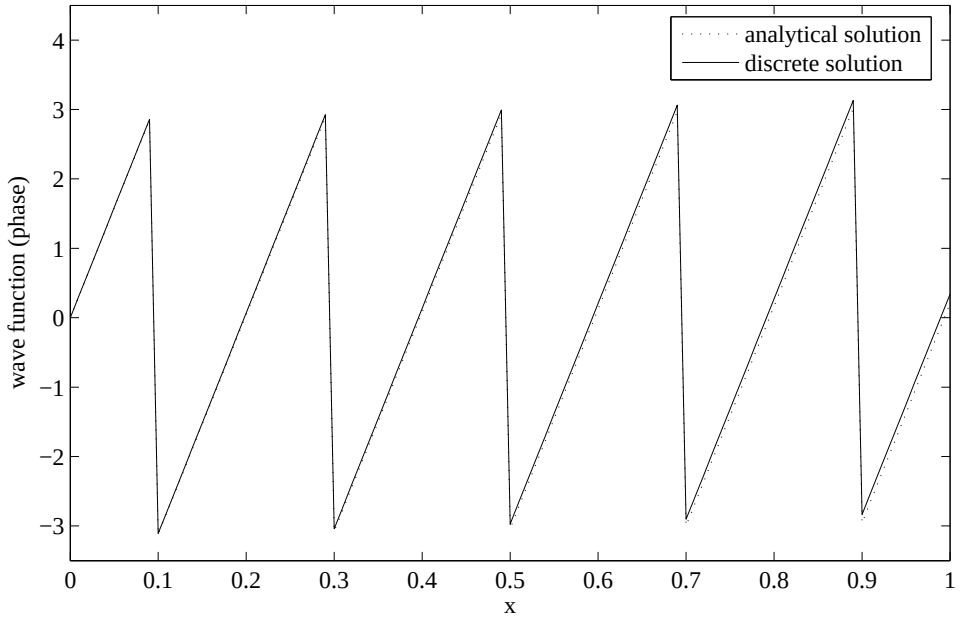

(b) Phases of the analytical (dotted line) and discrete (solid line) solutions.

Figure 2.3: Comparison of the analytical solution $\psi(x) = e^{\mathrm{i}\hat{k}x}$ and the discrete solution of the second order standard FDS using DTBCs for a step size $h = 1/100$, an energy $E = 500$ and a potential $V \equiv 0$.

Let us consider the Schrödinger equation of the BVP (2.17), and let us rewrite it in the form

$$\psi_{xx} = -2\left(E - V\left(x\right)\right)\psi, \qquad 0 < x < L. \tag{2.30}$$

As before, we use the uniform grid $x_j = jh,\ j = 0, \ldots, J$ with $L = Jh$. From Eq. (2.30) together with the standard second order finite difference operator $\mathrm{D}_h^{\mathrm{std}}$ we find that

$$\begin{aligned} h^2\psi_j^{(iv)} &= h^2 \left.\frac{\mathrm{d}^2}{\mathrm{d}x^2}\psi_{xx}\left(x\right)\right|_{x=x_j} \\ &= h^2\left(-2\left.\frac{\mathrm{d}^2}{\mathrm{d}x^2}\left(\left(E - V\left(x\right)\right)\psi\right)\right|_{x=x_j}\right) \\ &= h^2\left(-2\mathrm{D}_h^{\mathrm{std}}\left(\left(E - V_j\right)\psi_j\right) + \mathcal{O}\left(h^2\right)\right) \\ &= -2\left(E - V_{j+1}\right)\psi_{j+1} + 4\left(E - V_j\right)\psi_j - 2\left(E - V_{j-1}\right)\psi_{j-1} + \mathcal{O}\left(h^4\right). \end{aligned} \tag{2.31}$$

On the other hand, the Taylor series

$$\psi(x \pm h) = \psi(x) \pm h\psi_x(x) + \frac{h^2}{2}\psi_{xx}(x) \pm \frac{h^3}{6}\psi_{xxx}(x) + \frac{h^4}{24}\psi^{(iv)}(x) \pm \frac{h^5}{96}\psi^{(v)}(x) + \mathcal{O}(h^6)$$

gives

$$\psi(x+h) + \psi(x-h) = 2\psi(x) + h^2\psi_{xx}(x) + \frac{h^4}{12}\psi^{(iv)}(x) + \mathcal{O}(h^6),$$

which implies

$$h^2\psi_j^{(iv)} = \frac{12}{h^2}\left(\psi_{j+1} - 2\psi_j + \psi_{j-1}\right) - 12\left.\psi_{xx}(x)\right|_{x=x_j} + \mathcal{O}(h^4).$$

If we apply Eq. (2.30) to the above equation we get

$$h^2\psi_j^{(iv)} = \frac{12}{h^2}\left(\psi_{j+1} - 2\left(1 - \left(E - V_j\right)h^2\right)\psi_j + \psi_{j-1}\right) + \mathcal{O}(h^4). \tag{2.32}$$

A comparison of Eqs. (2.31) and (2.32) gives the Numerov FDS

$$\begin{aligned} \left(1 + \frac{h^2}{6}\left(E - V_{j+1}\right)\right)\psi_{j+1} - 2\left(1 - \frac{5h^2}{6}\left(E - V_j\right)\right)\psi_j \\ + \left(1 + \frac{h^2}{6}\left(E - V_{j-1}\right)\right)\psi_{j-1} = 0, \qquad j = 1, \ldots, J-1. \end{aligned} \tag{2.33}$$

The Numerov FDS is of of fourth order if $\psi \in C^6(0, L)$ compared to second order accuracy of the standard FDS if $\psi \in C^4(0, L)$.

Now we will examine the discrete exterior problem of the Numerov FDS with V constant. We want to determine a solution of the discrete exterior problem in order to apply the DTBCs (2.29).

If V is constant Eq. (2.33) is a linear second order difference equation with constant coefficients whose solution takes the form

$$\psi_j = \hat{\psi}_h\alpha^j = \hat{\psi}_h e^{\mathrm{i}k_h jh}, \tag{2.34}$$

with $\alpha \in \mathbb{C}$. Again we will refer to $\hat{\psi}_h$ as the *discrete amplitude* of the discrete wave ψ_j and

$$k_h = -\mathrm{i}\frac{1}{h}\ln\left(\alpha\right) = \frac{1}{h}\left(\arg\left(\alpha\right) - \mathrm{i}\ln\left|\alpha\right|\right) \tag{2.35}$$

as the *discrete wave vector*. Analogously to the standard FDS we get the discrete solution α by applying Eq. (2.34) to Eq. (2.33). Under the assumption that the energy E satisfies the energy condition (2.7), i.e.

$$E > V,$$

and the step size h satisfies

$$h < \frac{3}{\sqrt{E-V}}, \tag{2.36}$$

α is complex and reads

$$\alpha_{1,2} = 1 - \frac{6\,(E-V)\,h^2}{6+(E-V)\,h^2} \pm \mathrm{i}\frac{\sqrt{24\,(E-V)\,h^2\,(3-(E-V)\,h^2)}}{6+(E-V)\,h^2}. \tag{2.37}$$

The modulus of α is

$$|\alpha_{1,2}| = \left(1 - \frac{6\,(E-V)\,h^2}{6+(E-V)\,h^2}\right)^2 + \frac{24\,(E-V)\,h^2\left(3-(E-V)\,h^2\right)}{\left(6+(E-V)\,h^2\right)^2} = 1.$$

Thus, the discrete wave vector k_h is real and takes the form

$$k_h = \pm\hat{k}_h, \tag{2.38}$$

with the propagation coefficient

$$\hat{k}_h = \frac{1}{h}\arg(\alpha) = \frac{1}{h}\arccos\frac{\operatorname{Re}\alpha}{|\alpha|} = \frac{1}{h}\arccos\left(1 - \frac{6\,(E-V)\,h^2}{6+(E-V)\,h^2}\right).$$

Again we can neglect to add the term $n\frac{2\pi}{h}$, $n \in \mathbb{Z}$, to this formula since for any $n \neq 0$ this term diverges for $h \to 0$. On the other hand, it is easy to show that the discrete wave vector k_h as given in Eq. (2.38), i.e. with $n = 0$, tends to the analytical wave vector k as given in Eq. (2.8) for $h \to 0$ and $\hbar = m^* = 1$. Fig. 2.4 shows the discrete wave vector $\hat{k}_h$ of the Numerov FDS versus the number of grid points $J = 1/h$ compared to the analytical wave vector $\hat{k}$ for an energy $E = 500$ and a potential $V = 0$. Considering that the step size h has to satisfy Eq. (2.36), i.e. $h < 1/13$ in our example, the Numerov FDS overestimates the wave vector for any admissible step size h. Compared to the discrete wave vector of the standard FDS, see Fig. 2.1, the discrete wave vector of the Numerov FDS gives a better approximation of the analytical wave vector.

Hence, we get two traveling waves, the right-traveling wave

$$\psi_j = \alpha_1^j = e^{\mathrm{i}\hat{k}_h jh},$$

and the left-traveling wave

$$\psi_j = \alpha_2^j = e^{-\mathrm{i}\hat{k}_h jh}.$$

On the other hand, if the step size h does not satisfy the step size restriction (2.36) or the energy E does not satisfy the energy condition (2.7), α is real and yields evanescent waves.

Finally, we derive the *discrete dispersion relation* of the Numerov FDS in the same way as for the standard FDS. The wave $\psi_j = \hat{\psi}e^{\mathrm{i}k_h jh}$ implies

$$\psi_{j+1}e^{-\mathrm{i}k_h h} = \psi_j = \psi_{j-1}e^{\mathrm{i}k_h h},$$

and hence, applied to the Numerov difference equation (2.33) we get

$$E = E_h^{\mathrm{Num}}(k) = \frac{6}{5+\cos k_h h}\frac{2}{h^2}\sin^2\frac{k_h h}{2}. \tag{2.39}$$

Now we will prove an analogon to Thm. 2.4.

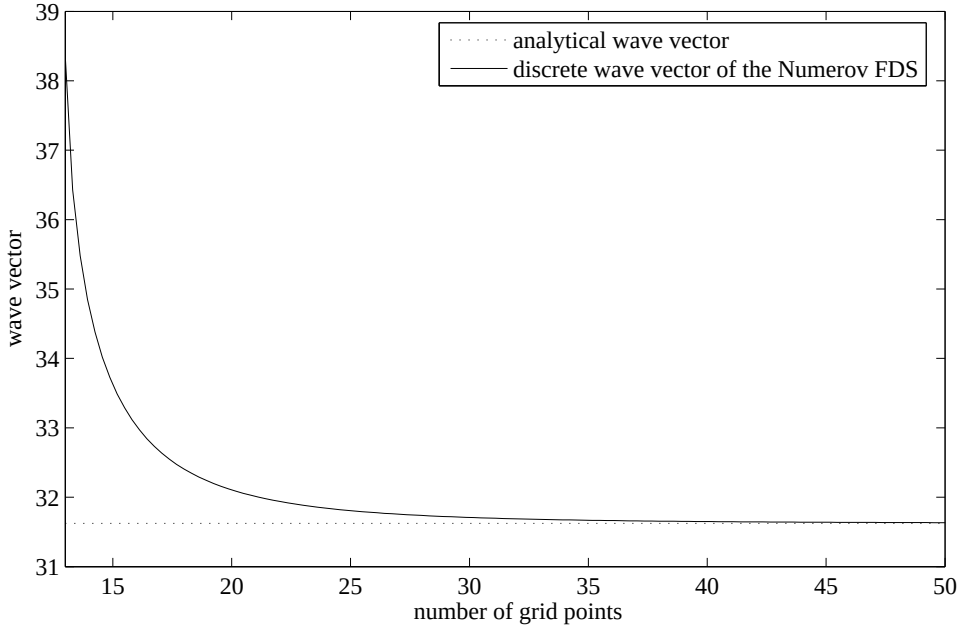

Figure 2.4: Analytical wave vector and discrete wave vector of the Numerov FDS against the number of grid points $J = 1/h$ for an energy $E = 500$ and a potential $V = 0$.

Theorem 2.5. Let $\{V_j\}, j = 0, \ldots, J$, and $E > \max\{0, V_L\}$ be given, and suppose

$$h < \min\left\{\sqrt{\frac{3}{E}}, \sqrt{\frac{3}{E - V_L}}, \sqrt{\frac{6}{|E - V_1|}}, \sqrt{\frac{6}{|E - V_{J-1}|}}, \frac{\pi}{\hat{k}_{h,0}}, \frac{\pi}{\hat{k}_{h,L}}\right\}.$$

Then the discrete BVP (2.33) of the Numerov FDS with the DTBCs (2.29) has a unique solution $\{\psi_j\}, j = 0, \ldots, J$.

Proof. We show that for homogeneous DTBCs the discrete solution is zero at every grid point. Therefore, let us introduce

$$\varphi_j = \sigma_j \psi_j,$$

with $\sigma_j = 1 + \frac{h^2}{6}(E - V_j) \in \mathbb{R}$. Note that $\sigma_j > 0$ for $j = 0, 1, J-1, J$.

Now we can rewrite the Numerov FDS in the form

$$\varphi_{j+1} - 2\varphi_j + \varphi_{j-1} = -2h^2 (E - V_j)\psi_j = -2h^2 (E - V_j)\sigma_j^{-1}\varphi_j,$$

or

$$\mathrm{D}_h^{\mathrm{std}}\varphi_j = -2(E - V_j)\sigma_j^{-1}\varphi_j.$$

The homogeneous left DTBC can be written in the form

$$-\gamma_1\psi_0 + \psi_1 = -\gamma_1\sigma_0^{-1}\varphi_0 + \sigma_1^{-1}\varphi_1,$$

that reduces to

$$\mathrm{D}_h^{\mathrm{bwd}}\varphi_1 = \left(\gamma_1\sigma_1\sigma_0^{-1} - 1\right)\varphi_0,$$

with

$$\gamma_1 = e^{-\mathrm{i}\hat{k}_{h,0}h}.$$

On the other hand, the right DTBC is

$$\psi_{J-1} - \gamma_2\psi_J = \sigma_{J-1}^{-1}\varphi_{J-1} - \gamma_2\sigma_J^{-1}\varphi_J,$$

which becomes

$$\mathrm{D}_h^{\mathrm{bwd}}\varphi_J = \left(\gamma_2^{-1}\sigma_J\sigma_{J-1}^{-1} - 1\right)\varphi_{J-1},$$

with

$$\gamma_2 = e^{-\mathrm{i}\hat{k}_{h,L}h}.$$

Analogously to the proof of Thm. 2.3, we multiply the sum of the Numerov FDS for $j = 1, \ldots, J-1$ by $\bar{\varphi}_j$, apply Lem. 2.2 and take the imaginary part. This gives

$$0 = -\sigma_1\sigma_0^{-1}\operatorname{Im}\gamma_1\left|\varphi_0\right|^2 + \sigma_J\sigma_{J-1}^{-1}\operatorname{Im}\gamma_2^{-1}\left|\varphi_{J-1}\right|^2,$$

with

$$\operatorname{Im}\gamma_1 = -\sin\hat{k}_{h,0}h < 0, \qquad h < \frac{\pi}{\hat{k}_{h,0}},$$

and

$$\operatorname{Im}\gamma_2^{-1} = -\frac{1}{\left|\gamma_2\right|^2}\operatorname{Im}\gamma_2 = \sin\hat{k}_{h,0}h > 0, \qquad h < \frac{\pi}{\hat{k}_{h,L}}.$$

Hence, we end up with the equation

$$0 = \sigma_1\sigma_0^{-1}\sin\hat{k}_{h,0}h\left|\varphi_0\right|^2 + \sigma_J\sigma_{J-1}\sin\hat{k}_{h,L}h\left|\varphi_{J-1}\right|^2.$$

Since $\sigma_j > 0$ for $j = 0, 1, J-1, J$, the above equation implies $\left|\varphi_0\right|^2 = \left|\varphi_{J-1}\right|^2 = 0$. Thus, $\psi_0 = \psi_{J-1} = 0$ and by using the homogeneous DTBCs we get $\psi_1 = 0$ and $\psi_J = 0$. Successively applying the Numerov FDS gives $\psi_j = 0$ for $j = 0, \ldots, J$ and hence, the discrete solution vanishes at every grid point if the DTBCs are homogeneous. Thus, the coefficient matrix of the system of linear equations formed by the discrete BVP and the two DTBCs is regular. This implies that the discrete solution is unique. □

Let us recall the numerical example in Sec. 2.5. When using the standard FDS we observed a phase error yielding a smaller discrete wave length than the analytical wave length. This is also the case for the Numerov FDS but the error is significantly smaller so that the discrete solution coincides with the analytical solution for the step size $h = 1/100$ and the used level of detail in Fig. 2.3.

2.6.2 The Mickens Discretization

We recall the Schrödinger equation (2.1)

$$\psi_{xx} + 2\left(E - V\left(x\right)\right)\psi = 0, \qquad 0 < x < L. \tag{2.40}$$

Let us assume that the potential $V\left(x\right) \equiv V$ is constant. As shown in Sec. 2.1 the Schrödinger equation (2.40) yields a traveling wave if $E > V$ and an evanescent wave otherwise. Hence, in the case $2\left(E - V\right) \equiv c_1 > 0$, Eq. (2.40) has the solution

$$\psi\left(x\right) = a_1\cos\left(\sqrt{c_1}x\right) + b_1\sin\left(\sqrt{c_1}x\right), \tag{2.41a}$$

and if $2\left(E - V\right) \equiv -c_2 < 0$, Eq. (2.40) has the solution

$$\psi\left(x\right) = a_2\cosh\left(\sqrt{c_2}x\right) + b_2\sinh\left(\sqrt{c_2}x\right), \tag{2.41b}$$

where $a_1, a_2, b_1, b_2 \in \mathbb{C}$ are arbitrary constants. The *Mickens nonstandard finite difference discretization*

$$\psi_{j+1} - 2\cos\left(h\sqrt{c_1}\right)\psi_j + \psi_{j-1} = 0, \qquad j = 1, \ldots, J-1, \tag{2.42a}$$

if $E > V$, and

$$\psi_{j+1} - 2\cosh\left(h\sqrt{c_2}\right)\psi_j + \psi_{j-1} = 0, \qquad j = 1, \ldots, J-1, \tag{2.42b}$$

if $E \leq V$, is a so-called *exact FDS* of Eq. (2.40) with the solutions (2.41), cf. [29]. An FDS is said to be *exact* if the numerical solution equals the analytical solution at the grid points, see [27]. It is easy to see that if V is constant the difference equation (2.42a) has the solution (2.41a) whereas the difference equation (2.42b) has the solution (2.41b). Therefore, the Mickens FDS gives a numerical solution that is equal to the analytical solution at the grid points, in other words, the Mickens FDS is exact.

Now we allow the potential $V(x)$ to vary inside the computational domain $(0, L)$. The Mickens FDS (2.42) becomes

$$\psi_{j+1} - 2D_j\psi_j + \psi_{j-1} = 0, \qquad j = 1, \ldots, J-1, \tag{2.43}$$

with

$$D_j = \begin{cases} \cos\left(h\sqrt{2\left(E - V_j\right)}\right), & E > V_j, \\ \cosh\left(h\sqrt{2\left(V_j - E\right)}\right), & E \leq V_j. \end{cases}$$

While the Mickens FDS (2.43) is exact for a constant potential V it is formally of order $\mathcal{O}(h^2)$ if the potential V is not constant, cf. [15].

In order to use the DTBCs for the Mickens FDS (2.43) we have to determine a discrete solution of the Mickens FDS in the exterior domains. The Mickens FDS is exact in the exterior domains since the potential V is assumed to be constant in these domains. Hence, the discrete solution is given by the analytical solution as derived in Sec. 2.1. The discrete wave vector k_h of the Mickens FDS is equal to the analytical wave vector k as given in Eq. (2.8), and the discrete dispersion relation $E_h^{\mathrm{Mic}}(\hat{k})$ is equal to the analytical dispersion relation (2.13).

Theorem 2.6. Let $\{V_j\}, j = 0, \ldots, J$, and $E > \max\{0, V_L\}$ be given, and assume $h < \min\left\{\frac{\pi}{\hat{k}_{h,0}}, \frac{\pi}{\hat{k}_{h,L}}\right\}$. Then the discrete BVP (2.42) of the Mickens FDS with the DTBCs (2.29) has a unique solution $\{\psi_j\}, j = 0, \ldots, J$.

Proof. Let us rewrite the Mickens FDS in the form

$$\mathrm{D}_h^{\mathrm{std}}\psi_j = -\frac{2}{h^2}\left(1 - D_j\right)\psi_j.$$

Since $-\frac{2}{h^2}\left(1 - D_j\right) \in \mathbb{R}$ for all $j = 1, \ldots, J-1$, it becomes clear that this theorem is a direct corollary of Thm. 2.4 and hence, the solution is unique. □

Since this scheme is exact for a constant potential, the Mickens FDS using DTBCs does not give an error when applied to the numerical example we introduced in Sec. 2.5. Later we will analyze its numerical behavior for non-constant potentials V and compare it to the other FDSs.

2.6.3 The Numerov-Mickens Discretization

Chen et al. [15] combined the Numerov discretization with the Mickens discretization and proposed the so-called *combined Numerov-Mickens finite-difference scheme*

$$\left(1 + \frac{h^2}{6}\left(E - V_{j+1}\right)\right)\psi_{j+1} - 2D_j\psi_j + \left(1 + \frac{h^2}{6}\left(E - V_{j-1}\right)\right)\psi_{j-1} = 0, \tag{2.44}$$

for $j = 1, \ldots, J-1$, with

$$D_j = \begin{cases} \cos\left(h\sqrt{2\left(E - V_j\right)}\right), & E > V_j, \\ \cosh\left(h\sqrt{2\left(V_j - E\right)}\right), & E \leq V_j. \end{cases}$$

It can be shown that the Numerov-Mickens FDS (2.44) is of order $\mathcal{O}\left(h^4\right)$, just as the Numerov FDS, and that it is an exact FDS if the potential V is constant, just as the Mickens FDS, cf. [15].

Let us now study the discrete exterior problem of the Numerov-Mickens FDS with a constant potential V. If V is constant Eq. (2.44) is a linear second order difference equation with constant coefficients whose solution takes the form

$$\psi_j = \hat{\psi}_h \alpha^j = \hat{\psi}_h e^{\mathrm{i}k_h jh}, \tag{2.45}$$

with $\alpha \in \mathbb{C}$, the *discrete amplitude* ψ_j and the *discrete wave vector*

$$k_h = -\mathrm{i}\frac{1}{h}\ln(\alpha) = \frac{1}{h}\left(\arg(\alpha) - \mathrm{i}\ln|\alpha|\right). \tag{2.46}$$

By applying Eq. (2.45) to Eq. (2.44) and under the assumption that the energy E satisfies the energy condition (2.7), i.e.

$$E > V,$$

α is complex and reads

$$\alpha_{1,2} = \frac{\cos\left(h\sqrt{2(E-V)}\right)}{1+h^2(E-V)/6} \pm \mathrm{i}\sqrt{1 - \frac{\cos^2\left(h\sqrt{2(E-V)}\right)}{\left(1+h^2(E-V)/6\right)^2}}. \tag{2.47}$$

Note that the step size h has to satisfy

$$\cos^2\left(h\sqrt{2(E-V)}\right) < \left(1+h^2(E-V)/6\right)^2. \tag{2.48}$$

But this condition is fulfilled for any step size $h > 0$ since the left hand side of Eq. (2.48) is in $[0,1]$, while the right hand side is always greater than 1. It is easy to show that $|\alpha| = 1$ and hence, the discrete wave vector k_h of the Numerov-Mickens FDS is real and reads

$$k_h = \pm\hat{k}_h, \tag{2.49}$$

with

$$\hat{k}_h = \frac{1}{h}\arg(\alpha) = \frac{1}{h}\arccos\frac{\mathrm{Re}\,\alpha}{|\alpha|} = \frac{1}{h}\arccos\frac{\cos\left(h\sqrt{2(E-V)}\right)}{1+h^2(E-V)/6} \in (0,\pi).$$

Again we shall neglect to add the term $n\frac{2\pi}{h}$, $n \in \mathbb{Z}$, to this formula since for any $n \neq 0$ this term diverges for $h \to 0$. However, the limit for $h \to 0$ of the discrete wave vector k_h as given in Eq. (2.49), i.e. with $n = 0$, is undefined. For an energy $E = 500$ and a potential $V = 0$ Fig. 2.5 shows the discrete wave vector $k_h = \hat{k}_h$ against the number of grid points $J = 1/h$. The value of the analytical wave vector for $E = 500$ and $V = 0$ is $k = \sqrt{2(E-V)} \approx 31.6$.

This illustrates the bad numerical behavior of the Numerov-Mickens FDS. Nevertheless, we will continue to analyze this FDS and formulate DTBCs with the right-traveling wave

$$\psi_j = \alpha_1^j = e^{\mathrm{i}\hat{k}jh},$$

and the left-traveling wave

$$\psi_j = \alpha_2^j = e^{-\mathrm{i}\hat{k}jh}.$$

An explicit formula of the *discrete dispersion relation* of the Numerov-Mickens FDS cannot be derived. However, the discrete wave $\psi_j = \hat{\psi}e^{\mathrm{i}k_h jh}$ implies

$$\psi_{j+1}e^{-\mathrm{i}kh} = \psi_j = \psi_{j-1}e^{\mathrm{i}kh}.$$

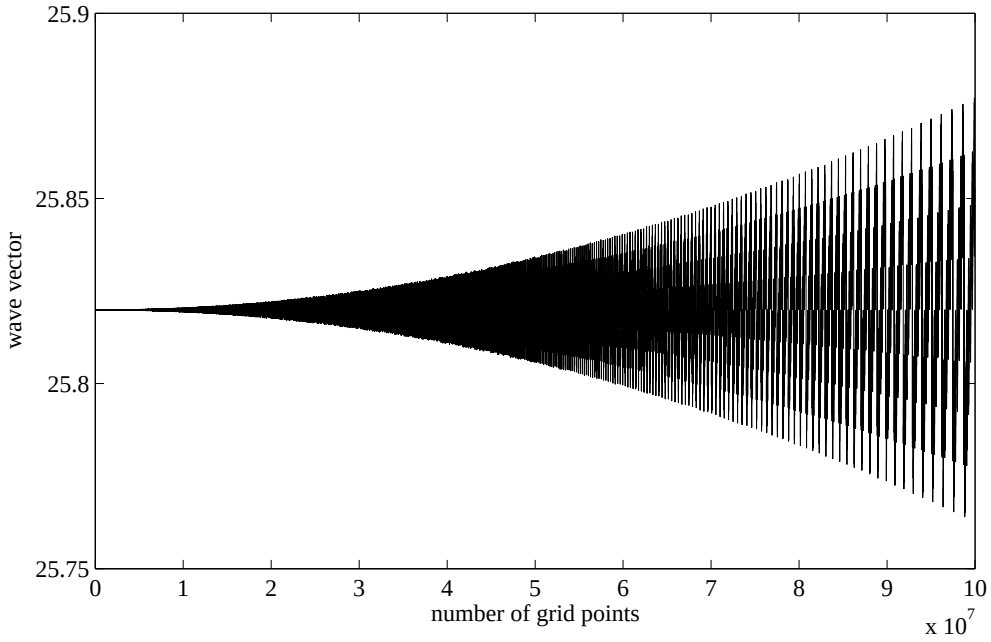

Figure 2.5: Discrete wave vector of the Numerov-Mickens FDS against the number of grid points $J = 1/h$ for an energy $E = 500$ and a potential $V = 0$. The analytical wave vector is $k = \sqrt{2\,(E - V)} \approx 31.6$.

Applied to the difference equation (2.44) we get

$$\cos\left(h\sqrt{2\left(E_h^{\mathrm{NumMic}} - v\right)}\right) - \left(\frac{h^2}{6}\cos kh\right)\left(E_h^{\mathrm{NumMic}} - V\right) - \cos kh = 0. \tag{2.50}$$

By numerically evaluating Eq. (2.50) for $h = 1/100$ and $V = 0$ with the MATLAB procedure `fsolve` using the tolerance 10^{-9}, we obtain the discrete dispersion relation E_h^{NumMic} as shown in Fig. 2.7.

Although the bad numerical behavior has been illustrated we shall prove

Theorem 2.7. Let $\{V_j\}, j = 0, \ldots, J$, and $E > \max\{0, V_L\}$ be given, and assume

$$h < \min\left\{\sqrt{\frac{6}{|E - V_1|}}, \sqrt{\frac{6}{|E - V_{J-1}|}}, \frac{\pi}{\hat{k}_{h,0}}, \frac{\pi}{\hat{k}_{h,L}}\right\}.$$

Then the discrete BVP (2.44) of the combined Numerov-Mickens FDS with the DTBCs (2.29) has a unique solution $\{\psi_j\}, j = 0, \ldots, J$.

Proof. Let us introduce

$$\varphi_j = \sigma_j \psi_j,$$

with $\sigma_j = 1 + \frac{h^2}{6}(E - V_j) \in \mathbb{R}$. Note that $\sigma_j > 0$ for $j = 0, 1, J-1, J$.

We rewrite the Numerov-Mickens FDS in the form

$$\mathrm{D}_h^{\mathrm{std}}\varphi_j = -\frac{2}{h^2}\left(1 - \sigma_j^{-1} D_j\right)\varphi_j.$$

Since $-\frac{2}{h^2}\left(1 - \sigma_j^{-1} D_j\right) \in \mathbb{R}$ for all $j = 1, \ldots, J-1$, it becomes clear that this theorem is a direct corollary of Thm. 2.5 and hence, the solution is unique. □

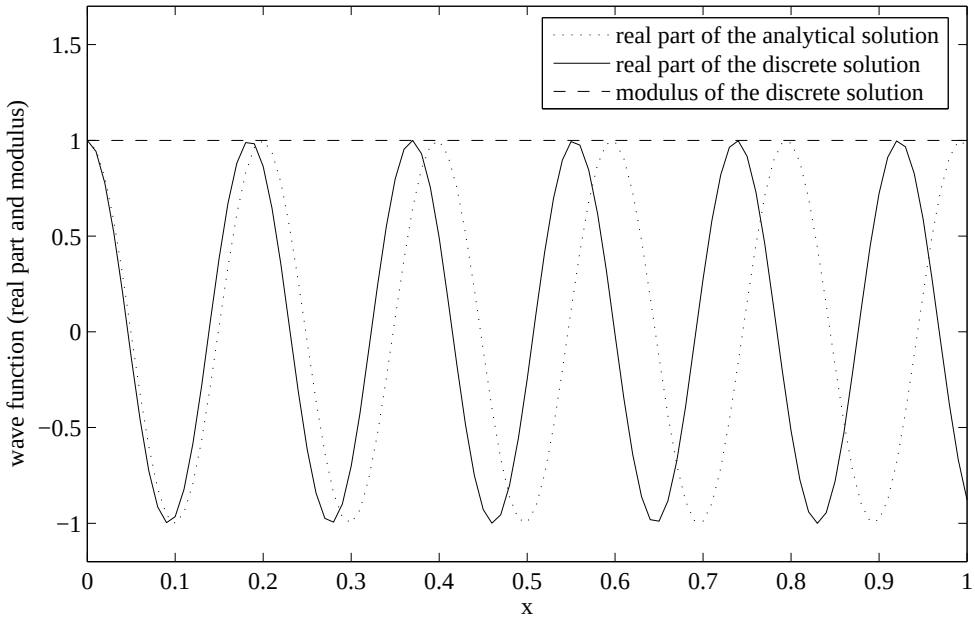

(a) Real parts of the analytical (dotted line) and discrete (solid line) solutions and modulus (dashed line) of the discrete solution, which coincides with the modulus of the analytical solution.

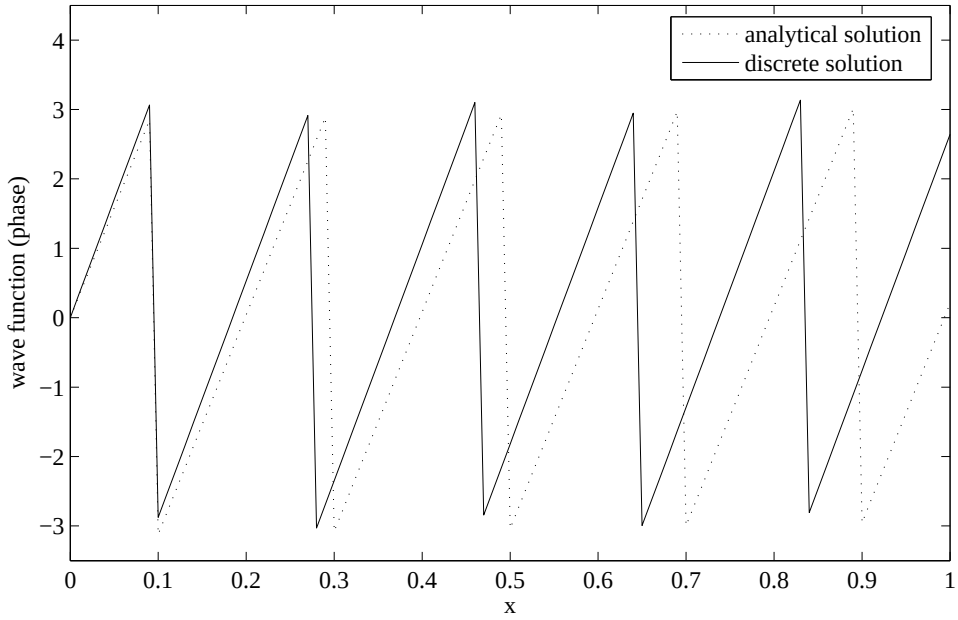

(b) Phases of the analytical (dotted line) and discrete (solid line) solutions.

Figure 2.6: Comparison of the analytical solution $\psi(x) = e^{\mathrm{i}\hat{k}x}$ and the discrete solution of the combined Numerov-Mickens FDS using DTBCs for a step size $h = 1/100$, an energy $E = 500$ and a potential $V \equiv 0$.

The bad numerical properties of Numerov-Mickens FDS that were shown by examining the limit of the discrete wave vector k_h can also be observed when applying the Numerov-Mickens FDS with corresponding DTBCs to the numerical example in Sec. 2.5. Fig. 2.6(a) shows that the modulus of the discrete solution is coincides with the modulus of the analytical solution as it did for the other FDSs, but the phase of the discrete solution differs significantly from the phase of the analytical solution, see Fig. 2.6(b). This results in a significantly smaller wave length of the real part of the discrete solution than the wave length of the real part of the analytical solution, see Fig. 2.6(a).

2.6.4 Comparison of the Discrete Dispersion Relations

In the previous sections we introduced FDSs for the BVP (2.17) and derived the corresponding discrete dispersion relations. Now we want to compare these discrete dispersion relations with the analytical quantum mechanical dispersion relation (2.13). Fig. 2.7 shows the analytical and discrete dispersion relations for a step size $h = 1/100$ and a potential $V = 0$.

All discrete dispersion relations except the dispersion relation of the Mickens FDS are periodic in the wave vector k_h with the period $\frac{2\pi}{h} \approx 628$. We can see that for small values of the wave vector, i.e. $k_h < 100$, the dispersion relation of the Numerov FDS coincides with the analytical dispersion relation for the used level of detail in Fig. 2.7, while the dispersion relation of the combined Numerov-Mickens FDS differs significantly from the analytical dispersion relation. Particularly, for $E = 500$, the value of the energy we used in our examples, the error of the dispersion relation of the Numerov-Mickens FDS is greater than of the other FDSs. This explains the significantly greater phase error of the Numerov-Mickens FDS we observed in Sec. 2.6.3.

2.7 Numerical Examples

2.7.1 The Single Barrier Potential

In this section we analyze the results of the four introduced FDSs in the case of a single barrier potential. We consider a semiconductor of length L composed of two different materials, e.g. GaAs (gallium arsenide) and AlGaAs (aluminium gallium arsenide), where the latter is built between two parts of the first material. Let $0 < x_1 < x_2 < L$ and let the domain $[x_1, x_2)$ be composed of AlGaAs, while the two outer domains $[0, x_1)$ and $[x_2, L]$ are composed of GaAs. $V(x) = E_c(x)$ describes the band edge profile or the variation of the conduction band edge of the semiconductor materials. We call $V_0 = \Delta E_c = E_c|_{\text{AlGaAs}} - E_c|_{\text{GaAs}}$ *band edge offset* between the semiconductor materials or band edge discontinuity of the material interface. The inner domain $[x_1, x_2)$ is called *quantum barrier* if its potential $V(x) = E_c|_{\text{AlGaAs}}$ is greater than the potential $V(x) = E_c|_{\text{GaAs}}$ of the outer domains and *quantum well* if it is smaller.

For simplicity we set $E_c|_{\text{GaAs}} = 0$ and we assume that $E_c|_{\text{AlGaAs}} = 500$, i.e. the band edge offset is $V_0 = \Delta E_c = 500$ and we have a quantum barrier at $x_1 \leq x < x_2$. Furthermore, we set $L = 1$, $x_1 = 1/3$ and $x_2 = 2/3$. Fig. 2.8 illustrates the band edge profile.

For a single barrier potential the BVP (2.17) can be solved analytically, cf. [21]. Since the potential V is constant in the three domains $[0, x_1)$, $[x_1, x_2)$ and $[x_2, L]$ and by assuming that the energy E satisfies

$$E > \max\{ E_c|_{\text{GaAs}}, E_c|_{\text{AlGaAs}}\} = V_0 = 500,$$

the wave function takes the form

$$\psi(x) = ae^{\mathrm{i}\hat{k}x} + be^{-\mathrm{i}\hat{k}x}, \tag{2.51}$$

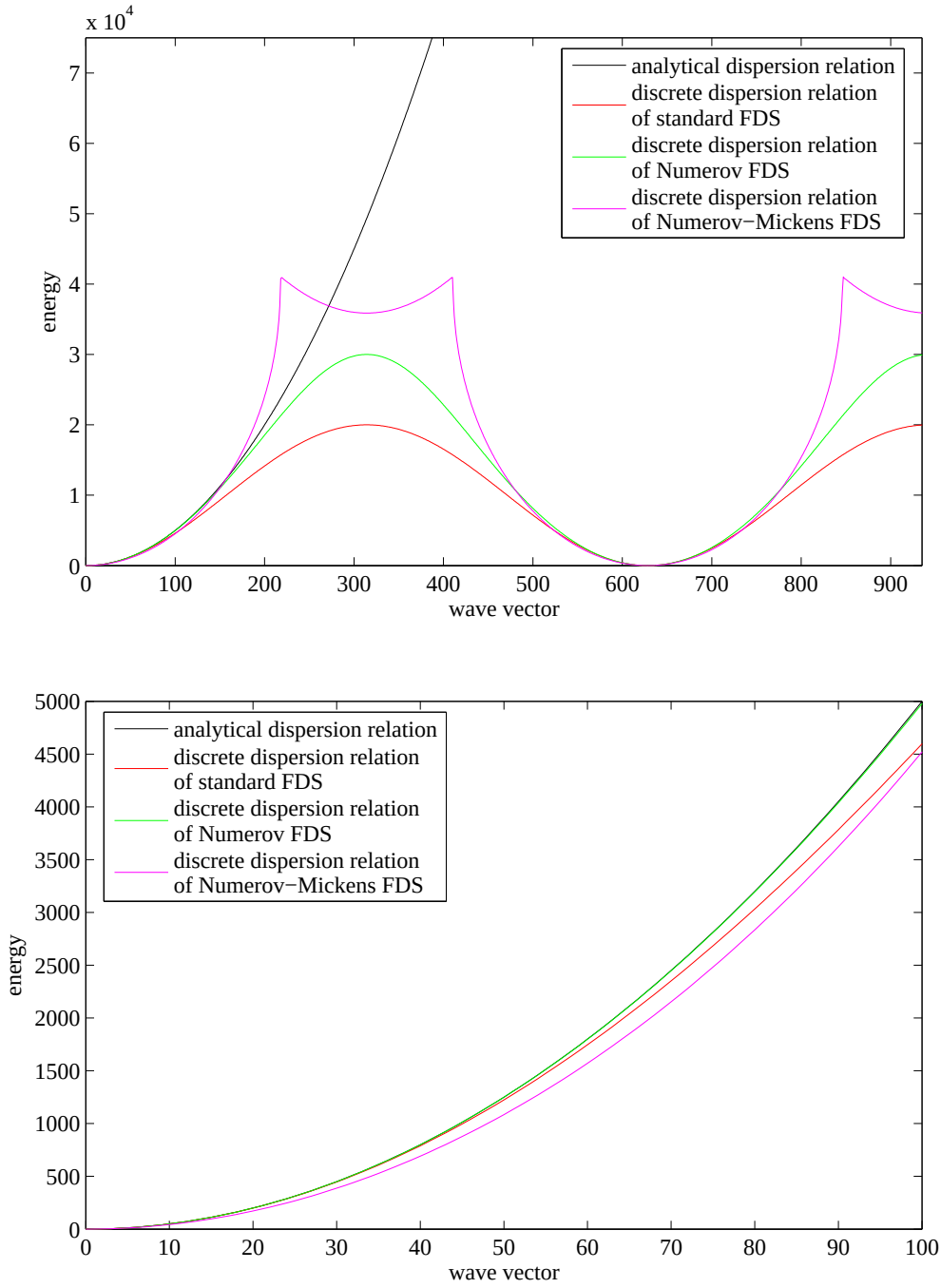

Figure 2.7: Analytical quantum mechanical dispersion relation $E(k)$ (black), the discrete dispersion relation of the standard discretization $E_h^{\mathrm{std}}(k_h)$ (red), the discrete dispersion relation of the Numerov discretization $E_h^{\mathrm{Num}}(k_h)$ (green) and the discrete dispersion relation of the combined Numerov-Mickens discretization $E_h^{\mathrm{NumMic}}(k_h)$ (magenta) for the step size $h = 1/100$. Note that the discrete dispersion relation of the Mickens discretization $E_h^{\mathrm{Mic}}(k_h)$ coincides with the analytical quantum mechanical dispersion relation $E(k)$.

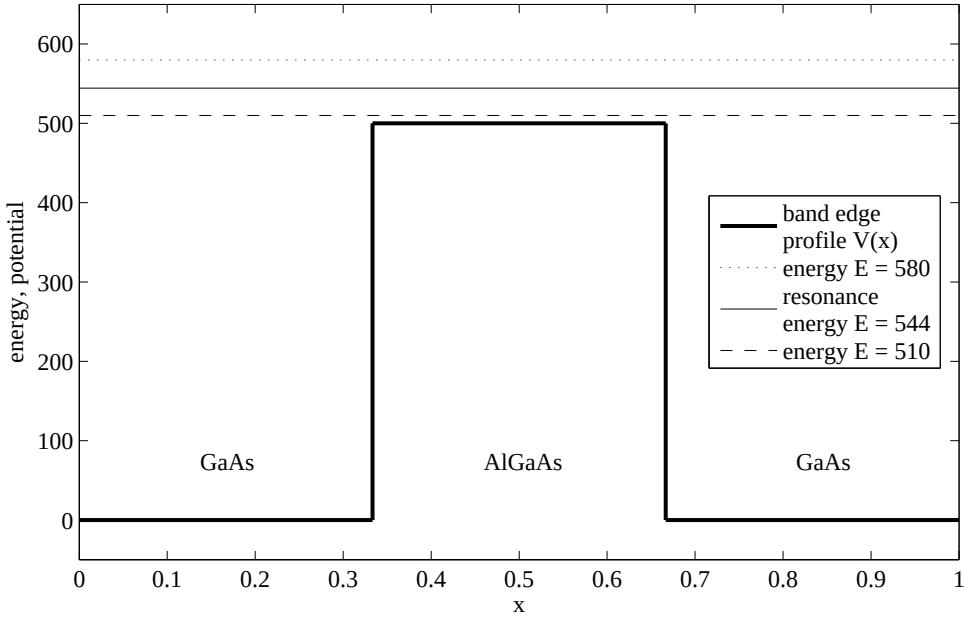

Figure 2.8: Band edge profile $V(x)$ and energies $E = 510$, $E = 544$, i.e. the first resonance state, and $E = 580$

where the amplitudes a and b are constant in each domain and the wave vector reads

$$\hat{k} = \hat{k}(0) = \sqrt{2E}, \qquad \text{if } x \in [0, x_1) \cup [x_2, L],$$

and

$$\hat{k} = \hat{k}(V_0) = \sqrt{2\,(E - V_0)}, \qquad \text{if } x \in [x_1, x_2).$$

Let us assume that a right-traveling wave with amplitude $\hat{\psi} = 1$ enters the semiconductor at $x = 0$. Since $V(x) = 0$ for $x \in [0, x_1)$, i.e. the same physical properties as in the exterior domain $x < 0$, the incoming wave is not reflected but completely transmitted into the domain $[0, x_1)$. At the boundary of the two materials at $x = x_1$ the wave is partly reflected. On the other hand, in the domain $[x_2, L]$ we expect a transmitted, right-traveling wave that leaves the semiconductor at $x = L$. For the same reason as at $x = 0$ we do not expect any reflections of the transmitted wave at $x = L$. Thus, the wave function reads

$$\psi(x) = \begin{cases} e^{\mathrm{i}\sqrt{2E}x} + re^{-\mathrm{i}\sqrt{2E}x}, & \text{if } x \in [0, x_1), \\ ae^{\mathrm{i}\sqrt{2(E-V_0)}x} + be^{-\mathrm{i}\sqrt{2(E-V_0)}x}, & \text{if } x \in [x_1, x_2), \\ te^{\mathrm{i}\sqrt{2E}x}, & \text{if } x \in [x_2, L], \end{cases} \tag{2.52}$$

cf. (2.51).

On the other hand, if the energy E satisfies $0 < E \leq V_0$, the waves in the domain $[x_1, x_2)$ are evanescent and take the form

$$\psi(x) = ae^{\check{k}x} + be^{-\check{k}x},$$

with

$$\check{k} = \check{k}(V_0) = \sqrt{2\,(V_0 - E)}.$$

But since $\check{k} = \mathrm{i}\hat{k}$ for $E \leq V$, Eq. (2.52) is the correct analytical solution also for the case $0 < E \leq V_0$. Hence, we can continue with the solution as given in Eq. (2.52) without having to neglect the case $0 < E \leq V_0$ in our numerical examples.

According to [24], the wave function $\psi(x)$ and its derivative

$$\psi_x(x) = \begin{cases} \mathrm{i}\sqrt{2E}e^{\mathrm{i}\sqrt{2E}x} - \mathrm{i}\sqrt{2E}re^{-\mathrm{i}\sqrt{2E}x}, & \text{if } x \in [0, x_1), \\ \mathrm{i}\sqrt{2\left(E-V_0\right)}ae^{\mathrm{i}\sqrt{2(E-V_0)}x} - \mathrm{i}\sqrt{2\left(E-V_0\right)}be^{-\mathrm{i}\sqrt{2(E-V_0)}x}, & \text{if } x \in [x_1, x_2), \\ \mathrm{i}\sqrt{2E}te^{\mathrm{i}\sqrt{2E}x}, & \text{if } x \in [x_2, L], \end{cases}$$

are continuous. In particular, they are continuous at the material interfaces at $x = x_1$ and $x = x_2$. Thus, we get a system of linear equation that yields

$$\begin{aligned} r &= \frac{-2\mathrm{i}\left(\sqrt{2\left(E-V_0\right)}^2 - \sqrt{2E}^2\right)e^{2\mathrm{i}\sqrt{2E}x_1}\sin\left(\sqrt{2\left(E-V_0\right)}(x_1-x_2)\right)}{\left(\sqrt{2\left(E-V_0\right)}+\sqrt{2E}\right)^2 e^{\mathrm{i}\sqrt{2(E-V_0)}(x_1-x_2)} - \left(\sqrt{2\left(E-V_0\right)}-\sqrt{2E}\right)^2 e^{-\mathrm{i}\sqrt{2(E-V_0)}(x_1-x_2)}} \\ a &= \frac{2\sqrt{2E}\left(\sqrt{2\left(E-V_0\right)}+\sqrt{2E}\right)e^{\mathrm{i}\left(\sqrt{2E}x_1-\sqrt{2(E-V_0)}x_2\right)}}{\left(\sqrt{2\left(E-V_0\right)}+\sqrt{2E}\right)^2 e^{\mathrm{i}\sqrt{2(E-V_0)}(x_1-x_2)} - \left(\sqrt{2\left(E-V_0\right)}-\sqrt{2E}\right)^2 e^{-\mathrm{i}\sqrt{2(E-V_0)}(x_1-x_2)}} \\ b &= \frac{2\sqrt{2E}\left(\sqrt{2\left(E-V_0\right)}-\sqrt{2E}\right)e^{\mathrm{i}\left(\sqrt{2E}x_1+\sqrt{2(E-V_0)}x_2\right)}}{\left(\sqrt{2\left(E-V_0\right)}+\sqrt{2E}\right)^2 e^{\mathrm{i}\sqrt{2(E-V_0)}(x_1-x_2)} - \left(\sqrt{2\left(E-V_0\right)}-\sqrt{2E}\right)^2 e^{-\mathrm{i}\sqrt{2(E-V_0)}(x_1-x_2)}} \\ t &= \frac{4\sqrt{2\left(E-V_0\right)}\sqrt{2E}e^{\mathrm{i}\sqrt{2E}(x_1-x_2)}}{\left(\sqrt{2\left(E-V_0\right)}+\sqrt{2E}\right)^2 e^{\mathrm{i}\sqrt{2(E-V_0)}(x_1-x_2)} - \left(\sqrt{2\left(E-V_0\right)}-\sqrt{2E}\right)^2 e^{-\mathrm{i}\sqrt{2(E-V_0)}(x_1-x_2)}}. \end{aligned} \tag{2.53}$$

This implies that the reflection and transmission coefficients satisfy

$$|r|^2 + |t|^2 = 1. \tag{2.54}$$

Note that the solution of the so-called *transfer-matrix method* coincides with the analytical solution in the case of a single barrier potential, cf. [36].

Since we have three domains of the same length the step size h has to be of the form $h = \frac{1}{3n}$ with $n = 1, 2, \ldots$, so that the discretized domains also have the same length. Otherwise the FDSs would not solve the problem as stated above and the results would differ significantly from the analytical solution.

2.7.1.1 The Transmission Coefficient

First we want to examine the behavior of the transmission coefficient $\tau = |t|$ against the energy E for a given edge band offset V_0. In Fig. 2.9 the analytical transmission coefficient τ is compared with the transmission coefficient of the combined Numerov-Mickens FDS. The transmission coefficients of the standard FDS, the Numerov FDS and the Mickens FDS coincide with the analytical transmission coefficient for the level of detail of Fig. 2.9. In order to evaluate the numerical transmission coefficients we take the modulus of the numerical solution at the right boundary at $x = L$. This straightforward procedure is possible since the transmitted wave is not reflected at the boundary $x = L$ and hence, the modulus of the numerical solutions is constant behind the barrier. Therefore, the modulus in this domain equals the transmission coefficients of the numerical schemes.

If $|\tau| = 1$, i.e. there is no reflection and the wave is transmitted completely, we say that there is a *resonance*. The first resonance of the analytical transmission coefficient is located at $E = E_{\text{resonance}} \approx 544$.

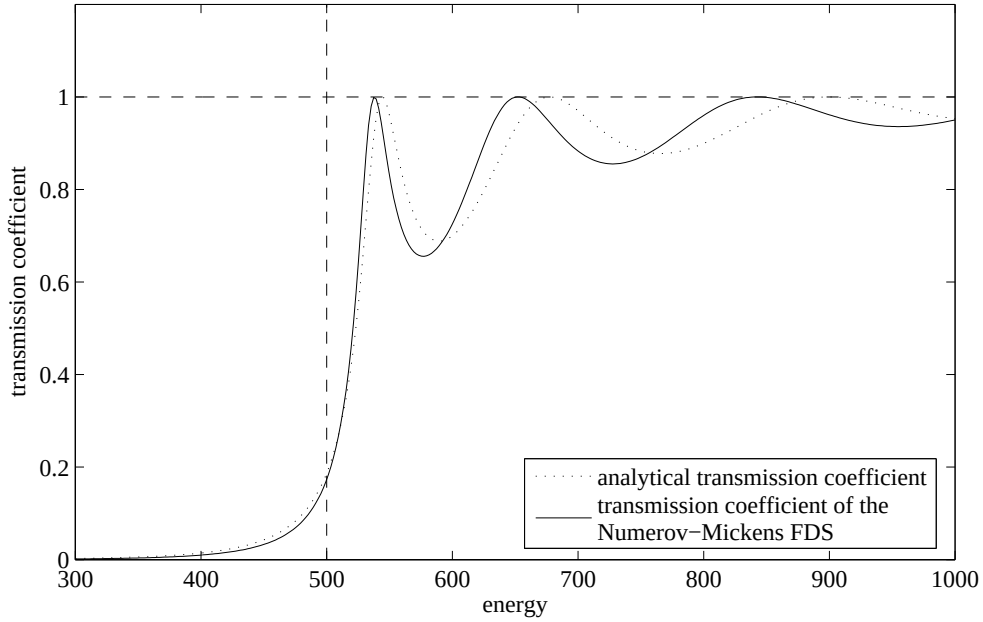

Figure 2.9: Analytical transmission coefficient (dotted line) and the transmission coefficient of the combined Numerov-Mickens FDS (solid line) for the step size $h = 1/300$. The transmission coefficients of the standard FDS, the Numerov FDS and the Mickens FDS coincide with the analytical transmission coefficient for the used level of detail.

2.7.1.2 Numerical Solutions of the Wave Function

In this section we want to compare the numerical results for three different values of the energy E. We choose the resonance energy $E = 544$, one smaller energy ($E = 510$) and one greater energy ($E = 580$), see Fig. 2.8. Figs. 2.10–2.12 show a comparison of the modulus and the phases of the the analytical solution and the solutions of the four FDSs for the step size $h = 1/300$. Note that the results of the Numerov FDS and the Mickens FDS coincide with the results of the standard FDS for the used level of detail in Figs. 2.10–2.12.

For all three energy states the standard FDS, the Numerov FDS and the Mickens FDS give reasonable results while the combined Numerov-Mickens FDS leads to a significant error.

2.7.1.3 The L^2-Error

Next we want to investigate the numerical error of the introduced FDSs for the single barrier problem. The evaluation of the discrete L^2-error, however, is not straightforward for a complex function. Since the numerical results of a stationary problem such as the BVP (2.17) has an arbitrary phase, we have to optimize the L^2-error with respect to a phase offset $\varphi \in [-\pi, \pi]$. In other words we have to solve the nonlinear problem

$$\Delta\psi_h^{\min} = \min_{\varphi\in[-\pi,\pi]} \Delta\psi_h = \min_{\varphi\in[-\pi,\pi]} \frac{1}{J+1}\sqrt{\sum_{j=0}^{J} |\psi(x_j) - \psi_h(x_j)e^{\mathrm{i}\varphi}|^2}, \tag{2.55}$$

where ψ denotes the analytical solution and ψ_h is the numerical solution using the step size $h = 1/J$. Fig. 2.13 shows the L^2-error $\Delta\psi_{300}$ of the standard FDS against the phase offset φ for the resonance energy $E = E_{\text{resonance}} \approx 544$ and the step size $h = 1/300$. In order to evaluate the minimal L^2-error $\Delta\psi_h^{\min}$ we discretize the domain $[-\pi, \pi]$ with a step size $h_\varphi = 2\pi/1000$ and analyze the L^2-error $\Delta\psi_h$ at every grid point. However, it is unclear why nonlinear optimization

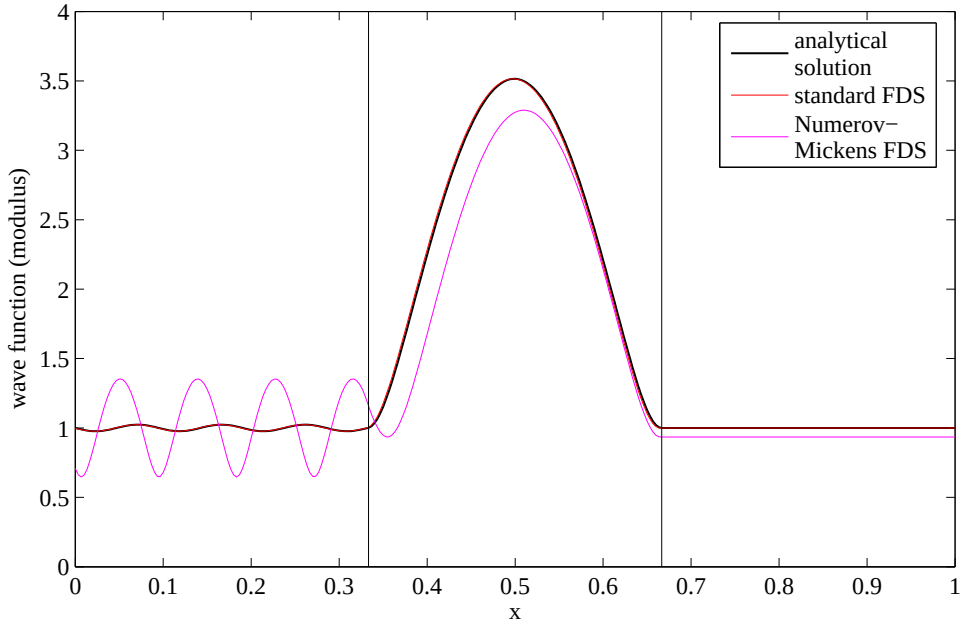

(a) Modulus of the analytical and numerical solutions.

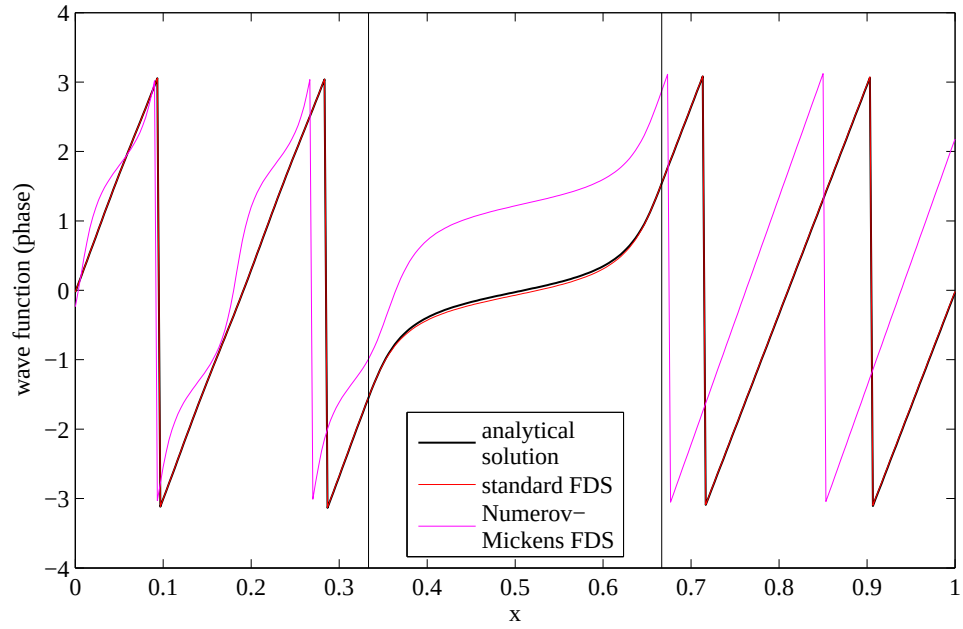

(b) Phases of the analytical and numerical solutions.

Figure 2.10: Comparison of the analytical solution (black) of the single barrier problem and the solutions of the standard FDS (red) and the combined Numerov-Mickens discretization (magenta) for the step size $h = 1/300$ and the resonance energy $E = E_{\text{resonance}} \approx 544$. Note that the results of the Numerov FDS and the Mickens FDS coincide with the results of the standard FDS for the used level of detail.

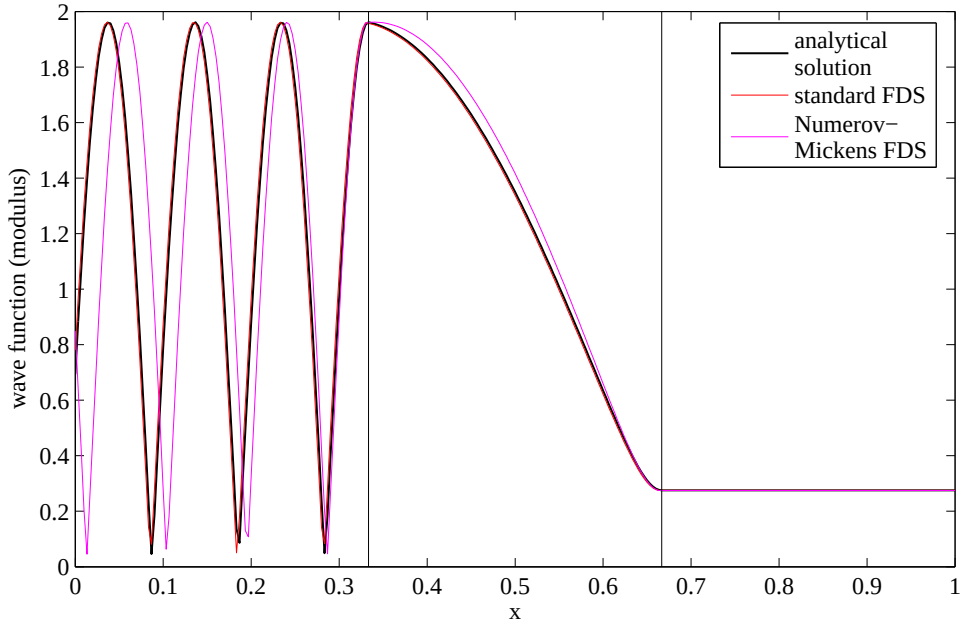

(a) Modulus of the analytical and numerical solutions.

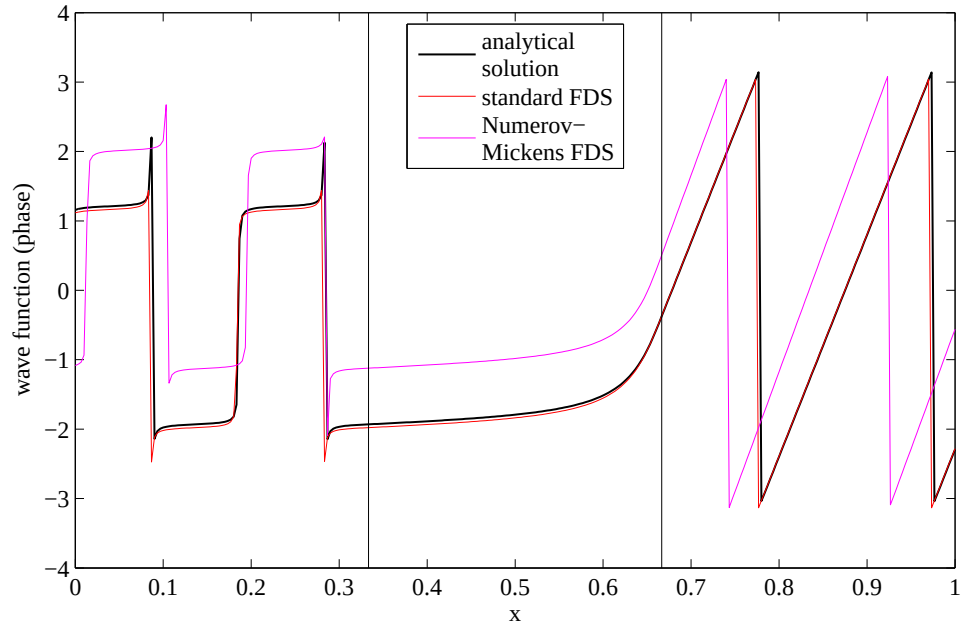

(b) Phases of the analytical and numerical solutions.

Figure 2.11: Comparison of the analytical solution (black) of the single barrier problem and the solutions of the standard FDS (red) and the combined Numerov-Mickens discretization (magenta) for the step size $h = 1/300$ and the energy $E = 510$. Note that the results of the Numerov FDS and the Mickens FDS coincide with the results of the standard FDS for the used level of detail.

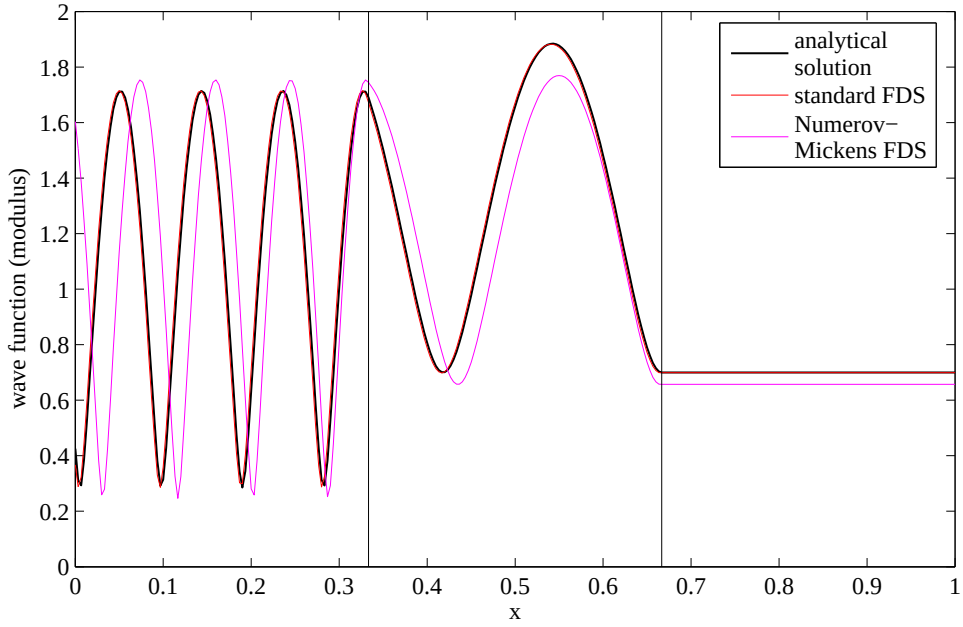

(a) Modulus of the analytical and numerical solutions.

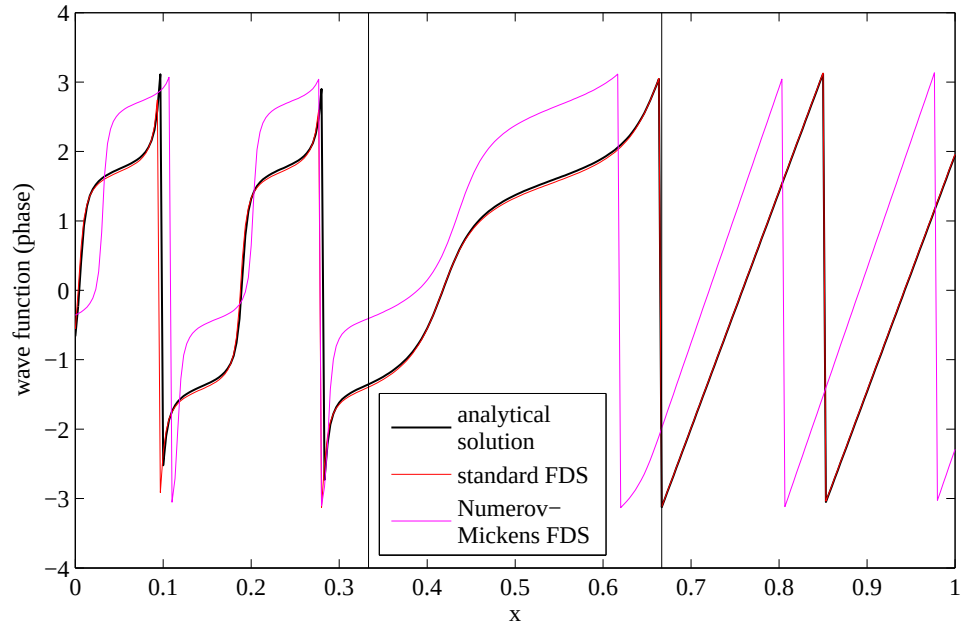

(b) Phases of the analytical and numerical solutions.

Figure 2.12: Comparison of the analytical solution (black) of the single barrier problem and the solutions of the standard FDS (red) and the combined Numerov-Mickens discretization (magenta) for the step size $h = 1/300$ and the energy $E = 580$. Note that the results of the Numerov FDS and the Mickens FDS coincide with the results of the standard FDS for the used level of detail.

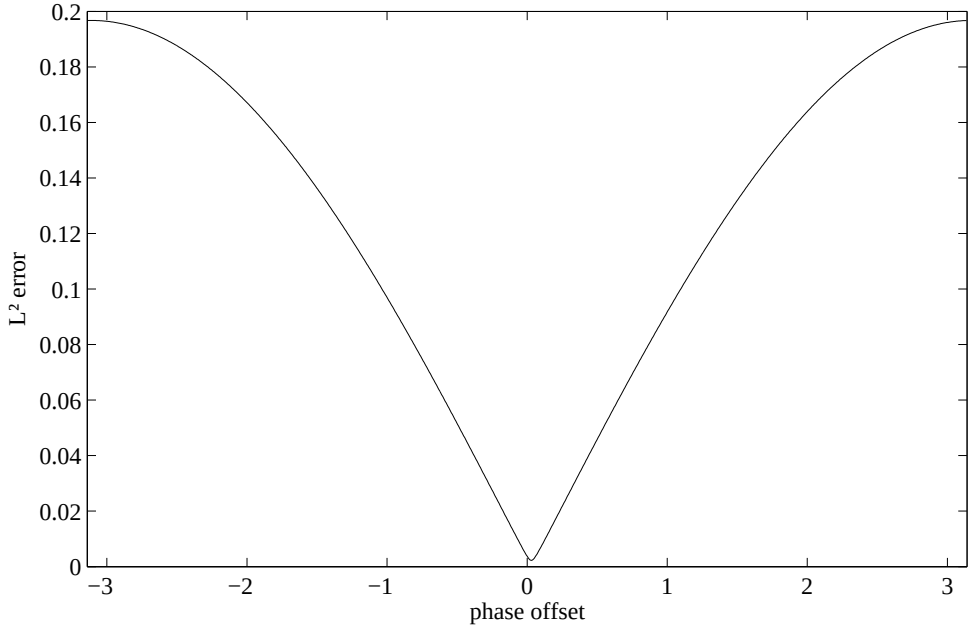

Figure 2.13: L^2-error $\Delta\psi_h$ of the standard FDS against the phase offset φ for the resonance energy $E = E_{\text{resonance}} \approx 544$ and the step size $h = 1/300$.

methods such as the MATLAB procedure `fminsearch` do not give acceptable results for this problem and hence, cannot be used.

In Fig. 2.14(a) the L^2-errors $\Delta\psi_h^{\min}$ of the standard FDS and the combined Numerov-Mickens FDS are plotted against the number of grid points $J = 1/h$ for the resonance energy $E = E_{\text{resonance}} \approx 544$. The error of the Numerov FDS and the error of the Mickens FDS coincide with the error of the standard discretization for the level of detail of Fig. 2.14(a). For these three FDSs the L^2-error is in $\mathcal{O}(h^2)$. The L^2-error of the combined Numerov-Mickens FDS, however, is only in $\mathcal{O}(h)$.

Fig. 2.14(b) shows that the phase shift adjusted L^2-errors of the Numerov FDS almost coincides with the standard FDS and the Mickens FDS, i.e. the Numerov FDS turns out to be not of higher order than the standard FDS and the Mickens FDS. Although the higher order of the Numerov FDS is considered to be an advantage compared to the standard FDS and the Mickens FDS, it is this property that leads to the observed error of the scheme. By applying the identity

$$\psi_{xx} = \left(\left(\frac{\psi_x}{\psi} \right)_x + \left(\frac{\psi_x}{\psi} \right)^2 \right) \psi$$

to the Schrödinger equation (2.1) we get

$$\left(\frac{\psi_x}{\psi} \right)_x + \left(\frac{\psi_x}{\psi} \right)^2 = V(x) - E. \tag{2.56}$$

Under the assumption of the Numerov FDS, i.e. that the discretization is of fourth order, the left hand side of Eq. (2.56) is second order differentiable. The right hand side, however, is not second order differentiable as the potential V comprises two jump discontinuities at the barrier's ends. For the standard discretization, the left hand side of Eq. (2.56) is continuous but not necessarily differentiable. Hence, the jump discontinuities of the potential also lead to an error but we expect this error to be smaller than for the Numerov scheme.

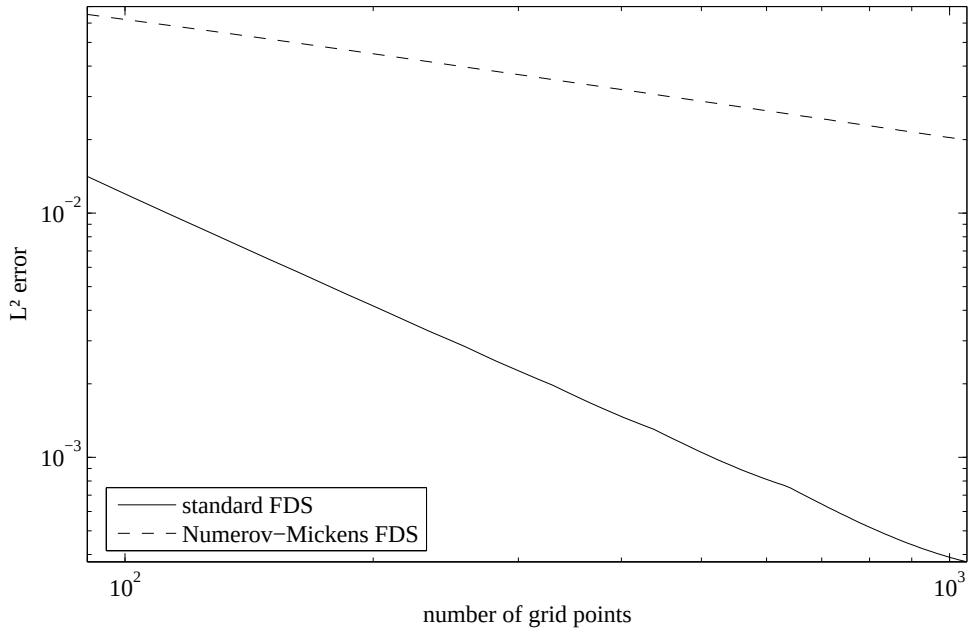

(a) L^2-error of the standard FDS (solid line) and the Numerov-Mickens FDS (dashed line).

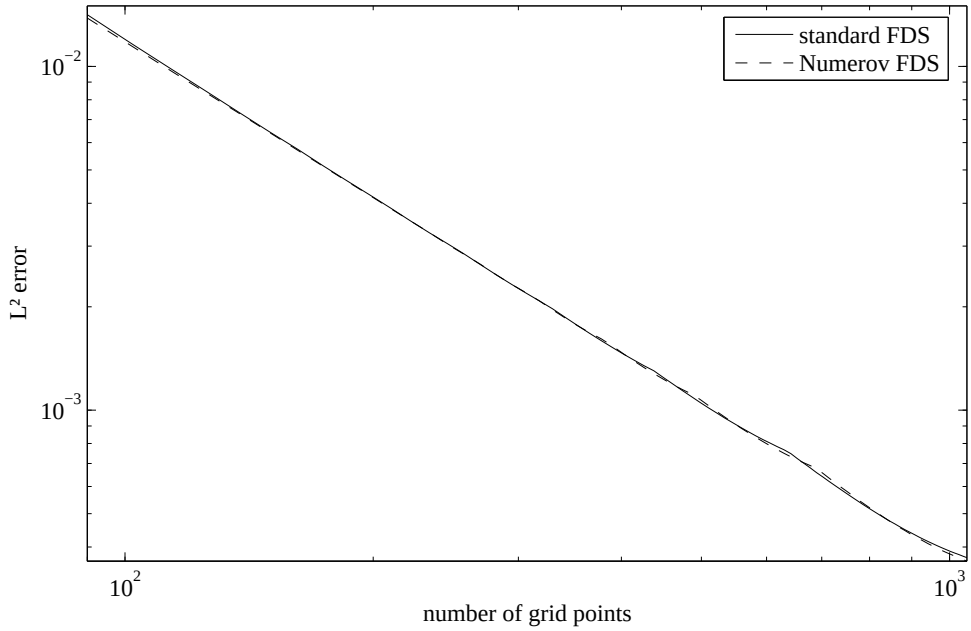

(b) L^2-error of the standard FDS (solid line) and the Numerov FDS (dashed line).

Figure 2.14: Comparison of the L^2-errors of the numerical schemes for the resonance energy $E = E_{\text{resonance}} \approx 544$. Note that the L^2-errors of the Numerov FDS and the Mickens FDS coincide with the L^2-error of the standard FDS for the used level of detail in (a), while the L^2-error of the Mickens FDS coincides with the L^2-error of the Numerov FDS for the used level of detail in (b).

An approach to improve the behavior of the Numerov FDS for a discontinuous potential V is to use the standard FDS of the Schrödinger equation at the point of discontinuity of the potential V and the Numerov FDS elsewhere. Although spurious oscillations due to possible incompatibility of the two schemes cannot be observed, numerical testing shows that the results cannot be improved significantly.

2.7.2 The Double Barrier Potential – Quantum Tunneling

As a final numerical example we will examine the results of the introduced FDSs for the double barrier potential. In particular, we want to check if the FDSs model the so-called *quantum tunneling* correctly. If there exists a resonance for an energy E that is smaller than the potential barrier V_0 we call this state quantum tunneling.

Analogously to the single barrier problem we can derive an analytical solution. Let $0 < x_1 < x_2 < x_3 < x_4 < L$. Assume that the domains $[x_1, x_2)$ and $[x_3, x_4)$ are quantum barriers with $V(x) = V_0$, while the domains $[0, x_1)$, $[x_2, x_3)$ and $[x_4, L]$ have zero potential, i.e. $V(x) = 0$. Again let us set $V_0 = 500$. Furthermore, we set $L = 1$ and $x_j = j/5$, $j = 1, \ldots, 4$.

Since the potential V is piecewise constant the wave function takes the form

$$\psi(x) = ae^{\mathrm{i}\hat{k}x} + be^{-\mathrm{i}\hat{k}x},$$

where the amplitudes a and b are constant in each domain and the wave vector reads

$$\hat{k} = \hat{k}(0) = \sqrt{2E}, \qquad \text{if } x \in [0, x_1) \cup [x_2, x_3) \cup [x_4, L],$$

and

$$\hat{k} = \hat{k}(V_0) = \sqrt{2\,(E - V_0)}, \qquad \text{if } x \in [x_1, x_2) \cup [x_3, x_4).$$

Note that we do not have to require the energy E to satisfy $E > V_0$, as we illustrated in the previous section.

Suppose that a right-traveling wave with amplitude $\hat{\psi} = 1$ enters the semiconductor from the left at $x = 0$. Since $V(x) = 0$ for $x \in [0, x_1)$, i.e. the same physical properties as in the exterior domain $x < 0$, the incoming wave is not reflected but completely transmitted into the domain $[0, x_1)$. At the potential barrier $x = x_1$ the wave is partially reflected. In domain $[x_4, L]$ we expect a transmitted, right-traveling wave to leave the semiconductor at the right boundary at $x = L$. For the same reason as at $x = 0$ we do not expect any reflections of the transmitted wave at $x = L$. Thus, the wave function reads

$$\psi(x) = \begin{cases} e^{\mathrm{i}\sqrt{2E}x} + re^{-\mathrm{i}\sqrt{2E}x}, & \text{if } x \in [0, x_1), \\ a_1 e^{\mathrm{i}\sqrt{2(E-V_0)}x} + b_1 e^{-\mathrm{i}\sqrt{2(E-V_0)}x}, & \text{if } x \in [x_1, x_2), \\ a_2 e^{\mathrm{i}\sqrt{2E}x} + b_2 e^{-\mathrm{i}\sqrt{2E}x}, & \text{if } x \in [x_2, x_3), \\ a_3 e^{\mathrm{i}\sqrt{2(E-V_0)}x} + b_3 e^{-\mathrm{i}\sqrt{2(E-V_0)}x}, & \text{if } x \in [x_3, x_4), \\ te^{\mathrm{i}\sqrt{2E}x}, & \text{if } x \in [x_4, L], \end{cases} \tag{2.57}$$

with the unknown reflection coefficient r, transmission coefficient t and the unknown coefficients a_j, b_j, $j = 1, \ldots, 3$.

Since the wave function (2.52) and its derivative

$$\psi_x(x) = \begin{cases} i\sqrt{2E}e^{\mathrm{i}\sqrt{2E}x} - \mathrm{i}\sqrt{2E}re^{-\mathrm{i}\sqrt{2E}x}, & \text{if } x \in [0, x_1), \\ i\sqrt{2\,(E - V_0)}a_1 e^{\mathrm{i}\sqrt{2(E-V_0)}x} - \mathrm{i}\sqrt{2\,(E - V_0)}b_1 e^{-\mathrm{i}\sqrt{2(E-V_0)}x}, & \text{if } x \in [x_1, x_2), \\ \mathrm{i}\sqrt{2E}a_2 e^{\mathrm{i}\sqrt{2E}x} - \mathrm{i}\sqrt{2E}b_2 e^{-\mathrm{i}\sqrt{2E}x}, & \text{if } x \in [x_2, x_3), \\ i\sqrt{2\,(E - V_0)}a_3 e^{\mathrm{i}\sqrt{2(E-V_0)}x} - \mathrm{i}\sqrt{2\,(E - V_0)}b_3 e^{-\mathrm{i}\sqrt{2(E-V_0)}x}, & \text{if } x \in [x_3, x_4), \\ i\sqrt{2E}te^{\mathrm{i}\sqrt{2E}x}, & \text{if } x \in [x_4, L], \end{cases}$$

are continuous at $x = x_j$, $j = 1, \ldots, 3$, cf. [24], we get a system of eight linear equations for the eight unknown coefficients.

However, we will not state the results of the system of linear equations since the expressions for the coefficients are very long.

2.7.2.1 The Transmission Coefficient

In this section we will study the transmission coefficient $\tau = |t|$ against the energy E. As explained above we expect a resonance for an energy E that is smaller than the potential barrier V_0. In Fig. 2.15(a) the analytical transmission coefficient τ is compared with the transmission coefficients of the standard FDS. The results of the Numerov FDS and the Mickens FDS coincide with the results of the standard FDS. Since the results of the combined Numerov-Mickens FDS with single barrier potential differed significantly from the analytical results we will omit to use this FDS for the double barrier potential.

As can be seen in Fig. 2.15(b) the standard FDS, the Numerov FDS and Mickens FDS model the tunneling resonance with a certain error while the error of the standard FDS is greater than the error of the Numerov FDS and Mickens FDS. If we choose a smaller step size h the error decreases.

2.8 Summary

We introduced four different FDSs of the BVP (2.17) and derived for each of them DTBCs. We showed that all FDSs together with the DTBCs have a unique solution. We found that the spurious oscillations of the modulus we observed when using discretized TBCs vanish when using DTBCs instead. Except the Mickens FDS all other introduced FDSs lead to a phase error in the free scattering state with constant potential that is directly caused by the difference of the analytical quantum mechanical dispersion relation (2.13) and the discrete dispersion relations (2.26), (2.39) and (2.50) respectively. We showed that this error vanishes when $h \to 0$ as the discrete dispersion relations converge to the analytical dispersion relation for $h \to 0$.

Considering the numerical results we point out that the Mickens FDS is the most promising FDS we introduced. If the potential is constant the Mickens FDS is an exact FDS and if the potential is not constant it is of order $\mathcal{O}(h^2)$. Which is the best possible order of convergence of the FDSs we introduced since the Numerov FDS which is formally of order $\mathcal{O}(h^4)$ is in fact also only $\mathcal{O}(h^2)$ since it requires the potential to be in $C^2(0, L)$. While the standard FDS and the Numerov FDS are also applicable, the combined Numerov-Mickens FDS, however, leads to significant errors.

Apart from the list of FDSs we introduced in this chapter there are a plenty of FDSs that can be used for the stationary linear Schrödinger equation (2.1). However, the chosen FDSs demonstrate the principle of using FDSs for the Schrödinger equation clearly. The reader is referred to Simos and Williams [40] for a concise review on FDSs for the Schrödinger equation.

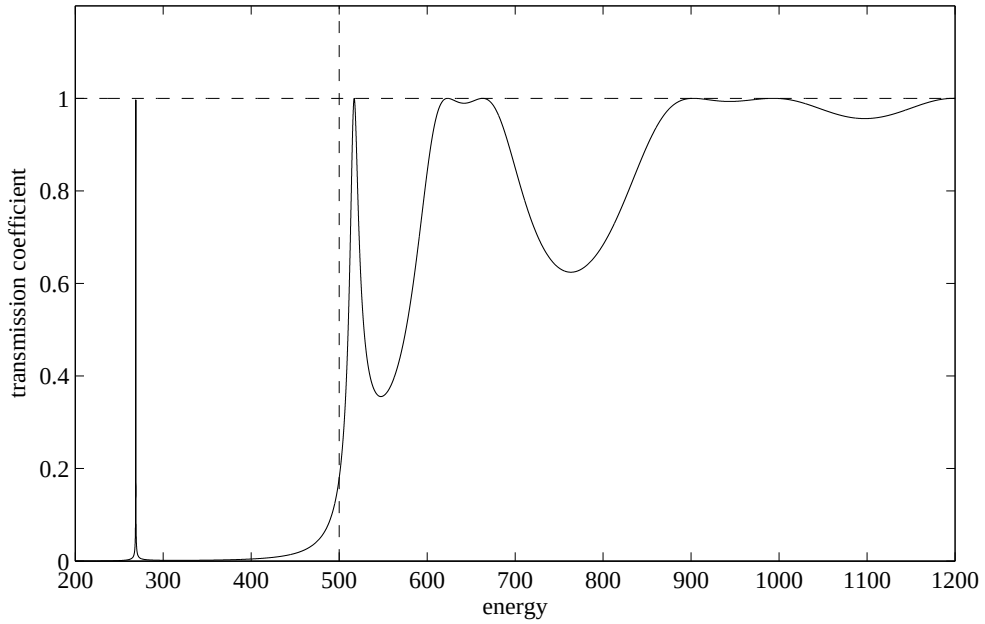

(a) Analytical transmission coefficient.

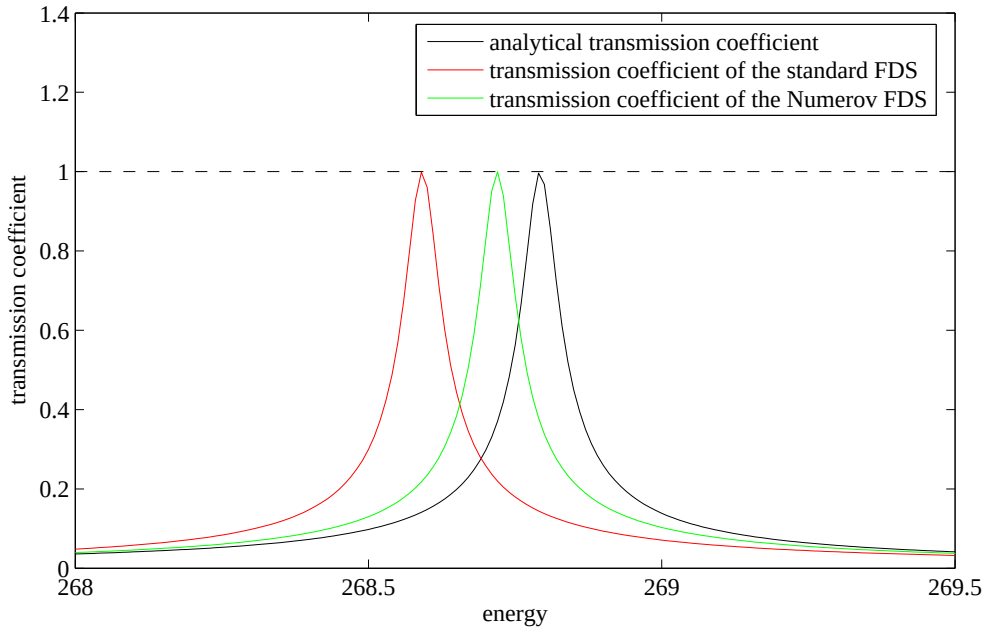

(b) Analytical and discrete transmission coefficients at the tunneling resonance at $E \approx 269$.

Figure 2.15: Analytical transmission coefficient (black), the transmission coefficient of the standard FDS (red) and the transmission coefficient of the Numerov FDS (green) for the step size $h = 1/300$. The transmission coefficient of the Mickens FDS coincides with the transmission coefficient of the Numerov FDS for the used level of detail in (b), while the transmission coefficients of the standard FDS, the Numerov FDS and the Mickens FDS coincide with the analytical transmission coefficient for the used level of detail in (a).

Chapter 3

The Two-Band Kane-Model

As a first step of generalization, we introduce the two-band *Kane-model*, cf. [22],

$$\mathbf{HF} = E\mathbf{F}, \qquad x \in \mathbb{R}, \tag{3.1}$$

with

$$\mathbf{H} = \begin{pmatrix} \frac{1}{2}E_{\mathrm{g}}(x) + E_0(x) & -\mathrm{i}P_0(x)\frac{\mathrm{d}}{\mathrm{d}x} \\ -\mathrm{i}P_0(x)\frac{\mathrm{d}}{\mathrm{d}x} & -\frac{1}{2}E_{\mathrm{g}}(x) + E_0(x) \end{pmatrix}, \tag{3.2}$$

where $P_0(x) > 0$ denotes the *Kane-parameter* that is given by the relation

$$E_{\mathrm{p}} = \frac{2m^*}{\hbar^2}P_0^2. \tag{3.3}$$

The energy E_{p} is called *optical matrix element* and is a measure of the coupling of the conduction and valence band. E_{g} denotes the so-called *band gap* which is the difference of the conduction and valence band edges E_{c} and E_{v}, i.e.

$$E_{\mathrm{g}}(x) = E_{\mathrm{c}}(x) - E_{\mathrm{v}}(x).$$

E_0 is called *middle of the band gap* and is the arithmetic mean of the conduction and valence band edges E_{c} and E_{v}, i.e.

$$E_0(x) = \frac{E_{\mathrm{c}}(x) + E_{\mathrm{v}}(x)}{2}.$$

In contrast to the approach of the single-band effective mass approximation in Chap. 2, the Kane-model considers not only the conduction band of the semiconductor but also the valence band. The two bands are coupled with a first order derivative of the envelope functions $F_{\mathrm{c}}(x)$ and $F_{\mathrm{v}}(x)$ of the conduction band and valence band respectively. However, the Hamiltonian $\mathbf{H}$ does not contain second order derivatives of $\mathbf{F}(x)$ on the diagonal. In other words, the Kane-model has no second order intra-band coupling.

Again, we consider a semiconductor of length L connected to reservoirs at $x = 0$ and $x = L$. Let us assume that the Kane-parameter $P_0(x)$ as well as the band edges $E_{\mathrm{c}}(x)$ and $E_{\mathrm{v}}(x)$ are constant in the reservoirs, i.e.

$$\begin{aligned} P_0(x) &= P_{0,0}, \qquad x \leq 0, \\ P_0(x) &= P_{0,L}, \qquad x \geq L, \end{aligned}$$

and

$$\begin{aligned} E_{\mathrm{g}}(x) &= E_{\mathrm{g},0}, \qquad x \leq 0, \\ E_{\mathrm{g}}(x) &= E_{\mathrm{g},L}, \qquad x \geq L, \end{aligned}$$

and

$$\begin{aligned} E_0(x) &= 0, \qquad x \leq 0, \\ E_0(x) &= E_{0,L}, \qquad x \geq L. \end{aligned}$$

3.1 The Exterior Problem and the Dispersion Relation

We will now analyze the exterior problem of the Kane-model. In the exterior domains the Kane-parameter P_0, the band gap E_g and the middle of the band gap E_0 are constant. However, we shall not analyze the exterior domains explicitly. Instead we will state the analytical dispersion relation and the solution of the free scattering state for some constant Kane-parameter P_0, some constant band gap E_g and some constant middle of the band gap E_0.

If P_0, E_g and E_0 are constant, Eq. (3.1) is a first order system of ODEs with constant coefficients that can be written in the form

$$\frac{\mathrm{d}}{\mathrm{d}x}\mathbf{F} = \mathbf{A}\mathbf{F}, \qquad x \in \mathbb{R}, \tag{3.4}$$

with

$$\mathbf{A} = \begin{pmatrix} 0 & \mathrm{i}\frac{1}{P_0}\left(E + \frac{1}{2}E_g - E_0\right) \\ \mathrm{i}\frac{1}{P_0}\left(E - \frac{1}{2}E_g - E_0\right) & 0 \end{pmatrix}.$$

As shown in the basic theory on systems of ODEs, e.g. see [41], the solution of Eq. (3.4) takes the form

$$\mathbf{F}(x) = \hat{\mathbf{F}}e^{\kappa x} = \hat{\mathbf{F}}e^{\mathrm{i}kx}, \tag{3.5}$$

where $\kappa = \kappa_{1,2} \in \mathbb{C}$ denotes an eigenvalue of the matrix $\mathbf{A}$ and $\hat{\mathbf{F}} = \hat{\mathbf{F}}(k) \in \mathbb{C}^2$ the corresponding eigenvector. We shall call $\hat{\mathbf{F}}$ *amplitude* of the vector $\mathbf{F}$ of the envelope functions and $k = \hat{k} + \mathrm{i}\check{k} = -\mathrm{i}\kappa$ *wave vector* of $\mathbf{F}$ with the *propagation coefficient* $\hat{k}$ and the *attenuation coefficient* $\check{k}$. If the attenuation coefficient $\check{k}$ is zero we say that the vector $\mathbf{F}$ of the envelope functions is *traveling* while it is called *evanescent* if $\check{k}$ is nonzero. In the sequel we shall refer to the vector $\mathbf{F}$ of the envelope functions as *envelope wave* since it can be expressed in the form of a plane wave.

If we apply the solution (3.5) to the Kane-model (3.1) we get

$$\hat{\mathbf{H}}\hat{\mathbf{F}} = E\hat{\mathbf{F}}, \tag{3.6}$$

with

$$\hat{\mathbf{H}} = \hat{\mathbf{H}}(k) = \begin{pmatrix} \hat{H}_{11}(k) & \hat{H}_{12}(k) \\ \hat{H}_{21}(k) & \hat{H}_{22}(k) \end{pmatrix} = \begin{pmatrix} \frac{1}{2}E_g + E_0 & P_0 k \\ P_0 k & -\frac{1}{2}E_g + E_0 \end{pmatrix}. \tag{3.7}$$

The characteristic polynomial of $\hat{\mathbf{H}}$ gives

$$(E - E_0)^2 - \frac{1}{4}E_g^2 - P_0^2 k^2 = 0.$$

and hence,

$$k^2 = \frac{1}{P_0^2}\left((E - E_0)^2 - \frac{1}{4}E_g^2\right).$$

If the energy E satisfies the energy condition

$$|E - E_0| > \frac{1}{2}E_g, \tag{3.8}$$

the wave vector k is real and reads

$$k = \pm\hat{k} \in \mathbb{R}, \tag{3.9}$$

with the *propagation coefficient*

$$\hat{k} = \frac{1}{P_0}\sqrt{(E - E_0)^2 - \frac{1}{4}E_g^2} > 0.$$

Thus, under the energy assumption (3.8), we obtain two traveling envelope waves, one being a right-traveling envelope wave (if $k = \hat{k}$) and the other being a left-traveling envelope wave (if $k = -\hat{k}$).

On the other hand, if

$$|E - E_0| \leq \frac{1}{2} E_{\mathrm{g}}, \tag{3.10}$$

the wave vector is purely imaginary and takes the form

$$k = \pm \mathrm{i}\check{k} \in \mathrm{i}\mathbb{R}, \tag{3.11}$$

with the *attenuation coefficient*

$$\check{k} = \frac{1}{P_0} \sqrt{\frac{1}{4} E_{\mathrm{g}}^2 - (E - E_0)^2} \geq 0.$$

Hence, under the assumption (3.10) we obtain two evanescent envelope waves, one decaying for $x \to -\infty$ (if $k = -\mathrm{i}\check{k}$, i.e. $\kappa = \check{k}$) and the other decaying for $x \to \infty$ (if $k = \mathrm{i}\check{k}$, i.e. $\kappa = -\check{k}$). In the case of identity in Eq. (3.10) we obtain a constant solution.

Eqs. (3.9) and (3.11) are called the *dispersion relations* of the Kane-model. Let us state the reciprocal form of these relations. Therefore, we evaluate the energy eigenvalue of $\hat{\mathbf{H}}$. It yields

$$E = E^{\mathrm{e/h}}(k) = E_0 \pm \sqrt{\frac{1}{4} E_{\mathrm{g}}^2 + k^2 P_0^2}. \tag{3.12}$$

The energy E^{e} associated with the positive sign in Eq. (3.12) denotes the energy of the electrons, while E^{h} associated with the negative sign in Eq. (3.12) denotes the energy of the holes. Clearly, $E^{\mathrm{e/h}}(k)$ satisfies the energy condition (3.8) if and only if the wave vector k is real. In this case, i.e. in the case of traveling envelope waves, we will refer to the energy E^{e} as the energy of the conduction band and the energy E^{h} as the energy of the valence band.

In order to complete the analysis of the exterior problem we will give the results of the amplitude $\hat{\mathbf{F}}(k)$. Note that in Chap. 2 we did not have to specify the amplitude since it was a scalar and we were free to set it to 1. In the two-band Kane-model, however, the amplitude

$$\hat{\mathbf{F}}(k) = \hat{\mathbf{F}}^{\mathrm{e/h}}(k) = \begin{pmatrix} \hat{F}_{\mathrm{c}}^{\mathrm{e/h}}(k) \\ \hat{F}_{\mathrm{v}}^{\mathrm{e/h}}(k) \end{pmatrix},$$

is an eigenvector of $\hat{\mathbf{H}}(k)$ with the corresponding energy eigenvalue $E^{\mathrm{e/h}}(k)$, see Eq. (3.6). Clearly, the amplitude $\hat{\mathbf{F}}^{\mathrm{e/h}}(k)$, as an eigenvector of $\hat{\mathbf{H}}(k)$, is not defined uniquely. But we know that it solves the under-determined linear equation

$$\left(\hat{H}_{11}(k) - E^{\mathrm{e/h}}(k)\right) \hat{F}_{\mathrm{c}}^{\mathrm{e/h}}(k) + \hat{H}_{12}(k) \hat{F}_{\mathrm{v}}^{\mathrm{e/h}}(k) = 0. \tag{3.13}$$

This gives

$$\hat{\mathbf{F}}^{\mathrm{e/h}}(k) = c \begin{pmatrix} \hat{H}_{12}(k) \\ E^{\mathrm{e/h}}(k) - \hat{H}_{11}(k) \end{pmatrix} = c \begin{pmatrix} kP_0 \\ E^{\mathrm{e/h}}(k) - \frac{1}{2} E_{\mathrm{g}} - E_0 \end{pmatrix}, \tag{3.14}$$

with some arbitrary constant $c \in \mathbb{C}$. Note that $\mathbf{F}^{\mathrm{e}}(x,k) = \hat{\mathbf{F}}^{\mathrm{e}}(k) e^{\pm \mathrm{i}kx}$ is the energy eigenstate associated with the energy E^{e} of the electrons, while $\mathbf{F}^{\mathrm{h}}(x,k) = \hat{\mathbf{F}}^{\mathrm{h}}(k) e^{\pm \mathrm{i}kx}$ corresponds to the energy E^{h} of the holes, see Eq. (3.12).

If the energy condition $|E - E_0| > \frac{1}{2} E_{\mathrm{g}}$ is fulfilled we obtain traveling envelope waves with a real wave vector $k = \pm \hat{k}$. For those traveling envelope waves we shall additionally assume that they are unitary waves, i.e. the amplitude $\hat{\mathbf{F}}^{\mathrm{e/h}}(\hat{k})$ is of norm 1 and hence, it satisfies the *normalization condition*

$$\left\| \hat{\mathbf{F}}^{\mathrm{e/h}}(\hat{k}) \right\|_{\mathbb{C}}^2 = \left\langle \hat{\mathbf{F}}^{\mathrm{e/h}}(\hat{k}), \overline{\hat{\mathbf{F}}^{\mathrm{e/h}}(\hat{k})} \right\rangle = 1. \tag{3.15}$$

In this case $\hat{\mathbf{H}}(\hat{k})$ and its eigenvalues $E^{\mathrm{e/h}}(\hat{k})$ are real-valued and thus, the eigenvectors $\hat{\mathbf{F}}^{\mathrm{e/h}}(\hat{k})$ are either also real-valued or purely imaginary. But since our approach in Eq. (3.5) implies that

$\hat{\mathbf{F}}^{\mathrm{e/h}}(\hat{k})$ is the modulus of $\mathbf{F}$, we shall assume that the amplitude $\hat{\mathbf{F}}^{\mathrm{e/h}}(\hat{k})$ is real. Hence, the normalization condition (3.15) becomes

$$\hat{F}_{\mathrm{c}}^{\mathrm{e/h}}(\hat{k})^2 + \hat{F}_{\mathrm{v}}^{\mathrm{e/h}}(\hat{k})^2 = 1. \tag{3.16}$$

Thus, the amplitude $\hat{\mathbf{F}}^{\mathrm{e/h}}(k)$ of a traveling envelope wave with norm 1 takes the form

$$\begin{aligned}\hat{\mathbf{F}}^{\mathrm{e/h}}(\hat{k}) &= \pm \begin{pmatrix} \frac{\hat{H}_{12}(\hat{k})}{\sqrt{\left(E^{\mathrm{e/h}}(\hat{k}) - \hat{H}_{11}(\hat{k})\right)^2 + \hat{H}_{12}(\hat{k})^2}} \\ \frac{E^{\mathrm{e/h}}(\hat{k}) - \hat{H}_{11}(\hat{k})}{\sqrt{\left(E^{\mathrm{e/h}}(\hat{k}) - \hat{H}_{11}(\hat{k})\right)^2 + \hat{H}_{12}(\hat{k})^2}} \end{pmatrix} \\ &= \pm \begin{pmatrix} \frac{\hat{k}P_0}{\sqrt{\left(E^{\mathrm{e/h}}(\hat{k}) - \frac{1}{2}E_{\mathrm{g}} - E_0\right)^2 + \hat{k}^2 P_0^2}} \\ \frac{E^{\mathrm{e/h}}(\hat{k}) - \frac{1}{2}E_{\mathrm{g}} - E_0}{\sqrt{\left(E^{\mathrm{e/h}}(\hat{k}) - \frac{1}{2}E_{\mathrm{g}} - E_0\right)^2 + \hat{k}^2 P_0^2}} \end{pmatrix}. \end{aligned} \tag{3.17}$$

Since the two solutions of the amplitude are linearly dependent, we can neglect the solution with negative sign and set

$$\hat{\mathbf{F}}^{\mathrm{e/h}}(\hat{k}) = \begin{pmatrix} \frac{\hat{k}P_0}{\sqrt{\left(E^{\mathrm{e/h}}(\hat{k}) - \frac{1}{2}E_{\mathrm{g}} - E_0\right)^2 + \hat{k}^2 P_0^2}} \\ \frac{E^{\mathrm{e/h}}(\hat{k}) - \frac{1}{2}E_{\mathrm{g}} - E_0}{\sqrt{\left(E^{\mathrm{e/h}}(\hat{k}) - \frac{1}{2}E_{\mathrm{g}} - E_0\right)^2 + \hat{k}^2 P_0^2}} \end{pmatrix}. \tag{3.18}$$

In the remainder of this section we will prove

Proposition 3.1. Let $k \in \mathbb{R}$ be the wave vector of a traveling envelope wave. Then the two vectors $\mathbf{F}^{\mathrm{e}}(x,k)$ and $\mathbf{F}^{\mathrm{h}}(x,k)$ of the envelope functions of the free scattering state are orthogonal, i.e.

$$\left\langle \mathbf{F}^{\mathrm{e}}(x,k), \mathbf{F}^{\mathrm{h}}(x,k) \right\rangle = 0.$$

Proof. The scalar product of $\mathbf{F}^{\mathrm{e}}(x,k)$ and $\mathbf{F}^{\mathrm{h}}(x,k)$ is given by

$$\left\langle \mathbf{F}^{\mathrm{e}}(x,k), \mathbf{F}^{\mathrm{h}}(x,k) \right\rangle = \left\langle \hat{\mathbf{F}}^{\mathrm{e}}(k)e^{\mathrm{i}kx}, \hat{\mathbf{F}}^{\mathrm{h}}(k)e^{\mathrm{i}kx} \right\rangle = e^{2\mathrm{i}kx} \left\langle \hat{\mathbf{F}}^{\mathrm{e}}(k), \hat{\mathbf{F}}^{\mathrm{h}}(k) \right\rangle.$$

Hence, we only have to show that the amplitudes $\hat{\mathbf{F}}^{\mathrm{e}}(k)$ and $\hat{\mathbf{F}}^{\mathrm{h}}(k)$ are orthogonal. Taking Eq. (3.18) into account, the scalar product of $\hat{\mathbf{F}}^{\mathrm{e}}(k)$ and $\hat{\mathbf{F}}^{\mathrm{h}}(k)$ becomes

$$\begin{aligned}\left\langle \hat{\mathbf{F}}^{\mathrm{e}}(k), \hat{\mathbf{F}}^{\mathrm{h}}(k) \right\rangle = &\frac{\hat{H}_{12}(k)}{\sqrt{\left(E^{\mathrm{e}}(k) - \hat{H}_{11}(k)\right)^2 + \hat{H}_{12}(k)^2}} \frac{\hat{H}_{12}(k)}{\sqrt{\left(E^{\mathrm{h}}(k) - \hat{H}_{11}(k)\right)^2 + \hat{H}_{12}(k)^2}} \\ &+ \frac{E^{\mathrm{e}}(k) - \hat{H}_{11}(k)}{\sqrt{\left(E^{\mathrm{e}}(k) - \hat{H}_{11}(k)\right)^2 + \hat{H}_{12}(k)^2}} \frac{E^{\mathrm{h}}(k) - \hat{H}_{11}(k)}{\sqrt{\left(E^{\mathrm{h}}(k) - \hat{H}_{11}(k)\right)^2 + \hat{H}_{12}(k)^2}}. \end{aligned}$$

Considering the dispersion relation (3.12) we get

$$\left\langle \hat{\mathbf{F}}^{\mathrm{e}}(k), \hat{\mathbf{F}}^{\mathrm{h}}(k) \right\rangle = \frac{\hat{H}_{12}(k)^2 + \left(E_0 - \hat{H}_{11}(k) + \sqrt{\frac{1}{4}E_{\mathrm{g}}^2 + P_0^2 k^2}\right)\left(E_0 - \hat{H}_{11}(k) - \sqrt{\frac{1}{4}E_{\mathrm{g}}^2 + P_0^2 k^2}\right)}{\sqrt{\left(E^{\mathrm{e}}(k) - \hat{H}_{11}(k)\right)^2 + \hat{H}_{12}(k)^2}\sqrt{\left(E^{\mathrm{h}}(k) - \hat{H}_{11}(k)\right)^2 + \hat{H}_{12}(k)^2}},$$

which gives

$$\left\langle \hat{\mathbf{F}}^{\mathrm{e}}(k), \hat{\mathbf{F}}^{\mathrm{h}}(k) \right\rangle = \frac{\left(\hat{H}_{11}(k) - E_0\right)^2 + \hat{H}_{12}(k)^2 - \frac{1}{4}E_{\mathrm{g}}^2 - P_0^2 k^2}{\sqrt{\left(E^{\mathrm{e}}(k) - \hat{H}_{11}(k)\right)^2 + \hat{H}_{12}(k)^2}\sqrt{\left(E^{\mathrm{h}}(k) - \hat{H}_{11}(k)\right)^2 + \hat{H}_{12}(k)^2}}.$$

By using the identities

$$\left(\hat{H}_{11}(k) - E_0\right)^2 = \frac{1}{4}E_\mathrm{g}^2$$

and

$$\hat{H}_{12}(k)^2 = P_0^2 k^2,$$

we obtain

$$\left\langle \hat{\mathbf{F}}^\mathrm{e}(k), \hat{\mathbf{F}}^\mathrm{h}(k) \right\rangle = 0,$$

and hence, the two vectors $\mathbf{F}^\mathrm{e}(x,k)$ and $\mathbf{F}^\mathrm{h}(x,k)$ of the envelope functions are orthogonal. □

3.2 Transparent Boundary Conditions

The TBCs are derived in the same way as in Chap. 2. Let $\hat{k}_0$ denote the propagation coefficient of the wave vector of a right-traveling envelope wave in the left exterior domain $x \leq 0$ and $\hat{k}_L$ the corresponding propagation coefficient in the right exterior domain $x \geq L$. We consider an incoming envelope wave

$$\mathbf{F}^\mathrm{in} = \hat{\mathbf{F}}_0^{\mathrm{e/h}}(\hat{k}_0) e^{\hat{k}_0 x}, \qquad x < 0. \tag{3.19}$$

This incoming envelope wave is partly reflected at the left boundary at $x = 0$,

$$\mathbf{F}^\mathrm{r} = \mathbf{r} e^{-\mathrm{i}\hat{k}_0 x}, \qquad x < 0, \tag{3.20}$$

with the reflection coefficient vector $\mathbf{r} = r\hat{\mathbf{F}}_0^{\mathrm{e/h}}(-\hat{k}_0)$, $r \in \mathbb{C}$, and partly transmitted at the right boundary at $x = L$,

$$\mathbf{F}^\mathrm{t} = \mathbf{t} e^{\mathrm{i}\hat{k}_L x}, \qquad x > L, \tag{3.21}$$

with the transmission coefficient vector $\mathbf{t} = t\hat{\mathbf{F}}_L^{\mathrm{e/h}}(\hat{k}_L)$, $t \in \mathbb{C}$. Hence, the solution in the left exterior domain reads

$$\mathbf{F} = \mathbf{F}^\mathrm{in} + \mathbf{F}^\mathrm{r}, \qquad x < 0, \tag{3.22}$$

while the solution in the right exterior domain is given by

$$\mathbf{F} = \mathbf{F}^\mathrm{t}, \qquad x > L. \tag{3.23}$$

Note that $\mathbf{F}^\mathrm{in}$ and $\mathbf{F}^\mathrm{t}$ are right-traveling envelope waves, whereas $\mathbf{F}^\mathrm{r}$ is a left-traveling envelope wave.

Let us recall that the envelope wave and its first derivative are continuous at the two boundaries. We eliminate the reflection coefficient vector $\mathbf{r}$ by comparing Eq. (3.22) and its first derivative at $x = 0$. It yields

$$\frac{\mathrm{d}}{\mathrm{d}x}\mathbf{F}(0,\hat{k}_0) + \mathrm{i}\hat{k}_0 \mathbf{F}(0,\hat{k}_0) = 2\mathrm{i}\hat{k}_0 \hat{\mathbf{F}}_0^{\mathrm{e/h}}, \tag{3.24a}$$

cf. the left TBC (2.17b) of the scalar Schrödinger equation. Analogously, we can eliminate the transmission coefficient vector $\mathbf{t}$ when comparing Eq. (3.23) and its first derivative at $x = L$. We get

$$\frac{\mathrm{d}}{\mathrm{d}x}\mathbf{F}(L,\hat{k}_L) - \mathrm{i}\hat{k}_L \mathbf{F}(L,\hat{k}_L) = \mathbf{0}, \tag{3.24b}$$

compared to the right TBC (2.17c) of the scalar Schrödinger equation in the previous chapter.

3.3 Reduction to a Second Order Scalar ODE

If we do not assume P_0, E_0 and E_g to be constant, the matrix $\mathbf{A}$ in the ODE (3.4) is not constant in x and takes the form

$$\mathbf{A}(x) = \begin{pmatrix} 0 & \mathrm{i}\frac{1}{P_0(x)}\left(E - \left(-\frac{1}{2}E_\mathrm{g}(x) + E_0(x)\right)\right) \\ \mathrm{i}\frac{1}{P_0(x)}\left(E - \left(\frac{1}{2}E_\mathrm{g}(x) + E_0(x)\right)\right) & 0 \end{pmatrix}.$$

We can derive a second order scalar ODE for the conduction band and the valence band respectively, that is equivalent to the Kane-model (3.1). We get

$$\begin{aligned} \frac{\mathrm{d}^2}{\mathrm{d}x^2}F_\mathrm{c} &= \mathrm{i}\frac{1}{P_0(x)}\left(E - \left(-\frac{1}{2}E_\mathrm{g}(x) + E_0(x)\right)\right)\frac{\mathrm{d}}{\mathrm{d}x}F_\mathrm{v} \\ &= \mathrm{i}\frac{1}{P_0(x)}\left(E - \left(-\frac{1}{2}E_\mathrm{g}(x) + E_0(x)\right)\right)\ \mathrm{i}\frac{1}{P_0(x)}\left(E - \left(\frac{1}{2}E_\mathrm{g}(x) + E_0(x)\right)\right)F_\mathrm{c} \\ &= -\frac{1}{P_0^2(x)}\left(\left(E - \left(-\frac{1}{2}E_\mathrm{g}(x) + E_0(x)\right)\right)\left(E - \left(\frac{1}{2}E_\mathrm{g}(x) + E_0(x)\right)\right)\right)F_\mathrm{c} \\ &= -\frac{1}{P_0^2(x)}\left(\left(E - E_0(x)\right)^2 - \frac{1}{4}E_\mathrm{g}^2(x)\right)F_\mathrm{c}. \end{aligned} \tag{3.25}$$

Together with definition of the Kane-parameter P_0 in Eq. (3.3), Eq. (3.25) yields

$$-\frac{\hbar^2}{2m^*}\frac{\mathrm{d}^2}{\mathrm{d}x^2}F_\mathrm{c} = \frac{1}{E_\mathrm{p}(x)}\left(\left(E - E_0(x)\right)^2 - \frac{1}{4}E_\mathrm{g}^2(x)\right)F_\mathrm{c}, \tag{3.26}$$

which is a non-linear eigenvalue problem in E.

The components of the vectorial TBCs (3.24) are not coupled, thus

$$\frac{\mathrm{d}}{\mathrm{d}x}F_\mathrm{c}(0,\hat{k}_0) + \mathrm{i}\hat{k}_0 F_\mathrm{c}(0,\hat{k}_0) = 2\mathrm{i}\hat{k}_0\hat{F}_{0,\mathrm{c}}^{\mathrm{e/h}}, \tag{3.27a}$$

and

$$\frac{\mathrm{d}}{\mathrm{d}x}F_\mathrm{c}(L,\hat{k}_L) - \mathrm{i}\hat{k}_L F_\mathrm{c}(L,\hat{k}_L) = 0, \tag{3.27b}$$

are the corresponding scalar TBCs of the scalar ODE (3.26). Together they form a scalar BVP that differs from the BVP (2.17) of the scalar Schrödinger equation in Sec. 2 only in the potential and energy. Therefore, we can prove

Theorem 3.2. Let E_p, E_g and E_0 be in $L^\infty(0,L)$ and real valued. Then the BVP of the ODE (3.26) and the TBCs (3.27) has a unique solution $F_\mathrm{c} \in W^{2,\infty}(0,L)$.

Proof. This theorem is a corollary of Thm. 2.1. If we set

$$E_\mathrm{scalar} = 0,$$

and

$$V(x) = -\frac{1}{E_\mathrm{p}(x)}\left(\left(E - E_0(x)\right)^2 - \frac{1}{4}E_\mathrm{g}^2(x)\right),$$

which is in $L^\infty(0,L)$ since E_p, E_g and E_0 are in $L^\infty(0,L)$, we can apply Thm. 2.1 and thus, the uniqueness of the solution is shown. □

Corollary 3.3. Let E_p, E_g and E_0 be in $L^\infty(0,L)$ and real valued. Then the BVP of the systems of ODEs (3.1) and the vectorial TBCs (3.24) has a unique solution $\mathbf{F} \in \left(W^{2,\infty}(0,L)\right)^2$.

Proof. We already showed the uniqueness of F_c in Thm. 3.2. The uniqueness of F_v and hence, $\mathbf{F}$ can be obtained by defining the scalar ODE for F_v and then applying a corresponding version of Thm. 3.2. □

3.4 Discretization

We recall the uniform discretization $x_j = jh$, $j = 0, \ldots, J$, with $L = Jh$, of the computational interval $(0, L)$ with $P_{0,j} = P_0(x_j)$, $E_{\mathrm{g},j} = E_{\mathrm{g}}(x_j)$, $E_{0,j} = E_0(x_j)$ and the approximation $\mathbf{F}_j \approx \mathbf{F}(x_j)$, $j = 0, \ldots, J$.

In general, the discretization of the Kane-Model takes the form

$$\mathbf{M}_j^+ \mathbf{F}_{j+1} + \left(\mathbf{M}_j^0 - E\mathbb{1}\right) \mathbf{F}_j + \mathbf{M}_j^- \mathbf{F}_{j-1} = \mathbf{0}, \qquad j = 1, \ldots, J-1, \tag{3.28}$$

where the matrices $\mathbf{M}_j^+$, $\mathbf{M}_j^0$ and $\mathbf{M}_j^-$ depend on the choice of the difference scheme.

In this section we will state different FDSs including their respective coefficient matrices $\mathbf{M}_j^+$, $\mathbf{M}_j^0$ and $\mathbf{M}_j^-$. We will analyze the discrete exterior problem of the introduced FDSs, i.e. the free scattering state with constant Kane-parameter P_0, constant band gap E_{g} and constant middle of the band gap E_0. However, we will not explicitly derive the discrete solutions of the exterior domains $x \leq 0$ and $x \geq L$. Instead we will give results for some constant Kane-parameter P_0, some constant band gap E_{g} and some constant middle of the band gap E_0. In order to determine the discrete solutions of the exterior domains one shall apply the respective values of the Kane-parameter P_0, the band gap E_{g} and the middle of the band gap E_0 to the results that we will state.

If P_0, E_{g} and E_0 are constant then the coefficient matrices $\mathbf{M}_j^+$, $\mathbf{M}_j^0$ and $\mathbf{M}_j^-$ are constant. In this case we will omit the subscript j.

Before we introduce a first FDS we prove

Proposition 3.4. Let $\alpha \in \mathbb{C}$ be an eigenvalue of $\mathbf{A} \in \mathbb{C}^{n\times n}$ with corresponding eigenvector $\mathbf{a} \in \mathbb{C}^n$. Then the first order difference equation with constant coefficients

$$\mathbf{y}_j = \mathbf{A}\mathbf{y}_{j-1}$$

with the initial value $\mathbf{y}_0 = \mathbf{a}$ has a solution of the form

$$\mathbf{y}_j = \alpha^j \mathbf{a}, \qquad j \geq 0.$$

Proof. By assumption the proposition holds for $j = 0$. Then it also holds for any $j \geq 1$ since

$$\mathbf{y}_{j+1} = \mathbf{A}\mathbf{y}_j = \mathbf{A}\alpha^j\mathbf{a} = \alpha^j\mathbf{A}\mathbf{a} = \alpha^j\alpha\mathbf{a} = \alpha^{j+1}\mathbf{a}.$$

Therefore,

$$\mathbf{y}_j = \alpha^j \mathbf{a}, \qquad j \geq 0,$$

is a solution of the above difference equation. □

Remark 3.5. The premise $\mathbf{y}_0 = \mathbf{a}$ in Prop. 3.4 sets the initial value of the first order finite difference equation $\mathbf{y}_j = \mathbf{A}\mathbf{y}_{j-1}$ to some eigenvector $\mathbf{a}$ of the matrix $\mathbf{A}$. However, if the n eigenvectors of the matrix $\mathbf{A}$ are linearly independent, the premise $\mathbf{y}_0 = \mathbf{a}$ means no loss of generality, since any vector $\mathbf{v} \in \mathbb{C}^n$ can be expressed as a linear combination of the n eigenvectors of $\mathbf{A}$. Hence, at $j = 0$ any vector $\mathbf{v} \in \mathbb{C}^n$ can be expressed as a linear combination of the n solutions $\mathbf{y}_j$.

The matrices $\mathbf{A}$ we will consider in this chapter as well as in the following chapter have mutually distinct eigenvalues and hence, the corresponding eigenvectors of $\mathbf{A}$ are linearly independent. On the other hand, in Chap. 5 where we will analyze the general d-band $\mathbf{k}\cdot\mathbf{p}$-model the eigenvalues are not necessarily distinct and thus, further analysis of the eigenspace is required.

If P_0, E_{g} and E_0 are constant then Eq. (3.28) is a difference equation with constant coefficients, but it is of second order. By using the first order difference operator $\mathrm{D}_h^{\mathrm{fwd}}$ and $\mathrm{D}_h^{\mathrm{bwd}}$, respectively, the matrix $\mathbf{M}^-$ or $\mathbf{M}^+$ vanishes and hence, we obtain a first order difference equation with constant coefficients we can apply Prop. 3.4 to.

3.4.1 One-Sided Finite Difference Schemes

Let us start with the first order forward FDS. We apply the first order forward difference operator $\mathrm{D}_h^{\mathrm{fwd}}$ to the Kane-model (3.1). This gives the coefficient matrices

$$\begin{aligned}\mathbf{M}_j^{+,\mathrm{fwd}} &= \begin{pmatrix} 0 & -\mathrm{i}P_{0,j}\frac{1}{h} \\ -\mathrm{i}P_{0,j}\frac{1}{h} & 0 \end{pmatrix}, \\ \mathbf{M}_j^{0,\mathrm{fwd}} &= \begin{pmatrix} \frac{1}{2}E_{\mathrm{g},j} + E_{0,j} & \mathrm{i}P_{0,j}\frac{1}{h} \\ \mathrm{i}P_{0,j}\frac{1}{h} & -\frac{1}{2}E_{\mathrm{g},j} + E_{0,j} \end{pmatrix}, \\ \mathbf{M}_j^{-,\mathrm{fwd}} &= \mathbf{0}. \end{aligned} \tag{3.29}$$

With these matrices and by assuming that the band gap E_{g} and the middle of the band gap E_0 are constant, Eq. (3.28) can be written in the form

$$\mathbf{F}_{j+1} = \mathbf{A}^{\mathrm{fwd}}\mathbf{F}_j, \qquad j = 0, \ldots, J-1, \tag{3.30}$$

with

$$\begin{aligned}\mathbf{A}^{\mathrm{fwd}} &= -\left(\mathbf{M}^{+,\mathrm{fwd}}\right)^{-1}\left(\mathbf{M}^{0,\mathrm{fwd}} - E\mathbb{1}\right) \\ &= \begin{pmatrix} 1 & -\mathrm{i}\frac{h}{P_0}\left((E_0 - E) - \frac{1}{2}E_{\mathrm{g}}\right) \\ -\mathrm{i}\frac{h}{P_0}\left((E_0 - E) + \frac{1}{2}E_{\mathrm{g}}\right) & 1 \end{pmatrix}.\end{aligned}$$

According to Prop. 3.4, the solution of this first order difference equation is

$$\mathbf{F}_j = \hat{\mathbf{F}}_h \alpha^j,$$

where $\alpha \in \mathbb{C}$ denotes an eigenvalue of $\mathbf{A}^{\mathrm{fwd}}$ and $\hat{\mathbf{F}}_h \in \mathbb{C}^2$ the corresponding eigenvector. Note that we can write the discrete solution $\mathbf{F}_j$ in the form

$$\mathbf{F}_j = \hat{\mathbf{F}}_h e^{\mathrm{i}k_h jh}, \tag{3.31}$$

with the *discrete amplitude* $\hat{\mathbf{F}}_h$ and the *discrete wave vector*

$$k_h = \hat{k}_h + \mathrm{i}\check{k}_h = \frac{1}{h}\left(\arg(\alpha) - \mathrm{i}\ln|\alpha|\right),$$

where $\hat{k}_h$ is called *discrete propagation coefficient* and $\check{k}_h$ is the *discrete attenuation coefficient*. If the discrete attenuation coefficient $\check{k}_h$ is zero the discrete envelope wave $\mathbf{F}_j$ is said to be traveling while it is called evanescent otherwise.

The eigenvalues α of $\mathbf{A}^{\mathrm{fwd}}$ are given by the relation

$$(\alpha - 1)^2 = \frac{h^2}{P_0^2}\left(\frac{1}{4}E_{\mathrm{g}}^2 - (E - E_0)^2\right). \tag{3.32}$$

If we assume that the energy E satisfies the complement of the energy condition (3.8), i.e.

$$|E - E_0| \leq \frac{1}{2}E_{\mathrm{g}},$$

the right hand side of Eq. (3.32) is nonnegative and hence, the roots $\alpha_{1,2}$ of Eq. (3.32) are real, and if

$$h < \frac{P_0}{\sqrt{\frac{1}{4}E_{\mathrm{g}}^2 - (E - E_0)^2}},$$

the roots $\alpha_{1,2}$ are positive. This implies that the wave vectors are purely imaginary and the discrete envelope waves are evanescent.

On the other hand, if the energy condition (3.8) is satisfied, i.e.

$$|E - E_0| > \frac{1}{2}E_\mathrm{g},$$

then the roots $\alpha_{1,2}$ of Eq. (3.32) are complex and read

$$\alpha_{1,2} = 1 \pm \mathrm{i}\frac{h}{P_0}\sqrt{(E-E_0)^2 - \frac{1}{4}E_\mathrm{g}^2}.$$

Since the modulus of the complex eigenvalues $\alpha_{1,2}$ is greater than 1, the discrete wave vector k_h has a nonzero discrete attenuation coefficient $\check{k}_h$ and hence, yields evanescent envelope waves.

However, we require traveling envelope waves to model the continuous case. But both pairs of eigenvalues result in evanescent envelope waves and thus, the first order forward FDS is not applicable to the Kane-model (3.1).

The first order backward FDS with the coefficient matrices

$$\begin{aligned}
\mathbf{M}_j^{+,\mathrm{bwd}} &= \mathbf{0}, \\
\mathbf{M}_j^{0,\mathrm{bwd}} &= \begin{pmatrix} \frac{1}{2}E_{\mathrm{g},j} + E_{0,j} & -\mathrm{i}P_{0,j}\frac{1}{h} \\ -\mathrm{i}P_{0,j}\frac{1}{h} & -\frac{1}{2}E_{\mathrm{g},j} + E_{0,j} \end{pmatrix}, \\
\mathbf{M}_j^{-,\mathrm{bwd}} &= \begin{pmatrix} 0 & \mathrm{i}P_{0,j}\frac{1}{h} \\ \mathrm{i}P_{0,j}\frac{1}{h} & 0 \end{pmatrix},
\end{aligned} \tag{3.33}$$

gives similar results. In this case the eigenvalues α of the matrix

$$\begin{aligned}
\mathbf{A}^\mathrm{bwd} &= -\left(\mathbf{M}^{0,\mathrm{bwd}} - E\mathbb{1}\right)^{-1}\mathbf{M}^{-,\mathrm{bwd}} \\
&= \frac{P_0}{P_0^2 + h^2\left((E-E_0)^2 - \frac{1}{4}E_\mathrm{g}^2\right)} \begin{pmatrix} P_0 & -\mathrm{i}h\left((E_0-E) - \frac{1}{2}E_\mathrm{g}\right) \\ -\mathrm{i}h\left((E_0-E) + \frac{1}{2}E_\mathrm{g}\right) & P_0 \end{pmatrix}
\end{aligned}$$

of the discrete exterior problem read

$$\alpha_{1,2} = \frac{P_0}{P_0^2 + h^2\left((E-E_0)^2 - \frac{1}{4}E_\mathrm{g}^2\right)}\left(P_0 \pm h\sqrt{\frac{1}{4}E_\mathrm{g}^2 - (E-E_0)^2}\right),$$

if the energy E satisfies

$$|E - E_0| \leq \frac{1}{2}E_\mathrm{g},$$

and

$$\alpha_{1,2} = \frac{P_0}{P_0^2 + h^2\left((E-E_0)^2 - \frac{1}{4}E_\mathrm{g}^2\right)}\left(P_0 \pm \mathrm{i}h\sqrt{(E-E_0)^2 - \frac{1}{4}E_\mathrm{g}^2}\right),$$

if the energy E satisfies

$$|E - E_0| > \frac{1}{2}E_\mathrm{g}.$$

Both cases do not yield a pair of real discrete wave vectors and hence, the first order backward FDS is not applicable either.

3.4.2 The Centered Finite Difference Scheme

If we apply the second order centered difference operator $\mathrm{D}_h^{\mathrm{cen}}$ to the Kane-model (3.1) the coefficient matrices become

$$\begin{aligned}
\mathbf{M}_j^{+,\mathrm{cen}} &= \begin{pmatrix} 0 & -\mathrm{i}P_{0,j}\frac{1}{2h} \\ -\mathrm{i}P_{0,j}\frac{1}{2h} & 0 \end{pmatrix}, \\
\mathbf{M}_j^{0,\mathrm{cen}} &= \begin{pmatrix} \frac{1}{2}E_{\mathrm{g},j} + E_{0,j} & 0 \\ 0 & -\frac{1}{2}E_{\mathrm{g},j} + E_{0,j} \end{pmatrix}, \\
\mathbf{M}_j^{-,\mathrm{cen}} &= \begin{pmatrix} 0 & \mathrm{i}P_{0,j}\frac{1}{2h} \\ \mathrm{i}P_{0,j}\frac{1}{2h} & 0 \end{pmatrix}.
\end{aligned} \tag{3.34}$$

Since neither $\mathbf{M}_j^{+,\mathrm{cen}}$ nor $\mathbf{M}_j^{-,\mathrm{cen}}$ vanishes, the difference equation (3.28) is of second order. However, every second order difference equation can be reduced to first order by introducing the substitution

$$\Phi_j = \begin{pmatrix} \mathbf{F}_j \\ \mathbf{F}_{j+1} \end{pmatrix}. \tag{3.35}$$

In the case of a constant Kane-parameter P_0, a constant band gap E_{g} as well as a constant middle of the band gap E_0 and with the help of the substitution (3.35) we get the first order difference equation with constant coefficients

$$\Phi_j = \mathbf{A}^{\mathrm{cen}}\Phi_{j-1}, \tag{3.36}$$

with

$$\begin{aligned}
\mathbf{A}^{\mathrm{cen}} &= \begin{pmatrix} \mathbf{0} & \mathbb{1} \\ (\mathbf{M}^{+,\mathrm{cen}})^{-1}\mathbf{M}^{-,\mathrm{cen}} & (\mathbf{M}^{+,\mathrm{cen}})^{-1}\left(\mathbf{M}^{0,\mathrm{cen}} - E\mathbb{1}\right) \end{pmatrix} \\
&= \begin{pmatrix} 0 & 0 & 1 & 0 \\ 0 & 0 & 0 & 1 \\ 1 & 0 & 0 & -2\mathrm{i}\frac{h}{P_0}\left(E_0 - E - \frac{1}{2}E_{\mathrm{g}}\right) \\ 0 & 1 & -2\mathrm{i}\frac{h}{P_0}\left(E_0 - E + \frac{1}{2}E_{\mathrm{g}}\right) & 0 \end{pmatrix}.
\end{aligned}$$

The solution of the first order difference equation is

$$\Phi_j = \mathbf{a}\alpha^j,$$

where $\alpha \in \mathbb{C}$ denotes an eigenvalue of $\mathbf{A}^{\mathrm{cen}}$ and $\mathbf{a} \in \mathbb{C}^4$ the corresponding eigenvector, cf. Prop. 3.4. Note that the discrete solution $\mathbf{F}_j \in \mathbb{C}^2$ of the second order centered FDS is given by the first two components of $\Phi_j \in \mathbb{C}^4$. Therefore, we introduce the *discrete amplitude* $\hat{\mathbf{F}}_h \in \mathbb{C}^2$ that contains the first two components of $\mathbf{a}$. Then the discrete solution $\mathbf{F}_j$ takes the form

$$\mathbf{F}_j = \hat{\mathbf{F}}_h\alpha^j = \hat{\mathbf{F}}_h e^{\mathrm{i}k_h jh}, \tag{3.37}$$

with the *discrete wave vector*

$$k_h = \hat{k}_h + \mathrm{i}\check{k}_h = \frac{1}{h}\left(\arg(\alpha) - \mathrm{i}\ln|\alpha|\right).$$

Again we shall refer to $\hat{k}_h$ as *discrete propagation coefficient* and $\check{k}_h$ as *discrete attenuation coefficient*.

The form of the discrete solution (3.37) implies

$$\mathbf{F}_{j+1}e^{-\mathrm{i}k_h h} = \mathbf{F}_j = \mathbf{F}_{j-1}e^{\mathrm{i}k_h h},$$

and thus, the difference equation (3.28) reduces to

$$\hat{\mathbf{H}}_h^{\mathrm{cen}}\hat{\mathbf{F}}_h = E\hat{\mathbf{F}}_h, \tag{3.38}$$

with

$$\begin{aligned}\hat{\mathbf{H}}_h^{\mathrm{cen}} &= \hat{\mathbf{H}}_h^{\mathrm{cen}}(k_h)\\ &= \mathbf{M}^{+,\mathrm{cen}}e^{\mathrm{i}k_h h} + \mathbf{M}^{0,\mathrm{cen}} + \mathbf{M}^{-,\mathrm{cen}}e^{-\mathrm{i}k_h h}\\ &= \begin{pmatrix} \frac{1}{2}E_{\mathrm{g}} + E_0 & -\mathrm{i}\frac{1}{2h}P_0\left(e^{\mathrm{i}k_h h} - e^{-\mathrm{i}k_h h}\right)\\ -\mathrm{i}\frac{1}{2h}P_0\left(e^{\mathrm{i}k_h h} - e^{-\mathrm{i}k_h h}\right) & -\frac{1}{2}E_{\mathrm{g}} + E_0\end{pmatrix}\\ &= \begin{pmatrix} \frac{1}{2}E_{\mathrm{g}} + E_0 & \frac{1}{h}P_0\sin k_h h\\ \frac{1}{h}P_0\sin k_h h & -\frac{1}{2}E_{\mathrm{g}} + E_0\end{pmatrix}.\end{aligned}$$

The characteristic polynomial of $\hat{\mathbf{H}}_h^{\mathrm{cen}}$ gives

$$(E - E_0)^2 - \frac{1}{4}E_{\mathrm{g}}^2 - P_0^2\frac{\sin^2 k_h h}{h^2} = 0,$$

which implies that the discrete wave vector k_h satisfies

$$\sin^2 k_h h = \frac{h^2}{P_0^2}\left((E - E_0)^2 - \frac{1}{4}E_{\mathrm{g}}^2\right). \tag{3.39}$$

Let us assume that energy condition (3.8) is fulfilled, i.e.

$$|E - E_0| > \frac{1}{2}E_{\mathrm{g}},$$

then the discrete wave vector is given by the relation

$$\sin k_h h = \pm\frac{h}{P_0}\sqrt{(E - E_0)^2 - \frac{1}{4}E_{\mathrm{g}}^2}.$$

Since

$$\sin(-k_h h) = -\sin(k_h h),$$

the wave vector reads

$$k_h = \pm\hat{k}_h \in \mathbb{R}, \tag{3.40}$$

with

$$\hat{k}_h = \frac{1}{h}\arcsin\left(\frac{h}{P_0}\sqrt{(E - E_0)^2 - \frac{1}{4}E_{\mathrm{g}}^2}\right) + n\frac{2\pi}{h}, \qquad n \in \mathbb{Z}.$$

However, by applying l'Hôpital's rule it is easy to show that the discrete wave vector $k_h = \pm\hat{k}_h$ only tends to the analytical wave vector $k = \pm\mathrm{i}\hat{k}$ of the continuous problem if $n = 0$, whereas for $n \neq 0$ the limit of $k_h = \pm\hat{k}_h$ for $h \to 0$ does not exist. Thus, we shall neglect solutions of the discrete wave vector with $n \neq 0$ and set

$$\hat{k}_h = \frac{1}{h}\arcsin\left(\frac{h}{P_0}\sqrt{(E - E_0)^2 - \frac{1}{4}E_{\mathrm{g}}^2}\right). \tag{3.41}$$

On the other hand, if the complement of the energy condition (3.8) is fulfilled, i.e.

$$|E - E_0| \leq \frac{1}{2}E_{\mathrm{g}},$$

the discrete wave vector k_h satisfies

$$\sin k_h h = \pm \mathrm{i} \frac{h}{P_0} \sqrt{\frac{1}{4} E_\mathrm{g}^2 - (E - E_0)^2}.$$

By using the identity $\sin k_h h = -\mathrm{i} \sinh \mathrm{i} k_h h$, we get

$$\sinh \mathrm{i} k_h h = \pm \frac{h}{P_0} \sqrt{\frac{1}{4} E_\mathrm{g}^2 - (E - E_0)^2}.$$

Considering that $\sinh(-\mathrm{i} k_h h) = -\sinh(i k_h h)$ and $\operatorname{arsinh}(x) = \ln\left(x + \sqrt{x^2+1}\right)$ for $x \in \mathbb{R}$, the discrete wave vector is purely imaginary and reads

$$k_h = \pm \mathrm{i} \check{k}_h, \tag{3.42}$$

with the discrete attenuation coefficient

$$\check{k} = \frac{1}{h} \ln\left(z + \sqrt{z^2+1}\right),$$

and

$$z = \frac{h}{P_0} \sqrt{\frac{1}{4} E_\mathrm{g}^2 - (E - E_0)^2} \in \mathbb{R}.$$

Hence, under the assumption (3.10) we obtain two evanescent envelope waves, one decaying for $x \to -\infty$ and the other one decaying for $x \to \infty$.

Eqs. (3.40) and (3.42) form the so-called *discrete dispersion relations* of the second order centered FDS. From the characteristic polynomial of $\hat{\mathbf{H}}_h^{\mathrm{cen}}$ we can derive the reciprocal form

$$E = E_h^{\mathrm{e/h}}(k) = E_0 \pm \sqrt{\frac{1}{4} E_\mathrm{g}^2 + P_0^2 \frac{\sin^2 k_h h}{h^2}}. \tag{3.43}$$

Analogously to the continuous case, the energy E_h^{e} associated with the positive sign in Eq. (3.43) denotes the energy of the electrons, while E_h^{h} corresponding to the negative sign in Eq. (3.43) describes the energy of the holes. Clearly, $E_h^{\mathrm{e/h}}(k_h)$ satisfies the energy condition (3.8) if and only if the discrete wave vector k_h is real. In this case, i.e. in the case of discrete traveling envelope waves, we will refer to the energy E_h^{e} as the energy of the conduction band and the energy E_h^{h} as the energy of the valence band.

In order to finish the analysis of the discrete exterior problem we will now specify the discrete amplitude $\hat{\mathbf{F}}_h(k_h)$. We know that the amplitude

$$\hat{\mathbf{F}}_h(k_h) = \hat{\mathbf{F}}_h^{\mathrm{e/h}}(k_h) = \begin{pmatrix} \hat{F}_{h,\mathrm{c}}^{\mathrm{e/h}}(k_h) \\ \hat{F}_{h,\mathrm{v}}^{\mathrm{e/h}}(k_h) \end{pmatrix},$$

is an eigenvector of $\hat{\mathbf{H}}_h^{\mathrm{cen}}(k_h)$ with the corresponding energy eigenvalue $E_h^{\mathrm{e/h}}(k_h)$. Hence, the discrete amplitude is not defined uniquely and solves the under-determined linear equation

$$\left(\hat{H}_{h,11}^{\mathrm{cen}}(k_h) - E_h^{\mathrm{e/h}}(k_h)\right) \hat{F}_{h,\mathrm{c}}^{\mathrm{e/h}}(k_h) + \hat{H}_{h,12}^{\mathrm{cen}}(k_h) \hat{F}_{h,\mathrm{v}}^{\mathrm{e/h}}(k_h) = 0. \tag{3.44}$$

Thus, the discrete amplitude reads

$$\hat{\mathbf{F}}_h^{\mathrm{e/h}}(k_h) = c \begin{pmatrix} \hat{H}_{h,12}^{\mathrm{cen}}(k_h) \\ E_h^{\mathrm{e/h}}(k_h) - \hat{H}_{h,11}^{\mathrm{cen}}(k_h) \end{pmatrix} = c \begin{pmatrix} P_0 \frac{\sin k_h h}{h} \\ E_h^{\mathrm{e/h}}(k_h) - \frac{1}{2} E_\mathrm{g} - E_0 \end{pmatrix}, \tag{3.45}$$

with some arbitrary $c \in \mathbb{C}$. Note that $\mathbf{F}_j^{\mathrm{e}}(k_h) = \hat{\mathbf{F}}_h^{\mathrm{e}}(k_h)e^{\pm \mathrm{i}k_h jh}$ describes the energy eigenstate associated with the energy E_h^{e} of the electrons while $\mathbf{F}_j^{\mathrm{h}}(k_h) = \hat{\mathbf{F}}_h^{\mathrm{h}}(k_h)e^{\pm \mathrm{i}k_h jh}$ corresponds to the energy E_h^{h} of the holes, see Eq. (3.43).

If $|E - E_0| > \frac{1}{2}E_{\mathrm{g}}$ is fulfilled the resulting discrete wave vectors are real, yielding discrete traveling envelope waves. In this case we shall additionally assume that the discrete waves are unitary, i.e. the discrete amplitude $\hat{\mathbf{F}}_h^{\mathrm{e/h}}(\hat{k}_h)$ has norm 1. Then it also satisfies the normalization condition

$$\left\|\hat{\mathbf{F}}^{\mathrm{e/h}}(\hat{k}_h)\right\|_{\mathbb{C}}^2 = \left\langle \hat{\mathbf{F}}^{\mathrm{e/h}}(\hat{k}_h), \overline{\hat{\mathbf{F}}^{\mathrm{e/h}}(\hat{k}_h)} \right\rangle = 1. \tag{3.46}$$

Since $\hat{\mathbf{H}}_h^{\mathrm{cen}}(\hat{k}_h)$ and its eigenvalues $E_h^{\mathrm{e/h}}(\hat{k}_h)$ are real-valued the eigenvectors $\hat{\mathbf{F}}_h^{\mathrm{e/h}}(\hat{k}_h)$ are either also real-valued or purely imaginary. But since our approach in Eq. (3.37) implies that $\hat{\mathbf{F}}_h^{\mathrm{e/h}}(\hat{k}_h)$ is the modulus of $\mathbf{F}_j$, we shall assume that the discrete amplitude $\hat{\mathbf{F}}_h^{\mathrm{e/h}}(\hat{k}_h)$ is real. Hence, the normalization condition (3.46) becomes

$$\hat{F}_{h,\mathrm{c}}^{\mathrm{e/h}}(\hat{k}_h)^2 + \hat{F}_{h,\mathrm{v}}^{\mathrm{e/h}}(\hat{k}_h)^2 = 1. \tag{3.47}$$

Thus, the amplitude $\hat{\mathbf{F}}_h^{\mathrm{e/h}}(\hat{k}_h)$ of the discrete traveling envelope wave with norm 1 reads

$$\begin{aligned}\hat{\mathbf{F}}_h^{\mathrm{e/h}}(\hat{k}_h) &= \pm \begin{pmatrix} \frac{\hat{H}_{h,12}^{\mathrm{cen}}(\hat{k}_h)}{\sqrt{\left(E_h^{\mathrm{e/h}}(\hat{k}_h) - \hat{H}_{h,11}^{\mathrm{cen}}(\hat{k}_h)\right)^2 + \hat{H}_{h,12}^{\mathrm{cen}}(\hat{k}_h)^2}} \\ \frac{E_h^{\mathrm{e/h}}(\hat{k}_h) - \hat{H}_{h,11}^{\mathrm{cen}}(\hat{k}_h)}{\sqrt{\left(E_h^{\mathrm{e/h}}(\hat{k}_h) - \hat{H}_{h,11}^{\mathrm{cen}}(\hat{k}_h)\right)^2 + \hat{H}_{h,12}^{\mathrm{cen}}(\hat{k}_h)^2}} \end{pmatrix} \\ &= \pm \begin{pmatrix} \frac{P_0 \frac{\sin \hat{k}_h h}{h}}{\sqrt{\left(E_h^{\mathrm{e/h}}(\hat{k}_h) - \frac{1}{2}E_{\mathrm{g}} - E_0\right)^2 + P_0^2 \frac{\sin^2 \hat{k}_h h}{h^2}}} \\ \frac{E_h^{\mathrm{e/h}}(\hat{k}_h) - \frac{1}{2}E_{\mathrm{g}} - E_0}{\sqrt{\left(E_h^{\mathrm{e/h}}(\hat{k}_h) - \frac{1}{2}E_{\mathrm{g}} - E_0\right)^2 + P_0^2 \frac{\sin^2 \hat{k}_h h}{h^2}}} \end{pmatrix}. \end{aligned} \tag{3.48}$$

Since the two solutions in Eq. (3.48) of the amplitude are linearly dependent, we can neglect the solution with negative sign and set

$$\hat{\mathbf{F}}_h^{\mathrm{e/h}}(\hat{k}_h) = \begin{pmatrix} \frac{P_0 \frac{\sin \hat{k}_h h}{h}}{\sqrt{\left(E_h^{\mathrm{e/h}}(\hat{k}_h) - \frac{1}{2}E_{\mathrm{g}} - E_0\right)^2 + P_0^2 \frac{\sin^2 \hat{k}_h h}{h^2}}} \\ \frac{E_h^{\mathrm{e/h}}(\hat{k}_h) - \frac{1}{2}E_{\mathrm{g}} - E_0}{\sqrt{\left(E_h^{\mathrm{e/h}}(\hat{k}_h) - \frac{1}{2}E_{\mathrm{g}} - E_0\right)^2 + P_0^2 \frac{\sin^2 \hat{k}_h h}{h^2}}} \end{pmatrix}. \tag{3.49}$$

In the remainder of this section, let us analyze the periodicity of the discrete dispersion relation of the centered FDS and compare it with the periodicity of the discrete envelope function. Let us focus on traveling envelope waves with a real wave vector $k_h \in \mathbb{R}$. The discrete amplitude satisfies

$$\hat{\mathbf{F}}_h^{\mathrm{e/h}}\left(k_h + n\frac{2\pi}{h}\right) = \hat{\mathbf{F}}_h^{\mathrm{e/h}}(k_h), \qquad \forall n \in \mathbb{Z}, k_h \in \mathbb{R}, \tag{3.50}$$

and hence, it has a period of $2\frac{\pi}{h}$ in k_h. Thus, the discrete envelope function

$$\mathbf{F}_j = \hat{\mathbf{F}}_h^{\mathrm{e/h}}(k_h)e^{\mathrm{i}k_h jh}$$

is $\frac{2\pi}{h}$-periodic in k_h. On the other hand, the discrete dispersion relation of the centered FDS satisfies

$$E_h^{\mathrm{e/h}}\left(k_h + n\frac{\pi}{h}\right) = E_h^{\mathrm{e/h}}(k_h), \qquad \forall n \in \mathbb{Z}, k_h \in \mathbb{R}, \tag{3.51}$$

i.e. the discrete dispersion relation is $\frac{\pi}{h}$-periodic in k_h. Fig. 3.1 in the following section demonstrates this behavior. It shows a comparison of the discrete dispersion relation of the centered FDS with the analytical dispersion relation and the discrete dispersion relation of the symmetrized FDS we will introduce in the following section.

Since the discrete envelope function is $2\frac{\pi}{h}$-periodic we shall focus on the interval $\left(-\frac{\pi}{h}, \frac{\pi}{h}\right)$. Recall that solutions with $k_h < 0$ are left-traveling, while solutions with $k_h > 0$ are right-traveling. Both the discrete envelope function as well as the discrete dispersion relation of the centered FDS are even functions and hence, without loss of generality we shall restrict our considerations to the interval $\left(0, \frac{\pi}{h}\right)$ of right-traveling solutions. But since the discrete dispersion relation is $\frac{\pi}{h}$-periodic with a maximum at $k_h = \frac{\pi}{2h}$ it is not injective in this domain. Without loss of generality, let us focus on the electron energy $E = E^{\mathrm{e}}$. Thus, for any energy E with

$$E_0 + \frac{1}{2}E_{\mathrm{g}} = E_h^{\mathrm{e}}(0) = \min_{k_h \in \mathbb{R}} E_h^{\mathrm{e}}(k_h) < E < \max_{k_h \in \mathbb{R}} E_h^{\mathrm{e}}(k_h) = E_h^{\mathrm{e}}\left(\frac{\pi}{2h}\right),$$

there are exactly two discrete wave vectors k_h in the interval $\left(0, \frac{\pi}{h}\right)$ that solve the discrete dispersion relation. These discrete wave vectors are given by

$$k_{h,1} = \frac{1}{h}\arcsin\left(\frac{h}{P_0}\sqrt{(E - E_0)^2 - \frac{1}{4}E_{\mathrm{g}}^2}\right),$$

see Eq. (3.40), and

$$k_{h,2} = \frac{\pi}{h} - k_{h,1}.$$

This implies that for any admissible energy E there exist two solutions of the discrete envelope function

$$\mathbf{F}_j = \hat{\mathbf{F}}_h^{\mathrm{e/h}}(k_{h,1})e^{\mathrm{i}k_{h,1}jh} \tag{3.52a}$$

and

$$\mathbf{F}_j = \hat{\mathbf{F}}_h^{\mathrm{e/h}}(k_{h,2})e^{\mathrm{i}k_{h,2}jh} = \hat{\mathbf{F}}_h^{\mathrm{e/h}}\left(\frac{\pi}{h} - k_{h,1}\right)e^{\mathrm{i}\left(\frac{\pi}{h} - k_{h,1}\right)jh}. \tag{3.52b}$$

However, only the first solution (3.52a) is an appropriate estimate of the analytical solution since the wave vector $k_{h,2} = \frac{\pi}{h} - k_{h,1}$ does not tend to the analytical wave k for $h \to 0$ while the wave vector $k_{h,1}$ does, as described above.

Note that the same is true for left-traveling solutions in the interval $\left(-\frac{\pi}{h}, 0\right)$ and hence, for any admissible energy E there are exactly two positive and two negative wave vectors k_h in the domain $\left(-\frac{\pi}{h}, \frac{\pi}{h}\right)$ that solve the discrete dispersion relation. All other solutions of the discrete wave vector that are not in the domain $\left(-\frac{\pi}{h}, \frac{\pi}{h}\right)$ can be ascribed to the four solutions in $\left(-\frac{\pi}{h}, \frac{\pi}{h}\right)$.

What does this mean for the numerical result of a certain problem? We know that the discrete solution of the centered FDS within a domain of a constant Kane-parameter P_0, a constant band gap E_{g} and a constant middle of the band gap E_0 is

$$\mathbf{F}_j = \hat{\mathbf{F}}_h^{\mathrm{e/h}}(k_h)e^{\mathrm{i}k_h jh},$$

with some discrete wave vector k_h that satisfies the discrete dispersion relation (3.43) and a discrete amplitude $\hat{\mathbf{F}}_h^{\mathrm{e/h}}(k_h)$ of the form as given in Eq. (3.48). Hence, if we apply the centered FDS to an example where these parameters are constant we do not expect solutions of the incorrect form (3.52b) since the DTBCs we will derive later define the discrete wave vector in the inner part of the semiconductor. For simplicity let us denote the correct discrete wave vector $k_{h,1}$ by k_h. When using this discrete wave vector instead of $\frac{\pi}{h} - k_h$ to form the DTBCs, the discrete solution of a problem with constant parameters P_0, E_{g} and E_0 is in fact

$$\mathbf{F}_j = \hat{\mathbf{F}}_h^{\mathrm{e/h}}(k_h)e^{\mathrm{i}k_h jh},$$

which tends to the analytical solution for $h \to 0$. However, if we allow the parameters to vary along the computational interval we expect some complications. For example, let us consider a semiconductor heterostructure with a single barrier potential, where the Kane-parameter P_0 and the band gap E_g are constant whereas the middle of the band gap E_0 is piecewise constant. Then we know that the solution in each of the three subdomains takes the form

$$\mathbf{F}_j = \hat{\mathbf{F}}_h^{\mathrm{e/h}}(k_h) e^{\mathrm{i}k_h jh},$$

where the discrete wave vector k_h and the discrete amplitude $\hat{\mathbf{F}}_h^{\mathrm{e/h}}(k_h)$ are constant within each subdomain but differ between these subdomains. Now let us consider an incoming wave, entering the semiconductor at $x = 0$. This envelope wave is reflected at the barrier. While the DTBCs define the discrete wave vector of the incoming envelope wave, the discrete wave vector of the reflected envelope wave is not defined uniquely. Instead the numerical solver gives a solution inside the left subdomain that reads

$$\mathbf{F}_j = \hat{\mathbf{F}}_h^{\mathrm{e/h}}(k_h) e^{\mathrm{i}k_h jh} + r_1 \hat{\mathbf{F}}_h^{\mathrm{e/h}}(-k_h) e^{-\mathrm{i}k_h jh} + r_2 \hat{\mathbf{F}}_h^{\mathrm{e/h}}(\frac{\pi}{h} - k_h) e^{-\mathrm{i}(\frac{\pi}{h} - k_h) jh},$$

with some reflection coefficients r_1 and r_2. The correct discrete solution does not comprise terms with the incorrect wave vector $\frac{\pi}{h} - k_h$, i.e. $r_2 = 0$. In general, the numerical solver does not set $r_2 = 0$, and hence the numerical solution comprises terms with the incorrect wave vector $\frac{\pi}{h} - k_h$ that we will refer to as *spurious oscillations*. The same is true for the second subdomain, while the solution in the right subdomain is defined uniquely by the right DTBC since we do not expect a reflection at the boundary at $x = L$. However, the amplitude of the solution in the right subdomain, that is equal to the transmission coefficient, might differ significantly from the analytical solution since the sum of the squared norms of all resulting transmission and reflection coefficients including those yielding the spurious oscillations is equal to the squared norm of the incoming envelope function. This means that if the reflection coefficients yielding the spurious oscillations are nonzero the discrete transmission coefficient differs significantly from the analytical transmission coefficient.

Before we will test this behavior of the centered FDS we will introduce an alternative FDS in the following section that prevents the problem of the periodicity of the discrete dispersion relation.

3.4.3 The Symmetrized Finite Difference Scheme

Let us introduce a combined backward and forward FDS, that we will refer to as *symmetrized FDS*. It is an approach to find a discrete dispersion relation and a discrete solution with the same periodicity. We apply the left-sided operator $\mathrm{D}_h^{\mathrm{bwd}}$ to the coupling in the first column of the Hamiltonian $\mathbf{H}$ whereas we apply the right-sided operator $\mathrm{D}_h^{\mathrm{fwd}}$ to the coupling in the second column of $\mathbf{H}$. This gives the coefficient matrices

$$\begin{aligned}
\mathbf{M}_j^{+,\mathrm{sym}} &= \begin{pmatrix} 0 & -\mathrm{i}P_{0,j}\frac{1}{h} \\ 0 & 0 \end{pmatrix}, \\
\mathbf{M}_j^{0,\mathrm{sym}} &= \begin{pmatrix} \frac{1}{2}E_{\mathrm{g},j} + E_{0,j} & \mathrm{i}P_{0,j}\frac{1}{h} \\ -\mathrm{i}P_{0,j}\frac{1}{h} & -\frac{1}{2}E_{\mathrm{g},j} + E_{0,j} \end{pmatrix}, \\
\mathbf{M}_j^{-,\mathrm{sym}} &= \begin{pmatrix} 0 & 0 \\ \mathrm{i}P_{0,j}\frac{1}{h} & 0 \end{pmatrix}.
\end{aligned} \tag{3.53}$$

However, $\mathbf{M}^{+,\mathrm{sym}}$ is not regular and hence, we cannot transform the second order difference equation into a difference equation of order one. In order to perform this transformation a regularization term is needed. This regularization term leads us to the next step of generalization of the multi-band effective mass approximations and is discussed later in Chap. 4.

Nevertheless, we shall assume that the discrete solution takes the form

$$\mathbf{F}_j = \hat{\mathbf{F}}_h e^{\mathrm{i}k_h jh}, \tag{3.54}$$

with the *discrete wave vector*

$$k_h = \hat{k}_h + \mathrm{i}\check{k} \in \mathbb{C},$$

and the discrete amplitude $\hat{\mathbf{F}}_h \in \mathbb{C}^2$. Note that in contrast to the centered FDS, this approach is mathematically not evident.

The form of the discrete solution (3.54) implies

$$\mathbf{F}_{j+1} e^{-\mathrm{i}k_h h} = \mathbf{F}_j = \mathbf{F}_{j-1} e^{\mathrm{i}k_h h},$$

and thus, applied to the difference equation (3.28) it yields

$$\hat{\mathbf{H}}_h^{\mathrm{sym}} \hat{\mathbf{F}}_h = E \hat{\mathbf{F}}_h, \tag{3.55}$$

with

$$\begin{aligned}
\hat{\mathbf{H}}_h^{\mathrm{sym}} &= \hat{\mathbf{H}}_h^{\mathrm{sym}}(k_h) \\
&= \mathbf{M}^{+,\mathrm{sym}} e^{\mathrm{i}k_h h} + \mathbf{M}^{0,\mathrm{sym}} + \mathbf{M}^{-,\mathrm{sym}} e^{-\mathrm{i}k_h h} \\
&= \begin{pmatrix} \frac{1}{2}E_{\mathrm{g}} + E_0 & -\mathrm{i}\frac{1}{h}P_0\left(e^{\mathrm{i}k_h h} - 1\right) \\ -\mathrm{i}\frac{1}{h}P_0\left(1 - e^{-\mathrm{i}k_h h}\right) & -\frac{1}{2}E_{\mathrm{g}} + E_0 \end{pmatrix} \\
&= \begin{pmatrix} \frac{1}{2}E_{\mathrm{g}} + E_0 & \frac{1}{h}P_0\left(-\sin k_h h - \mathrm{i}\left(1 - \cos k_h h\right)\right) \\ \frac{1}{h}P_0\left(-\sin k_h h + \mathrm{i}\left(1 - \cos k_h h\right)\right) & -\frac{1}{2}E_{\mathrm{g}} + E_0 \end{pmatrix}.
\end{aligned}$$

By analyzing the characteristic polynomial

$$\begin{aligned}
0 &= (E - E_0)^2 - \frac{1}{4}E_{\mathrm{g}}^2 - \frac{1}{h^2}P_0^2\left(\sin^2 k_h h + \left(1 - \cos k_h h\right)^2\right) \\
&= (E - E_0)^2 - \frac{1}{4}E_{\mathrm{g}}^2 - \frac{4}{h^2}P_0^2 \sin^2 \frac{k_h h}{2},
\end{aligned}$$

of $\hat{\mathbf{H}}_h^{\mathrm{sym}}$ which implies

$$\sin^2 \frac{k_h h}{2} = \frac{h^2}{4P_0^2}\left((E - E_0)^2 - \frac{1}{4}E_{\mathrm{g}}^2\right), \tag{3.56}$$

and proceeding analogously to the derivation of the discrete wave vector k_h of the centered FDS, we end up with the following discrete wave vectors of the symmetrized FDS.

If the energy condition (3.8) is fulfilled, i.e.

$$|E - E_0| > \frac{1}{2}E_{\mathrm{g}},$$

the discrete wave vector k_h is real and reads

$$k_h = \pm\hat{k}_h \in \mathbb{R}, \tag{3.57}$$

with the propagation coefficient

$$\hat{k}_h = \frac{2}{h}\arcsin\left(\frac{h}{2P_0}\sqrt{(E - E_0)^2 - \frac{1}{4}E_{\mathrm{g}}^2}\right).$$

On the other hand, if the energy condition (3.8) is not fulfilled, i.e.

$$|E - E_0| \leq \frac{1}{2}E_{\mathrm{g}},$$

then the discrete wave vector k_h is purely imaginary and takes the form

$$k_h = \pm \mathrm{i}\check{k}_h, \tag{3.58}$$

with the discrete attenuation coefficient

$$\check{k} = \frac{2}{h} \ln\left(z + \sqrt{z^2+1}\right),$$

where $z \in \mathbb{R}$ is given by

$$z = \frac{h}{2P_0}\sqrt{\frac{1}{4}E_\mathrm{g}^2 - (E-E_0)^2}.$$

The reciprocal of the dispersion relations (3.57) and (3.58) can be derived directly from the characteristic polynomial of $\hat{\mathbf{H}}_h^{\mathrm{sym}}$. We get

$$E = E_h^{\mathrm{e/h}}(k) = E_0 \pm \sqrt{\frac{1}{4}E_\mathrm{g}^2 + \frac{4}{h^2}P_0^2 \sin^2\frac{k_h h}{2}}, \tag{3.59}$$

where the positive sign corresponds to the energy E_h^{e} of the electrons while the negative sign is associated with the energy E_h^{h} of the holes.

No we will specify the discrete amplitude $\hat{\mathbf{F}}_h(k_h)$ of the symmetrized FDS. Analogously to the centered FDS the discrete amplitude

$$\hat{\mathbf{F}}_h(k_h) = \hat{\mathbf{F}}_h^{\mathrm{e/h}}(k_h) = \begin{pmatrix} \hat{F}_{h,\mathrm{c}}^{\mathrm{e/h}}(k_h) \\ \hat{F}_{h,\mathrm{v}}^{\mathrm{e/h}}(k_h) \end{pmatrix},$$

is given by

$$\hat{\mathbf{F}}_h^{\mathrm{e/h}}(k_h) = c\begin{pmatrix} \hat{H}_{h,12}^{\mathrm{sym}}(k_h) \\ E_h^{\mathrm{e/h}}(k_h) - \hat{H}_{h,11}^{\mathrm{sym}}(k_h) \end{pmatrix} = c\begin{pmatrix} \frac{1}{h}P_0\left(\sin k_h h + \mathrm{i}\left(1-\cos k_h h\right)\right) \\ E_h^{\mathrm{e/h}}(k_h) - \frac{1}{2}E_\mathrm{g} - E_0 \end{pmatrix}, \tag{3.60}$$

with some arbitrary $c \in \mathbb{C}$. Note that $\mathbf{F}_j^{\mathrm{e}}(k_h) = \hat{\mathbf{F}}_h^{\mathrm{e}}(k_h)e^{\pm \mathrm{i}k_h jh}$ is the energy eigenstate associated with the energy E_h^{e} of the electrons while $\mathbf{F}_j^{\mathrm{h}}(k_h) = \hat{\mathbf{F}}_h^{\mathrm{h}}(k_h)e^{\pm \mathrm{i}k_h jh}$ corresponds to the energy E_h^{h} of the holes, see Eq. (3.59).

Let us additionally assume that the discrete waves are unitary, i.e. the discrete amplitude $\hat{\mathbf{F}}_h^{\mathrm{e/h}}(\hat{k}_h)$ has norm 1. Then it also satisfies the normalization condition

$$\left\|\hat{\mathbf{F}}^{\mathrm{e/h}}(\hat{k}_h)\right\|_{\mathbb{C}}^2 = \left\langle \hat{\mathbf{F}}^{\mathrm{e/h}}(\hat{k}_h), \overline{\hat{\mathbf{F}}^{\mathrm{e/h}}(\hat{k}_h)}\right\rangle = 1,$$

and the constant c is determined by

$$\begin{aligned} c &= \left(\hat{F}_{h,\mathrm{c}}^{\mathrm{e/h}}(k_h)\overline{\hat{F}_{h,\mathrm{c}}^{\mathrm{e/h}}(k_h)} + \hat{F}_{h,\mathrm{v}}^{\mathrm{e/h}}(k_h)\overline{\hat{F}_{h,\mathrm{v}}^{\mathrm{e/h}}(k_h)}\right)^{-1/2} \\ &= \left(\frac{4}{h^2}P_0^2\sin^2\frac{k_h h}{2} + \left(E_h^{\mathrm{e/h}}(k_h) - \frac{1}{2}E_\mathrm{g} - E_0\right)^2\right)^{-1/2}. \end{aligned}$$

The discrete amplitude of a traveling envelope wave of the symmetrized FDS is not real-valued. While the valence band component is real, the conduction band component is complex if $h \neq n\frac{2\pi}{k_h}$, $n \in \mathbb{N}$. Thus, the resulting discrete wave is not plane since the two components have a different phase. This indicates that the approach (3.54) we could not prove mathematically leads to physically incorrect solutions. However, the numerical examples in the following sections show that the symmetrized scheme gives reasonable results.

Finally, we note that the periodicities of the discrete dispersion relation of the symmetrized FDS and the discrete envelope function are in fact the same, which is not the case for the centered FDS. Both, the discrete dispersion relation and the discrete envelope function of the symmetrized FDS are $2\frac{\pi}{h}$-periodic in k_h, see Eqs. (3.59) and (3.60). However, it is important to note that the discrete dispersion relation, which is again an even function, is injective in the interval $\left(0, \frac{\pi}{h}\right)$. This means that for any admissible energy E there exists only one positive and one negative discrete wave vector k_h in $\left(-\frac{\pi}{h}, \frac{\pi}{h}\right)$, that solves the discrete dispersion relation of the symmetrized FDS. Hence, we do not expect any spurious oscillations due to incorrect wave vectors as we do for the centered FDS.

This behavior is illustrated in Fig. 3.1 that shows a comparison of the discrete dispersion relation of the symmetrized FDS with the analytical dispersion relation and the discrete dispersion relation of the centered FDS for a step size $h = 1/300$, a Kane-parameter $P_0 \equiv 1$, a band gap $E_\mathrm{g} \equiv 200$ and a middle of the band gap $E_0 \equiv 0$.

3.5 Discrete Transparent Boundary Conditions

We derive the DTBCs for the Kane-model by applying the discrete solution with the discrete amplitudes (3.49) and (3.60) as well as the discrete wave vectors (3.41) and (3.57) to the reflection and transmission conditions (3.22) and (3.23). We assume that these conditions hold in a small vicinity of the two boundaries, i.e. $j = 0, 1$ and $j = J-1, J$ respectively. Let $\hat{k}_{h,0}$ denote the propagation coefficient of the discrete wave vector and $\hat{\mathbf{F}}_{h,0}(\hat{k}_{h,0})$ the corresponding discrete amplitude of a traveling discrete envelope wave in the left exterior domain $x \leq 0$. On the other hand, let $\hat{k}_{h,L}$ denote the propagation coefficient of the discrete wave vector and $\hat{\mathbf{F}}_{h,L}(\hat{k}_{h,L})$ the corresponding discrete amplitude of a traveling discrete envelope wave in the right exterior domain $x \geq L$. Thus, we have

$$\mathbf{F}_j = \mathbf{F}_j^{\mathrm{in}} + \mathbf{F}_j^{\mathrm{r}} = \hat{\mathbf{F}}_{h,0} e^{\mathrm{i}\hat{k}_{h,0} x_j} + \mathbf{r} e^{-\mathrm{i}\hat{k}_{h,0} x_j}, \qquad j = 0, 1,$$

and

$$\mathbf{F}_j = \mathbf{F}_j^{\mathrm{t}} = \mathbf{t} e^{\mathrm{i}\hat{k}_{h,L} x_j}, \qquad j = J-1, J,$$

with $\mathbf{r} = r\hat{\mathbf{F}}_{h,0}(-\hat{k}_{h,0})$, $r \in \mathbb{C}$, and $\mathbf{t} = t\hat{\mathbf{F}}_{h,L}(\hat{k}_{h,L})$, $t \in \mathbb{C}$. By eliminating the reflection and transmission coefficients we obtain the DTBCs

$$-\mathbf{F}_0 e^{-\mathrm{i}\hat{k}_{h,0} h} + \mathbf{F}_1 = \hat{\mathbf{F}}_{h,0} 2\mathrm{i} \sin \hat{k}_{h,0} h, \tag{3.61a}$$

and

$$\mathbf{F}_{J-1} e^{\mathrm{i}\hat{k}_{h,L} h} - \mathbf{F}_J = \mathbf{0}, \tag{3.61b}$$

compared to the scalar DTBCs in Eq. (2.29).

Remark 3.6. Note that the discrete formulation of the two-band Kane-model as given in Eq. (3.28) together with the DTBCs (3.61) has a unique solution for all considered examples, i.e. the band matrix consisting of the coefficients of Eq. (3.28) for $j = 1, \ldots, J-1$, and the two DTBCs is regular. It remains to prove a general existence theorem for the discrete problem. However, this proof is not a discrete analogon of Cor. 3.3 since we can not reduce the discrete problem of the Kane-model to a problem that is equivalent to the scalar discrete problem.

3.6 Numerical Examples

3.6.1 The Free Scattering State

In a first numerical example we briefly analyze the numerical results of the centered FDS and the symmetrized FDS in the case of the free scattering state. In particular we are interested if

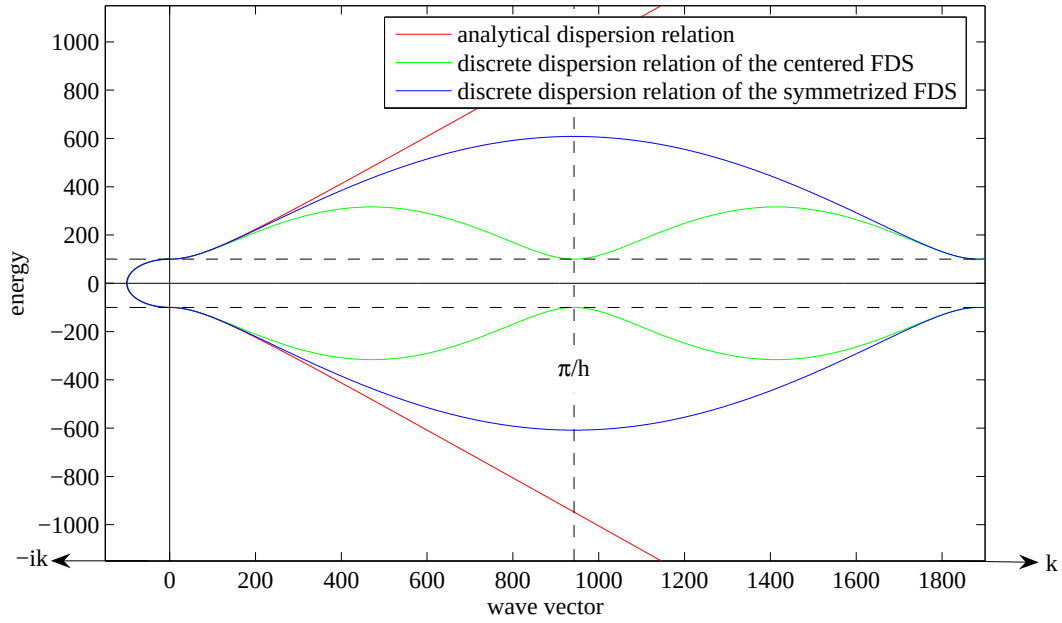

(a) Discrete and analytical dispersion relations.

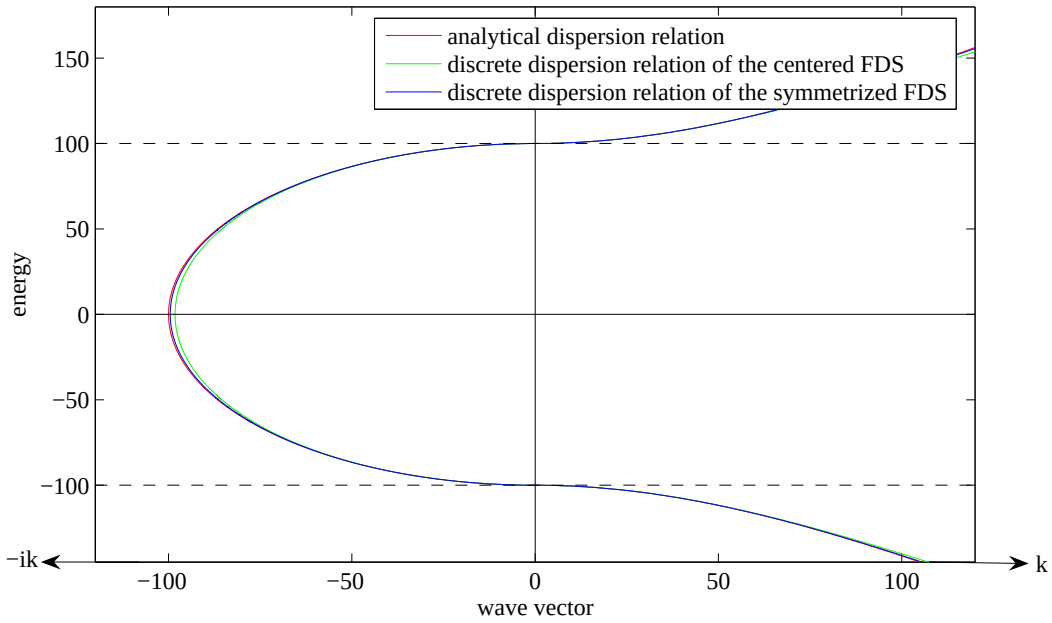

(b) Detail view of (a).

Figure 3.1: Comparison of the analytical dispersion relation (red) of the Kane-model and the discrete dispersion relations of the centered FDS (green) and the symmetrized FDS (blue) for a step size $h = 1/300$, a Kane-parameter $P_0 \equiv 1$, a band gap $E_g \equiv 200$ and a middle of the band gap $E_0 \equiv 0$. The horizontal dashed lines indicate the level of the energy values $E = E_g/2$ and $E = -E_g/2$. The negative wave vector axis corresponds to the purely imaginary wave vector $k = \mathrm{i}\check{k}$ of evanescent envelope waves while the positive wave vector axis corresponds to the real wave vector $k = \hat{k}$ of traveling envelope waves. The vertical dashed line in (a) indicates the the location of the wave vector value $k = \pi/h$.

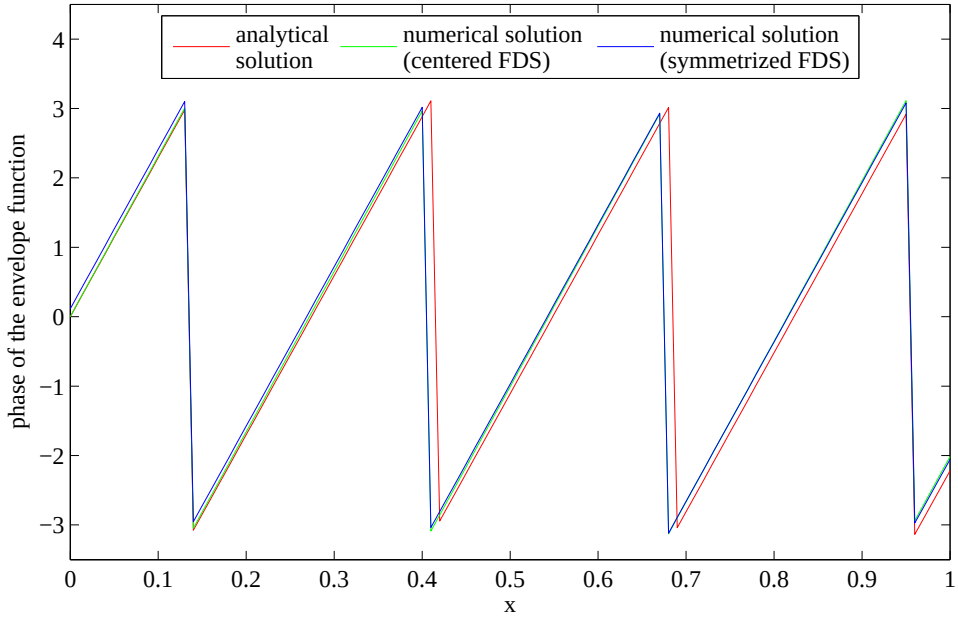

Figure 3.2: Comparison of the phases of the analytical solution (red) and the numerical solutions of the centered FDS (green) and the symmetrized FDS (blue) for the free scattering state with $P_0 \equiv 1$, $E_\mathrm{g} \equiv 20$, $E_0 \equiv 0$, a step size $h = 1/100$ and an energy $E = 25$.

the results of the centered FDS in fact do not oscillate in the free scattering state. Moreover, we want to check if the symmetrized FDS delivers acceptable results although it does not give plane waves in the discrete exterior problem.

We shall set $P_0 \equiv 1$, $E_0(x) \equiv 20$, $E_\mathrm{g}(x) \equiv 0$ and $E = 25$.

The analytical solution of the free scattering state has norm 1. Both the centered FDS and the symmetrized FDS using the corresponding DTBCs give results with norm 1 without any oscillations. The phases of the analytical solution and the numerical solutions of the two FDSs are plotted in Fig. 3.2 for a step size $h = 1/100$. While the phases of the numerical results of both schemes almost coincide for the used level of detail in Fig. 3.2, the phases of the numerical schemes differ slightly from the phase of analytical scheme. The numerical wave lengths are smaller than the analytical wave length. This error is directly related to the difference of the analytical wave vector and the discrete wave vectors. Thus, this error decreases for smaller step sizes.

Analogously to the evaluation of the discrete L^2-error in Chap. 2, we have to optimize the L^2-error with respect to a phase offset $\varphi \in [-\pi, \pi]$. In other words we have to solve the nonlinear problem

$$\Delta\mathbf{F}_h^{\min} = \min_{\varphi\in[-\pi,\pi]} \Delta\mathbf{F}_h = \min_{\varphi\in[-\pi,\pi]} \frac{1}{J+1} \sqrt{\sum_{j=0}^{J} \left\|\mathbf{F}(x_j) - \mathbf{F}_j e^{\mathrm{i}\varphi}\right\|^2}, \tag{3.62}$$

where $\mathbf{F}(x_j)$ denotes the analytical solution at $x = x_j$ and $\mathbf{F}_j$ the numerical solution using the step size $h = 1/J$. As in Chap. 2, nonlinear optimization methods such as the MATLAB procedure `fminsearch` do not give acceptable results. Hence, we discretize the domain $[-\pi, \pi]$ with a step size $h_\varphi = 2\pi/1000$ and analyze the L^2-error $\Delta\mathbf{F}_h$ at every grid point in order to evaluate the minimal L^2-error $\Delta\mathbf{F}_h^{\min}$.

The L^2-errors of the numerical solutions are shown in Fig. 3.3. The numerical order evaluated experimentally coincides for both FDSs with their formal order. While the discrete L^2-error of the centered FDS is in $\mathcal{O}(h^2)$ the discrete L^2-error of the symmetrized FDS decays like $\mathcal{O}(h)$.

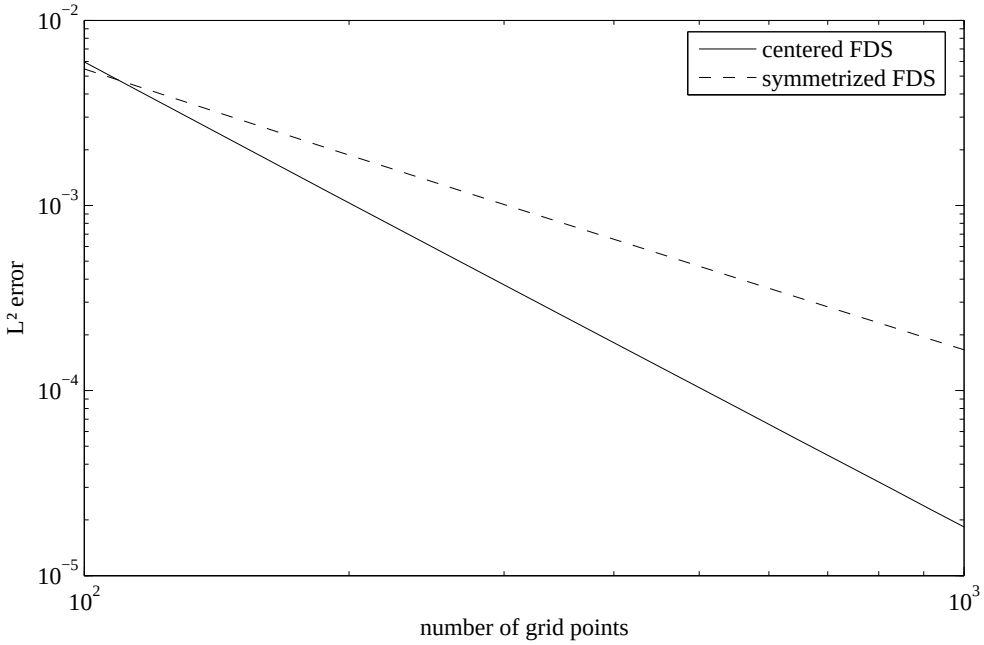

Figure 3.3: Discrete L^2-errors of the numerical solution of the centered FDS (solid line) and the symmetrized FDS (dashed line) against the number of grid points $J = 1/h$ for the free scattering state with $P_0 \equiv 1$, $E_g \equiv 20$, $E_0 \equiv 0$ and an energy $E = 25$.

We note that both the centered FDS and the symmetrized FDS give reasonable results. Hence, the difference of the periodicity of the discrete dispersion relation of the centered FDS and its discrete solution do not affect the results of the free scattering state. Similarly, the non-plane discrete solution of the symmetrized FDS does not produce notable errors.

3.6.2 The Single Barrier Potential

Analogously to the numerical examples in Chap. 2 we want to compare the numerical results with the analytical results when applied to a single barrier potential. We consider a semiconductor of length L that is split into three parts. Let $0 < x_1 < x_2 < L$, then the three subdomains of the semiconductor are defined by $[0, x_1)$, $[x_1, x_2)$ and $[x_2, L]$. The two outer subdomains are denoted by $A = [0, x_1) \cup [x_2, L]$, while the inner subdomain is called $B = [x_1, x_2)$.

The Kane-parameter P_0 and the band gap E_g are assumed to be constant, while the middle of the band gap E_0 is piecewise constant and satisfies

$$E_0(x) = 0, \qquad x \in A,$$

and

$$E_0(x) = E_{0,B}, \qquad x \in B.$$

In other words, we add some potential $E_{0,B}$ to the band edges in the domain B. Note that we can additionally define a piecewise constant band gap and proceed analogously. However, for simplicity we shall restrict the variation to the middle of the band gap only.

First let us derive the analytical solution. We suppose that the energy E satisfies the energy condition (3.8) in the whole semiconductor, i.e.

$$E > E_0(x) + \frac{1}{2}E_g(x), \qquad x \in [0, L].$$

In the three domains $[0, x_1)$, $[x_1, x_2)$ and $[x_2, L]$ both the band gap E_g and the middle of the band gap E_0 are constant. Hence, in each domain the vector of the envelope functions takes the form

$$\mathbf{F}(x) = a\hat{\mathbf{F}}^{\mathrm{e/h}}(\hat{k})e^{\mathrm{i}\hat{k}x} + b\hat{\mathbf{F}}^{\mathrm{e/h}}(-\hat{k})e^{-\mathrm{i}\hat{k}x},$$

with $a, b \in \mathbb{C}$ and the propagation coefficient $\hat{k}$ of the wave vector k. Let $\hat{k}_A$ be the propagation coefficient in A and let $\hat{k}_B$ denote the propagation coefficient in B. Then we have

$$\hat{k}_A = \frac{1}{P_0}\sqrt{E^2 - \frac{1}{4}E_\mathrm{g}^2}$$

and

$$\hat{k}_B = \frac{1}{P_0}\sqrt{(E - E_{0,B})^2 - \frac{1}{4}E_\mathrm{g}^2}.$$

Let $\hat{\mathbf{F}}_A^{\mathrm{e/h}}(k)$ denote the unitary amplitude of a wave with wave vector k in the domain A and let $\hat{\mathbf{F}}_B^{\mathrm{e/h}}(k)$ denote the corresponding, unitary amplitude in the domain B. We consider a right-traveling envelope wave with amplitude $\hat{\mathbf{F}}_A^{\mathrm{e/h}}(\hat{k})$ that enters the semiconductor at $x = 0$. Since E_g is constant and $E_0 \equiv 0$ in A, which is also the case in the exterior domain $x < 0$, the incoming wave is not reflected but completely transmitted into the domain $[0, x_1)$. At $x = x_1$ the envelope wave is partly reflected. In the domain $[x_2, L]$ we expect a transmitted, right-traveling envelope wave that leaves the semiconductor at $x = L$. For the same reason as at $x = 0$ we do not expect any reflection of the transmitted wave at $x = L$. Thus, the vector of the envelope functions is determined by

$$\mathbf{F}(x) = \begin{cases} \hat{\mathbf{F}}_A^{\mathrm{e/h}}(\hat{k}_A)e^{\mathrm{i}\hat{k}_A x} + r\hat{\mathbf{F}}_A^{\mathrm{e/h}}(-\hat{k}_A)e^{-\mathrm{i}\hat{k}_A x}, & \text{if } x \in [0, x_1), \\ a\hat{\mathbf{F}}_B^{\mathrm{e/h}}(\hat{k}_B)e^{\mathrm{i}\hat{k}_B x} + b\hat{\mathbf{F}}_B^{\mathrm{e/h}}(-\hat{k}_B)e^{-\mathrm{i}\hat{k}_B x}, & \text{if } x \in [x_1, x_2), \\ t\hat{\mathbf{F}}_A^{\mathrm{e/h}}(\hat{k}_A)e^{\mathrm{i}\hat{k}_A x}, & \text{if } x \in [x_2, L]. \end{cases} \tag{3.63}$$

Since only the band edges vary between the three subdomains, the resulting vector of envelope functions $\mathbf{F}$ is continuous, cf. [24]. In particular, $\mathbf{F}$ is continuous at $x = x_1, x_2$. Hence, we get the following system of linear equations

$$\begin{aligned} \hat{\mathbf{F}}_A^{\mathrm{e/h}}(\hat{k}_A)e^{\mathrm{i}\hat{k}_A x_1} + r\hat{\mathbf{F}}_A^{\mathrm{e/h}}(-\hat{k}_A)e^{-\mathrm{i}\hat{k}_A x_1} &= a\hat{\mathbf{F}}_B^{\mathrm{e/h}}(\hat{k}_B)e^{\mathrm{i}\hat{k}_B x_1} + b\hat{\mathbf{F}}_B^{\mathrm{e/h}}(-\hat{k}_B)e^{-\mathrm{i}\hat{k}_B x_1} \\ a\hat{\mathbf{F}}_B^{\mathrm{e/h}}(\hat{k}_B)e^{\mathrm{i}\hat{k}_B x_2} + b\hat{\mathbf{F}}_B^{\mathrm{e/h}}(-\hat{k}_B)e^{-\mathrm{i}\hat{k}_B x_2} &= t\hat{\mathbf{F}}_A^{\mathrm{e/h}}(\hat{k}_A)e^{\mathrm{i}\hat{k}_A x_2} \end{aligned}$$

for the four scalar unknowns r, a, b and t. Let us rewrite the system of linear equations in the form

$$\mathbf{Q}\begin{pmatrix} r \\ a \\ b \\ t \end{pmatrix} = \begin{pmatrix} -\hat{\mathbf{F}}_A^{\mathrm{e/h}}(\hat{k}_A)e^{\mathrm{i}\hat{k}_A x_1} \\ \mathbf{0} \end{pmatrix},$$

with $\mathbf{Q} \in \mathbb{C}^{4\times 4}$ given by

$$\mathbf{Q} = \begin{pmatrix} \hat{\mathbf{F}}_A^{\mathrm{e/h}}(-\hat{k}_A)e^{-\mathrm{i}\hat{k}_A x_1} & -\hat{\mathbf{F}}_B^{\mathrm{e/h}}(\hat{k}_B)e^{\mathrm{i}\hat{k}_B x_1} & -\hat{\mathbf{F}}_B^{\mathrm{e/h}}(-\hat{k}_B)e^{-\mathrm{i}\hat{k}_B x_1} & \mathbf{0} \\ \mathbf{0} & \hat{\mathbf{F}}_B^{\mathrm{e/h}}(\hat{k}_B)e^{\mathrm{i}\hat{k}_B x_2} & \hat{\mathbf{F}}_B^{\mathrm{e/h}}(-\hat{k}_B)e^{-\mathrm{i}\hat{k}_B x_2} & -\hat{\mathbf{F}}_A^{\mathrm{e/h}}(\hat{k}_A)e^{\mathrm{i}\hat{k}_A x_2} \end{pmatrix}.$$

It remains to show that the matrix $\mathbf{Q}$ is regular in order to get uniquely defined coefficients r, a, b and t. We omit to give a mathematical proof. Instead we point out that if the matrix $\mathbf{Q}$ is not regular, the homogeneous case of the system of linear equations, i.e. with no incoming envelope wave, does not necessarily imply that the coefficients r, a, b and t are zero. This means that there can exist envelope waves inside the computational domain without the existence of an incoming envelope wave which is a physical contradiction. Moreover, we point out, that in our particular example the matrix $\mathbf{Q}$ is in fact regular and hence, the unknown coefficients r, a, b and t are defined uniquely.

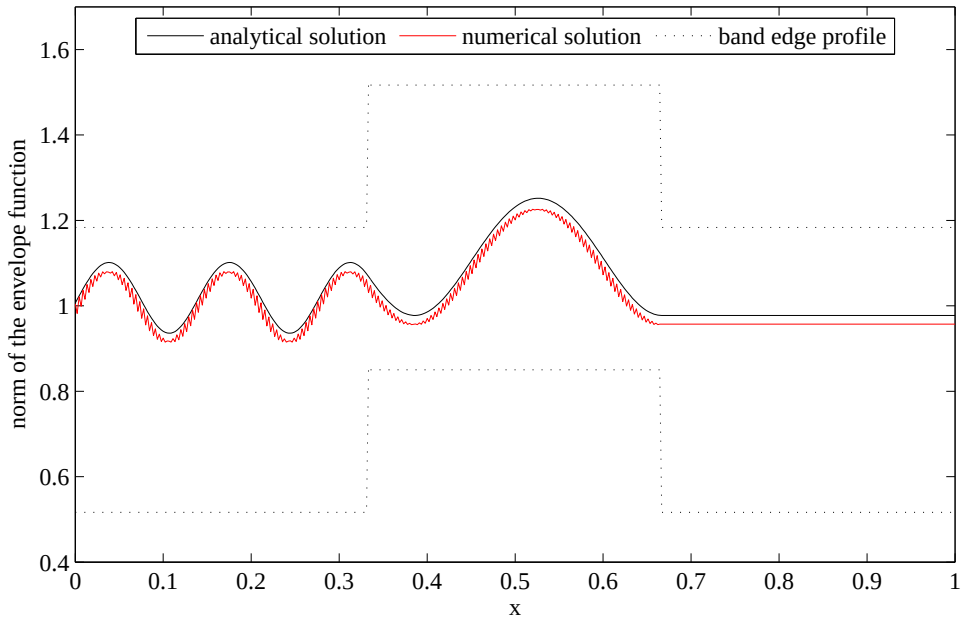

(a) Norm of the analytical and numerical solutions.

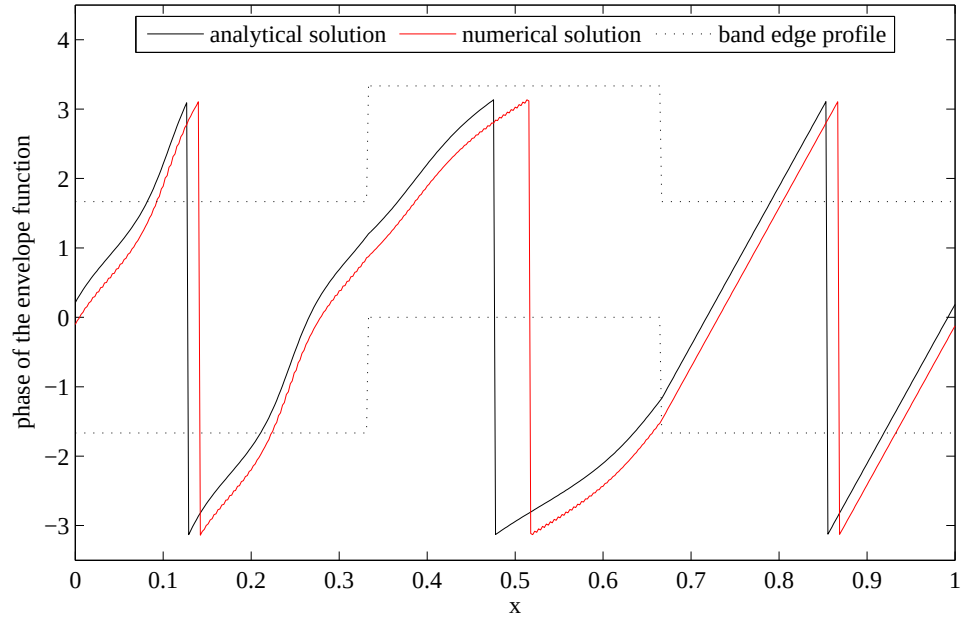

(b) Phases of the analytical and numerical solutions.

Figure 3.4: Comparison of the analytical solution (black) of the single barrier problem and the numerical solution (red) using the centered FDS with the step size $h = 1/450$ and an energy $E = 25$. The dotted line indicates schematically the band edge profile.

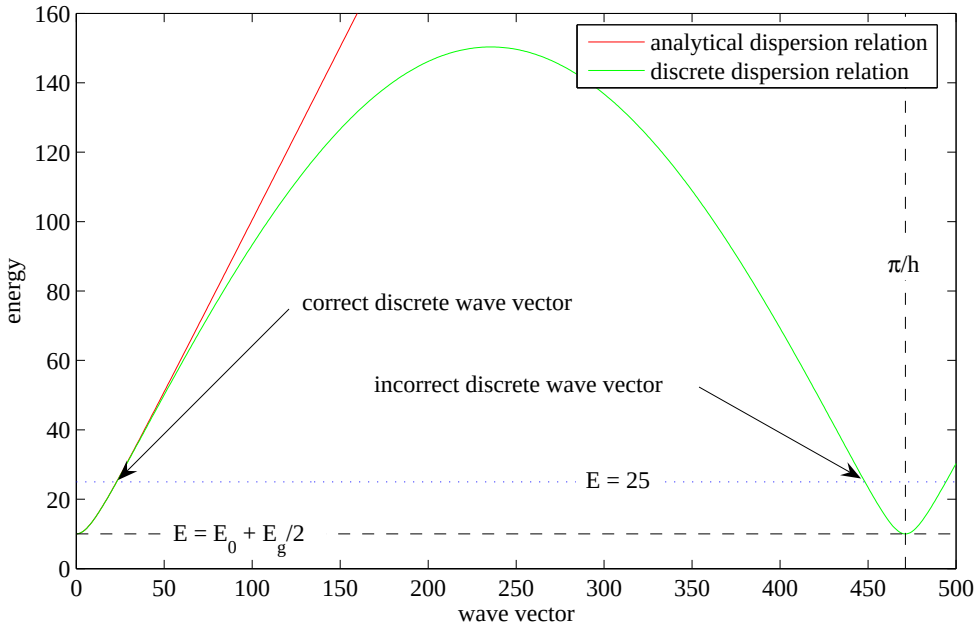

Figure 3.5: Positive trunk of the discrete dispersion relation of the centered FDS for a band gap $E_g = 20$, a middle of the band gap $E_0 = 0$, a Kane-parameter $P_0 = 1$ and a step size $h = 1/450$. The blue line indicates the energy $E = 25$, used in this example with single barrier potential.

3.6.2.1 Numerical Solutions of the Envelope Functions

In this section we want to analyze the norm and the phase of the numerical results of the introduced FDSs. Let us start with the second order centered FDS. We choose an energy $E = 25$ and set $E_{0,B} = 10$, $E_g = 20$ and $P_0 = 1$. Moreover we set $x_1 = 1/3$, $x_2 = 2/3$ and $L = 1$. Fig. 3.4 shows a comparison of the norms and the phases of the analytical solution and the numerical solution for the step size $h = 1/450$.

We observe that the norm as well as the phase of the numerical solution using the centered FDS oscillates in front of the barrier, i.e. in the domain $[0, x_1)$, and in the barrier, in the domain $[x_1, x_2)$. Behind the barrier, i.e. in the domain $[x_2, 1]$, the numerical solution does not oscillate and the norm is constant. However, the norm is not equal to the norm of the analytical solution, i.e. the numerical transmission coefficient differs significantly from the analytical transmission coefficient. These oscillations and the difference of the analytical and numerical transmission coefficient becomes smaller when using a smaller step size but the oscillations do not vanish.

This observation is in line with analysis of the discrete dispersion relation of the centered FDS. In Fig. 3.5 the positive trunk of the discrete dispersion relation of the centered FDS is shown. The parameters used are equal to the parameters in the domain A, i.e. $E_g = 20$, $E_0 = 0$, $P_0 = 1$ and $h = 1/450$. The blue line indicates the energy $E = 25$, used in this example. Its intersections with the green line of the discrete dispersion relation show the two solutions of the discrete wave vector. The solution on the left is the correct value of the discrete wave vector while the solution on the right is the wave vector that leads to the spurious oscillations.

Let us now apply the symmetrized FDS instead of the centered FDS. Fig. 3.4 shows a comparison of the norms and the phases of the the analytical solution and the numerical solution using the symmetrized FDS for the step size $h = 1/450$. We can see that the spurious oscillations of the norm and the phase, we observed when using the centered FDS, vanish. Moreover, the transmission is modeled more correctly and the norm as well as the phase are estimated significantly better in the entire domain $[0, 1]$.

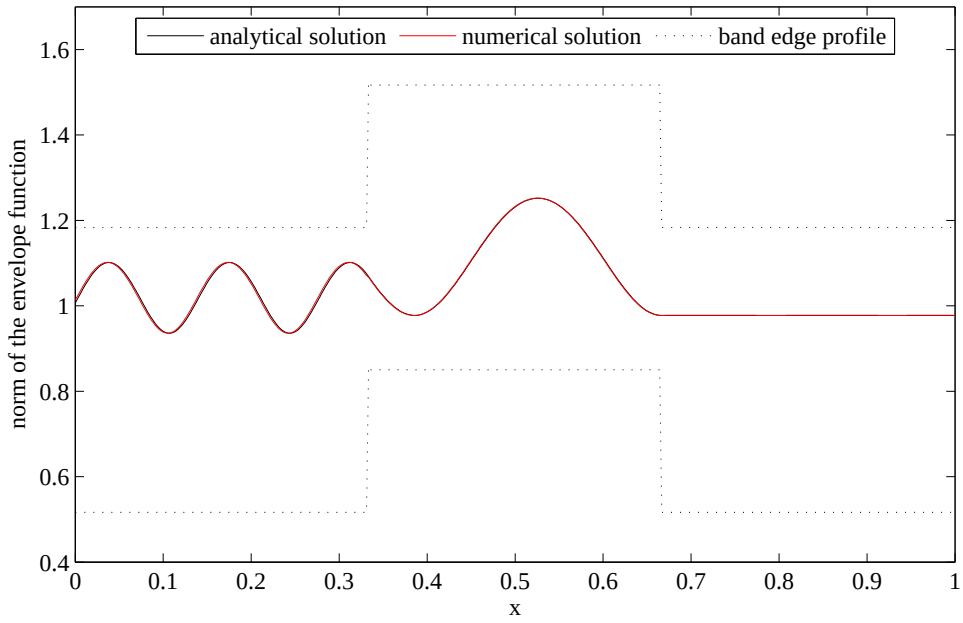

(a) Norm of the analytical and numerical solutions.

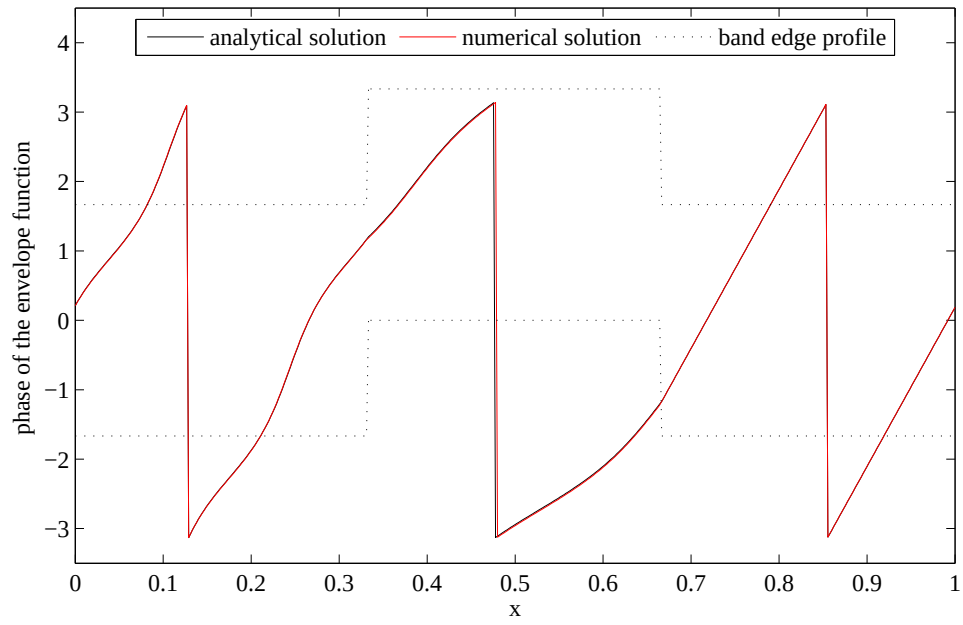

(b) Phases of the analytical and numerical solutions.

Figure 3.6: Comparison of the analytical solution (black) of the single barrier problem and the numerical solution (red) using the symmetrized FDS with the step size $h = 1/450$ and an energy $E = 25$. The dotted line indicates schematically the band edge profile.

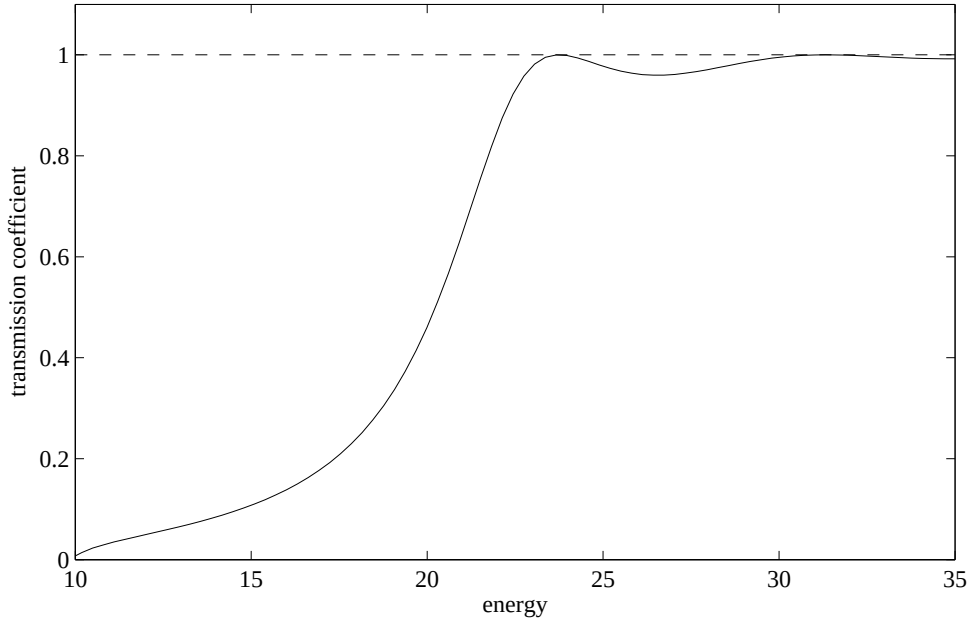

Figure 3.7: Analytical transmission coefficient.

As expected, the symmetrized FDS does not lead to spurious oscillations. Moreover, we note that the non-plane discrete exterior solution of the symmetrized FDS again does not affect the numerical results. Therefore, we shall use the symmetrized FDS in the remainder of this chapter.

3.6.2.2 The Transmission Coefficient

Now let us examine the behavior of the transmission coefficient versus the energy E. Therefore, we set again $E_g = 20$, $E_{0,B} = 10$ and $P_0 = 1$ as well as $L = 1$, $x_1 = 1/3$ and $x_2 = 2/3$. Fig. 3.7 shows the analytical transmission coefficient. The smallest energy yielding a resonance is located at $E \approx 23.8$.

In Fig. 3.8 the analytical transmission coefficient is compared with the numerical transmission coefficient of the symmetrized FDS in the vicinity of the first two resonance energies. As can be seen in Fig. 3.8(a), the numerical transmission coefficient using the step size $h = 1/300$ overestimates the analytical transmission coefficient. This implies that the numerical transmission coefficient is greater than 1 near the resonance energies $E \approx 23.8$ and $E \approx 31.3$. This error decreases if we use a smaller step size such as $h = 1/450$ in Fig. 3.8(b).

3.6.2.3 The L^2-Error

Finally, we want to study the discrete L^2-error of the numerical solution using the symmetrized FDS and check if its formal numerical order can be confirmed numerically for the example with single barrier potential. Recall that we have to solve the nonlinear problem (3.62) in order to compute the discrete L^2-error. In Fig. 3.9 the discrete L^2-error $\Delta\mathbf{F}_h^{\min}$ of the symmetrized FDS is plotted against the number of grid points $J = 1/h$ for an energy $E = 25$, a band gap $E_g = 20$ and a middle of the band gap $E_{0,B} = 10$ at the barrier. We observe, that for the example with single barrier potential, the discrete L^2-error of the symmetrized FDS, which is formally of first order, converges in fact in $\mathcal{O}(h)$.

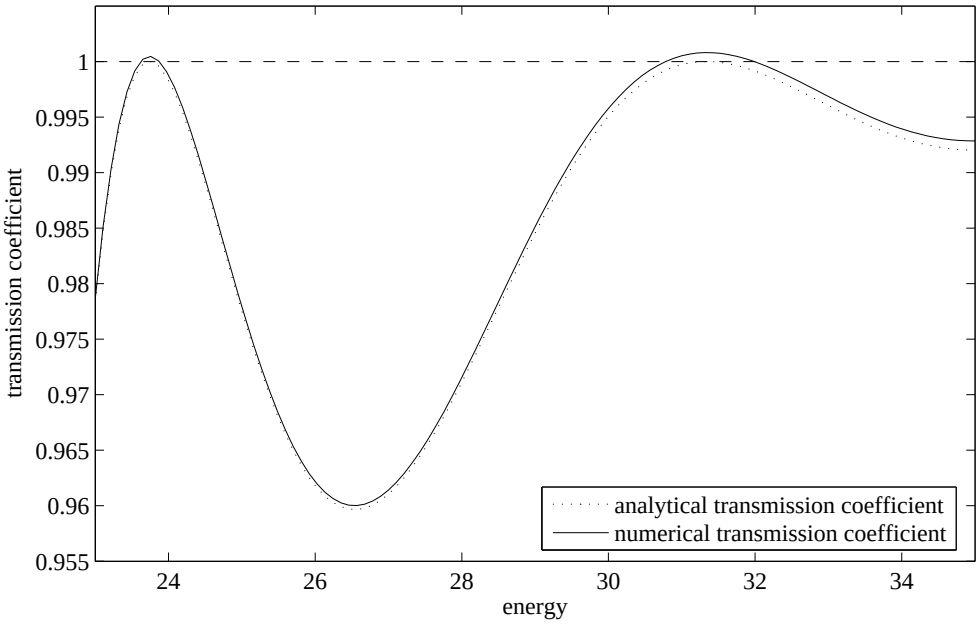

(a) Analytical and numerical transmission coefficient for $h = 1/300$.

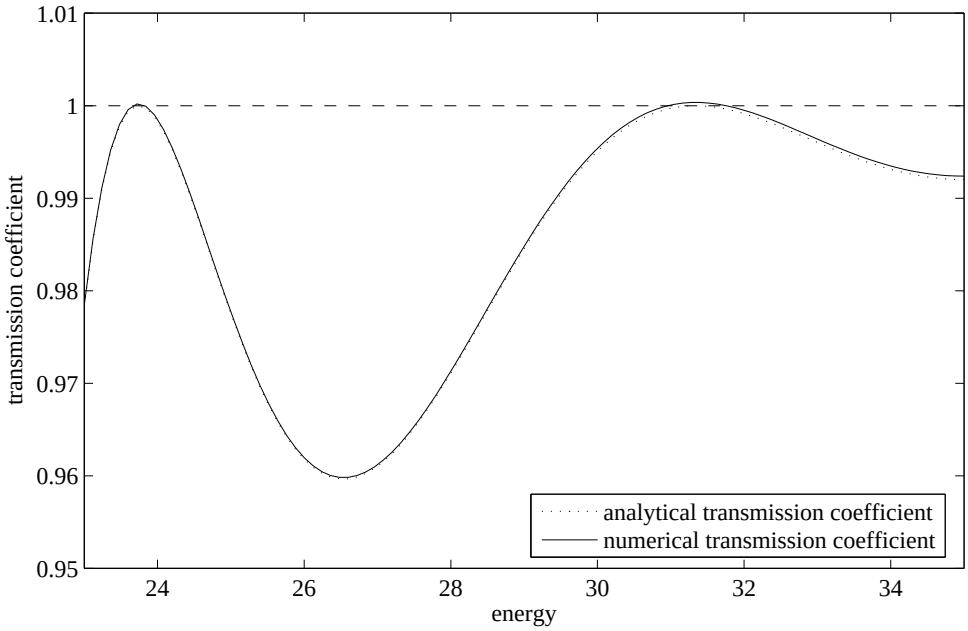

(b) Analytical and numerical transmission coefficient for $h = 1/450$.

Figure 3.8: Analytical transmission coefficient (black) and the transmission coefficient of the symmetrized FDS (red) in the vicinity of the first two resonances for a step size $h = 1/300$ in (a) and $h = 1/450$ in (b).

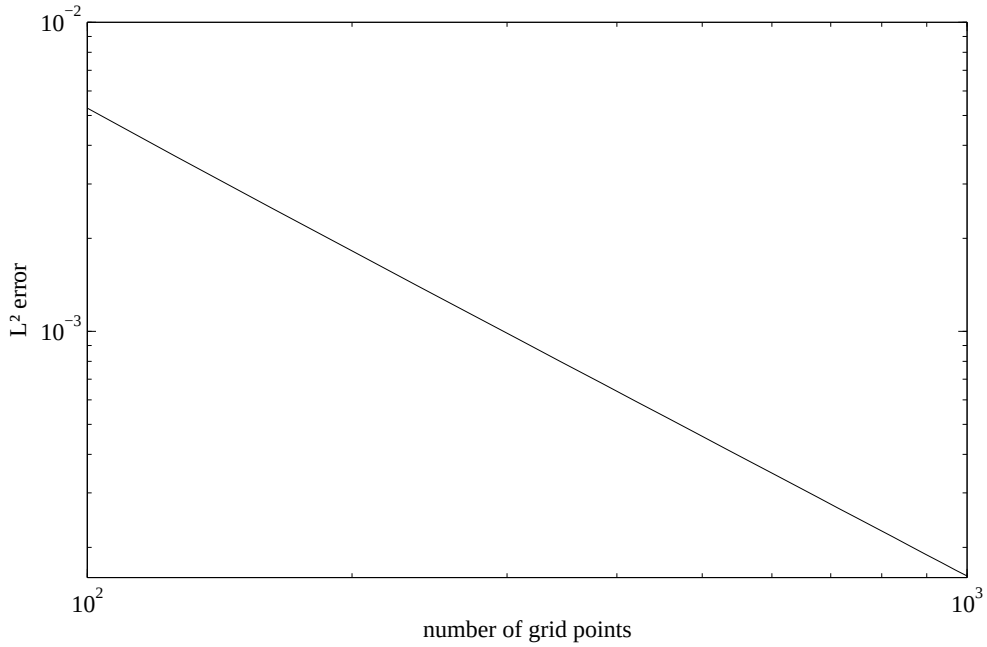

Figure 3.9: L^2-error of the symmetrized FDS for an energy $E = 25$, a band gap $E_\mathrm{g} = 20$ and a middle of the band gap $E_{0,B} = 10$ at the barrier.

3.7 Summary

We introduced the so-called two-band Kane-model, solved the analytical exterior problem and derived TBCs. By reducing the system to a scalar second order ODE we showed that it has a unique solution.

Four different FDSs were introduced, the first order backward and forward FDSs, the second order centered FDS and the first order symmetrized FDS. The discrete exterior problem, however, could only be analyzed when using the second order centered FDS. The approach of a discrete plane wave as a solution of the exterior problem of the symmetrized FDS could not be verified mathematically and yields discrete waves that are not plane.

With the help of the discrete amplitudes and the discrete wave vectors we derived DTBCs.

We showed that the second order centered FDS leads to a significant error in the example with single barrier potential including spurious oscillations. These oscillations are caused by the discrete dispersion relation of the centered FDS. Since it is not injective in the interval $\left(0, \frac{\pi}{h}\right)$, the discrete wave vector k_h of the centered FDS corresponding to some energy E is not unique. The discrete dispersion relation of the symmetrized FDS, however, is injective in $\left(0, \frac{\pi}{h}\right)$ and hence, the symmetrized FDS does not lead to spurious oscillations.

Chapter 4

The Two-Band $\mathbf{k} \cdot \mathbf{p}$-Model

In Chap. 3 we pointed out that we need a certain regularization term on the diagonal of the Hamiltonian $\mathbf{H}$ in order to use advanced discretization methods for the two-band model. This regularization term leads us to the so-called *two-band* $\mathbf{k} \cdot \mathbf{p}$*-model*. Basically, there are two kinds of two-band $\mathbf{k} \cdot \mathbf{p}$-models that differ in the choice of the regularization term, one being a model of the coupling of conduction and valence band, a so-called *inter-band model* such as the Kane-model, and the other being a model of the coupling of heavy and light hole band, a so-called *intra-band model* of the valence bands.

The regularization term of the two-band $\mathbf{k} \cdot \mathbf{p}$-model with inter-band coupling that is added to the Hamiltonian (3.2) of the Kane-model reads

$$-\mathbf{N}\frac{\mathrm{d}^2}{\mathrm{d}x^2}, \tag{4.1}$$

with

$$\mathbf{N} = \begin{pmatrix} \epsilon & 0 \\ 0 & -\epsilon \end{pmatrix}. \tag{4.2}$$

Hence, the Hamiltonian of the two-band $\mathbf{k} \cdot \mathbf{p}$ model

$$\mathbf{HF} = E\mathbf{F}, \tag{4.3}$$

with inter-band coupling takes the form

$$\mathbf{H} = \begin{pmatrix} -\epsilon\frac{\mathrm{d}^2}{\mathrm{d}x^2} + \frac{1}{2}E_\mathrm{g}(x) + E_0(x) & -\mathrm{i}P_0(x)\frac{\mathrm{d}}{\mathrm{d}x} \\ -\mathrm{i}P_0(x)\frac{\mathrm{d}}{\mathrm{d}x} & \epsilon\frac{\mathrm{d}^2}{\mathrm{d}x^2} - \frac{1}{2}E_\mathrm{g}(x) + E_0(x) \end{pmatrix}. \tag{4.4}$$

On the other hand, the regularization term of the two-band $\mathbf{k} \cdot \mathbf{p}$-model with intra-band coupling is defined by

$$\mathbf{N}^{\mathrm{intra}} = \begin{pmatrix} \epsilon & 0 \\ 0 & \epsilon \end{pmatrix}. \tag{4.5}$$

In this chapter we will analyze the two-band $\mathbf{k} \cdot \mathbf{p}$-model with inter-band coupling. For the two-band $\mathbf{k} \cdot \mathbf{p}$-model with intra-band coupling we refer to [23] and [9] as well as to Chap. 5 where we will study the general d-band $\mathbf{k} \cdot \mathbf{p}$-model.

As before, we consider a semiconductor of length L connected to reservoirs at $x = 0$ and $x = L$. We assume that the Kane-parameter $P_0(x)$ and the band edges $E_\mathrm{c}(x)$ and $E_\mathrm{v}(x)$ are constant in the reservoirs, i.e.

$$\begin{aligned} P_0(x) &= P_{0,0}, \qquad x \le 0, \\ P_0(x) &= P_{0,L}, \qquad x \ge L, \end{aligned}$$

and

$$\begin{aligned} E_\mathrm{g}(x) &= E_{\mathrm{g},0}, \qquad x \le 0, \\ E_\mathrm{g}(x) &= E_{\mathrm{g},L}, \qquad x \ge L, \end{aligned}$$

and

$$E_0(x) = 0, \qquad x \leq 0,$$
$$E_0(x) = E_{0,L}, \qquad x \geq L.$$

4.1 The Exterior Problem and the Dispersion Relation

In this section we will analyze the exterior problem of the two-band $\mathbf{k}\cdot\mathbf{p}$-model with a constant Kane-parameter P_0, a constant band gap E_g and a constant middle of the band gap E_0. Instead of deriving results for the explicit values of the parameters in the exterior domains, we shall consider some constant Kane-parameter P_0, some constant band gap E_g and some constant middle of the band gap E_0. In order to determine the results of the exterior domains that are needed in the following sections, we shall apply the specific values of the Kane-parameter P_0, the band gap E_g and the middle of the band gap E_0 in the exterior domains to the results stated.

If P_0, E_g and E_0 are constant Eq. (4.3) is a second order system of ODEs with constant coefficients that can be written in the form

$$-\mathbf{N}\frac{\mathrm{d}^2}{\mathrm{d}x^2}\mathbf{F} + \mathrm{i}\mathbf{M}\frac{\mathrm{d}}{\mathrm{d}x}\mathbf{F} + (\mathbf{V} - E\mathbb{1})\,\mathbf{F} = \mathbf{0}, \tag{4.6}$$

with

$$\mathbf{M} = \begin{pmatrix} 0 & -P_0 \\ -P_0 & 0 \end{pmatrix} \tag{4.7a}$$

and

$$\mathbf{V} = \begin{pmatrix} \frac{1}{2}E_\mathrm{g} + E_0 & \\ 0 & -\frac{1}{2}E_\mathrm{g} + E_0 \end{pmatrix}. \tag{4.7b}$$

In order to reduce Eq. (4.6) to a first order system of ODEs with constant coefficients we introduce the substitution

$$\Phi = \begin{pmatrix} \mathbf{F} \\ \frac{\mathrm{d}}{\mathrm{d}x}\mathbf{F} \end{pmatrix}, \tag{4.8}$$

to give the first order system of ODEs with constant coefficients

$$\frac{\mathrm{d}}{\mathrm{d}x}\Phi = \mathbf{A}\Phi, \tag{4.9}$$

with

$$\mathbf{A} = \begin{pmatrix} \mathbf{0} & \mathbb{1} \\ \mathbf{N}^{-1}\,(\mathbf{V} - E\mathbb{1}) & \mathrm{i}\mathbf{N}^{-1}\mathbf{M} \end{pmatrix} \in \mathbb{C}^{4\times 4}. \tag{4.10}$$

The solution of Eq. (4.9) takes the form

$$\Phi(x) = \mathbf{a}e^{\kappa x}, \tag{4.11}$$

where $\kappa = \kappa_1, \ldots, \kappa_4 \in \mathbb{C}$ is an eigenvalue and $\mathbf{a} = \mathbf{a}(\kappa) \in \mathbb{C}^4$ the corresponding eigenvector of the matrix $\mathbf{A}$, cf. [41]. Let $\hat{\mathbf{F}} \in \mathbb{C}^2$ denote the *amplitude* of the vector $\mathbf{F}$ of envelope functions that contains the first two components of $\mathbf{a}(\kappa) \in \mathbb{C}^4$, then the vector $\mathbf{F}$ of the envelope functions becomes

$$\mathbf{F}(x) = \hat{\mathbf{F}}e^{\mathrm{i}kx}, \tag{4.12}$$

where $k = \hat{k} + \mathrm{i}\check{k} = -\mathrm{i}\kappa$ is called *wave vector* of $\mathbf{F}$ with the *propagation coefficient* $\hat{k}$ and the *attenuation coefficient* $\check{k}$. If the attenuation coefficient $\check{k}$ is zero we say that $\mathbf{F}$ is traveling while $\mathbf{F}$ is called evanescent otherwise. Analogously to Chap. 3, we shall refer to the vector $\mathbf{F}$ of the envelope functions as *envelope wave* since it can be expressed in terms of a plane wave.

By applying the solution (4.12) to the two-band $\mathbf{k}\cdot\mathbf{p}$-model (4.3) we get

$$\hat{\mathbf{H}}\hat{\mathbf{F}} = E\hat{\mathbf{F}}, \tag{4.13}$$

with

$$\hat{\mathbf{H}} = \hat{\mathbf{H}}(k) = \begin{pmatrix} \hat{H}_{11}(k) & \hat{H}_{12}(k) \\ \hat{H}_{21}(k) & \hat{H}_{22}(k) \end{pmatrix} = \begin{pmatrix} \epsilon k^2 + \frac{1}{2}E_{\mathrm{g}} + E_0 & P_0 k \\ P_0 k & -\epsilon k^2 - \frac{1}{2}E_{\mathrm{g}} + E_0 \end{pmatrix}. \tag{4.14}$$

The characteristic polynomial implies

$$(E - E_0)^2 - \left(\epsilon k^2 + \frac{1}{2}E_{\mathrm{g}}\right)^2 - P_0^2 k^2 = 0,$$

and hence, the wave vector k satisfies the relation

$$k^4 + \frac{1}{\epsilon^2}\left(\epsilon E_{\mathrm{g}} + P_0^2\right)k^2 - \frac{1}{\epsilon^2}\left((E - E_0)^2 - \frac{1}{4}E_{\mathrm{g}}^2\right) = 0,$$

that leads to

$$\left(k^2 + \frac{1}{2\epsilon^2}\left(\epsilon E_{\mathrm{g}} + P_0^2\right)\right)^2 = \frac{1}{4\epsilon^4}\left(\epsilon E_{\mathrm{g}} + P_0^2\right)^2 + \frac{1}{\epsilon^2}\left((E - E_0)^2 - \frac{1}{4}E_{\mathrm{g}}^2\right). \tag{4.15}$$

Since the right hand side of Eq. (4.15) can be written in the form

$$\frac{1}{4\epsilon^4}\left(\epsilon E_{\mathrm{g}} + P_0^2\right)^2 + \frac{1}{\epsilon^2}\left((E - E_0)^2 - \frac{1}{4}E_{\mathrm{g}}^2\right) = \frac{P_0^2}{4\epsilon^4}\left(P_0^2 + 2\epsilon E_{\mathrm{g}}\right) + \frac{1}{\epsilon^2}(E - E_0)^2 \geq 0,$$

the roots of Eq. (4.15) are real and read

$$k^2 = -\frac{1}{2\epsilon^2}\left(\epsilon E_{\mathrm{g}} + P_0^2\right) \pm \sqrt{\frac{P_0^2}{4\epsilon^4}\left(P_0^2 + 2\epsilon E_{\mathrm{g}}\right) + \frac{1}{\epsilon^2}(E - E_0)^2}.$$

If the energy E satisfies the complement of the energy condition (3.8), i.e.

$$|E - E_0| \leq \frac{1}{2}E_{\mathrm{g}}, \tag{4.16}$$

then we have

$$\frac{1}{2\epsilon^2}\left(\epsilon E_{\mathrm{g}} + P_0^2\right) \geq \sqrt{\frac{P_0^2}{4\epsilon^4}\left(P_0^2 + 2\epsilon E_{\mathrm{g}}\right) + \frac{1}{\epsilon^2}(E - E_0)^2}.$$

Hence, the wave vector k is purely imaginary and given by

$$k = \pm \mathrm{i}\check{k}_{1,2} \in \mathrm{i}\mathbb{R}, \tag{4.17}$$

with the attenuation coefficient

$$\check{k}_{1,2} = \sqrt{\frac{1}{2\epsilon^2}\left(\epsilon E_{\mathrm{g}} + P_0^2\right) \pm \sqrt{\frac{P_0^2}{4\epsilon^4}\left(P_0^2 + 2\epsilon E_{\mathrm{g}}\right) + \frac{1}{\epsilon^2}(E - E_0)^2}} \geq 0.$$

Thus, if Eq. (4.16) is fulfilled we obtain four evanescent envelope waves and no traveling envelope wave.

On the other hand, if the energy condition (3.8) is fulfilled, i.e.

$$|E - E_0| > \frac{1}{2}E_{\mathrm{g}}, \tag{4.18}$$

we get two real wave vectors

$$k = \pm\hat{k} \in \mathbb{R}, \tag{4.19a}$$

with the propagation coefficient

$$\hat{k} = \sqrt{-\frac{1}{2\epsilon^2}\left(\epsilon E_\mathrm{g} + P_0^2\right) + \sqrt{\frac{P_0^2}{4\epsilon^4}\left(P_0^2 + 2\epsilon E_\mathrm{g}\right) + \frac{1}{\epsilon^2}\left(E - E_0\right)^2}} > 0,$$

and two purely imaginary wave vectors

$$k = \pm\mathrm{i}\check{k} \in \mathrm{i}\mathbb{R}, \tag{4.19b}$$

with

$$\check{k} = \sqrt{\frac{1}{2\epsilon^2}\left(\epsilon E_\mathrm{g} + P_0^2\right) + \sqrt{\frac{P_0^2}{4\epsilon^4}\left(P_0^2 + 2\epsilon E_\mathrm{g}\right) + \frac{1}{\epsilon^2}\left(E - E_0\right)^2}} > 0.$$

This means that if Eq. (4.18) holds, we obtain two traveling envelope waves with the wave vector $k = \pm\hat{k}$ and two evanescent envelope waves with the wave vector $k = \pm\mathrm{i}\check{k}$.

Eqs. (4.17) and (4.19) are called *dispersion relations* of the two-band $\mathbf{k}\cdot\mathbf{p}$-model. Usually, they are given in the reciprocal form, that can be obtained by calculating the energy eigenvalue E of $\hat{\mathbf{H}}$. It yields

$$E = E^{\mathrm{e/h}}(k) = E_0 \pm \sqrt{\left(\epsilon k^2 + \frac{1}{2}E_\mathrm{g}\right)^2 + k^2 P_0^2}. \tag{4.20}$$

The energy E^e that corresponds to the positive sign in Eq. (4.20) denotes the energy of the electrons, while E^h associated with the negative sign in Eq. (4.20) is the energy of the holes. Clearly, $E^{\mathrm{e/h}}(k)$ satisfies the energy condition (3.8) if and only if the wave vector k is real. In this case, we will refer to the energy E^e as the energy of the conduction band and the energy E^h as the energy of the valence band.

As a last step of the analysis of the exterior problem we will now specify the amplitude $\hat{\mathbf{F}}$ of the exterior solution. The amplitude

$$\hat{\mathbf{F}}(k) = \hat{\mathbf{F}}^{\mathrm{e/h}}(k) = \begin{pmatrix} \hat{F}_\mathrm{c}^{\mathrm{e/h}}(k) \\ \hat{F}_\mathrm{v}^{\mathrm{e/h}}(k) \end{pmatrix},$$

is an eigenvector of $\hat{\mathbf{H}}(k)$ with the corresponding eigenvalue $E^{\mathrm{e/h}}(k)$. Therefore, it is not defined uniquely and solves the under-determined linear equation

$$\left(\hat{H}_{11}(k) - E^{\mathrm{e/h}}(k)\right)\hat{F}_\mathrm{c}^{\mathrm{e/h}}(k) + \hat{H}_{12}(k)\hat{F}_\mathrm{v}^{\mathrm{e/h}}(k) = 0. \tag{4.21}$$

Hence, the amplitude satisfies

$$\hat{\mathbf{F}}^{\mathrm{e/h}}(k) = c\begin{pmatrix} \hat{H}_{12}(k) \\ E^{\mathrm{e/h}}(k) - \hat{H}_{11}(k) \end{pmatrix} = c\begin{pmatrix} kP_0 \\ E^{\mathrm{e/h}}(k) - \epsilon k^2 - \frac{1}{2}E_\mathrm{g} - E_0 \end{pmatrix}, \tag{4.22}$$

with some arbitrary constant $c \in \mathbb{C}$. Note that $\mathbf{F}^\mathrm{e}(x,k) = \hat{\mathbf{F}}^\mathrm{e}(k)e^{\pm\mathrm{i}kx}$ is the energy eigenstate associated with the energy E^e of the electrons while $\mathbf{F}^\mathrm{h}(x,k) = \hat{\mathbf{F}}^\mathrm{h}(k)e^{\pm\mathrm{i}kx}$ corresponds to the energy E^h of the holes, see Eq. (4.20).

If the energy condition $|E - E_0| > \frac{1}{2}E_\mathrm{g}$ is fulfilled, we obtain two evanescent and two traveling envelope waves. For the two traveling solutions we assume additionally that they are unitary and hence, the amplitude $\hat{\mathbf{F}}^{\mathrm{e/h}}(\hat{k})$ has norm 1 and it satisfies the *normalization condition*

$$\left\|\hat{\mathbf{F}}^{\mathrm{e/h}}(\hat{k})\right\|_\mathbb{C}^2 = \left\langle \hat{\mathbf{F}}^{\mathrm{e/h}}(\hat{k}), \overline{\hat{\mathbf{F}}^{\mathrm{e/h}}(\hat{k})} \right\rangle = 1. \tag{4.23}$$

Since the matrix $\hat{\mathbf{H}}(\hat{k})$ and its eigenvalues $E^{\mathrm{e/h}}(\hat{k})$ are real-valued, the eigenvectors $\hat{\mathbf{F}}^{\mathrm{e/h}}(\hat{k})$ are either also real-valued or purely imaginary. But since our approach in Eq. (4.12) implies that $\hat{\mathbf{F}}^{\mathrm{e/h}}(\hat{k})$ is the modulus of $\mathbf{F}$, we shall assume that the amplitude $\hat{\mathbf{F}}^{\mathrm{e/h}}(\hat{k})$ is real. Hence, the normalization condition (3.15) becomes

$$\hat{F}_{\mathrm{c}}^{\mathrm{e/h}}(\hat{k})^2 + \hat{F}_{\mathrm{v}}^{\mathrm{e/h}}(\hat{k})^2 = 1. \tag{4.24}$$

Thus, the amplitude $\hat{\mathbf{F}}^{\mathrm{e/h}}(\hat{k})$ of a traveling envelope wave with norm 1 reads

$$\begin{aligned}\hat{\mathbf{F}}^{\mathrm{e/h}}(\hat{k}) &= \pm \begin{pmatrix} \frac{\hat{H}_{12}(\hat{k})}{\sqrt{\left(E^{\mathrm{e/h}}(\hat{k})-\hat{H}_{11}(\hat{k})\right)^2+\hat{H}_{12}(\hat{k})^2}} \\ \frac{E^{\mathrm{e/h}}(\hat{k})-\hat{H}_{11}(\hat{k})}{\sqrt{\left(E^{\mathrm{e/h}}(\hat{k})-\hat{H}_{11}(\hat{k})\right)^2+\hat{H}_{12}(\hat{k})^2}} \end{pmatrix} \\ &= \pm \begin{pmatrix} \frac{\hat{k}P_0}{\sqrt{\left(E^{\mathrm{e/h}}(\hat{k})-\epsilon\hat{k}^2-\frac{1}{2}E_{\mathrm{g}}-E_0\right)^2+\hat{k}^2P_0^2}} \\ \frac{E^{\mathrm{e/h}}(\hat{k})-\epsilon\hat{k}^2-\frac{1}{2}E_{\mathrm{g}}-E_0}{\sqrt{\left(E^{\mathrm{e/h}}(\hat{k})-\epsilon\hat{k}^2-\frac{1}{2}E_{\mathrm{g}}-E_0\right)^2+\hat{k}^2P_0^2}} \end{pmatrix}. \end{aligned} \tag{4.25}$$

Since the two solutions of the amplitude are linearly dependent, we can neglect the solution with negative sign and set

$$\hat{\mathbf{F}}^{\mathrm{e/h}}(\hat{k}) = \begin{pmatrix} \frac{\hat{k}P_0}{\sqrt{\left(E^{\mathrm{e/h}}(\hat{k})-\epsilon\hat{k}^2-\frac{1}{2}E_{\mathrm{g}}-E_0\right)^2+\hat{k}^2P_0^2}} \\ \frac{E^{\mathrm{e/h}}(\hat{k})-\epsilon\hat{k}^2\,\frac{1}{2}E_{\mathrm{g}}-E_0}{\sqrt{\left(E^{\mathrm{e/h}}(\hat{k})-\epsilon\hat{k}^2-\frac{1}{2}E_{\mathrm{g}}-E_0\right)^2+\hat{k}^2P_0^2}} \end{pmatrix}. \tag{4.26}$$

Remark 4.1. Since the amplitudes $\hat{\mathbf{F}}^{\mathrm{e/h}}(\pm\hat{k})$ of traveling envelope waves are real-valued while the amplitudes $\hat{\mathbf{F}}^{\mathrm{e/h}}(\pm\mathrm{i}\check{k})$ of evanescent envelope waves have one purely imaginary component and one real component, the amplitudes $\hat{\mathbf{F}}^{\mathrm{e/h}}(\pm\hat{k})$ of traveling envelope waves are linearly independent from the amplitudes $\hat{\mathbf{F}}^{\mathrm{e/h}}(\pm\mathrm{i}\check{k})$ of evanescent envelope waves.

Analogously to Chap. 3 we will now prove

Proposition 4.2. Let $k \in \mathbb{R}$ be the wave vector of a traveling envelope wave. Then the two solutions $\mathbf{F}^{\mathrm{e}}(x,k)$ and $\mathbf{F}^{\mathrm{h}}(x,k)$ of the free scattering state are orthogonal, i.e.

$$\left\langle \mathbf{F}^{\mathrm{e}}(x,k), \mathbf{F}^{\mathrm{h}}(x,k) \right\rangle = 0.$$

Proof. The scalar product of $\mathbf{F}^{\mathrm{e}}(x,k)$ and $\mathbf{F}^{\mathrm{h}}(x,k)$ can be reduced to

$$\left\langle \mathbf{F}^{\mathrm{e}}(x,k), \mathbf{F}^{\mathrm{h}}(x,k) \right\rangle = \left\langle \hat{\mathbf{F}}^{\mathrm{e}}(k)e^{\mathrm{i}kx}, \hat{\mathbf{F}}^{\mathrm{h}}(k)e^{\mathrm{i}kx} \right\rangle = e^{2\mathrm{i}kx} \left\langle \hat{\mathbf{F}}^{\mathrm{e}}(k), \hat{\mathbf{F}}^{\mathrm{h}}(k) \right\rangle,$$

and therefore, we only have to show that the amplitudes $\hat{\mathbf{F}}^{\mathrm{e}}(k)$ and $\hat{\mathbf{F}}^{\mathrm{h}}(k)$ are orthogonal. By applying Eq. (4.26) to the scalar product of $\hat{\mathbf{F}}^{\mathrm{e}}(k)$ and $\hat{\mathbf{F}}^{\mathrm{h}}(k)$, we can rewrite it in the form

$$\begin{aligned}\left\langle \hat{\mathbf{F}}^{\mathrm{e}}(k), \hat{\mathbf{F}}^{\mathrm{h}}(k) \right\rangle = &\frac{\hat{H}_{12}(k)}{\sqrt{\left(E^{\mathrm{e}}(k)-\hat{H}_{11}(k)\right)^2+\hat{H}_{12}(k)^2}} \frac{\hat{H}_{12}(k)}{\sqrt{\left(E^{\mathrm{h}}(k)-\hat{H}_{11}(k)\right)^2+\hat{H}_{12}(k)^2}} \\ &+ \frac{E^{\mathrm{e}}(k)-\hat{H}_{11}(k)}{\sqrt{\left(E^{\mathrm{e}}(k)-\hat{H}_{11}(k)\right)^2+\hat{H}_{12}(k)^2}} \frac{E^{\mathrm{h}}(k)-\hat{H}_{11}(k)}{\sqrt{\left(E^{\mathrm{h}}(k)-\hat{H}_{11}(k)\right)^2+\hat{H}_{12}(k)^2}}. \end{aligned}$$

Considering the dispersion relation (4.20), we obtain

$$\left\langle \hat{\mathbf{F}}^{\mathrm{e}}(k), \hat{\mathbf{F}}^{\mathrm{h}}(k) \right\rangle = \frac{\left(\hat{H}_{11}(k) - E_0\right)^2 + \hat{H}_{12}(k)^2 - \left(\epsilon k^2 + \frac{1}{2}E_{\mathrm{g}}\right)^2 - P_0^2 k^2}{\sqrt{\left(E^{\mathrm{e}}(k) - \hat{H}_{11}(k)\right)^2 + \hat{H}_{12}(k)^2}\sqrt{\left(E^{\mathrm{h}}(k) - \hat{H}_{11}(k)\right)^2 + \hat{H}_{12}(k)^2}}.$$

By using the identities

$$\left(\hat{H}_{11}(k) - E_0\right)^2 = \left(\epsilon k^2 + \frac{1}{2}E_{\mathrm{g}}\right)^2$$

and

$$\hat{H}_{12}(k)^2 = P_0^2 k^2,$$

we get

$$\left\langle \hat{\mathbf{F}}^{\mathrm{e}}(k), \hat{\mathbf{F}}^{\mathrm{h}}(k) \right\rangle = 0,$$

and hence, the two solutions $\mathbf{F}^{\mathrm{e}}(x,k)$ and $\mathbf{F}^{\mathrm{h}}(x,k)$ are orthogonal. □

4.2 Transparent Boundary Conditions

In order to derive the TBCs for the two-band $\mathbf{k}\cdot\mathbf{p}$-model we will proceed as in Chaps. 2 and 3. We will assume that a plane envelope wave with amplitude of norm 1 enters the computational domain at $x = 0$. This implies that we require the energy to satisfy the energy condition $|E - E_0| > \frac{1}{2}E_{\mathrm{g}}$ in the exterior domain. In contrast to the TBCs of the Kane-model, the resulting reflected and transmitted envelope waves are a superposition of a traveling and an evanescent envelope wave. Hence, we will use the fact that we know the amplitudes of traveling and evanescent envelope waves in the exterior domains except for an arbitrary scalar.

Let $\hat{k}_0 > 0$ denote the propagation coefficient of the wave vector k_0 in the left exterior domain $x \leq 0$, and $\hat{k}_L > 0$ the corresponding propagation coefficient of the wave vector k_L in the right exterior domain $x \geq L$. Moreover, we will refer to $\check{k}_0 > 0$ as the attenuation coefficient of an evanescent envelope wave in the left-exterior domain $x \leq 0$, and $\check{k}_L > 0$ as the attenuation coefficient of an evanescent envelope wave in the right exterior domain $x \geq L$. Note that there cannot exist an evanescent envelope wave with negative attenuation coefficient in the left exterior domain since this wave would tend to infinity for $x \to -\infty$. The opposite is true for the right exterior domain.

The incoming envelope wave takes the form

$$\mathbf{F}^{\mathrm{in}} = \hat{\mathbf{F}}_0^{\mathrm{e/h}}(\hat{k}_0)e^{\mathrm{i}\hat{k}_0 x}, \qquad x < 0. \tag{4.27}$$

This wave is partly reflected at the left boundary at $x = 0$, yielding a superposition of a left-traveling envelope wave and an evanescent envelope wave given by

$$\mathbf{F}^{\mathrm{r}} = \hat{r}\hat{\mathbf{F}}_0^{\mathrm{e/h}}(-\hat{k}_0)e^{-\mathrm{i}\hat{k}_0 x} + \check{r}\hat{\mathbf{F}}_0^{\mathrm{e/h}}(-\mathrm{i}\check{k}_0)e^{\check{k}_0 x}, \qquad x < 0, \tag{4.28}$$

with the reflection coefficients $\hat{r}$ and $\check{r}$. Furthermore, the incoming envelope wave is partly transmitted at the right boundary at $x = L$, which results in a superposition of a right-traveling envelope wave and an evanescent envelope wave that takes the form

$$\mathbf{F}^{\mathrm{t}} = \hat{t}\hat{\mathbf{F}}_L^{\mathrm{e/h}}(\hat{k}_L)e^{\mathrm{i}\hat{k}_L x} + \check{t}\hat{\mathbf{F}}_L^{\mathrm{e/h}}(\mathrm{i}\check{k}_L)e^{-\check{k}_L x}, \qquad x > L, \tag{4.29}$$

with the transmission coefficients $\hat{t}$ and $\check{t}$. Thus, the solution in the left exterior domain can be written in the form

$$\mathbf{F} = \mathbf{F}^{\mathrm{in}} + \mathbf{F}^{\mathrm{r}}, \qquad x < 0, \tag{4.30}$$

and the solution in the right exterior domain is

$$\mathbf{F} = \mathbf{F}^{\mathrm{t}}, \qquad x > L. \tag{4.31}$$

In order to determine the TBC at the left boundary we evaluate the vector of the envelope functions $\mathbf{F}$ and its first derivative $\frac{\mathrm{d}}{\mathrm{d}x}\mathbf{F}$ at $x = 0$. We get

$$\mathbf{F}(0) = \hat{\mathbf{F}}_0^{\mathrm{e/h}}(\hat{k}_0) + \hat{r}\hat{\mathbf{F}}_0^{\mathrm{e/h}}(-\hat{k}_0) + \check{r}\hat{\mathbf{F}}_0^{\mathrm{e/h}}(-\mathrm{i}\check{k}_0), \tag{4.32a}$$

and

$$\frac{\mathrm{d}}{\mathrm{d}x}\mathbf{F}(0) = \mathrm{i}\hat{k}_0\hat{\mathbf{F}}_0^{\mathrm{e/h}}(\hat{k}_0) - \mathrm{i}\hat{k}_0\hat{r}\hat{\mathbf{F}}_0^{\mathrm{e/h}}(-\hat{k}_0) + \check{k}_0\check{r}\hat{\mathbf{F}}_0^{\mathrm{e/h}}(-\mathrm{i}\check{k}_0). \tag{4.32b}$$

Let us introduce

$$\mathbf{P}_0 = \left(\hat{\mathbf{F}}_0^{\mathrm{e/h}}(-\hat{k}_0) \quad \hat{\mathbf{F}}_0^{\mathrm{e/h}}(-\mathrm{i}\check{k}_0)\right) \in \mathbb{C}^{2\times 2},$$

and

$$\mathbf{K}_0 = \mathrm{diag}\left(-\mathrm{i}\hat{k}_0, \check{k}_0\right) \in \mathbb{C}^{2\times 2},$$

as well as

$$\mathbf{r} = \begin{pmatrix}\hat{r}\\ \check{r}\end{pmatrix} \in \mathbb{C}^2.$$

Then we can rewrite the vector of the envelope functions $\mathbf{F}$ and its first derivative $\frac{\mathrm{d}}{\mathrm{d}x}\mathbf{F}$ at $x = 0$ in the form

$$\mathbf{P}_0\mathbf{r} = \mathbf{F}(0) - \hat{\mathbf{F}}_0^{\mathrm{e/h}}(\hat{k}_0), \tag{4.33a}$$

and

$$\mathbf{P}_0\mathbf{K}_0\mathbf{r} = \frac{\mathrm{d}}{\mathrm{d}x}\mathbf{F}(0) - \mathrm{i}\hat{k}_0\hat{\mathbf{F}}_0^{\mathrm{e/h}}(\hat{k}_0). \tag{4.33b}$$

Since the amplitudes $\hat{\mathbf{F}}_0^{\mathrm{e/h}}(-\hat{k}_0)$ and $\hat{\mathbf{F}}_0^{\mathrm{e/h}}(-\mathrm{i}\check{k}_0)$ are linearly independent, cf. Remark 4.1, the matrix $\mathbf{P}_0$ is regular and hence, its inverse $\mathbf{P}_0^{-1}$ exists. Then the reflection coefficient vector $\mathbf{r}$ reads

$$\mathbf{r} = \mathbf{P}_0^{-1}\left(\mathbf{F}(0) - \hat{\mathbf{F}}_0^{\mathrm{e/h}}(\hat{k}_0)\right),$$

cf. Eq. (4.33a). Applied to Eq. (4.33b) we get the left TBC

$$\mathbf{F}_x(0) - \mathbf{P}_0\mathbf{K}_0\mathbf{P}_0^{-1}\mathbf{F}(0) = \left(\mathrm{i}\hat{k}\mathbb{1} - \mathbf{P}_0\mathbf{K}_0\mathbf{P}_0^{-1}\right)\hat{\mathbf{F}}_0^{\mathrm{e/h}}(\hat{k}_0). \tag{4.34}$$

At the right boundary we proceed analogously. The function $\mathbf{F}$ and its first derivative $\frac{\mathrm{d}}{\mathrm{d}x}\mathbf{F}$ at $x = L$ read

$$\mathbf{F}(L) = \hat{t}\hat{\mathbf{F}}_L^{\mathrm{e/h}}(\hat{k}_L)e^{\mathrm{i}\hat{k}_L L} + \check{t}\hat{\mathbf{F}}_L^{\mathrm{e/h}}(\mathrm{i}\check{k}_L)e^{-\check{k}_L L}, \tag{4.35a}$$

and

$$\frac{\mathrm{d}}{\mathrm{d}x}\mathbf{F}(L) = \mathrm{i}\hat{k}_L\hat{t}\hat{\mathbf{F}}_L^{\mathrm{e/h}}(\hat{k}_L)e^{\mathrm{i}\hat{k}_L L} - \check{k}_L\check{t}\hat{\mathbf{F}}_L^{\mathrm{e/h}}(\mathrm{i}\check{k}_L)e^{-\check{k}_L L}. \tag{4.35b}$$

Let us introduce

$$\mathbf{P}_L = \left(\hat{\mathbf{F}}_L^{\mathrm{e/h}}(\hat{k}_L)e^{\mathrm{i}\hat{k}_L L} \quad \hat{\mathbf{F}}_L^{\mathrm{e/h}}(\mathrm{i}\check{k}_L)e^{-\check{k}_L L}\right) \in \mathbb{C}^{2\times 2},$$

and

$$\mathbf{K}_L = \mathrm{diag}\left(\mathrm{i}\hat{k}_L, -\check{k}_L\right) \in \mathbb{C}^{2\times 2},$$

as well as

$$\mathbf{t} = \begin{pmatrix}\hat{t}\\ \check{t}\end{pmatrix} \in \mathbb{C}^2.$$

Then we can rewrite the vector of the envelope functions $\mathbf{F}$ and its first derivative $\frac{\mathrm{d}}{\mathrm{d}x}\mathbf{F}$ at $x = L$ in the form

$$\mathbf{P}_L\mathbf{t} = \mathbf{F}(L), \tag{4.36a}$$

and

$$\mathbf{P}_L\mathbf{K}_L\mathbf{t} = \frac{\mathrm{d}}{\mathrm{d}x}\mathbf{F}(L). \tag{4.36b}$$

Since the amplitudes $\hat{\mathbf{F}}_L^{\mathrm{e/h}}(\hat{k}_L)$ and $\hat{\mathbf{F}}_L^{\mathrm{e/h}}(\mathrm{i}\check{k}_L)$ are linearly independent, cf. Remark 4.1, the vectors $\hat{\mathbf{F}}_L^{\mathrm{e/h}}(\hat{k}_L)e^{\mathrm{i}\hat{k}_L L}$ and $\hat{\mathbf{F}}_L^{\mathrm{e/h}}(\mathrm{i}\check{k}_L)e^{-\check{k}_L L}$ are also linearly independent. Hence, the matrix $\mathbf{P}_L$ is regular and its inverse $\mathbf{P}_L^{-1}$ exists. Then the transmission coefficient vector $\mathbf{t}$ takes the form

$$\mathbf{t} = \mathbf{P}_L^{-1}\mathbf{F}(L),$$

cf. Eq. (4.36a). Applied to Eq. (4.36b) we get the right TBC

$$\mathbf{F}_x(L) - \mathbf{P}_L\mathbf{K}_L\mathbf{P}_L^{-1}\mathbf{F}(L) = \mathbf{0}. \tag{4.37}$$

Remark 4.3. Ben Abdallah and Kefi-Ferhane showed in [9] that the two-band $\mathbf{k}\cdot\mathbf{p}$-model with intra-band coupling together with the corresponding TBCs has a unique solution. However, it is not trivial to transfer this proof to the two-band $\mathbf{k}\cdot\mathbf{p}$-model with inter-band coupling as given in Eq. (4.3) together with the TBCs (4.34) and (4.37).

The strategy used in [9] is similar to the strategy used to show the uniqueness of the solution of the scalar Schrödinger equation and its TBCs, cf. [8]. First the Eq. (4.3) is multiplied by some arbitrary test function $\mathbf{G}$ and then integrated by parts. The resulting expression can be split into a sum of a coercive form $C(\mathbf{F},\mathbf{G})$, a sesquilinear form $S(\mathbf{F},\mathbf{G})$ and a anti-linear form $A(\mathbf{G})$. According to the Riesz representation theorem, there exist compact operators R_C and R_S as well as a function a_L such that the coercive, sesquilinear and anti-linear forms can be expressed as

$$\begin{aligned} C(\mathbf{F},\mathbf{G}) &= \langle R_C\mathbf{F},\mathbf{G}\rangle, \\ S(\mathbf{F},\mathbf{G}) &= \langle R_S\mathbf{F},\mathbf{G}\rangle, \\ A(\mathbf{G}) &= \langle a_L,\mathbf{G}\rangle. \end{aligned}$$

Then we obtain the weak formulation

$$(R_C + R_S)\,\mathbf{F} = a_L,$$

and by applying the Fredholm alternative we can show that this expression has a unique solution if $R_C + R_S$ is injective. This is equivalent to show that the solution of

$$(R_C + R_S)\,\mathbf{F} = 0$$

is identically to zero. By setting $\mathbf{G} = \mathbf{F}$ and taking the imaginary part of this expression we end up with

$$\mathbf{S}_L\mathbf{B}_L\mathbf{F}\cdot\mathbf{B}_L\mathbf{F}(L) - \mathbf{S}_0\mathbf{B}_0\mathbf{F}\cdot\mathbf{B}_0\mathbf{F}(0) = 0,$$

where $\mathbf{B}_0$ and $\mathbf{B}_L$ are some regular matrices and $\mathbf{S}_L$ is a positive definite matrix, while $\mathbf{S}_0$ is negative definite. Hence, we have $\mathbf{F}(0) = \mathbf{F}(L) = \mathbf{0}$. By taking the homogeneous TBCs and the Cauchy-Lipschitz theorem into account, this implies that $\mathbf{F}$ vanishes everywhere.

In the appendix A.1 we prove that the two-band $\mathbf{k}\cdot\mathbf{p}$-model with inter-band coupling can also be expressed in terms of a coercive form $C(\mathbf{F},\mathbf{G})$, a sesquilinear form $S(\mathbf{F},\mathbf{G})$ and a anti-linear form $A(\mathbf{G})$. However, it remains to show the existence of a positive definite matrix $\mathbf{S}_L$ and a negative definite matrix $\mathbf{S}_0$ in order to finish the proof. While the two-band $\mathbf{k}\cdot\mathbf{p}$-model with intra-band coupling has only real wave vectors, the two-band $\mathbf{k}\cdot\mathbf{p}$-model with inter-band coupling has two real wave vectors and a complex conjugate pair of wave vectors. Basically, this is the reason that transferring the proof of the two-band $\mathbf{k}\cdot\mathbf{p}$-model with intra-band coupling to our model is not trivial.

4.3 Discretization

We recall the uniform grid $x_j = jh,\ j = 0, \ldots, J$, with $L = Jh$, of the computational interval $(0, L)$, with $P_{0,j} = P_0(x_j)$, $E_{\mathrm{g},j} = E_{\mathrm{g}}(x_j)$, $E_{0,j} = E_0(x_j)$ and the approximation $\mathbf{F}_j \approx \mathbf{F}(x_j)$, $j = 0, \ldots, J$.

Moreover, we recall the second order standard difference operator $\mathrm{D}_h^{\mathrm{std}}$ in order to discretize the second derivative of the regularization term, as well as the second order centered difference operator $\mathrm{D}_h^{\mathrm{cen}}$ and the first order symmetrized discretization we introduced in Chap. 3 in order to discretize the first order derivative.

In general, the discretization of the two-band $\mathbf{k}\cdot\mathbf{p}$-model takes the form

$$\mathbf{M}_j^+ \mathbf{F}_{j+1} + \left(\mathbf{M}_j^0 - E\mathbb{1}\right)\mathbf{F}_j + \mathbf{M}_j^- \mathbf{F}_{j-1} = \mathbf{0}, \qquad j = 1, \ldots, J-1, \tag{4.38}$$

where the matrices $\mathbf{M}_j^+$, $\mathbf{M}_j^0$ and $\mathbf{M}_j^-$ depend on the choice of the difference operator.

In Chap. 3 we showed that the matrices $\mathbf{M}_j^+$ and $\mathbf{M}_j^-$ are not regular if we use the symmetrized discretization. The two-band $\mathbf{k}\cdot\mathbf{p}$-model contains a second derivative regularization term such that the matrices $\mathbf{M}_j^+$ and $\mathbf{M}_j^-$ are regular if we use the symmetrized discretization for the first derivative in the Hamiltonian $\mathbf{H}$ and the standard discretization for the second derivative regularization term. But first let us start with the second order centered difference operator $\mathrm{D}_h^{\mathrm{cen}}$ to discretize the first derivative.

4.3.1 The Standard and Centered Finite Difference Scheme

When applying the second order centered difference operator $\mathrm{D}_h^{\mathrm{cen}}$ to the first order derivative, we get

$$\begin{aligned}
\mathbf{M}_j^{+,\mathrm{cen}} &= \begin{pmatrix} -\epsilon\frac{1}{h^2} & -\mathrm{i}P_{0,j}\frac{1}{2h} \\ -\mathrm{i}P_{0,j}\frac{1}{2h} & \epsilon\frac{1}{h^2} \end{pmatrix}, \\
\mathbf{M}_j^{0,\mathrm{cen}} &= \begin{pmatrix} \epsilon\frac{2}{h^2} + \frac{1}{2}E_{\mathrm{g},j} + E_{0,j} & 0 \\ 0 & -\epsilon\frac{2}{h^2} - \frac{1}{2}E_{\mathrm{g}} + E_0 \end{pmatrix}, \\
\mathbf{M}_j^{-,\mathrm{cen}} &= \begin{pmatrix} -\epsilon\frac{1}{h^2} & \mathrm{i}P_{0,j}\frac{1}{2h} \\ \mathrm{i}P_{0,j}\frac{1}{2h} & \epsilon\frac{1}{h^2} \end{pmatrix}.
\end{aligned} \tag{4.39}$$

In order to derive the DTBCs we have to find a solution of the discrete exterior problem. In the exterior domains $x \le 0$ and $x \ge L$ the Kane-parameter P_0, the band gap E_{g} and the middle of the band gap E_0 are constant. In this section, however, we will not use the specific values of these parameters in the exterior domains. Instead we shall derive the results for some constant Kane-parameter P_0, some constant band gap E_{g} and some constant middle of the band gap E_0. Later we can use these results to determine the explicit solution in the exterior domains.

If P_0, E_{g} and E_0 are constant, the matrices $\mathbf{M}^{+,\mathrm{cen}}$, $\mathbf{M}^{0,\mathrm{cen}}$ and $\mathbf{M}^{-,\mathrm{cen}}$ are constant. In the sequel we shall omit the subscript j of these matrices.

In this case Eq. (4.38) is a second order linear difference equation with constant coefficients. By introducing the substitution

$$\Phi_j = \begin{pmatrix} \mathbf{F}_j \\ \mathbf{F}_{j+1} \end{pmatrix},$$

Eq. (4.38) can be transformed into a first order difference equation with constant coefficients that reads

$$\Phi_j = \mathbf{A}^{\mathrm{cen}}\Phi_{j-1}, \tag{4.40}$$

with

$$\mathbf{A}^{\mathrm{cen}} = \begin{pmatrix} \mathbf{0} & \mathbb{1} \\ (-\mathbf{M}^{+,\mathrm{cen}})^{-1}\mathbf{M}^{-,\mathrm{cen}} & (-\mathbf{M}^{+,\mathrm{cen}})^{-1}\left(\mathbf{M}^{0,\mathrm{cen}} - E\mathbb{1}\right) \end{pmatrix} \in \mathbb{C}^{4\times 4}.$$

The solution of the first order difference equation is

$$\Phi_j = \mathbf{a}\alpha^j,$$

where $\alpha \in \mathbb{C}$ denotes an eigenvalue of $\mathbf{A}^{\text{cen}}$ and $\mathbf{a} \in \mathbb{C}^4$ the corresponding eigenvector, cf. Prop. 3.4. The first two components of $\Phi_j \in \mathbb{C}^4$ represent the discrete solution $\mathbf{F}_j \in \mathbb{C}^2$ of the second order centered FDS. Thus, we introduce the *discrete amplitude* $\hat{\mathbf{F}}_h \in \mathbb{C}^2$ that contains the first two components of $\mathbf{a}$. Then the discrete solution $\mathbf{F}_j$ takes the form

$$\mathbf{F}_j = \hat{\mathbf{F}}_h \alpha^j = \hat{\mathbf{F}}_h e^{\mathrm{i}k_h jh}, \tag{4.41}$$

with the *discrete wave vector*

$$k_h = \frac{1}{h}\left(\arg(\alpha) - \mathrm{i}\ln|\alpha|\right).$$

The form of the discrete solution (4.41) implies

$$\mathbf{F}_{j+1}e^{-\mathrm{i}k_h h} = \mathbf{F}_j = \mathbf{F}_{j-1}e^{\mathrm{i}k_h h},$$

and thus, applied to the difference equation (4.38) we obtain

$$\hat{\mathbf{H}}_h^{\text{cen}}\hat{\mathbf{F}}_h = E\hat{\mathbf{F}}_h, \tag{4.42}$$

with

$$\begin{aligned}
\hat{\mathbf{H}}_h^{\text{cen}} &= \hat{\mathbf{H}}_h^{\text{cen}}(k_h) \\
&= \mathbf{M}^{+,\text{cen}}e^{\mathrm{i}k_h h} + \mathbf{M}^{0,\text{cen}} + \mathbf{M}^{-,\text{cen}}e^{-\mathrm{i}k_h h} \\
&= \begin{pmatrix} -\epsilon\frac{1}{h^2}\left(e^{\mathrm{i}k_h h} + e^{-\mathrm{i}k_h h}\right) + \epsilon\frac{2}{h^2} + \frac{1}{2}E_{\text{g}} + E_0 & -\mathrm{i}\frac{1}{2h}P_0\left(e^{\mathrm{i}k_h h} - e^{-\mathrm{i}k_h h}\right) \\ -\mathrm{i}\frac{1}{2h}P_0\left(e^{\mathrm{i}k_h h} - e^{-\mathrm{i}k_h h}\right) & \epsilon\frac{1}{h^2}\left(e^{\mathrm{i}k_h h} + e^{-\mathrm{i}k_h h}\right) - \epsilon\frac{2}{h^2} - \frac{1}{2}E_{\text{g}} + E_0 \end{pmatrix} \\
&= \begin{pmatrix} \epsilon\frac{2}{h^2}\left(1 - \cos k_h h\right) + \frac{1}{2}E_{\text{g}} + E_0 & \frac{1}{h}P_0 \sin k_h h \\ \frac{1}{h}P_0 \sin k_h h & -\epsilon\frac{2}{h^2}\left(1 - \cos k_h h\right) - \frac{1}{2}E_{\text{g}} + E_0 \end{pmatrix}.
\end{aligned}$$

The characteristic polynomial of $\hat{\mathbf{H}}_h^{\text{cen}}$ can be written in the form

$$(E - E_0)^2 - \left(\epsilon\frac{2}{h^2}\left(1 - \cos k_h h\right) + \frac{1}{2}E_{\text{g}}\right)^2 + \frac{1}{h^2}P_0^2\left(\cos^2 k_h h - 1\right) = 0. \tag{4.43}$$

Let us introduce the substitution

$$\gamma = \cos k_h h = \cosh \mathrm{i}k_h h, \tag{4.44}$$

with the reciprocal

$$\begin{aligned}
k_h &= \pm\mathrm{i}\frac{1}{h}\ln\left(\gamma + \sqrt{\gamma^2 - 1}\right) \\
&= \pm\frac{1}{h}\left(\arg\left(\gamma + \sqrt{\gamma^2 - 1}\right) - \mathrm{i}\ln\left|\gamma + \sqrt{\gamma^2 - 1}\right|\right) + n\frac{2\pi}{h},
\end{aligned}$$

with $n \in \mathbb{Z}$.

Note that γ is real and greater than -1 if $k_h h \in \mathbb{R} \cup \mathrm{i}\mathbb{R}$. More precisely, $\gamma \in [-1, 1]$ if and only if $k_h h \in \mathbb{R}$ and $\gamma > 1$ if and only if $k_h h \in \mathrm{i}\mathbb{R}$.

Let us suppose that γ is real and greater than -1. If $-1 < \gamma < 1$, we have

$$\ln\left|\gamma + \sqrt{\gamma^2 - 1}\right| = \ln\left|\gamma + \mathrm{i}\sqrt{1 - \gamma^2}\right| = \ln\sqrt{\gamma^2 + 1 - \gamma^2} = 0,$$

and hence, the wave vector is given by

$$k_h = \pm\frac{1}{h}\arg\left(\gamma + \mathrm{i}\sqrt{1 - \gamma^2}\right) + n\frac{2\pi}{h} \in \mathbb{R},$$

for $n \in \mathbb{Z}$. If $\gamma \geq 1$, then we have

$$\gamma + \sqrt{\gamma^2 - 1} > 0,$$

and hence,

$$\arg\left(\gamma + \sqrt{\gamma^2 - 1}\right) = 0.$$

Thus, the wave vector takes the form

$$k_h = \pm \mathrm{i}\frac{1}{h}\ln\left(\gamma + \sqrt{\gamma^2 - 1}\right) + n\frac{2\pi}{h} \in \mathbb{C},$$

for $n \in \mathbb{Z}$.

In other words, if $-1 < \gamma < 1$, then we get a real-valued pair of discrete wave vectors, yielding traveling envelope waves. On the other hand, if $\gamma \geq 1$, then the wave vectors are complex conjugate with zero real part for $n = 0$. If γ is real but less than -1, then the discrete wave vector is complex with nonzero real part and nonzero imaginary part. If $\gamma = -1$, then the discrete wave vector is undefined.

Let us suppose that $\lim_{h\to 0} k_h$ exists for $n = 0$. Then the limit does not exist for $n \neq 0$. Therefore, we shall set $n = 0$ in the sequel. We will see later that the limit of the discrete wave vectors with $n = 0$ in fact exists and equals the analytical values of the wave vector as given in Eqs. (4.17) and (4.19).

Now let us show, that under reasonable assumptions, γ is in fact real and greater than -1. Therefore, let us apply the substitution (4.44) to the characteristic polynomial (4.43). It yields

$$(E - E_0)^2 - \left(\epsilon\frac{2}{h^2}\gamma - \left(\epsilon\frac{2}{h^2} + \frac{1}{2}E_\mathrm{g}\right)\right)^2 + \frac{1}{h^2}P_0^2\left(\gamma^2 - 1\right) = 0,$$

which implies

$$\left(\gamma + \frac{\frac{2\epsilon}{h^2}\left(\frac{2\epsilon}{h^2} + \frac{1}{2}E_\mathrm{g}\right)}{\frac{P_0^2}{h^2} - \frac{4\epsilon^2}{h^4}}\right)^2 = \left(\frac{\frac{2\epsilon}{h^2}\left(\frac{2\epsilon}{h^2} + \frac{1}{2}E_\mathrm{g}\right)}{\frac{P_0^2}{h^2} - \frac{4\epsilon^2}{h^4}}\right)^2 - \left(\frac{(E - E_0)^2 - \left(\frac{2\epsilon}{h^2} + \frac{1}{2}E_\mathrm{g}\right)^2 - \frac{P_0^2}{h^2}}{\frac{P_0^2}{h^2} - \frac{4\epsilon^2}{h^4}}\right). \quad (4.45)$$

If we can show that the right hand side of Eq. (4.45) is nonnegative, the roots $\gamma_{1,2}$ of Eq. (4.45) are real. If the right hand side is positive, the real roots are distinct. First let us assume that the energy E satisfies the condition (4.16), i.e.

$$|E - E_0| \leq \frac{1}{2}E_\mathrm{g}.$$

Then the right hand side of Eq. (4.45) can be written in the form

$$\frac{1}{\left(\frac{4\epsilon^2}{h^2} - P_0^2\right)^2}\left(4\epsilon^2(E - E_0)^2 + P_0^4 + 2\epsilon P_0^2 E_\mathrm{g} + h^2 P_0^2\left(\frac{1}{4}E_\mathrm{g}^2 - (E - E_0)^2\right)\right).$$

Clearly, it is nonnegative if Eq. (4.16) is fulfilled and

$$h \neq \frac{2\epsilon}{P_0}.$$

Hence, γ is real.

On the other hand, if we assume that the energy E satisfies Eq. (4.18), i.e.

$$|E - E_0| > \frac{1}{2}E_\mathrm{g},$$

and if we write the right hand side of Eq. (4.45) in the form

$$\frac{1}{\left(\frac{4\epsilon^2}{h^2}-P_0^2\right)^2}\left(\left(\epsilon E_\mathrm{g}+P_0^2\right)^2+\left(4\epsilon^2-h^2P_0^2\right)\left((E-E_0)^2-\frac{1}{4}E_\mathrm{g}^2\right)\right),$$

we can see that it suffice to require the step size restriction

$$h<\frac{2\epsilon}{P_0}, \tag{4.46}$$

in order to get a positive right hand side of Eq. (4.45) and hence, distinct real roots of Eq. (4.45). Note that this inequality is not best possible, but since we need

$$h\neq\frac{2\epsilon}{P_0}$$

to avoid undefined right hand sides of Eq. (4.45) the condition (4.46) is most practicable.

Thus, γ takes the form

$$\begin{aligned}\gamma_{1,2}&=\frac{\frac{4\epsilon^2}{h^2}+\epsilon E_\mathrm{g}}{\frac{4\epsilon^2}{h^2}-P_0^2}\pm\frac{1}{\frac{4\epsilon^2}{h^2}-P_0^2}\sqrt{\left(\epsilon E_\mathrm{g}+P_0^2\right)^2+\left(4\epsilon^2-h^2P_0^2\right)\left((E-E_0)^2-\frac{1}{4}E_\mathrm{g}^2\right)}\\&=1+\frac{\epsilon E_\mathrm{g}+P_0^2}{\frac{4\epsilon^2}{h^2}-P_0^2}\pm\frac{1}{\frac{4\epsilon^2}{h^2}-P_0^2}\sqrt{\left(\epsilon E_\mathrm{g}+P_0^2\right)^2+\left(4\epsilon^2-h^2P_0^2\right)\left((E-E_0)^2-\frac{1}{4}E_\mathrm{g}^2\right)}.\end{aligned} \tag{4.47}$$

If the step size h suffices the step size condition (4.46), it is obvious that the root γ_1, that corresponds to the positive sign in Eq. (4.47), is greater than 1 and hence, yields a complex conjugate pair of purely imaginary discrete wave vectors. On the other hand, the root γ_2 is greater than or equal to 1 if the energy E satisfies

$$|E-E_0|\leq\frac{1}{2}E_\mathrm{g},$$

and less than 1, if

$$|E-E_0|>\frac{1}{2}E_\mathrm{g}.$$

In the first case, we obtain two complex conjugate pairs of purely imaginary discrete wave vectors, while we get one real-valued pair and one purely imaginary, complex conjugate pair of discrete wave vectors in the latter case.

Since the discrete wave vectors are either real-valued or purely imaginary, γ is always greater than -1.

Let us summarize the results of the discrete wave vector k_h. If the energy E satisfies

$$|E-E_0|\leq\frac{1}{2}E_\mathrm{g},$$

and the step size is sufficiently small, i.e. Eq. (4.46) is fulfilled, than we obtain two complex conjugate pairs of purely imaginary discrete wave vectors that read

$$k_h=\pm\mathrm{i}\check{k}_{h,1,2}, \tag{4.48}$$

with the discrete attenuation coefficients

$$\check{k}_{h,1,2}=\frac{1}{h}\ln\left(\gamma_{1,2}+\sqrt{\gamma_{1,2}^2-1}\right),$$

where $\gamma_{1,2}$ is given by

$$\gamma_{1,2} = 1 + \frac{\epsilon E_\mathrm{g} + P_0^2}{\frac{4\epsilon^2}{h^2} - P_0^2} \pm \frac{1}{\frac{4\epsilon^2}{h^2} - P_0^2} \sqrt{\left(\epsilon E_\mathrm{g} + P_0^2\right)^2 + \left(4\epsilon^2 - h^2 P_0^2\right)\left((E - E_0)^2 - \frac{1}{4}E_\mathrm{g}^2\right)}.$$

These real discrete wave vectors yield evanescent discrete waves.

On the other hand, if the energy E satisfies

$$|E - E_0| > \frac{1}{2}E_\mathrm{g},$$

and the step size is sufficiently small, i.e. Eq. (4.46) is fulfilled, then we obtain one pair of real discrete wave vectors, yielding traveling discrete waves, and one complex conjugate pair of purely imaginary discrete wave vectors, yielding evanescent discrete waves. The pair of real wave vectors takes the form

$$k_h = \pm \hat{k}_h, \tag{4.49a}$$

with the discrete propagation coefficient

$$\hat{k}_h = \frac{1}{h} \arg\left(\gamma + \mathrm{i}\sqrt{1 - \gamma^2}\right),$$

where γ is given by

$$\gamma = 1 + \frac{\epsilon E_\mathrm{g} + P_0^2}{\frac{4\epsilon^2}{h^2} - P_0^2} - \frac{1}{\frac{4\epsilon^2}{h^2} - P_0^2} \sqrt{\left(\epsilon E_\mathrm{g} + P_0^2\right)^2 + \left(4\epsilon^2 - h^2 P_0^2\right)\left((E - E_0)^2 - \frac{1}{4}E_\mathrm{g}^2\right)}.$$

The complex conjugate pair of purely imaginary wave vectors reads

$$k_h = \pm \mathrm{i}\check{k}_h, \tag{4.49b}$$

with the discrete attenuation coefficient

$$\check{k}_h = \frac{1}{h} \ln\left(\gamma + \sqrt{\gamma^2 - 1}\right),$$

and

$$\gamma = 1 + \frac{\epsilon E_\mathrm{g} + P_0^2}{\frac{4\epsilon^2}{h^2} - P_0^2} + \frac{1}{\frac{4\epsilon^2}{h^2} - P_0^2} \sqrt{\left(\epsilon E_\mathrm{g} + P_0^2\right)^2 + \left(4\epsilon^2 - h^2 P_0^2\right)\left((E - E_0)^2 - \frac{1}{4}E_\mathrm{g}^2\right)}.$$

Eqs. (4.48) and (4.49) are called *discrete dispersion relations* of the second order centered FDS of the two-band $\mathbf{k}\cdot\mathbf{p}$-model. Usually this relation is given in the reciprocal form which we get by calculating the eigenvalue E of $\hat{\mathbf{H}}_h^{\mathrm{cen}}$

$$E = E_h^{\mathrm{e/h}}(k_h) = E_0 \pm \sqrt{\left(\epsilon \frac{4}{h^2} \sin^2 \frac{k_h h}{2} + \frac{1}{2}E_\mathrm{g}\right)^2 + \frac{1}{h^2}P_0^2 \sin^2 k_h h}. \tag{4.50}$$

As in the continuous case, the energy E_h^{e} associated with the positive sign in Eq. (4.50) denotes the energy of the electrons, while E_h^{h} corresponding to the negative sign in Eq. (4.50) is the energy of the holes.

By applying l'Hôpital's rule, it can be shown that the discrete dispersion relation (4.50) tends to the analytical dispersion relation (4.20) for $h \to 0$. The same can be shown for the discrete wave vectors (4.48) and (4.49).

Fig. 4.1 shows a comparison of the analytical dispersion relation of the two-band $\mathbf{k}\cdot\mathbf{p}$-model and the discrete dispersion relation of the centered FDS for different Kane-parameters P_0. In

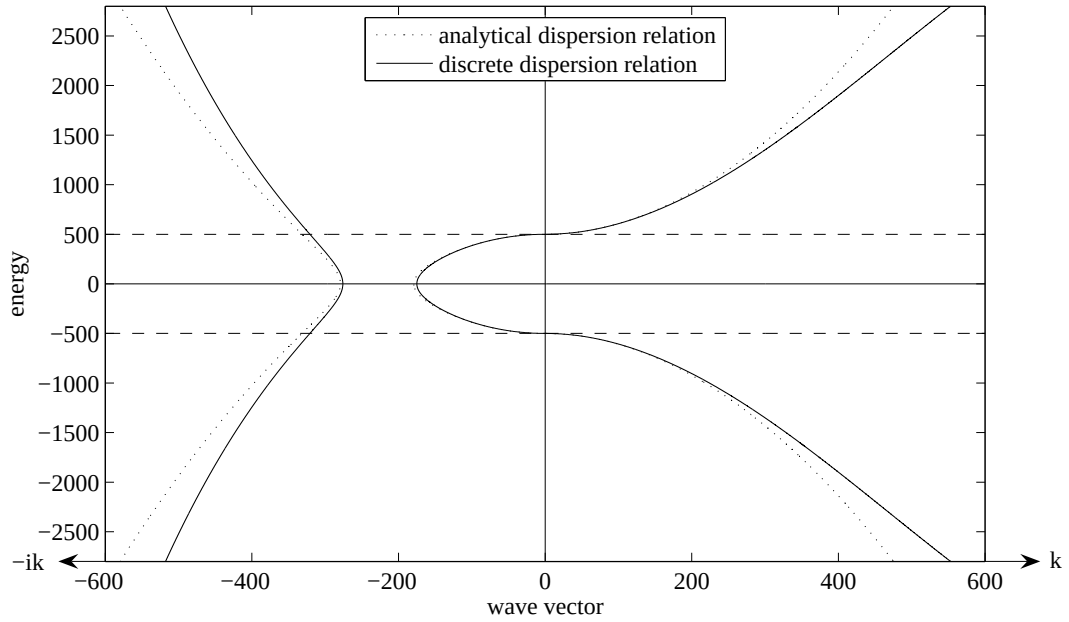

(a) Kane-parameter $P_0 = 1$

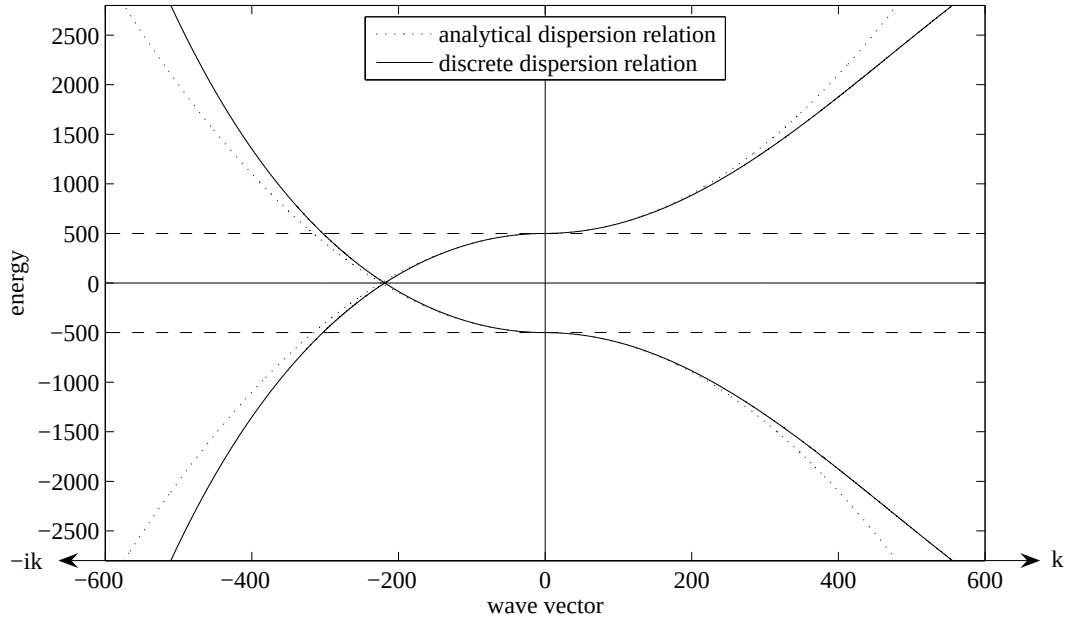

(b) Kane-parameter $P_0 = 0.01$

Figure 4.1: Comparison of the analytical dispersion relation (dotted line) of the two-band $\mathbf{k} \cdot \mathbf{p}$-model and the discrete dispersion relation of the centered FDS (solid line) for a step size $h = 1/300$, a band gap $E_\mathrm{g} = 1000$, a regularization parameter $\epsilon = 0.01$ and a Kane-parameter $P_0 = 1$ in Fig. (a) and a Kane-parameter $P_0 = 0.01$ in Fig. (b), respectively. The negative wave vector axis corresponds to the purely imaginary wave vector $k = \mathrm{i}\check{k}$ of evanescent envelope waves while the positive wave vector axis corresponds to the real wave vector $k = \hat{k}$ of traveling envelope waves. The dashed lines indicate the energy values $E_\mathrm{g}/2$ and $-E_\mathrm{g}/2$. Between these energy levels the energy condition (4.18) is not fulfilled and there exist only imaginary wave vectors.

particular the behavior of the attenuation coefficients is shown. We observe that for small values of the Kane-parameter, the trunk of the wave vector that is purely imaginary for all energies intersects with the trunk of the wave vector that is purely imaginary if the energy satisfies $|E - E_0| \leq E_\mathrm{g}/2$ and real otherwise.

Let us finish the analysis of the discrete exterior problem by giving the the discrete amplitude of the discrete exterior solutions. The discrete amplitude

$$\hat{\mathbf{F}}_h(k_h) = \hat{\mathbf{F}}_h^{\mathrm{e/h}}(k_h) = \begin{pmatrix} \hat{F}_{h,\mathrm{c}}^{\mathrm{e/h}}(k_h) \\ \hat{F}_{h,\mathrm{v}}^{\mathrm{e/h}}(k_h) \end{pmatrix}$$

is an eigenvector of $\hat{\mathbf{H}}_h^{\mathrm{cen}}(k_h)$ with the corresponding eigenvalue $E_h^{\mathrm{e/h}}(k_h)$. Hence, it is not defined uniquely and solves the under-determined linear equation

$$\left(\hat{H}_{h,11}^{\mathrm{cen}}(\hat{k}_h) - E_h^{\mathrm{e/h}}(\hat{k}_h)\right) \hat{F}_{h,\mathrm{c}}^{\mathrm{e/h}}(\hat{k}_h) + \hat{H}_{h,12}^{\mathrm{cen}}(\hat{k}_h)\hat{F}_{h,\mathrm{v}}^{\mathrm{e/h}}(\hat{k}_h) = 0. \tag{4.51}$$

Thus, the discrete amplitude can be written in the form

$$\hat{\mathbf{F}}_h^{\mathrm{e/h}}(k_h) = c \begin{pmatrix} \hat{H}_{h,12}^{\mathrm{cen}}(k_h) \\ E_h^{\mathrm{e/h}}(k_h) - \hat{H}_{h,11}^{\mathrm{cen}}(k_h) \end{pmatrix} = c \begin{pmatrix} P_0 \frac{\sin k_h h}{h} \\ E_h^{\mathrm{e/h}}(k_h) - \epsilon \frac{4}{h^2} \sin^2 \frac{k_h h}{2} - \frac{1}{2} E_\mathrm{g} - E_0 \end{pmatrix}, \tag{4.52}$$

with some arbitrary $c \in \mathbb{C}$. Note that $\mathbf{F}_j^{\mathrm{e}}(k_h) = \hat{\mathbf{F}}_h^{\mathrm{e}}(k_h) e^{\mathrm{i}k_h jh}$ is the energy eigenstate associated with the energy E_h^{e} of the electrons while $\mathbf{F}_j^{\mathrm{h}}(k_h) = \hat{\mathbf{F}}_h^{\mathrm{h}}(k_h) e^{\mathrm{i}k_h jh}$ corresponds to the energy E_h^{h} of the holes, see Eq. (4.50).

If we assume that the energy condition $|E - E_0| > \frac{1}{2} E_\mathrm{g}$ is fulfilled we obtain two traveling and two discrete evanescent envelope waves. For the two traveling envelope waves we shall additionally assume that they are unitary, i.e. the discrete amplitude $\hat{\mathbf{F}}_h^{\mathrm{e/h}}(\hat{k}_h)$ has norm 1 and it satisfies the normalization condition

$$\left\| \hat{\mathbf{F}}_h^{\mathrm{e/h}}(\hat{k}_h) \right\|_{\mathbb{C}}^2 = \left\langle \hat{\mathbf{F}}_h^{\mathrm{e/h}}(\hat{k}_h), \overline{\hat{\mathbf{F}}_h^{\mathrm{e/h}}(\hat{k}_h)} \right\rangle = 1. \tag{4.53}$$

Since $\hat{\mathbf{H}}_h^{\mathrm{cen}}(\hat{k}_h)$ and its eigenvalues $E_h^{\mathrm{e/h}}(\hat{k}_h)$ are real-valued, the eigenvectors $\hat{\mathbf{F}}_h^{\mathrm{e/h}}(\hat{k}_h)$ are either also real-valued or purely imaginary. But since our approach in Eq. (4.41) implies that $\hat{\mathbf{F}}_h^{\mathrm{e/h}}(k_h)$ is the modulus of $\mathbf{F}_j$, we shall assume that the discrete amplitude $\hat{\mathbf{F}}_h^{\mathrm{e/h}}(k_h)$ is real. Hence, the normalization condition (4.53) becomes

$$\hat{F}_{h,\mathrm{c}}^{\mathrm{e/h}}(\hat{k}_h)^2 + \hat{F}_{h,\mathrm{v}}^{\mathrm{e/h}}(\hat{k}_h)^2 = 1, \tag{4.54}$$

and the amplitude $\hat{\mathbf{F}}_h^{\mathrm{e/h}}(\hat{k}_h)$ of a discrete traveling envelope wave with norm 1 reads

$$\begin{aligned} \hat{\mathbf{F}}_h^{\mathrm{e/h}}(\hat{k}_h) &= \pm \begin{pmatrix} \frac{\hat{H}_{h,12}^{\mathrm{cen}}(\hat{k}_h)}{\sqrt{\left(E_h^{\mathrm{e/h}}(\hat{k}_h) - \hat{H}_{h,11}^{\mathrm{cen}}(\hat{k}_h)\right)^2 + \hat{H}_{h,12}^{\mathrm{cen}}(\hat{k}_h)^2}} \\ \frac{E_h^{\mathrm{e/h}}(\hat{k}_h) - \hat{H}_{h,11}^{\mathrm{cen}}(\hat{k}_h)}{\sqrt{\left(E_h^{\mathrm{e/h}}(\hat{k}_h) - \hat{H}_{h,11}^{\mathrm{cen}}(\hat{k}_h)\right)^2 + \hat{H}_{h,12}^{\mathrm{cen}}(\hat{k}_h)^2}} \end{pmatrix} \\ &= \pm \begin{pmatrix} \frac{P_0 \frac{\sin \hat{k}_h h}{h}}{\sqrt{\left(E_h^{\mathrm{e/h}}(\hat{k}_h) - \epsilon \frac{4}{h^2} \sin^2 \frac{\hat{k}_h h}{2} - \frac{1}{2} E_\mathrm{g} - E_0\right)^2 + P_0^2 \frac{\sin^2 \hat{k}_h h}{h^2}}} \\ \frac{E_h^{\mathrm{e/h}}(\hat{k}_h) - \epsilon \frac{4}{h^2} \sin^2 \frac{\hat{k}_h h}{2} - \frac{1}{2} E_\mathrm{g} - E_0}{\sqrt{\left(E_h^{\mathrm{e/h}}(\hat{k}_h) - \epsilon \frac{4}{h^2} \sin^2 \frac{\hat{k}_h h}{2} - \frac{1}{2} E_\mathrm{g} - E_0\right)^2 + P_0^2 \frac{\sin^2 \hat{k}_h h}{h^2}}} \end{pmatrix}. \end{aligned} \tag{4.55}$$

Since the two solutions of the amplitude in Eq. (4.55) are linearly dependent, we can neglect the solution with negative sign and set

$$\hat{\mathbf{F}}_h^{\mathrm{e/h}}(\hat{k}_h) = \begin{pmatrix} \frac{P_0 \frac{\sin \hat{k}_h h}{h}}{\sqrt{\left(E_h^{\mathrm{e/h}}(\hat{k}_h) - \epsilon \frac{4}{h^2} \sin^2 \frac{\hat{k}_h h}{2} - \frac{1}{2}E_{\mathrm{g}} - E_0\right)^2 + P_0^2 \frac{\sin^2 \hat{k}_h h}{h^2}}} \\ \frac{E_h^{\mathrm{e/h}}(\hat{k}_h) - \epsilon \frac{4}{h^2} \sin^2 \frac{\hat{k}_h h}{2} - \frac{1}{2}E_{\mathrm{g}} - E_0}{\sqrt{\left(E_h^{\mathrm{e/h}}(\hat{k}_h) - \epsilon \frac{4}{h^2} \sin^2 \frac{\hat{k}_h h}{2} - \frac{1}{2}E_{\mathrm{g}} - E_0\right)^2 + P_0^2 \frac{\sin^2 \hat{k}_h h}{h^2}}} \end{pmatrix}. \tag{4.56}$$

Remark 4.4. Since the discrete amplitudes $\hat{\mathbf{F}}_h^{\mathrm{e/h}}(\pm\hat{k}_h)$ of discrete traveling envelope waves are real-valued while the discrete amplitudes $\hat{\mathbf{F}}_h^{\mathrm{e/h}}(\pm\mathrm{i}\check{k}_h)$ of discrete evanescent envelope waves have a purely imaginary component and a real component, the discrete amplitudes $\hat{\mathbf{F}}_h^{\mathrm{e/h}}(\pm\hat{k}_h)$ of discrete traveling envelope waves are linearly independent from the discrete amplitudes $\hat{\mathbf{F}}_h^{\mathrm{e/h}}(\pm\mathrm{i}\check{k}_h)$ of discrete evanescent envelope waves.

Analogously to Chap. 3, let us now analyze the periodicity of the discrete dispersion relation (4.50) of the centered FDS. Let will focus on traveling envelope waves with a real wave vector $k_h \in \mathbb{R}$. The discrete amplitude satisfies

$$\hat{\mathbf{F}}_h^{\mathrm{e/h}}\left(k_h + n\frac{2\pi}{h}\right) = \hat{\mathbf{F}}_h^{\mathrm{e/h}}(k_h), \qquad \forall n \in \mathbb{Z}, k_h \in \mathbb{R}, \tag{4.57}$$

and hence, it has a period of $2\frac{\pi}{h}$ in k_h. Thus, the discrete envelope function

$$\mathbf{F}_j = \hat{\mathbf{F}}_h^{\mathrm{e/h}}(k_h) e^{\mathrm{i}k_h j h}$$

is $\frac{2\pi}{h}$-periodic in k_h. On the other hand, the discrete dispersion relation of the centered FDS satisfies

$$E_h^{\mathrm{e/h}}\left(k_h + n\frac{2\pi}{h}\right) = E_h^{\mathrm{e/h}}(k_h), \qquad \forall n \in \mathbb{Z}, k_h \in \mathbb{R}, \tag{4.58}$$

and hence, it is also $2\frac{\pi}{h}$ in k_h. However, it also consists of $\frac{\pi}{h}$-periodic terms. Before we will analyze the influence of these $\frac{\pi}{h}$-periodic terms, let us note that the discrete dispersion relation is an even function and hence, we can focus on the interval $\left(0, \frac{\pi}{h}\right)$.

Without loss of generality let us restrict our considerations to the energy of the electron $E = E^{\mathrm{e}}$. Then the discrete dispersion relation has a local minimum at $k_h = 0$ and a second local minimum at $k_h = \frac{\pi}{h}$, i.e. at the boundaries of the considered interval. By applying the extreme value theorem, we know that there exists a maximum of the discrete dispersion relation in the interval $\left(0, \frac{\pi}{h}\right)$. Hence, the discrete dispersion relation is not injective in the domain $\left(0, \frac{\pi}{h}\right)$. Obviously, there are no other extrema in this domain $\left(0, \frac{\pi}{h}\right)$. In other words, for any energy E that satisfies

$$E_0 + \frac{1}{2}E_{\mathrm{g}} = E^{\mathrm{e}}(0) < E < E^{\mathrm{e}}\left(\frac{\pi}{h}\right) = E_0 + \frac{1}{2}E_{\mathrm{g}} + \frac{4\epsilon}{h^2},$$

there exists a unique discrete wave vector k_h in the interval $\left(0, \frac{\pi}{h}\right)$ that solves the discrete dispersion relation. On the other hand, for any energy E that satisfies

$$E_0 + \frac{1}{2}E_{\mathrm{g}} + \frac{4\epsilon}{h^2} = E^{\mathrm{e}}\left(\frac{\pi}{h}\right) \leq E \leq \max_{0<k_h<\frac{\pi}{h}} E^{\mathrm{e}}(k_h),$$

there exist exactly two discrete wave vectors $k_{h,1}$ and $k_{h,2}$ in the interval $\left(0, \frac{\pi}{h}\right)$ that solve the discrete dispersion relation of the centered FDS. Fig. 4.2 illustrate this behavior of the discrete dispersion relation of the centered FDS and compares it with the analytical dispersion relation and the discrete dispersion relation of the symmetrized FDS we will introduce in the following section.

We will refer to the energy interval

$$E_0 + \frac{1}{2}E_\mathrm{g} = E^\mathrm{e}(0) < E < E^\mathrm{e}\left(\frac{\pi}{h}\right) = E_0 + \frac{1}{2}E_\mathrm{g} + \frac{4\epsilon}{h^2},$$

as *energy window* of the discrete dispersion relation of the centered FDS.

This means that for all energies E inside the energy window we do not expect spurious oscillations as we observed for the centered FDS of the Kane-model in Chap. 3, while for any energy outside the energy window we expect spurious oscillations if at least one of the parameters of the two-band $\mathbf{k}\cdot\mathbf{p}$-model is not constant in the computational domain of the semiconductor.

In the next section we will introduce the symmetrized FDS for the two-band $\mathbf{k}\cdot\mathbf{p}$-model and will check if its discrete dispersion relation is again injective in the interval $\left(0, \frac{\pi}{h}\right)$ as it is for the two-band Kane-model. If so, the scheme is applicable not only for energies inside some energy window.

4.3.2 The Standard and Symmetrized Finite Difference Scheme

When using the symmetrized FDS for the first order derivative in $\mathbf{H}$ we get the coefficient matrices

$$\begin{aligned}
\mathbf{M}_j^{+,\mathrm{sym}} &= \begin{pmatrix} -\epsilon\frac{1}{h^2} & -\mathrm{i}P_{0,j}\frac{1}{h} \\ 0 & \epsilon\frac{1}{h^2} \end{pmatrix}, \\
\mathbf{M}_j^{0,\mathrm{sym}} &= \begin{pmatrix} \epsilon\frac{2}{h^2} + \frac{1}{2}E_{\mathrm{g},j} + E_{0,j} & \mathrm{i}P_{0,j}\frac{1}{h} \\ -\mathrm{i}P_{0,j}\frac{1}{h} & -\epsilon\frac{2}{h^2} - \frac{1}{2}E_{\mathrm{g},j} + E_{0,j} \end{pmatrix}, \\
\mathbf{M}_j^{-,\mathrm{sym}} &= \begin{pmatrix} -\epsilon\frac{1}{h^2} & 0 \\ \mathrm{i}P_{0,j}\frac{1}{h} & \epsilon\frac{1}{h^2} \end{pmatrix}.
\end{aligned} \tag{4.59}$$

In the discrete exterior problem the Kane-parameter P_0, the band gap E_g and the middle of the band gap E_0 are constant. Hence, the matrices $\mathbf{M}^{+,\mathrm{sym}}$, $\mathbf{M}^{0,\mathrm{sym}}$ and $\mathbf{M}^{-,\mathrm{sym}}$ are constant. In the sequel we shall omit the subscript j of these matrices.

Thus, Eq. (4.38) with the matrices as given in Eq. (4.59) is a second order difference equation with constant coefficients. We recall the substitution

$$\Phi_j = \begin{pmatrix} \mathbf{F}_j \\ \mathbf{F}_{j+1} \end{pmatrix},$$

and transform Eq. (4.38) into a first order difference equation with constant coefficients

$$\Phi_j = \mathbf{A}^\mathrm{sym}\Phi_{j-1}, \tag{4.60}$$

with

$$\mathbf{A}^\mathrm{sym} = \begin{pmatrix} \mathbf{0} & \mathbb{1} \\ (\mathbf{M}^{+,\mathrm{sym}})^{-1}\mathbf{M}^{-,\mathrm{sym}} & (\mathbf{M}^{+,\mathrm{sym}})^{-1}\left(\mathbf{M}^{0,\mathrm{sym}} - E\mathbb{1}\right) \end{pmatrix} \in \mathbb{C}^{4\times 4}.$$

The solution of Eq. (4.60) has the form

$$\Phi_j = \mathbf{a}\alpha^j, \tag{4.61}$$

where $\alpha \in \mathbb{C}$ denotes an eigenvalue of $\mathbf{A}^\mathrm{sym}$ with the corresponding eigenvector $\mathbf{a} \in \mathbb{C}^4$, see Prop. 3.4. The first two components of $\Phi_j \in \mathbb{C}^4$ represent the discrete solution $\mathbf{F}_j \in \mathbb{C}^2$ of the first order symmetrized FDS. Thus, we introduce the *discrete amplitude* $\hat{\mathbf{F}}_h \in \mathbb{C}^2$ that contains the first two components of $\mathbf{a}$. The discrete solution $\mathbf{F}_j$ then takes the form

$$\mathbf{F}_j = \hat{\mathbf{F}}_h\alpha^j = \hat{\mathbf{F}}_h e^{\mathrm{i}k_h hj}, \tag{4.62}$$

with the *discrete wave vector*

$$k_h = \frac{1}{h}\left(\arg(\alpha) - \mathrm{i}\ln|\alpha|\right).$$

The form of the discrete solution (4.62) implies

$$\mathbf{F}_{j+1}e^{-\mathrm{i}k_h h} = \mathbf{F}_j = \mathbf{F}_{j-1}e^{\mathrm{i}k_h h},$$

and hence, applied to the difference equation (4.38) we obtain

$$\hat{\mathbf{H}}_h^{\mathrm{sym}}\hat{\mathbf{F}}_h = E\hat{\mathbf{F}}_h, \tag{4.63}$$

with

$$\begin{aligned}
\hat{\mathbf{H}}_h^{\mathrm{sym}} &= \hat{\mathbf{H}}_h^{\mathrm{sym}}(k_h)\\
&= \mathbf{M}^{+,\mathrm{sym}}e^{\mathrm{i}k_h h} + \mathbf{M}^{0,\mathrm{sym}} + \mathbf{M}^{-,\mathrm{sym}}e^{-\mathrm{i}k_h h}\\
&= \begin{pmatrix} -\epsilon\frac{1}{h^2}\left(e^{\mathrm{i}k_h h} + e^{-\mathrm{i}k_h h}\right) + \epsilon\frac{2}{h^2} + \frac{1}{2}E_{\mathrm{g}} + E_0 & -\mathrm{i}\frac{1}{h}P_0\left(e^{\mathrm{i}k_h h} - 1\right)\\ -\mathrm{i}\frac{1}{h}P_0\left(1 - e^{-\mathrm{i}k_h h}\right) & \epsilon\frac{1}{h^2}\left(e^{\mathrm{i}k_h h} + e^{-\mathrm{i}k_h h}\right) - \epsilon\frac{2}{h^2} - \frac{1}{2}E_{\mathrm{g}} + E_0\end{pmatrix}\\
&= \begin{pmatrix} \epsilon\frac{4}{h^2}\sin^2\frac{k_h h}{2} + \frac{1}{2}E_{\mathrm{g}} + E_0 & \frac{1}{h}P_0\left(-\sin k_h h - \mathrm{i}\left(1-\cos k_h h\right)\right)\\ \frac{1}{h}P_0\left(-\sin k_h h + \mathrm{i}\left(1-\cos k_h h\right)\right) & -\epsilon\frac{4}{h^2}\sin^2\frac{k_h h}{2} - \frac{1}{2}E_{\mathrm{g}} + E_0\end{pmatrix}.
\end{aligned}$$

Let us analyze the characteristic polynomial

$$\begin{aligned}
0 &= (E-E_0)^2 - \left(\epsilon\frac{4}{h^2}\sin^2\frac{k_h h}{2} + \frac{1}{2}E_{\mathrm{g}}\right)^2 - \frac{1}{h^2}P_0^2\left(\sin^2 k_h h + \left(1-\cos k_h h\right)^2\right)\\
&= (E-E_0)^2 - \left(\epsilon\frac{4}{h^2}\sin^2\frac{k_h h}{2} + \frac{1}{2}E_{\mathrm{g}}\right)^2 - \frac{4}{h^2}P_0^2\sin^2\frac{k_h h}{2}
\end{aligned}$$

of $\hat{\mathbf{H}}_h^{\mathrm{sym}}$. It implies

$$\sin^2\frac{k_h h}{2} = -\frac{h^2}{8\epsilon^2}\left(\epsilon E_{\mathrm{g}} + P_0^2\right) \pm \sqrt{\frac{h^4}{64\epsilon^4}\left(\epsilon E_{\mathrm{g}} + P_0^2\right)^2 + \frac{h^4}{16\epsilon^2}\left((E-E_0)^2 - \frac{1}{4}E_{\mathrm{g}}^2\right)}, \tag{4.64}$$

if

$$(E-E_0)^2 \geq \frac{P_0^2}{2\epsilon}\left(E_{\mathrm{g}} - \frac{P_0^2}{2\epsilon}\right). \tag{4.65}$$

Note that Eq. (4.65) is always satisfied if the energy E fulfills the energy condition (4.18), i.e.

$$|E-E_0| > \frac{1}{2}E_{\mathrm{g}}.$$

On the other hand, if the energy condition is not satisfied, then Eq. (4.65) forms an additional condition that needs to be satisfied to write the discrete wave vector k_h in the form as given in Eq. (4.64). However, we will neglect this case since it yields evanescent envelope waves only.

Hence, we get the following discrete wave vectors when applying the symmetrized FDS. If the energy condition (4.18) is satisfied, i.e.

$$|E-E_0| > \frac{1}{2}E_{\mathrm{g}},$$

we get one pair of real discrete wave vectors

$$k_h = \pm\hat{k}_h \in \mathbb{R}, \tag{4.66a}$$

with the propagation coefficient

$$\hat{k}_h = \frac{2}{h} \arcsin \sqrt{-\frac{h^2}{8\epsilon^2}\left(\epsilon E_\mathrm{g} + P_0^2\right) + \sqrt{\frac{h^4}{64\epsilon^4}\left(\epsilon E_\mathrm{g} + P_0^2\right)^2 + \frac{h^4}{16\epsilon^2}\left((E-E_0)^2 - \frac{1}{4}E_\mathrm{g}^2\right)}},$$

and one complex conjugate pair of purely imaginary discrete wave vectors

$$k_h = \pm \mathrm{i}\check{k}_h, \tag{4.66b}$$

with the attenuation coefficient

$$\hat{k}_h = \frac{2}{h} \ln\left(\sqrt{z^2+1} - z\right),$$

where $z \in \mathbb{R}$ is given by

$$z = \sqrt{\frac{h^2}{8\epsilon^2}\left(\epsilon E_\mathrm{g} + P_0^2\right) + \sqrt{\frac{h^4}{64\epsilon^4}\left(\epsilon E_\mathrm{g} + P_0^2\right)^2 + \frac{h^4}{16\epsilon^2}\left((E-E_0)^2 - \frac{1}{4}E_\mathrm{g}^2\right)}}.$$

On the other hand, if the energy condition (4.18) is not fulfilled, i.e.

$$|E - E_0| \leq \frac{1}{2}E_\mathrm{g},$$

and moreover,

$$\frac{1}{2}E_\mathrm{g} \leq \frac{2\epsilon^2}{P_0^2}(E-E_0)^2 + \frac{P_0^2}{2}$$

is satisfied, cf. Eq. (4.65), then the discrete wave vector k_h is purely imaginary and reads

$$k_h = \pm \mathrm{i}\check{k}_h, \tag{4.67}$$

with the discrete attenuation coefficient

$$\check{k} = \frac{2}{h} \ln\left(\sqrt{z^2+1} - z\right),$$

where $z \in \mathbb{R}$ is given by

$$z = \sqrt{\frac{h^2}{8\epsilon^2}\left(\epsilon E_\mathrm{g} + P_0^2\right) \pm \sqrt{\frac{h^4}{64\epsilon^4}\left(\epsilon E_\mathrm{g} + P_0^2\right)^2 + \frac{h^4}{16\epsilon^2}\left((E-E_0)^2 - \frac{1}{4}E_\mathrm{g}^2\right)}}.$$

From the characteristic polynomial of $\hat{\mathbf{H}}_h^{\mathrm{sym}}$ we can derive the reciprocal of the formulas of the discrete wave vectors (4.66) and (4.67) to get the discrete dispersion relation

$$E = E_h^{\mathrm{e/h}}(\hat{k}_h) = E_0 \pm \sqrt{\left(\epsilon\frac{4}{h^2}\sin^2\frac{\hat{k}_h h}{2} + \frac{E_\mathrm{g}}{2}\right)^2 + \frac{4}{h^2}P_0^2\sin^2\frac{\hat{k}_h h}{2}} \in \mathbb{R}, \tag{4.68}$$

where the positive sign corresponds to the energy E_h^{e} of the electrons and the negative sign corresponds to the energy E_h^{h} of the holes.

By applying l'Hôpital's rule, it can be shown that the discrete wave vectors (4.66) and (4.67) as well as the discrete dispersion relation (4.68) tend to their analytical form for $h \to 0$.

Now we will specify the discrete amplitude $\hat{\mathbf{F}}_h(k_h)$ of the symmetrized FDS. Analogously to the centered FDS, the discrete amplitude

$$\hat{\mathbf{F}}_h(k_h) = \hat{\mathbf{F}}_h^{\mathrm{e/h}}(k_h) = \begin{pmatrix} \hat{F}_{h,\mathrm{c}}^{\mathrm{e/h}}(k_h) \\ \hat{F}_{h,\mathrm{v}}^{\mathrm{e/h}}(k_h) \end{pmatrix},$$

reads

$$\hat{\mathbf{F}}_h^{\mathrm{e/h}}(k_h) = c\begin{pmatrix} \hat{H}_{h,12}^{\mathrm{sym}}(k_h) \\ E_h^{\mathrm{e/h}}(k_h) - \hat{H}_{h,11}^{\mathrm{sym}}(k_h) \end{pmatrix} = c\begin{pmatrix} -\frac{1}{h}P_0\left(\sin k_h h + \mathrm{i}\left(1-\cos k_h h\right)\right) \\ E_h^{\mathrm{e/h}}(k_h) - \epsilon\frac{4}{h^2}\sin^2\frac{k_h h}{2} - \frac{1}{2}E_{\mathrm{g}} - E_0 \end{pmatrix}, \tag{4.69}$$

with some arbitrary $c \in \mathbb{C}$. The envelope wave $\mathbf{F}_j^{\mathrm{e}}(k_h) = \hat{\mathbf{F}}_h^{\mathrm{e}}(k_h)e^{\pm\mathrm{i}k_h jh}$ denotes the energy eigenstate associated with the energy E_h^{e} of the electrons while $\mathbf{F}_j^{\mathrm{h}}(k_h) = \hat{\mathbf{F}}_h^{\mathrm{h}}(k_h)e^{\pm\mathrm{i}k_h jh}$ corresponds to the energy E_h^{h} of the holes, see Eq. (4.68).

Let us additionally assume that the discrete waves are unitary, i.e. the discrete amplitude $\hat{\mathbf{F}}_h^{\mathrm{e/h}}(\hat{k}_h)$ has norm 1. Then it also satisfies the normalization condition

$$\left\|\hat{\mathbf{F}}^{\mathrm{e/h}}(k_h)\right\|_{\mathbb{C}}^2 = \left\langle \hat{\mathbf{F}}^{\mathrm{e/h}}(k_h), \overline{\hat{\mathbf{F}}^{\mathrm{e/h}}(k_h)}\right\rangle = 1.$$

Hence, the constant c reads

$$\begin{aligned} c &= \left(\hat{F}_{h,\mathrm{c}}^{\mathrm{e/h}}(k_h)\overline{\hat{F}_{h,\mathrm{c}}^{\mathrm{e/h}}(k_h)} + \hat{F}_{h,\mathrm{v}}^{\mathrm{e/h}}(k_h)\overline{\hat{F}_{h,\mathrm{v}}^{\mathrm{e/h}}(k_h)}\right)^{-1/2} \\ &= \left(\frac{4}{h^2}P_0^2\sin^2\frac{k_h h}{2} + \left(E_h^{\mathrm{e/h}}(k_h) - \epsilon\frac{4}{h^2}\sin^2\frac{k_h h}{2} - \frac{1}{2}E_{\mathrm{g}} - E_0\right)^2\right)^{-1/2}. \end{aligned}$$

Analogously to Chap. 3, we observe that the symmetrized FDS leads to discrete traveling envelope waves that are not plane. For any real discrete wave vector $k_h \in \mathbb{R}$, the conduction band component is complex if $h \neq n\frac{2\pi}{k_h}$, $n \in \mathbb{N}$, while the valence band component is real.

Remark 4.5. In contrast to Remark 4.4, we can not show that the discrete amplitudes $\hat{\mathbf{F}}_h^{\mathrm{e/h}}(\pm\hat{k}_h)$ of discrete traveling envelope waves and the discrete amplitudes $\hat{\mathbf{F}}_h^{\mathrm{e/h}}(\pm\mathrm{i}\check{k}_h)$ of discrete evanescent envelope waves of the symmetrized FDS are generally linearly independent. However, we note that in all considered examples it is the case.

Finally, we note that both the discrete dispersion relation of the symmetrized FDS and the discrete envelope function are $2\frac{\pi}{h}$-periodic in k_h, see Eqs. (3.59) and (3.60). In contrast to the centered FDS, the discrete dispersion relation of the symmetrized FDS does not consist of any terms with other periodicity and it is injective in the domain $\left(0, \frac{\pi}{h}\right)$. This means that for any admissible energy E there exists only one positive and one negative discrete wave vector k_h that solves the discrete dispersion relation of the symmetrized FDS.

This behavior is illustrated in Fig. 4.2 that shows a comparison of the discrete dispersion relation of the symmetrized FDS with the analytical dispersion relation and the discrete dispersion relation of the centered FDS for a step size $h = 1/100$, a Kane-parameter $P_0 \equiv 1$, a band gap $E_{\mathrm{g}} \equiv 200$, a middle of the band gap $E_0 \equiv 0$ and two different values of the regularization coefficient ϵ. We observe that for greater values of the regularization coefficient ϵ, the energy window of the centered FDS almost coincides with the interval of admissible energies of the symmetrized FDS, see Fig. 4.2(a). This demonstrates that the symmetrized FDS does not imply a significant advantage compared to the centered FDS for the two-band $\mathbf{k}\cdot\mathbf{p}$-model.

4.4 Discrete Transparent Boundary Conditions

In order to derive the DTBCs for the two-band $\mathbf{k}\cdot\mathbf{p}$-model we apply the discrete solution derived in the previous section to the reflection and transmission conditions (4.30), (4.31) and assume that they hold in a small vicinity of the two boundaries, i.e. $j = 0, 1$ and $j = J-1, J$ respectively.

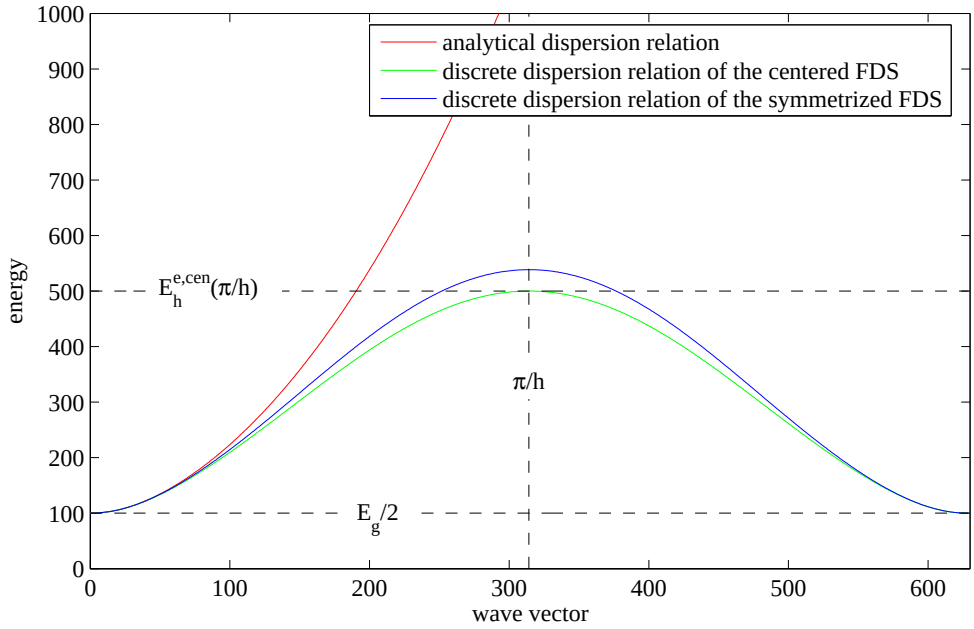

(a) Regularization coefficient $\epsilon = 0.01$

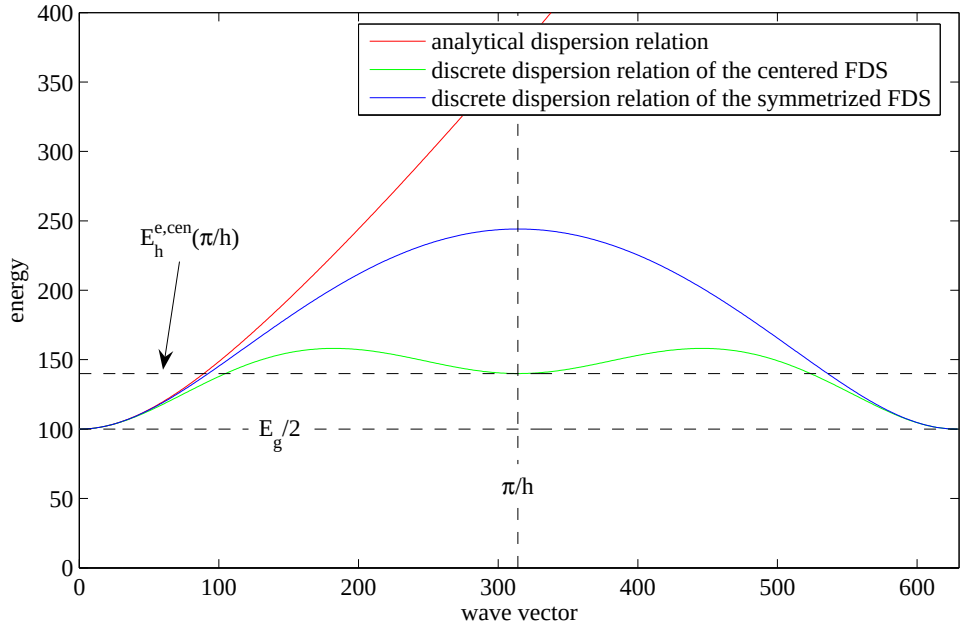

(b) Regularization coefficient $\epsilon = 0.001$

Figure 4.2: Comparison of the positive trunks of the analytical dispersion relation (red) of the two-band $\mathbf{k} \cdot \mathbf{p}$-model and the discrete dispersions relation of the centered FDS (green) and the symmetrized FDS (blue) for a step size $h = 1/100$, a Kane-parameter $P_0 = 1$, a band gap $E_g = 200$ and a regularization coefficient $\epsilon = 0.01$ in Fig. (a) and a regularization coefficient $\epsilon = 0.001$ in Fig. (b), respectively. The horizontal dashed lines indicate the energy window of the centered FDS.

Let us assume that the energy E satisfies the energy condition (4.18) and that the step size h is sufficiently small. Then we have one pair of real discrete wave vectors $k_h = \pm\hat{k}_h$, yielding discrete traveling envelope waves, and one complex conjugate pair of purely imaginary discrete wave vectors $k_h = \pm\mathrm{i}\check{k}_h$, yielding discrete evanescent envelope waves. The explicit values of the wave vectors in the exterior domains are identified by the subscripts 0 and L respectively. Let $\hat{\mathbf{F}}^{\mathrm{e/h}}_{h,0}(k_{h,0})$ denote the amplitude of a discrete wave with the discrete wave vector $k_{h,0}$ in the left exterior domain $x \leq 0$ and let $\hat{\mathbf{F}}^{\mathrm{e/h}}_{h,L}(k_{h,L})$ denote the amplitude of a discrete wave with the discrete wave vector $k_{h,L}$ in the right exterior domain $x \geq L$.

Then we have

$$\mathbf{F}_j = \mathbf{F}^{\mathrm{in}}_j + \mathbf{F}^{\mathrm{r}}_j = \hat{\mathbf{F}}^{\mathrm{e/h}}_{h,0}(\hat{k}_{h,0})e^{\mathrm{i}\hat{k}_{h,0}x_j} + \hat{r}_h\hat{\mathbf{F}}^{\mathrm{e/h}}_{h,0}(-\hat{k}_{h,0})e^{-\mathrm{i}\hat{k}_{h,0}x_j} + \check{r}_h\hat{\mathbf{F}}^{\mathrm{e/h}}_{h,0}(-\mathrm{i}\check{k}_{h,0})e^{\check{k}_{h,0}x_j},$$

$j = 0, 1$, at the left boundary and

$$\mathbf{F}_j = \mathbf{F}^{\mathrm{t}}_j = \hat{t}_h\hat{\mathbf{F}}^{\mathrm{e/h}}_{h,L}(\hat{k}_{h,L})e^{\mathrm{i}\hat{k}_{h,L}x_j} + \check{t}_h\hat{\mathbf{F}}^{\mathrm{e/h}}_{h,L}(\mathrm{i}\check{k}_{h,L})e^{-\check{k}_{h,L}x_j},$$

$j = J-1, J$, at the right boundary.

Let us introduce

$$\mathbf{P}_{h,0} = \begin{pmatrix}\hat{\mathbf{F}}^{\mathrm{e/h}}_{h,0}(-\hat{k}_{h,0}) & \hat{\mathbf{F}}^{\mathrm{e/h}}_{h,0}(-\mathrm{i}\check{k}_{h,0})\end{pmatrix} \in \mathbb{C}^{2\times 2},$$

and

$$\mathbf{K}_{h,0} = \operatorname{diag}\left(e^{-\mathrm{i}\hat{k}_{h,0}h}, e^{\check{k}_{h,0}h}\right) \in \mathbb{C}^{2\times 2},$$

as well as

$$\mathbf{r}_h = \begin{pmatrix}\hat{r}_h \\ \check{r}_h\end{pmatrix} \in \mathbb{C}^2.$$

Then we can rewrite the discrete wave $\mathbf{F}_j$ for $j = 0, 1$ in the form

$$\mathbf{P}_{h,0}\mathbf{r}_h = \mathbf{F}_0 - \hat{\mathbf{F}}^{\mathrm{e/h}}_{h,0}(\hat{k}_{h,0}), \tag{4.70a}$$

and

$$\mathbf{P}_{h,0}\mathbf{K}_{h,0}\mathbf{r}_h = \mathbf{F}_1 - \hat{\mathbf{F}}^{\mathrm{e/h}}_{h,0}(\hat{k}_{h,0})e^{\mathrm{i}\hat{k}_{h,0}h}. \tag{4.70b}$$

Since the discrete amplitudes $\hat{\mathbf{F}}^{\mathrm{e/h}}_{h,0}(-\hat{k}_{h,0})$ and $\hat{\mathbf{F}}^{\mathrm{e/h}}_{h,0}(-\mathrm{i}\check{k}_{h,0})$ are linearly independent, cf. Remarks 4.4 and 4.5, the matrix $\mathbf{P}_{h,0}$ is regular and hence, its inverse $\mathbf{P}^{-1}_{h,0}$ exists. Then the reflection coefficient vector $\mathbf{r}_h$ reads

$$\mathbf{r}_h = \mathbf{P}^{-1}_{h,0}\left(\mathbf{F}_0 - \hat{\mathbf{F}}^{\mathrm{e/h}}_{h,0}(\hat{k}_{h,0})\right),$$

cf. Eq. (4.70a). Applied to Eq. (4.70b) we get the left DTBC

$$\mathbf{F}_1 - \mathbf{P}_{h,0}\mathbf{K}_{h,0}\mathbf{P}^{-1}_{h,0}\mathbf{F}_0 = \left(e^{\mathrm{i}\hat{k}_{h,0}h}\mathbb{1} - \mathbf{P}_{h,0}\mathbf{K}_{h,0}\mathbf{P}^{-1}_{h,0}\right)\hat{\mathbf{F}}^{\mathrm{e/h}}_{h,0}(\hat{k}_{h,0}). \tag{4.71}$$

At the right boundary we proceed analogously. By introducing

$$\mathbf{P}_{h,L} = \begin{pmatrix}\hat{\mathbf{F}}^{\mathrm{e/h}}_{h,L}(\hat{k}_{h,L})e^{\mathrm{i}\hat{k}_{h,L}Jh} & \hat{\mathbf{F}}^{\mathrm{e/h}}_{h,L}(\mathrm{i}\check{k}_{h,L})e^{-\check{k}_{h,L}Jh}\end{pmatrix} \in \mathbb{C}^{2\times 2},$$

and

$$\mathbf{K}_{h,L} = \operatorname{diag}\left(e^{-\mathrm{i}\hat{k}_{h,L}h}, e^{\check{k}_{h,L}h}\right) \in \mathbb{C}^{2\times 2},$$

as well as

$$\mathbf{t}_h = \begin{pmatrix}\hat{t}_h \\ \check{t}_h\end{pmatrix} \in \mathbb{C}^2,$$

we can rewrite the discrete wave $\mathbf{F}_j$ for $j = J-1, J$ in the form

$$\mathbf{P}_{h,L}\mathbf{t}_h = \mathbf{F}_J, \tag{4.72a}$$

and

$$\mathbf{P}_{h,L}\mathbf{K}_{h,L}\mathbf{t}_h = \mathbf{F}_{J-1}. \tag{4.72b}$$

Since the discrete amplitudes $\hat{\mathbf{F}}^{\mathrm{e/h}}_{h,L}(\hat{k}_{h,L})$ and $\hat{\mathbf{F}}^{\mathrm{e/h}}_{h,L}(\mathrm{i}\check{k}_{h,L})$ are linearly independent, cf. Remarks 4.4 and 4.5, so are $\hat{\mathbf{F}}^{\mathrm{e/h}}_{h,L}(\hat{k}_{h,L})e^{\mathrm{i}\hat{k}_{h,L}Jh}$ and $\hat{\mathbf{F}}^{\mathrm{e/h}}_{h,L}(\mathrm{i}\check{k}_{h,L})e^{-\check{k}_{h,L}Jh}$ and hence, the matrix $\mathbf{P}_{h,L}$ is regular and therefore, its inverse $\mathbf{P}^{-1}_{h,L}$ exists. Then the transmission coefficient vector $\mathbf{t}_h$ reads

$$\mathbf{t}_h = \mathbf{P}^{-1}_{h,L}\mathbf{F}_J,$$

cf. Eq. (4.72a). Applied to Eq. (4.72b) we get the right DTBC

$$\mathbf{F}_{J-1} - \mathbf{P}_{h,L}\mathbf{K}_{h,L}\mathbf{P}^{-1}_{h,L}\mathbf{F}_J = \mathbf{0}. \tag{4.73}$$

Remark 4.6. Note that the discrete formulation of the two-band $\mathbf{k}\cdot\mathbf{p}$-model as given in Eq. (4.38) together with the DTBCs (4.71) and (4.73) has a unique solution for all considered examples, i.e. the band matrix of the coefficients of Eq. (4.38) for $j = 1, \ldots, J-1$, and the two DTBCs is regular. However, it remains to prove a general existence theorem for the discrete problem. We are confident that once a proof of the continuous problem is found, cf. Remark 4.6, we can prove a discrete analogon.

4.5 Numerical Examples

4.5.1 The Free Scattering State

In our first example we want to compare the numerical results of the centered FDS and the symmetrized FDS in the case of the free scattering state. We set $\epsilon = 1$, $P_0 \equiv 1$, $E_0 \equiv 200$ and $E_\mathrm{g} \equiv 0$. The energy E is set to $E = 250$. With the help of the analytical solution of the free scattering state given in Sec. 4.1, we will check the numerical order of the introduced FDSs.

The analytical solution of the free scattering has norm 1. Both the centered FDS and the symmetrized FDS give results with norm 1 without any oscillations. The phases of the analytical solution and the numerical solutions of the two FDSs are plotted in Fig. 4.3 for a step size $h = 1/100$. While the phases of the numerical results almost coincide for the used level of detail in Fig. 4.3, the phases of the numerical schemes differ slightly from the phase of analytical scheme. The numerical wave lengths are smaller than the analytical wave length. This error is directly caused by the difference of the analytical wave vector and the discrete wave vectors. Thus, this error decreases for smaller step sizes.

Now let us analyze the discrete L^2-error. Therefore we recall the nonlinear problem

$$\Delta\mathbf{F}^{\min}_h = \min_{\varphi\in[-\pi,\pi]} \Delta\mathbf{F}_h = \min_{\varphi\in[-\pi,\pi]} \frac{1}{J+1}\sqrt{\sum_{j=0}^{J} \|\mathbf{F}(x_j) - \mathbf{F}_j e^{\mathrm{i}\varphi}\|^2}, \tag{4.74}$$

with the analytical solution $\mathbf{F}(x_j)$ at $x = x_j$ and the numerical solution $\mathbf{F}_j$ using the step size $h = 1/J$.

The L^2-errors of the numerical solutions are shown in Fig. 4.4. The numerical order evaluated experimentally coincides for both FDSs with their formal order. While the discrete L^2-error of the centered FDS decays like $\mathcal{O}(h^2)$ the discrete L^2-error of the symmetrized FDS is in $\mathcal{O}(h)$.

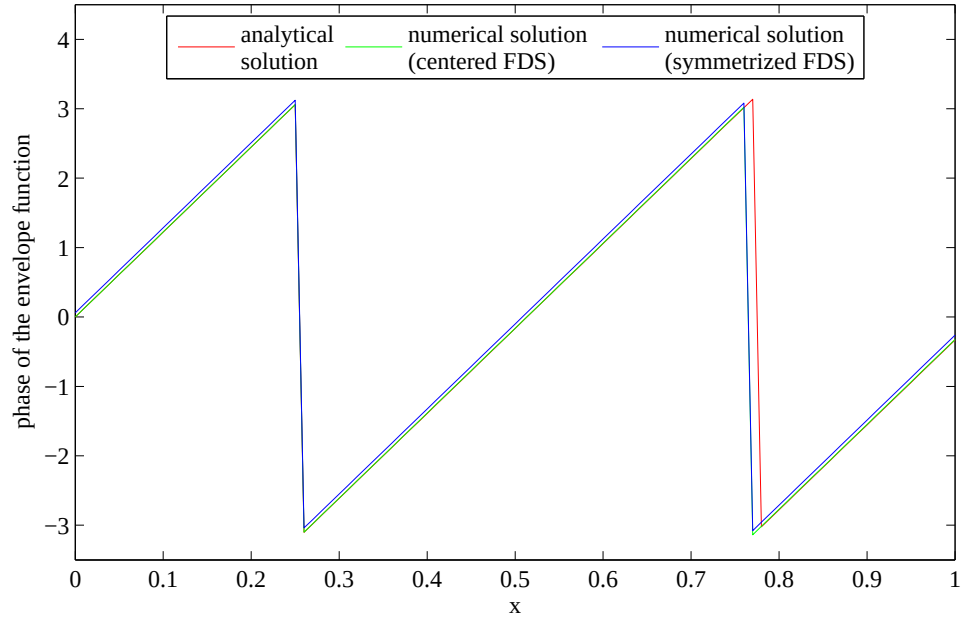

Figure 4.3: Comparison of the phases of the analytical solution (red) and the numerical solution of the centered FDS (green) and the symmetrized FDS (blue) for the free scattering state with $\epsilon = 1$, $P_0 \equiv 1$, $E_\mathrm{g} \equiv 200$, $E_0 \equiv 0$, a step size $h = 1/100$ and an energy $E = 250$.

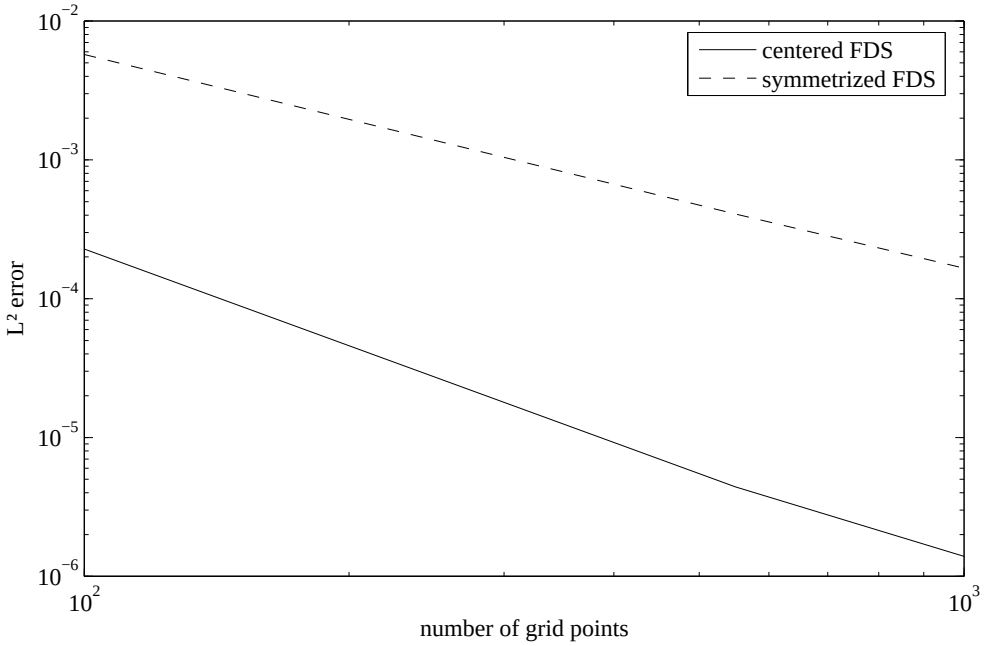

Figure 4.4: Discrete L^2-errors of the numerical solution of the centered FDS (solid line) and the symmetrized FDS (dashed line) against the number of grid points $J = 1/h$ for the free scattering state with $\epsilon = 1$, $P_0 \equiv 1$, $E_\mathrm{g} \equiv 200$, $E_0 \equiv 0$ and an energy $E = 250$.

4.5.2 The Single Barrier Potential

In this section we will study the behavior of the introduced FDS when applied to a single barrier potential. We will compare the numerical results with the analytical solution. In particular, we want to examine if the centered FDS leads to spurious oscillations as it did in Chap. 3 when applied to a single barrier potential.

We consider a semiconductor of length L that is split into three parts. Let $0 < x_1 < x_2 < L$, then the three subdomains of the semiconductor are defined by $[0, x_1)$, $[x_1, x_2)$ and $[x_2, L]$. The two outer subdomains have the same physical properties and are denoted by $A = [0, x_1) \cup [x_2, L]$. The inner subdomain is called $B = [x_1, x_2)$.

We assume that the Kane-parameter P_0 and the band gap E_g are constant, while the middle of the band gap E_0 is piecewise constant and satisfies

$$E_0(x) = 0, \qquad x \in A,$$

and

$$E_0(x) = E_{0,B}, \qquad x \in B.$$

In other words, we add some potential $E_{0,B}$ to the band edges in the domain B. Note that we can additionally vary the band gap and proceed analogously. But for simplicity we shall restrict the variation to the middle of the band gap.

First let us derive the analytical solution. We suppose that the energy E satisfies the energy condition (4.18) in the whole semiconductor, i.e.

$$E > E_0(x) + \frac{1}{2}E_\mathrm{g}(x), \qquad x \in [0, L].$$

In the three domains $[0, x_1)$, $[x_1, x_2)$ and $[x_2, L]$ both the band gap E_g and the middle of the band gap E_0 are constant. Hence, in each domain the vector of the envelope functions takes the form

$$\mathbf{F}(x) = \hat{a}\hat{\mathbf{F}}^{\mathrm{e/h}}(\hat{k})e^{\mathrm{i}\hat{k}x} + \check{a}\hat{\mathbf{F}}^{\mathrm{e/h}}(-\mathrm{i}\check{k})e^{\check{k}x} + \hat{b}\hat{\mathbf{F}}^{\mathrm{e/h}}(-\hat{k})e^{-\mathrm{i}\hat{k}x} + \check{b}\hat{\mathbf{F}}^{\mathrm{e/h}}(\mathrm{i}\check{k})e^{-\check{k}x},$$

with $\hat{a}, \check{a}, \hat{b}, \check{b} \in \mathbb{C}$. The propagation and attenuation coefficients are given by

$$\hat{k}_A = \sqrt{-\frac{1}{2\epsilon^2}\left(\epsilon E_\mathrm{g} + P_0^2\right) + \sqrt{\frac{P_0^2}{4\epsilon^4}\left(P_0^2 + 2\epsilon E_\mathrm{g}\right) + \frac{1}{\epsilon^2}E^2}},$$

and

$$\check{k}_A = \sqrt{\frac{1}{2\epsilon^2}\left(\epsilon E_\mathrm{g} + P_0^2\right) + \sqrt{\frac{P_0^2}{4\epsilon^4}\left(P_0^2 + 2\epsilon E_\mathrm{g}\right) + \frac{1}{\epsilon^2}E^2}},$$

in the domain A, and

$$\hat{k}_B = \sqrt{-\frac{1}{2\epsilon^2}\left(\epsilon E_\mathrm{g} + P_0^2\right) + \sqrt{\frac{P_0^2}{4\epsilon^4}\left(P_0^2 + 2\epsilon E_\mathrm{g}\right) + \frac{1}{\epsilon^2}\left(E - E_{0,B}\right)^2}},$$

and

$$\check{k}_B = \sqrt{\frac{1}{2\epsilon^2}\left(\epsilon E_\mathrm{g} + P_0^2\right) + \sqrt{\frac{P_0^2}{4\epsilon^4}\left(P_0^2 + 2\epsilon E_\mathrm{g}\right) + \frac{1}{\epsilon^2}\left(E - E_{0,B}\right)^2}},$$

in the domain B.

Let $\hat{\mathbf{F}}_A^{\mathrm{e/h}}(k)$ denote the unitary amplitude of a wave with wave vector k in the domain A and $\hat{\mathbf{F}}_B^{\mathrm{e/h}}(k)$ denote the corresponding, unitary amplitude in the domain B. We consider a right-traveling envelope wave with amplitude $\hat{\mathbf{F}}_A^{\mathrm{e/h}}(\hat{k})$ that enters the semiconductor at $x = 0$.

Since E_g is constant and $E_0 \equiv 0$ in A, which means that the physical properties are equal to the properties in the exterior domain $x < 0$, the incoming envelope wave is not reflected but completely transmitted into the domain $[0, x_1)$. At $x = x_1$ the envelope wave is partly reflected. In the domain $[x_2, L]$ we expect a transmitted, right-traveling envelope wave that leaves the semiconductor at $x = L$. For the same reason as at $x = 0$ we do not expect any reflection of the transmitted wave at $x = L$. This leads to the vector of the envelope functions

$$\mathbf{F}(x) = \begin{cases} \mathbf{F}_{A_1}(x) & \text{if } x \in [0, x_1), \\ \mathbf{F}_B(x) & \text{if } x \in [x_1, x_2), \\ \mathbf{F}_{A_2}(x) & \text{if } x \in [x_2, L], \end{cases} \tag{4.75}$$

where

$$\begin{aligned}
\mathbf{F}_{A_1}(x) &= \hat{\mathbf{F}}_A^{\mathrm{e/h}}(\hat{k}_A)e^{\mathrm{i}\hat{k}_A x} + \hat{r}\hat{\mathbf{F}}_A^{\mathrm{e/h}}(-\hat{k}_A)e^{-\mathrm{i}\hat{k}_A x} + \check{r}\hat{\mathbf{F}}_A^{\mathrm{e/h}}(-\mathrm{i}\check{k}_A)e^{\check{k}_A x}, \\
\mathbf{F}_B(x) &= \hat{a}\hat{\mathbf{F}}_B^{\mathrm{e/h}}(\hat{k}_B)e^{\mathrm{i}\hat{k}_B x} + \check{a}\hat{\mathbf{F}}_B^{\mathrm{e/h}}(-\mathrm{i}\check{k}_B)e^{\check{k}_B x} + \hat{b}\hat{\mathbf{F}}_B^{\mathrm{e/h}}(-\hat{k}_B)e^{-\mathrm{i}\hat{k}_B x} + \check{b}\hat{\mathbf{F}}_B^{\mathrm{e/h}}(\mathrm{i}\hat{k}_B)e^{-\check{k}_B x}, \\
\mathbf{F}_{A_2}(x) &= \hat{t}\hat{\mathbf{F}}_A^{\mathrm{e/h}}(\hat{k}_A)e^{\mathrm{i}\hat{k}_A x} + \check{t}\hat{\mathbf{F}}_A^{\mathrm{e/h}}(\mathrm{i}\check{k}_A)e^{-\check{k}_A x},
\end{aligned}$$

with the eight unknown coefficients $\hat{r}, \check{r}, \hat{a}, \check{a}, \hat{b}, \check{b}, \hat{t}, \check{t} \in \mathbb{C}$.

The vector of the envelope functions $\mathbf{F}$ and its derivative are continuous, see [24]. In particular, they are continuous at $x = x_1, x_2$. Hence, we get a system of eight linear equations that can be written in the form

$$\mathbf{Q}\mathbf{c} = \mathbf{s},$$

with

$$\mathbf{c} = \begin{pmatrix} \hat{r} & \check{r} & \hat{a} & \check{a} & \hat{b} & \check{b} & \hat{t} & \check{t} \end{pmatrix}^{\mathrm{T}} \in \mathbb{C}^8,$$

and

$$\mathbf{s} = \begin{pmatrix} -\hat{\mathbf{F}}_A^{\mathrm{e/h}}(\hat{k}_A)e^{\mathrm{i}\hat{k}_A x_1} \\ \mathbf{0} \\ -\mathrm{i}\hat{k}_A\hat{\mathbf{F}}_A^{\mathrm{e/h}}(\hat{k}_A)e^{\mathrm{i}\hat{k}_A x_1} \\ \mathbf{0} \end{pmatrix} \in \mathbb{C}^8,$$

and the coefficient matrix

$$\mathbf{Q} = \begin{pmatrix} \mathbf{q}_{\hat{r}} & \mathbf{q}_{\check{r}} & \mathbf{q}_{\hat{a}} & \mathbf{q}_{\check{a}} & \mathbf{q}_{\hat{b}} & \mathbf{q}_{\check{b}} & \mathbf{q}_{\hat{t}} & \mathbf{q}_{\check{t}} \end{pmatrix} \in \mathbb{C}^{8\times 8},$$

whose columns are given by

$$\begin{aligned}
\mathbf{q}_{\hat{r}} &= \begin{pmatrix} \hat{\mathbf{F}}_A^{\mathrm{e/h}}(-\hat{k}_A)e^{-\mathrm{i}\hat{k}_A x_1} \\ \mathbf{0} \\ -\mathrm{i}\hat{k}_A\hat{\mathbf{F}}_A^{\mathrm{e/h}}(-\hat{k}_A)e^{-\mathrm{i}\hat{k}_A x_1} \\ \mathbf{0} \end{pmatrix}, \quad
\mathbf{q}_{\check{r}} = \begin{pmatrix} \hat{\mathbf{F}}_A^{\mathrm{e/h}}(-\mathrm{i}\check{k}_A)e^{\check{k}_A x_1} \\ \mathbf{0} \\ \check{k}_A\hat{\mathbf{F}}_A^{\mathrm{e/h}}(-\mathrm{i}\check{k}_A)e^{\check{k}_A x_1} \\ \mathbf{0} \end{pmatrix}, \\
\mathbf{q}_{\hat{a}} &= \begin{pmatrix} -\hat{\mathbf{F}}_B^{\mathrm{e/h}}(\hat{k}_B)e^{\mathrm{i}\hat{k}_B x_1} \\ \hat{\mathbf{F}}_B^{\mathrm{e/h}}(\hat{k}_B)e^{\mathrm{i}\hat{k}_B x_2} \\ -\mathrm{i}\hat{k}_B\hat{\mathbf{F}}_B^{\mathrm{e/h}}(\hat{k}_B)e^{\mathrm{i}\hat{k}_B x_1} \\ i\hat{k}_B\hat{\mathbf{F}}_B^{\mathrm{e/h}}(\hat{k}_B)e^{\mathrm{i}\hat{k}_B x_2} \end{pmatrix}, \quad
\mathbf{q}_{\check{a}} = \begin{pmatrix} -\hat{\mathbf{F}}_B^{\mathrm{e/h}}(-\mathrm{i}\check{k}_B)e^{\check{k}_B x_1} \\ \hat{\mathbf{F}}_B^{\mathrm{e/h}}(-\mathrm{i}\check{k}_B)e^{\check{k}_B x_2} \\ -\check{k}_B\hat{\mathbf{F}}_B^{\mathrm{e/h}}(-\mathrm{i}\check{k}_B)e^{\check{k}_B x_1} \\ \check{k}_B\hat{\mathbf{F}}_B^{\mathrm{e/h}}(-\mathrm{i}\check{k}_B)e^{\check{k}_B x_2} \end{pmatrix}, \\
\mathbf{q}_{\hat{b}} &= \begin{pmatrix} -\hat{\mathbf{F}}_B^{\mathrm{e/h}}(-\hat{k}_B)e^{-\mathrm{i}\hat{k}_B x_1} \\ \hat{\mathbf{F}}_B^{\mathrm{e/h}}(-\hat{k}_B)e^{-\mathrm{i}\hat{k}_B x_2} \\ i\hat{k}_B\hat{\mathbf{F}}_B^{\mathrm{e/h}}(-\hat{k}_B)e^{-\mathrm{i}\hat{k}_B x_1} \\ -\mathrm{i}\hat{k}_B\hat{\mathbf{F}}_B^{\mathrm{e/h}}(-\hat{k}_B)e^{-\mathrm{i}\hat{k}_B x_2} \end{pmatrix}, \quad
\mathbf{q}_{\check{b}} = \begin{pmatrix} -\hat{\mathbf{F}}_B^{\mathrm{e/h}}(\mathrm{i}\check{k}_B)e^{-\check{k}_B x_1} \\ \hat{\mathbf{F}}_B^{\mathrm{e/h}}(\mathrm{i}\check{k}_B)e^{-\check{k}_B x_2} \\ \check{k}_B\hat{\mathbf{F}}_B^{\mathrm{e/h}}(\mathrm{i}\check{k}_B)e^{-\check{k}_B x_1} \\ -\check{k}_B\hat{\mathbf{F}}_B^{\mathrm{e/h}}(\mathrm{i}\check{k}_B)e^{-\check{k}_B x_2} \end{pmatrix}, \\
\mathbf{q}_{\hat{t}} &= \begin{pmatrix} \mathbf{0} \\ -\hat{\mathbf{F}}_A^{\mathrm{e/h}}(\hat{k}_A)e^{\mathrm{i}\hat{k}_A x_2} \\ \mathbf{0} \\ -\mathrm{i}\hat{k}_A\hat{\mathbf{F}}_A^{\mathrm{e/h}}(\hat{k}_A)e^{\mathrm{i}\hat{k}_A x_2} \end{pmatrix}, \quad
\mathbf{q}_{\check{t}} = \begin{pmatrix} \mathbf{0} \\ -\hat{\mathbf{F}}_A^{\mathrm{e/h}}(\mathrm{i}\check{k}_A)e^{-\check{k}_A x_2} \\ \mathbf{0} \\ \check{k}_A\hat{\mathbf{F}}_A^{\mathrm{e/h}}(\mathrm{i}\check{k}_A)e^{-\check{k}_A x_2} \end{pmatrix}.
\end{aligned}$$

Analogously to the single barrier problem in Chap. 3, we omit to give a mathematical proof that the matrix $\mathbf{Q}$ is regular. Instead we argue that a singular matrix $\mathbf{Q}$ would imply that the homogeneous case of the system of linear equations has a nonzero solution. This means that there can exist envelope waves inside the computational domain without the existence of an incoming envelope wave which is a physical contradiction. Furthermore, we note that in our particular example the matrix $\mathbf{Q}$ is in fact regular and thus, the unknown coefficients $\hat{r}$, $\check{r}$, $\hat{a}$, $\check{a}$, $\hat{b}$, $\check{b}$, $\hat{t}$ and $\check{t}$ are defined uniquely.

4.5.2.1 Numerical Solutions of the Envelope Functions

As shown above, we expect the centered FDS to have no spurious oscillations if the energy E is less than the upper bound $E_h^{\mathrm{e,\,cen}}(\pi/h)$. For the given values of the parameters this upper bound is

$$E_h^{\mathrm{e,\,cen}}(\pi/h) = E_{0,B} + \left(\epsilon\frac{4}{h^2} + \frac{1}{2}E_{\mathrm{g}}\right) = 810200.$$

Since we choose the energy to be $E = 250 < E_h^{\mathrm{e,\,cen}}(\pi/h)$ we expect no spurious oscillations.

Fig. 4.5 shows a comparison of the norms and the phases of the analytical solution and the numerical solution using the centered FDS. As the solution of the centered FDS and the symmetrized FDS coincide for the used level of detail in Fig. 4.5, only the norm and phase of the centered FDS is shown.

In fact, we do not observe any spurious oscillations of the numerical solution. In contrast, the norm of the numerical solution of the centered FDS almost coincides with the norm of the analytical solution in Fig. 4.5(a). However, we observe a small phase error in front of the barrier. This phase error decreases when using a smaller step size and hence, can be ascribed to the difference of the analytical and discrete wave vector.

4.5.2.2 The Transmission Coefficient

Let us briefly examine the behavior of the transmission coefficient versus the energy E. To do this, we use the same settings as before, i.e. $E_{\mathrm{g}} = 200$, $E_{0,B} = 100$, $P_0 = 1$ and $\epsilon = 1$ as well as $L = 1$, $x_1 = 1/3$ and $x_2 = 2/3$. Fig. 4.6(a) shows the analytical transmission coefficient. In Fig. 4.6(b) the analytical transmission coefficient is compared with the numerical transmission coefficient of the centered FDS for a step size $h = 1/60$. The results of the centered FDS coincide with the results of the symmetrized FDS for the used level of detail in Fig. 4.6(b). Therefore, only the numerical transmission coefficient of the centered FDS is plotted.

The smallest energy yielding a resonance is located at $E \approx 289$. Note that we cannot observe any numerical overestimation of the analytical transmission coefficient near the resonance as we did in Chap. 3.

4.5.2.3 The L^2-Error

Finally, we want to compare the discrete L^2-errors of the numerical solutions using the centered FDS and the symmetrized FDS respectively. In particular, we want to check if the numerical order of the schemes is the same as the numerical order we observed in the the free scattering state example. Let us recall the nonlinear problem (4.74) in order to evaluate the discrete L^2-error. In Fig. 4.7 the discrete L^2-errors $\Delta\mathbf{F}_h^{\min}$ of the centered and symmetrized FDS are plotted against the number of grid points $J = 1/h$ for an energy $E = 250$, a band gap $E_{\mathrm{g}} = 200$ and a middle of the band gap $E_{0,B} = 100$ at the barrier. The numerical results confirm the formal order of the symmetrized FDS. Its discrete L^2-error decays like $\mathcal{O}(h)$. However, the centered FDS is not of second order for this particular example while its discrete L^2-error of the free scattering state example is in $\mathcal{O}(h^2)$, cf. Fig. 4.4. In order to explain this, let us set the Kane-parameter to $P_0 = 0$. In other words, we neglect the coupling between the conduction band

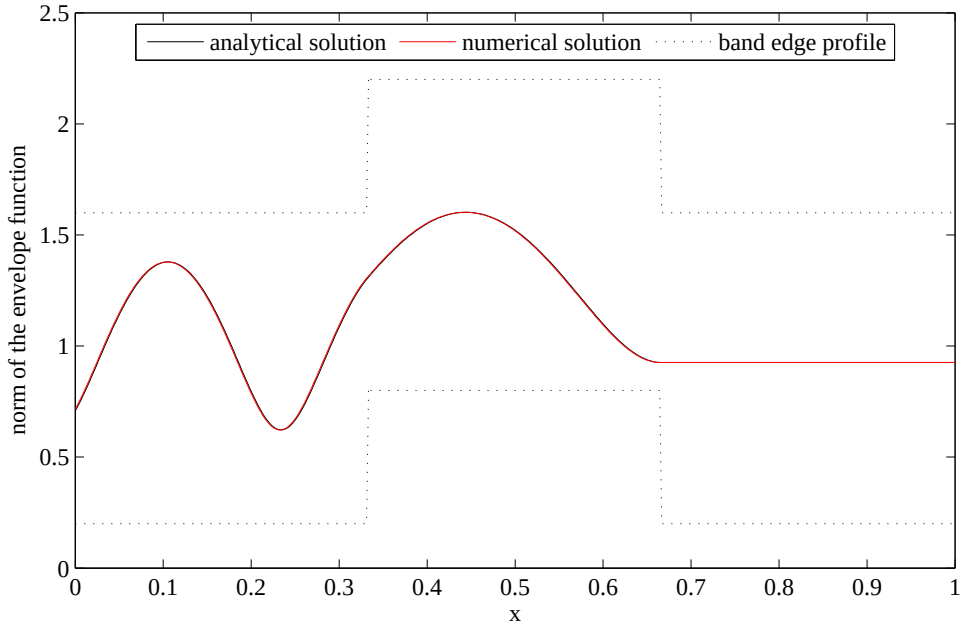

(a) Norm of the analytical and numerical solutions.

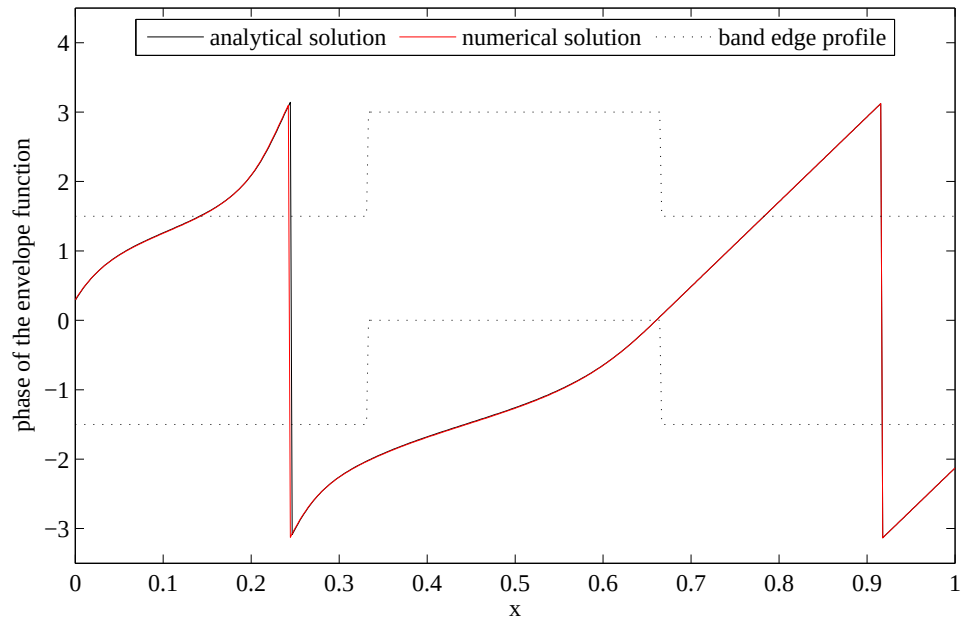

(b) Phases of the analytical and numerical solutions.

Figure 4.5: Comparison of the analytical solution (black) of the single barrier problem and the numerical solution (red) using the centered FDS for the step size $h = 1/450$ and an energy $E = 250$. The dotted line indicates schematically the band edge profile.

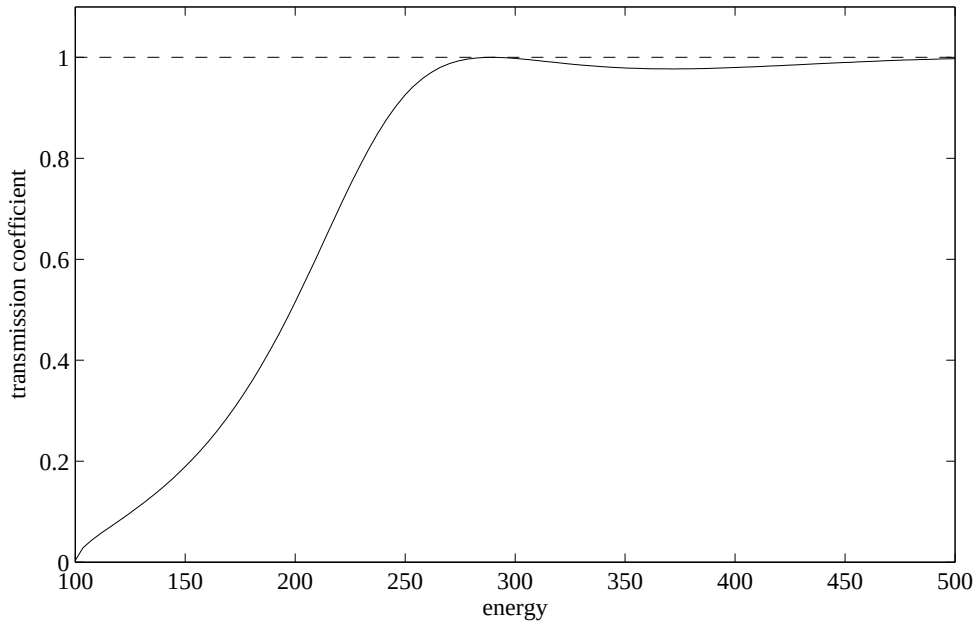

(a) Analytical transmission coefficient.

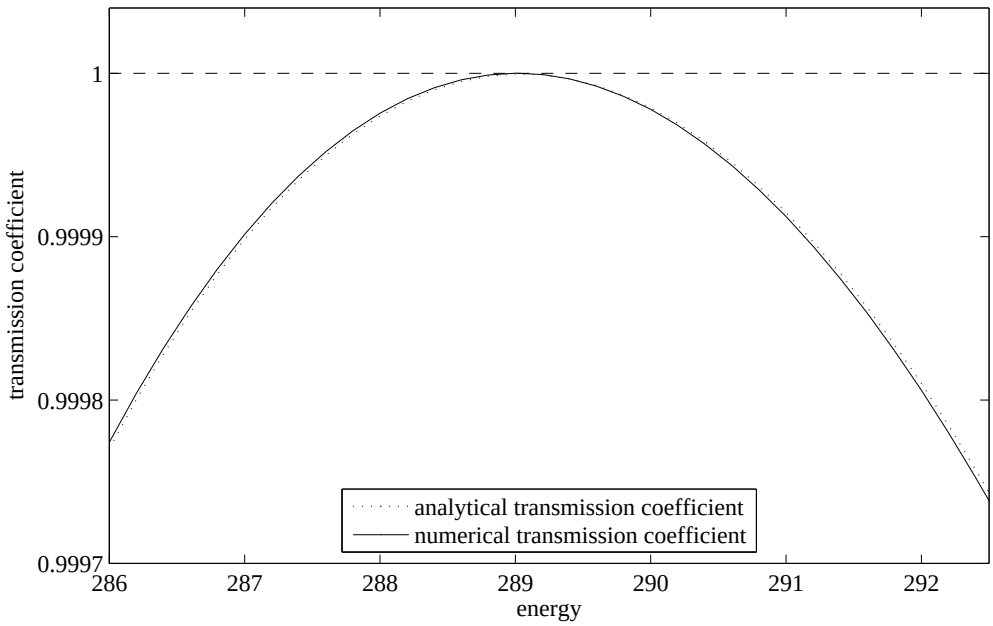

(b) Analytical (dotted line) and numerical (solid line) transmission coefficients for a step size $h = 1/60$.

Figure 4.6: Analytical transmission coefficient and the transmission coefficient of the centered FDS for the step size $h = 1/60$.

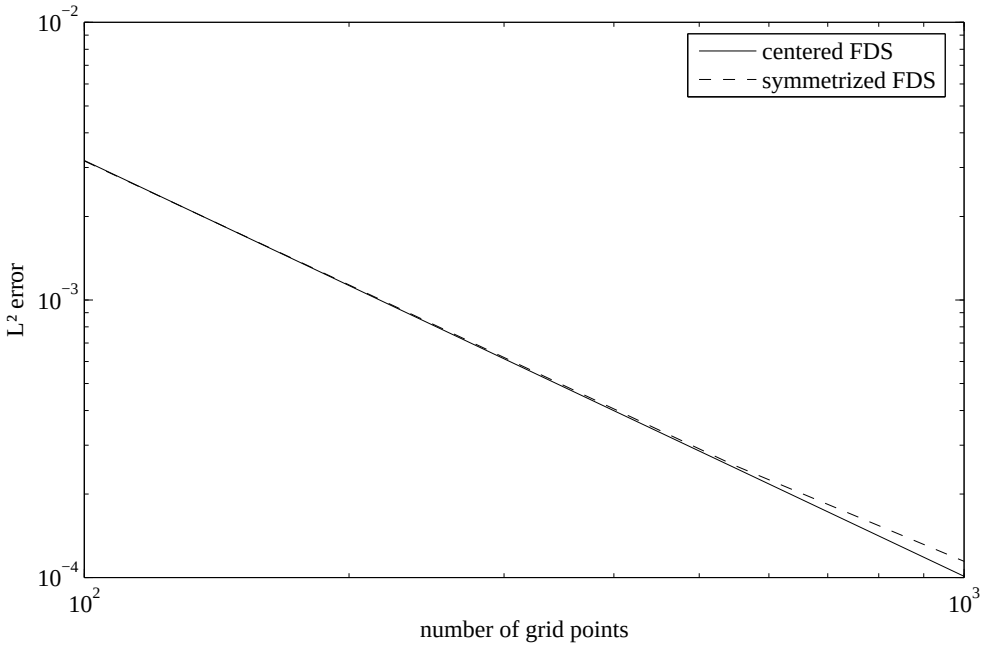

Figure 4.7: L^2-errors of the centered FDS (solid line) and the symmetrized FDS (dashed line) for an energy $E = 250$, a band gap $E_g = 200$ and a middle of the band gap $E_{0,B} = 100$ at the barrier.

and valence band. In this case we can analyze each band solution of the two-band $\mathbf{k}\cdot\mathbf{p}$-model separately. Let us focus on the conduction band. The two-band $\mathbf{k}\cdot\mathbf{p}$-model of the conduction band without coupling reduces to

$$-\epsilon\frac{\mathrm{d}^2}{\mathrm{d}x^2}F_\mathrm{c} + E_\mathrm{c}F_\mathrm{c} = EF_\mathrm{c}. \tag{4.76}$$

We use the identity

$$\frac{\mathrm{d}^2}{\mathrm{d}x^2}F_\mathrm{c} = \left(\frac{\mathrm{d}}{\mathrm{d}x}\left(\frac{\frac{\mathrm{d}}{\mathrm{d}x}F_\mathrm{c}}{F_\mathrm{c}}\right) + \left(\frac{\frac{\mathrm{d}}{\mathrm{d}x}F_\mathrm{c}}{F_\mathrm{c}}\right)^2\right)F_\mathrm{c}$$

and end up with

$$-\epsilon\left(\frac{\mathrm{d}}{\mathrm{d}x}\left(\frac{\frac{\mathrm{d}}{\mathrm{d}x}F_\mathrm{c}}{F_\mathrm{c}}\right) + \left(\frac{\frac{\mathrm{d}}{\mathrm{d}x}F_\mathrm{c}}{F_\mathrm{c}}\right)^2\right) = E_\mathrm{c} - E. \tag{4.77}$$

If we apply a numerical scheme to Eq. (4.76) that is formally of second order we require the envelope function F_c to be twice continuously differentiable. This implies that the left hand side of Eq. (4.77) needs to be continuous. However, the right hand side has two jump discontinuities at the barrier. Hence, the discrete L^2-error of any numerical scheme of order two or higher applied to an example with discontinuous band edge profile decays at most like $\mathcal{O}(h)$.

4.6 Summary

We introduced the two-band $\mathbf{k}\cdot\mathbf{p}$-model with inter-band coupling. Basically, this model is equal to two-band Kane-model with added Laplace-operator on the diagonal. The Laplace operator is multiplied by some regularization coefficient. We solved the analytical exterior problem and found that for energies outside the band gap there exist not only traveling waves but also a

pair of evanescent waves. These evanescent waves also had to be considered when deriving the TBCs.

We analyzed the discrete exterior problem by introducing a scheme consisting of the standard and centered FDS as well as a scheme that used the symmetrized FDS for the first order derivative. Analogously to the Kane-model, the discrete exterior solution of the symmetrized FDS is not plane but we showed that this has no notable effect on the numerical solution. We pointed out that there exists an energy window for the centered FDS. Energies inside this window do not yield spuriously oscillating solutions, as we observed for the Kane-model. This energy window is proportional to the square of the number of grid points and to the regularization coefficient. Hence, for greater values of the regularization coefficient the energy window increases and it is almost identical to the interval of admissible energies of the symmetrized FDS.

After deriving the DTBCs analogously to the TBCs, we performed a numerical example with constant band edge profile as well as an example with a single barrier potential. We showed that the discrete L^2-error of the centered FDS, which is formally of order two, converges only in $\mathcal{O}(h)$ if the band edge profile is discontinuous. Hence, the centered FDS does not imply any numerical advantage compared to the symmetrized FDS.

Chapter 5

The General $\mathbf{k}\cdot\mathbf{p}$-Model

In the last step of generalization, we introduce the general $\mathbf{k}\cdot\mathbf{p}$-model. Let $d\in\mathbb{N}$ denote the number of considered bands of the semiconductor and $\mathbf{F}(x)\in\mathbb{C}^d$ the vector of the envelope functions $F_1,\dots,F_d\in\mathbb{C}$. Let $\mathbf{m}(x),\mathbf{e}(x)\in\mathbb{R}^{d\times d}$ be diagonal, real and regular $d\times d$-matrices, $\mathbf{U}_p(x),\mathbf{U}_{pq}(x),\mathbf{v}(x)\in\mathbb{C}^{d\times d}$ Hermitian $d\times d$-matrices and $\mathbf{M}_0(x),\mathbf{M}_1(x),\mathbf{M}_2(x)\in\mathbb{C}^{d\times d}$ skew-Hermitian $d\times d$-matrices. Then we will refer to

$$\begin{aligned}E\mathbf{F}(x) =& -\frac{\mathrm{d}}{\mathrm{d}x}\left(\mathbf{m}(x)\frac{\mathrm{d}}{\mathrm{d}x}\mathbf{F}(x)\right)+\mathbf{M}_0(x)\frac{\mathrm{d}}{\mathrm{d}x}\mathbf{F}(x)-\frac{\mathrm{d}}{\mathrm{d}x}\left(\mathbf{M}_0^{\mathrm{H}}(x)\mathbf{F}(x)\right)\\ &+k_1\left(\mathbf{M}_1(x)\frac{\mathrm{d}}{\mathrm{d}x}\mathbf{F}(x)-\frac{\mathrm{d}}{\mathrm{d}x}\left(\mathbf{M}_1^{\mathrm{H}}(x)\mathbf{F}(x)\right)\right)\\ &+k_2\left(\mathbf{M}_2(x)\frac{\mathrm{d}}{\mathrm{d}x}\mathbf{F}(x)-\frac{\mathrm{d}}{\mathrm{d}x}\left(\mathbf{M}_2^{\mathrm{H}}(x)\mathbf{F}(x)\right)\right)\\ &+k_1\mathbf{U}_1(x)\mathbf{F}(x)+k_2\mathbf{U}_2(x)\mathbf{F}(x)\\ &+k_1^2\mathbf{U}_{11}(x)\mathbf{F}(x)+k_2^2\mathbf{U}_{22}(x)\mathbf{F}(x)+k_1k_2\left(\mathbf{U}_{12}(x)+\mathbf{U}_{21}(x)\right)\mathbf{F}(x)\\ &+\mathbf{v}(x)\mathbf{F}(x)+\mathbf{e}(x)\mathbf{F}(x),\end{aligned}\tag{5.1}$$

with $x\in\mathbb{R}$ and $k_1,k_2\in\mathbb{R}$, as *d-band* $\mathbf{k}\cdot\mathbf{p}$*-Schrödinger equation*, cf. [5]. In order to abbreviate this physical formulation we introduce the skew-Hermitian $d\times d$-matrix

$$\mathbf{M}_{\mathrm{S}}(x)=\mathbf{M}_0(x)+k_1\mathbf{M}_1(x)+k_2\mathbf{M}_2(x),\tag{5.2a}$$

and the Hermitian $d\times d$-matrix

$$\begin{aligned}\mathbf{V}(x) =& k_1\mathbf{U}_1(x)+k_2\mathbf{U}_2(x)\\ &+k_1^2\mathbf{U}_{11}(x)+k_2^2\mathbf{U}_{22}(x)+k_1k_2\left(\mathbf{U}_{12}(x)+\mathbf{U}_{21}(x)\right)+\mathbf{v}(x)+\mathbf{e}(x).\end{aligned}\tag{5.2b}$$

Then (5.1) reads

$$E\mathbf{F}(x)=-\frac{\mathrm{d}}{\mathrm{d}x}\left(\mathbf{m}(x)\frac{\mathrm{d}}{\mathrm{d}x}\mathbf{F}(x)\right)+\mathbf{M}_{\mathrm{S}}(x)\frac{\mathrm{d}}{\mathrm{d}x}\mathbf{F}(x)-\frac{\mathrm{d}}{\mathrm{d}x}\left(\mathbf{M}_{\mathrm{S}}^{\mathrm{H}}(x)\mathbf{F}(x)\right)+\mathbf{V}(x)\mathbf{F}(x),\tag{5.3}$$

with $x\in\mathbb{R}$.

We consider a semiconductor of length L connected to reservoirs at $x=0$ and $x=L$. Let us assume that the matrices $\mathbf{m}$, $\mathbf{M}_{\mathrm{S}}$ and $\mathbf{V}$ are constant in the reservoirs with

$$\mathbf{m}(x)\equiv\mathbf{m}_0,\quad \mathbf{M}_{\mathrm{S}}(x)\equiv\mathbf{M}_{\mathrm{S},0},\quad \mathbf{V}(x)\equiv\mathbf{V}_0\qquad x\le 0,$$

and

$$\mathbf{m}(x)\equiv\mathbf{m}_L,\quad \mathbf{M}_{\mathrm{S}}(x)\equiv\mathbf{M}_{\mathrm{S},L},\quad \mathbf{V}(x)\equiv\mathbf{V}_L\qquad x\ge L.$$

5.1 The Exterior Problem and the Dispersion Relation

Let us study the exterior problem of the general $\mathbf{k}\cdot\mathbf{p}$-model. In the exterior domains the matrices $\mathbf{m}$, $\mathbf{M}_\mathrm{S}$ and $\mathbf{V}$ are constant. Without loss of generality, we focus on the left exterior domain $x \leq 0$ with $\mathbf{m}(x) = \mathbf{m}_0$, $\mathbf{M}_\mathrm{S}(x) = \mathbf{M}_{\mathrm{S},0}$ and $\mathbf{V}(x) = \mathbf{V}_0$. Note that the results for the right exterior domain $x \geq L$ can be derived analogously. For simplicity let us omit the subscript 0 in $\mathbf{m}_0$, $\mathbf{M}_{\mathrm{S},0}$ and $\mathbf{V}_0$. With these simplifying assumptions, Eq. (5.1) regarded on the half line $x \leq 0$ is a second order system of ODEs with constant coefficients that can be written in the form

$$-\mathbf{N}\frac{\mathrm{d}^2}{\mathrm{d}x^2}\mathbf{F} + \mathrm{i}\mathbf{M}\frac{\mathrm{d}}{\mathrm{d}x}\mathbf{F} + (\mathbf{V} - E\mathbb{1})\,\mathbf{F} = \mathbf{0}, \qquad x \leq 0, \tag{5.4}$$

with

$$\mathbf{N} = \mathbf{m} \tag{5.5a}$$

and

$$\mathbf{M} = -\mathrm{i}\mathbf{M}_\mathrm{S} + \mathrm{i}\mathbf{M}_\mathrm{S}^\mathrm{H} = -2\mathrm{i}\mathbf{M}_\mathrm{S}. \tag{5.5b}$$

Note that $\mathbf{M}$ is Hermitian since $\mathbf{M}_\mathrm{S}$ is skew-Hermitian.

By introducing the substitution

$$\Phi = \begin{pmatrix} \mathbf{F} \\ \frac{\mathrm{d}}{\mathrm{d}x}\mathbf{F} \end{pmatrix}, \tag{5.6}$$

we can reduce Eq. (5.4) to a first order system of ODEs with constant coefficients

$$\mathbf{A}\frac{\mathrm{d}}{\mathrm{d}x}\Phi = \mathbf{B}\Phi, \qquad x \leq 0, \tag{5.7}$$

with

$$\mathbf{A} = \begin{pmatrix} \mathbf{M} & \mathrm{i}\mathbf{N} \\ -\mathrm{i}\mathbf{N} & \mathbf{0} \end{pmatrix} \in \mathbb{C}^{(2d)\times(2d)} \tag{5.8}$$

and

$$\mathbf{B} = \begin{pmatrix} \mathrm{i}\mathbf{V} - \mathrm{i}E\mathbb{1} & \mathbf{0} \\ \mathbf{0} & -\mathrm{i}\mathbf{N} \end{pmatrix} \in \mathbb{C}^{(2d)\times(2d)}. \tag{5.9}$$

Let us introduce the following notation

Definition 5.1 (cf. [35])**.** The inertia of the matrix $\mathbf{A} \in \mathbb{C}^{n\times n}$ is the ordered triple

$$\mathrm{in}(\mathbf{A}) = (\mathrm{in}_+(\mathbf{A}), \mathrm{in}_-(\mathbf{A}), \mathrm{in}_0(\mathbf{A}))\,,$$

where $\mathrm{in}_+(\mathbf{A})$ is the number of eigenvalues of $\mathbf{A}$ with positive real part, $\mathrm{in}_-(\mathbf{A})$ is the number of eigenvalues of $\mathbf{A}$ with negative real part and $\mathrm{in}_0(\mathbf{A})$ is the number of eigenvalues of $\mathbf{A}$ with zero real part, all counting multiplicity.

Zisowsky showed in [44] for the transient general $\mathbf{k}\cdot\mathbf{p}$-model that the matrices

$$\mathbf{A}_\mathrm{transient} = \mathbf{A},$$

and

$$\mathbf{B}_\mathrm{transient} = \begin{pmatrix} \mathrm{i}\mathbf{V} + s\mathbb{1} & \mathbf{0} \\ \mathbf{0} & -\mathrm{i}\mathbf{N} \end{pmatrix},$$

with the Laplace parameter s of the Laplace-transformed exterior problem, are regular for $\mathrm{Re}(s) > 0$. Moreover she proved a *splitting theorem* saying that the matrix $\mathbf{A}_\mathrm{transient}^{-1}\mathbf{B}_\mathrm{transient}$ has exactly d eigenvalues with positive real part and d eigenvalues with negative real part, i.e.

$$\mathrm{in}\left(\mathbf{A}_\mathrm{transient}^{-1}\mathbf{B}_\mathrm{transient}\right) = (d, d, 0)\,.$$

Our aim is to show a similar result for the stationary general $\mathbf{k}\cdot\mathbf{p}$-model (5.7). First let us show that $\mathbf{A}$ and $\mathbf{B}$ are regular and hence, $\mathbf{A}^{-1}\mathbf{B}$ exists and is also regular. Since $\mathbf{A}_{\text{transient}} = \mathbf{A}$, the matrix $\mathbf{A}$ is regular and $\mathbf{A}^{-1}\mathbf{B}$ exists. Since $\mathbf{V}$ is Hermitian, it is diagonalizable with the real eigenvalues $v_1, \dots, v_d$. Let us suppose that the energy E satisfies

$$E \neq v_p, \qquad p = 1, \dots, d. \tag{5.10}$$

then the matrix $\mathrm{i}\mathbf{V} - \mathrm{i}E\mathbb{1}$ is similar to $\operatorname{diag}(\mathrm{i}(v_1 - E), \dots, \mathrm{i}(v_d - E))$ which is regular. Considering that $\mathbf{N}$ is regular, the matrix $\mathbf{B}$ is regular and hence, the matrix $\mathbf{A}^{-1}\mathbf{B}$ is regular.

Thus, we can write Eq. (5.7) in the form

$$\frac{\mathrm{d}}{\mathrm{d}x}\Phi = \mathbf{A}^{-1}\mathbf{B}\Phi, \qquad x \leq 0, \tag{5.11}$$

with

$$\mathbf{A}^{-1}\mathbf{B} = \begin{pmatrix} \mathbf{0} & \mathbb{1} \\ \mathbf{N}^{-1}(\mathbf{V} - E\mathbb{1}) & \mathrm{i}\mathbf{N}^{-1}\mathbf{M} \end{pmatrix} \in \mathbb{C}^{(2d)\times(2d)}. \tag{5.12}$$

The solution of Eq. (5.7) takes the form

$$\Phi(x) = \mathbf{a}e^{\kappa x}, \qquad x \leq 0, \tag{5.13}$$

where $\kappa = \kappa_1, \dots, \kappa_{2d} \in \mathbb{C}$ denotes an eigenvalue and $\mathbf{a} = \mathbf{a}(\kappa) \in \mathbb{C}^{2d}$ the corresponding eigenvector of the matrix $\mathbf{A}^{-1}\mathbf{B}$, cf. [41]. Since the vector of the envelope functions $\mathbf{F}$ is represented by the first d components of Φ, we introduce the *amplitude* $\hat{\mathbf{F}} \in \mathbb{C}^d$ of $\mathbf{F}$ that contains the first d components of $\mathbf{a}(\kappa) \in \mathbb{C}^{2d}$. Then the vector of the envelope functions $\mathbf{F}$ takes the form

$$\mathbf{F}(x) = \hat{\mathbf{F}}e^{\mathrm{i}kx}, \tag{5.14}$$

where $k = \hat{k} + \mathrm{i}\check{k} = -\mathrm{i}\kappa$ is called *wave vector* of $\mathbf{F}$ with the *propagation coefficient* $\hat{k}$ and the *attenuation coefficient* $\check{k}$. If the attenuation coefficient $\check{k}$ is zero, we say that $\mathbf{F}$ is traveling, while $\mathbf{F}$ is called evanescent otherwise. Again we shall refer to the vector $\mathbf{F}$ of the envelope functions as *envelope wave* since it can be written in the form of a plane wave.

By applying the solution (5.13) to the general $\mathbf{k}\cdot\mathbf{p}$-model (5.1) we get

$$\hat{\mathbf{H}}\hat{\mathbf{F}} = E\hat{\mathbf{F}}, \tag{5.15}$$

with

$$\hat{\mathbf{H}} = \hat{\mathbf{H}}(k) = k^2\mathbf{N} - k\mathbf{M} + \mathbf{V}. \tag{5.16}$$

Note that $\hat{\mathbf{H}}$ is Hermitian if k is real.

Now we are ready to state the main theorem of this chapter.

Theorem 5.1 (Splitting Theorem)**.** Let n denote the number of positive eigenvalues of $\mathbf{N}$. Then there exists an energy $E_0^{\mathrm{e}} \in \mathbb{R}$ such that for all energies $E > E_0^{\mathrm{e}}$

(i) the matrix $\mathbf{A}^{-1}\mathbf{B}$ has exactly $2n$ purely imaginary eigenvalues, n with positive imaginary part and n with negative imaginary part,

(ii) the matrix $\mathbf{A}^{-1}\mathbf{B}$ has exactly $2(d-n)$ complex eigenvalues, $d-n$ with positive real part and $d-n$ with negative real part.

Furthermore, there exists an energy $E_0^{\mathrm{h}} < E_0^{\mathrm{e}}$ such that for all energies $E < E_0^{\mathrm{h}}$

(iii) the matrix $\mathbf{A}^{-1}\mathbf{B}$ has exactly $2(d-n)$ purely imaginary eigenvalues, $d-n$ with positive imaginary part and $d-n$ with negative imaginary part,

(iv) the matrix $\mathbf{A}^{-1}\mathbf{B}$ has exactly $2n$ complex eigenvalues, n with positive real part and n with negative real part.

Remark 5.2. The splitting theorem is needed in order to derive the TBCs in the following section. For the simple case $\mathbf{M} = 0$ and $\mathbf{V} = \operatorname{diag}(v_1, \ldots, v_d)$ a proof of Thm. 5.1 is provided in the appendix A.2. For the general case, i.e. for Hermitian matrices $\mathbf{M}$ and $\mathbf{V}$, numerical evidence shows the correctness of Thm. 5.1. However, a general proof has not been found yet and requires future work.

Considering that the wave vector k satisfies

$$k = -\mathrm{i}\kappa,$$

we can state the following corollary of Thm 5.1.

Corollary 5.3. Let n denote the number of positive eigenvalues of $\mathbf{N}$. Then there exists an energy $E_0^{\mathrm{e}} \in \mathbb{R}$ such that for all energies $E > E_0^{\mathrm{e}}$

(i) there are exactly n positive and n negative wave vectors (i.e. n right and n left-traveling envelope waves),

(ii) there are exactly $2(d-n)$ complex wave vectors, $d-n$ with positive imaginary part (i.e. $d-n$ evanescent envelope waves decaying for $x \to \infty$) and $d-n$ with negative imaginary part (i.e. $d-n$ evanescent envelope waves growing for $x \to \infty$).

Moreover, there exists an energy $E_0^{\mathrm{h}} < E_0^{\mathrm{e}}$ such that for all energies $E < E_0^{\mathrm{h}}$

(iii) there are exactly $d-n$ positive and $d-n$ negative wave vectors (i.e. $d-n$ right and $d-n$ left-traveling envelope waves) and

(iv) there are exactly $2n$ complex wave vectors, n with positive imaginary part (i.e. n evanescent envelope waves decaying for $x \to \infty$) and n with negative imaginary part (i.e. n evanescent envelope waves growing for $x \to \infty$).

Remark 5.4. In all considered examples the d amplitudes $\hat{\mathbf{F}}(k)$ that correspond to the n positive wave vectors and the $d-n$ complex wave vectors with positive imaginary part are linearly independent. Moreover, the d amplitudes $\hat{\mathbf{F}}(k)$ associated with the n negative wave vectors and the $d-n$ complex wave vectors with negative imaginary part are linearly independent.

5.2 Transparent Boundary Conditions

Let us recall the strategy we used in the previous chapters in order to derive the TBCs. We considered a traveling envelope wave $\mathbf{F}^{\mathrm{in}}$ with amplitude of norm 1 that enters the computational domain at $x = 0$. This means that depending on the energy E we require the matrix $\mathbf{N}$ to have at least one positive or negative eigenvalue in order to get at least one pair of traveling envelope waves.

Let us from now on assume that the energy E is greater than some lower bound E_0^{e} and hence, the number n of positive eigenvalues of $\mathbf{N}$ is equal to the number of pairs of traveling envelope waves.

If there are two or more pairs of traveling envelope waves, the incoming envelope wave is not unique. In this case we shall consider a unitary superposition of all right-traveling envelope waves to enter the semiconductor at $x = 0$. This means that we have to specify a priori the values of the n coefficients of the superposition of incoming envelope waves.

Let $\hat{k}_{0,l}^{+}$, $l = 1, \ldots, n$, denote the n positive wave vectors and $\hat{k}_{0,l}^{-}$, $l = 1, \ldots, n$, the n negative wave vectors in the left exterior domain. Moreover, let $\check{k}_{0,l}^{+}$, $l = 1, \ldots, d-n$, denote the $d-n$

complex wave vectors with positive imaginary part and $\check{k}_{0,l}^-$, $l = 1, \dots, d-n$, the $d-n$ complex wave vectors with negative imaginary part in the left exterior domain. The wave vectors in the right exterior domain are defined analogously with subscript L instead of 0.

Note that in all considered examples, e.g. the two-band $\mathbf{k} \cdot \mathbf{p}$-model in Chap. 4, $\hat{k}_l^+ = -\hat{k}_l^-$, for $l = 1, \dots, n$, and $\check{k}_l^+ = -\check{k}_l^-$, for $l = 1, \dots, d-n$.

Let $\hat{\mathbf{F}}_0(k)$ denote the amplitude of norm 1 in the left exterior domain that corresponds to the wave vector k, i.e. the eigenvector of norm 1 of $\hat{\mathbf{H}}(k)$ to the energy eigenvalue E. On the other hand, let $\hat{\mathbf{F}}_L(k)$ denote the corresponding amplitude in the right exterior domain.

Let us consider the superposition of all right-traveling envelope functions

$$\mathbf{F}^{\mathrm{in}} = \sum_{l=1}^{n} \omega_l \hat{\mathbf{F}}_0(\hat{k}_{0,l}^+) e^{\mathrm{i}\hat{k}_{0,l}^+ x}, \qquad x < 0, \tag{5.17}$$

with the coefficients $\omega_1, \dots, \omega_n \in \mathbb{C}$ that satisfy the normalization condition

$$\sum_{l=1}^{n} |\omega_l|^2 = 1. \tag{5.18}$$

This incoming superposition of envelope functions is partly reflected at the left boundary at $x = 0$, yielding a superposition of left-traveling and evanescent envelope functions that reads

$$\mathbf{F}^{\mathrm{r}} = \sum_{l=1}^{n} \hat{r}_l \hat{\mathbf{F}}_0(\hat{k}_{0,l}^-) e^{\mathrm{i}\hat{k}_{0,l}^- x} + \sum_{l=1}^{d-n} \check{r}_l \hat{\mathbf{F}}_0(\check{k}_{0,l}^-) e^{\mathrm{i}\check{k}_{0,l}^- x}, \qquad x < 0, \tag{5.19}$$

with the reflection coefficients $\hat{r}_l$ and $\check{r}_l$. Furthermore, the incoming waves are partly transmitted at the right boundary at $x = L$, which results in a superposition of right-traveling and evanescent envelope functions that takes the form

$$\mathbf{F}^{\mathrm{t}} = \sum_{l=1}^{n} \hat{t}_l \hat{\mathbf{F}}_0(\hat{k}_{0,l}^+) e^{\mathrm{i}\hat{k}_{0,l}^+ x} + \sum_{l=1}^{d-n} \check{t}_l \hat{\mathbf{F}}_0(\check{k}_{0,l}^+) e^{\mathrm{i}\check{k}_{0,l}^+ x}, \qquad x > L, \tag{5.20}$$

with the transmission coefficients $\hat{t}_l$ and $\check{t}_l$. Thus, the solution in the left exterior domain is given by

$$\mathbf{F} = \mathbf{F}^{\mathrm{in}} + \mathbf{F}^{\mathrm{r}}, \qquad x < 0, \tag{5.21}$$

while the solution in the right exterior domain is

$$\mathbf{F} = \mathbf{F}^{\mathrm{t}}, \qquad x > L. \tag{5.22}$$

In order to determine the TBC at the left boundary we evaluate the envelope function $\mathbf{F}$ and its first derivative $\frac{\mathrm{d}}{\mathrm{d}x}\mathbf{F}$ at $x = 0$. We get

$$\mathbf{F}(0) = \sum_{l=1}^{n} \omega_l \hat{\mathbf{F}}_0(\hat{k}_{0,l}^+) + \sum_{l=1}^{n} \hat{r}_l \hat{\mathbf{F}}_0(\hat{k}_{0,l}^-) + \sum_{l=1}^{d-n} \check{r}_l \hat{\mathbf{F}}_0(\check{k}_{0,l}^-) \tag{5.23a}$$

and

$$\frac{\mathrm{d}}{\mathrm{d}x}\mathbf{F}(0) = \sum_{l=1}^{n} \mathrm{i}\hat{k}_{0,l}^+ \omega_l \hat{\mathbf{F}}_0(\hat{k}_{0,l}^+) + \sum_{l=1}^{n} \mathrm{i}\hat{k}_{0,l}^- \hat{r}_l \hat{\mathbf{F}}_0(\hat{k}_{0,l}^-) + \sum_{l=1}^{d-n} \mathrm{i}\check{k}_{0,l}^- \check{r}_l \hat{\mathbf{F}}_0(\check{k}_{0,l}^-). \tag{5.23b}$$

Let us introduce

$$\mathbf{P}_0 = \begin{pmatrix} \hat{\mathbf{F}}_0(\hat{k}_{0,1}^-) & \cdots & \hat{\mathbf{F}}_0(\hat{k}_{0,n}^-) & \hat{\mathbf{F}}_0(\check{k}_{0,1}^-) & \cdots & \hat{\mathbf{F}}_0(\check{k}_{0,d-n}^-) \end{pmatrix} \in \mathbb{C}^{d \times d},$$

and

$$\mathbf{K}_0 = \operatorname{diag}\left(\mathrm{i}\hat{k}_{0,1}^-, \ldots, \mathrm{i}\hat{k}_{0,n}^-, \mathrm{i}\check{k}_{0,1}^-, \ldots, \mathrm{i}\check{k}_{0,d-n}^-\right) \in \mathbb{C}^{d\times d},$$

as well as

$$\mathbf{r} = \left(\hat{r}_1, \ldots, \hat{r}_n, \check{r}_1, \ldots, \check{r}_{d-n}\right)^{\mathrm{T}} \in \mathbb{C}^d.$$

Then we can rewrite the envelope wave $\mathbf{F}$ and its first derivative $\frac{\mathrm{d}}{\mathrm{d}x}\mathbf{F}$ at $x = 0$ in the form

$$\mathbf{P}_0\mathbf{r} = \mathbf{F}(0) - \sum_{l=1}^{n} \omega_l \hat{\mathbf{F}}_0(\hat{k}_{0,l}^+), \tag{5.24a}$$

and

$$\mathbf{P}_0\mathbf{K}_0\mathbf{r} = \frac{\mathrm{d}}{\mathrm{d}x}\mathbf{F}(0) - \sum_{l=1}^{n} \mathrm{i}\hat{k}_{0,l}^+ \omega_l \hat{\mathbf{F}}_0(\hat{k}_{0,l}^+). \tag{5.24b}$$

Since the amplitudes

$$\hat{\mathbf{F}}_0(\hat{k}_{0,1}^-), \ldots, \hat{\mathbf{F}}_0(\hat{k}_{0,n}^-), \hat{\mathbf{F}}_0(\check{k}_{0,1}^-), \ldots, \hat{\mathbf{F}}_0(\check{k}_{0,d-n}^-)$$

are linearly independent, cf. Remark 5.4, the matrix $\mathbf{P}_0$ is regular and hence, its inverse $\mathbf{P}_0^{-1}$ exists. Then the reflection coefficient vector $\mathbf{r}$ reads

$$\mathbf{r} = \mathbf{P}_0^{-1}\left(\mathbf{F}(0) - \sum_{l=1}^{n} \omega_l \hat{\mathbf{F}}_0(\hat{k}_{0,l}^+)\right),$$

cf. Eq. (5.24a). Applied to Eq. (5.24b) we get the left TBC

$$\mathbf{F}_x(0) - \mathbf{P}_0\mathbf{K}_0\mathbf{P}_0^{-1}\mathbf{F}(0) = \sum_{l=1}^{n}\left(\mathrm{i}\hat{k}_{0,l}^+\mathbb{1} - \mathbf{P}_0\mathbf{K}_0\mathbf{P}_0^{-1}\right)\omega_l\hat{\mathbf{F}}_0(\hat{k}_{0,l}^+). \tag{5.25}$$

At the right boundary we proceed analogously. The envelope wave $\mathbf{F}$ and its first derivative $\frac{\mathrm{d}}{\mathrm{d}x}\mathbf{F}$ at $x = L$ read

$$\mathbf{F}(L) = \sum_{l=1}^{n} \hat{t}_l \hat{\mathbf{F}}_L(\hat{k}_{L,l}^+) e^{\mathrm{i}\hat{k}_{L,l}^+ L} + \sum_{l=1}^{d-n} \check{t}_l \hat{\mathbf{F}}_L(\check{k}_{L,l}^+) e^{\mathrm{i}\check{k}_{L,l}^+ L}, \tag{5.26a}$$

and

$$\frac{\mathrm{d}}{\mathrm{d}x}\mathbf{F}(L) = \sum_{l=1}^{n} \mathrm{i}\hat{k}_{L,l}^+ \hat{t}_l \hat{\mathbf{F}}_L(\hat{k}_{L,l}^+) e^{\mathrm{i}\hat{k}_{L,l}^+ L} + \sum_{l=1}^{d-n} \mathrm{i}\check{k}_{L,l}^+ \check{t}_l \hat{\mathbf{F}}_L(\check{k}_{L,l}^+) e^{\mathrm{i}\check{k}_{L,l}^+ L}. \tag{5.26b}$$

Let us introduce

$$\mathbf{P}_L = \left(\hat{\mathbf{F}}_L(\hat{k}_{L,1}^+)e^{\mathrm{i}\hat{k}_{L,1}^+ L} \cdots \hat{\mathbf{F}}_L(\hat{k}_{L,n}^+)e^{\mathrm{i}\hat{k}_{L,n}^+ L} \quad \hat{\mathbf{F}}_L(\check{k}_{L,1}^+)e^{\mathrm{i}\check{k}_{L,1}^+ L} \cdots \hat{\mathbf{F}}_L(\check{k}_{L,d-n}^+)e^{\mathrm{i}\check{k}_{L,d-n}^+ L}\right) \in \mathbb{C}^{d\times d},$$

and

$$\mathbf{K}_L = \operatorname{diag}\left(\mathrm{i}\hat{k}_{L,1}^+, \ldots, \mathrm{i}\hat{k}_{L,n}^+, \mathrm{i}\check{k}_{L,1}^+, \ldots, \mathrm{i}\check{k}_{L,d-n}^+\right) \in \mathbb{C}^{d\times d},$$

as well as

$$\mathbf{t} = \left(\hat{t}_1, \ldots, \hat{t}_n, \check{t}_1, \ldots, \check{t}_{d-n}\right)^{\mathrm{T}} \in \mathbb{C}^d.$$

Then we can rewrite the envelope wave $\mathbf{F}$ and its first derivative $\frac{\mathrm{d}}{\mathrm{d}x}\mathbf{F}$ at $x = L$ in the form

$$\mathbf{P}_L\mathbf{t} = \mathbf{F}(L), \tag{5.27a}$$

and

$$\mathbf{P}_L\mathbf{K}_L\mathbf{t} = \frac{\mathrm{d}}{\mathrm{d}x}\mathbf{F}(L). \tag{5.27b}$$

Since the amplitudes

$$\hat{\mathbf{F}}_L(\hat{k}^+_{L,1}),\dots,\hat{\mathbf{F}}_L(\hat{k}^+_{L,n}),\hat{\mathbf{F}}_L(\check{k}^+_{L,1}),\dots,\hat{\mathbf{F}}_L(\check{k}^+_{L,d-n})$$

are linearly independent, cf. Remark 5.4, so are

$$\hat{\mathbf{F}}_L(\hat{k}^+_{L,1})e^{\mathrm{i}\hat{k}^+_{L,1}L},\dots,\hat{\mathbf{F}}_L(\hat{k}^+_{L,n})e^{\mathrm{i}\hat{k}^+_{L,n}L},\hat{\mathbf{F}}_L(\check{k}^+_{L,1})e^{\mathrm{i}\check{k}^+_{L,1}L},\dots,\hat{\mathbf{F}}_L(\check{k}^+_{L,d-n})e^{\mathrm{i}\check{k}^+_{L,d-n}L}$$

and hence, the matrix $\mathbf{P}_L$ is regular and its inverse $\mathbf{P}_L^{-1}$ exists. Then the transmission coefficient vector $\mathbf{t}$ becomes

$$\mathbf{t}=\mathbf{P}_L^{-1}\mathbf{F}(L),$$

cf. Eq. (5.27a). Applied to Eq. (5.27b) we get the right TBC

$$\mathbf{F}_x(L)-\mathbf{P}_L\mathbf{K}_L\mathbf{P}_L^{-1}\mathbf{F}(L)=\mathbf{0}. \tag{5.28}$$

Remark 5.5. The coefficients $\omega_1,\dots,\omega_n$ restrict the solution at the left boundary. However, in physical applications, for example the unstrained eight-band $\mathbf{k}\cdot\mathbf{p}$-model of the lowest conduction band and the three top-most valence bands, all doubly degenerate, with $\mathbf{k}_{||}=\mathbf{0}$ we will consider in our numerical examples in Sec. 5.5, one typically considers only a particular incoming wave. In the example mentioned above, we have $n=2$, for $E>E_0^{\mathrm{e}}$. As indicated, the bands are doubly degenerate. Mathematically, this means that the eigenvalues of $\mathbf{A}^{-1}\mathbf{B}$ are 2-fold degenerate, i.e. there exist d distinct wave vectors k and for every wave vector k there exist two corresponding amplitudes, if the geometric multiplicity equals the algebraic multiplicity which is the case in our example. In this particular example we have so-called *spin-up solutions* and *spin-down solutions*. If we only consider spin-up envelope functions for example, we set the coefficient ω_1 of the incoming spin-up envelope wave to one and the coefficient ω_2 of the incoming spin-down envelope wave to zero. Depending on the band edge profile the resulting transmitted envelope waves may also consist of spin-down solutions.

5.3 Discretization

We recall the uniform grid $x_j=jh,\ j=0,\dots,J$ with $L=Jh$, of the computational interval $(0,L)$ with $\mathbf{N}_j=\mathbf{N}(x_j)$, $\mathbf{M}_{\mathrm{S}j}=\mathbf{M}_{\mathrm{S}}(x_j)$, $\mathbf{V}_j=\mathbf{V}(x_j)$ and the approximation $\mathbf{F}_j\approx\mathbf{F}(x_j)$, $j=0,\dots,J$. In order to discretize the general $\mathbf{k}\cdot\mathbf{p}$-model (5.1) we apply the second order centered difference operator $\mathrm{D}_h^{\mathrm{cen}}$ as well as the standard second order difference operator D_h^{std} to the abbreviated continuous formulation of the general $\mathbf{k}\cdot\mathbf{p}$-model (5.1)

$$E\mathbf{F}=-\mathbf{N}\mathbf{F}_{xx}+\left(-\mathbf{N}_x+2\mathbf{M}_{\mathrm{S}}\right)\mathbf{F}_x+\left(\mathbf{V}-\mathbf{M}_{\mathrm{S}\,x}^{\mathrm{H}}\right)\mathbf{F}, \tag{5.29}$$

for $x\in(0,L)$.

Thus the discretization of the general $\mathbf{k}\cdot\mathbf{p}$-model leads to

$$E\mathbf{F}_j=-\mathbf{N}_jD_h^{\mathrm{std}}\mathbf{F}_j+\left(-\mathrm{D}_h^{\mathrm{cen}}\mathbf{N}_j+2\mathbf{M}_{\mathrm{S}j}\right)\mathrm{D}_h^{\mathrm{cen}}\mathbf{F}_j+\left(\mathbf{V}_j-\mathrm{D}_h^{\mathrm{cen}}\mathbf{M}_{\mathrm{S}\,j}^{\mathrm{H}}-E\mathbb{1}\right)\mathbf{F}_j, \tag{5.30}$$

with $j=1,\dots,J-1$, which implies

$$\begin{aligned}E\mathbf{F}_j=&\left(-\frac{1}{h^2}\mathbf{N}_j+\frac{1}{2h}\left(-\frac{1}{2h}\left(\mathbf{N}_{j+1}-\mathbf{N}_{j-1}\right)+2\mathbf{M}_{\mathrm{S}j}\right)\right)\mathbf{F}_{j+1}\\&+\left(\frac{2}{h^2}\mathbf{N}_j+\mathbf{V}_j-\frac{1}{2h}\left(\mathbf{M}_{\mathrm{S}\,j+1}^{\mathrm{H}}-\mathbf{M}_{\mathrm{S}\,j-1}^{\mathrm{H}}\right)\right)\mathbf{F}_j\\&+\left(-\frac{1}{h^2}\mathbf{N}_j-\frac{1}{2h}\left(-\frac{1}{2h}\left(\mathbf{N}_{j+1}-\mathbf{N}_{j-1}\right)+2\mathbf{M}_{\mathrm{S}j}\right)\right)\mathbf{F}_{j-1},\end{aligned} \tag{5.31}$$

with $j = 1, \ldots, J-1$.

In the exterior domains $x \leq 0$ and $x \geq L$, the matrices $\mathbf{N}$, $\mathbf{M}_{\mathrm{S}}$ and $\mathbf{V}$ are constant. Without loss of generality we focus on the left exterior domain $x \leq 0$ with $\mathbf{N}(x) = \mathbf{N}_0$, $\mathbf{M}_{\mathrm{S}}(x) = \mathbf{M}_{\mathrm{S},0}$ and $\mathbf{V}(x) = \mathbf{V}_0$. Note that the results for the right exterior domain $x \geq L$ can be derived analogously. For simplicity let us omit the subscript 0 in $\mathbf{N}_0$, $\mathbf{M}_{\mathrm{S},0}$ and $\mathbf{V}_0$. Hence, Eq. (5.31) is a second order difference equation with constant coefficients of the form

$$E\mathbf{F}_j = \mathbf{M}^+\mathbf{F}_{j+1} + \mathbf{M}^0\mathbf{F}_j + \mathbf{M}^-\mathbf{F}_{j-1}, \qquad j < 0, \tag{5.32}$$

with

$$\begin{aligned} \mathbf{M}^+ &= -\frac{1}{h^2}\mathbf{N} + \frac{1}{h}\mathbf{M}_{\mathrm{S}}, \\ \mathbf{M}^0 &= \frac{2}{h^2}\mathbf{N} + \mathbf{V}, \\ \mathbf{M}^- &= -\frac{1}{h^2}\mathbf{N} - \frac{1}{h}\mathbf{M}_{\mathrm{S}}. \end{aligned} \tag{5.33}$$

By introducing the substitution

$$\Phi_j = \begin{pmatrix} \mathbf{F}_j \\ \mathbf{F}_{j+1} \end{pmatrix},$$

Eq. (5.32) can be transformed into a first order difference equation with constant coefficients

$$\mathbf{A}_h\Phi_j = \mathbf{B}_h\Phi_{j-1}, \qquad j < 0, \tag{5.34}$$

with

$$\mathbf{A}_h = \begin{pmatrix} \mathbb{1} & \mathbf{0} \\ \mathbf{0} & -\mathbf{M}^+ \end{pmatrix}$$

and

$$\mathbf{B}_h = \begin{pmatrix} \mathbf{0} & \mathbb{1} \\ \mathbf{M}^- & \left(\mathbf{M}^0 - E\mathbb{1}\right) \end{pmatrix}.$$

Note that $\mathbf{M}^+$ and $\mathbf{M}^-$ are not necessarily regular. However, in all examples we examined $\mathbf{M}^+$ and $\mathbf{M}^-$ are regular. In this case, $\mathbf{A}_h$ and $\mathbf{B}_h$ are regular and hence, we can write Eq. (5.34) in the form

$$\Phi_j = \mathbf{A}_h^{-1}\mathbf{B}_h\Phi_{j-1}, \qquad j < 0,$$

with the regular matrix

$$\mathbf{A}_h^{-1}\mathbf{B}_h = \begin{pmatrix} \mathbf{0} & \mathbb{1} \\ (-\mathbf{M}^+)^{-1}\mathbf{M}^- & (-\mathbf{M}^+)^{-1}\left(\mathbf{M}^0 - E\mathbb{1}\right) \end{pmatrix}.$$

Remark 5.6. In all examples we examined the geometric multiplicity of the eigenvalues of $\mathbf{A}_h^{-1}\mathbf{B}_h$ is equal to their algebraic multiplicity. Hence, the eigenvectors of $\mathbf{A}_h^{-1}\mathbf{B}_h$ are linearly independent and form a basis of $\mathbb{C}^{4d}$. This property is important in order to use Prop. 3.4 where we set the discrete solution at the left boundary to some eigenvector $\mathbf{a}$ of $\mathbf{A}_h^{-1}\mathbf{B}_h$.

According to Prop. 3.4, the solution of the first order difference equation can be written in the form

$$\Phi_j = \mathbf{a}\alpha^j,$$

with an eigenvalue $\alpha \in \mathbb{C}$ of $\mathbf{A}_h^{-1}\mathbf{B}_h$ and the corresponding eigenvector $\mathbf{a} \in \mathbb{C}^{2d}$. The first d components of $\Phi_j \in \mathbb{C}^{2d}$ represent the discrete solution $\mathbf{F}_j \in \mathbb{C}^d$. Therefore, we introduce the *discrete amplitude* $\hat{\mathbf{F}}_h \in \mathbb{C}^d$ that contains the first d components of $\mathbf{a}$. The discrete solution $\mathbf{F}_j$ becomes

$$\mathbf{F}_j = \hat{\mathbf{F}}_h\alpha^j = \hat{\mathbf{F}}_h e^{\mathrm{i}k_h jh}, \tag{5.35}$$

with the *discrete wave vector*

$$k_h = \frac{1}{h}\left(\arg(\alpha) - \mathrm{i}\ln|\alpha|\right).$$

The discrete solution as given in Eq. (5.35) implies

$$\mathbf{F}_{j+1}e^{-\mathrm{i}k_h h} = \mathbf{F}_j = \mathbf{F}_{j-1}e^{\mathrm{i}k_h h},$$

and thus, applied to the difference equation (5.32) we obtain

$$\hat{\mathbf{H}}_h\hat{\mathbf{F}}_h = E\hat{\mathbf{F}}_h, \tag{5.36}$$

with

$$\hat{\mathbf{H}}_h = \hat{\mathbf{H}}_h(k_h) = \mathbf{M}^+e^{\mathrm{i}k_h h} + \mathbf{M}^0 + \mathbf{M}^-e^{-\mathrm{i}k_h h}.$$

Now we shall state the discrete analogon of Thm. 5.1.

Theorem 5.7 (Discrete Splitting Theorem)**.** Let n denote the number of positive eigenvalues of $\mathbf{N}$. Then there exists an energy $E^{\mathrm{e}}_{h,0} \in \mathbb{R}$ such that for all energies $E > E^{\mathrm{e}}_{h,0}$

(i) the matrix $\mathbf{A}_h^{-1}\mathbf{B}_h$ has exactly $2n$ eigenvalues with modulus 1, n having a positive complex argument and n having a negative complex argument,

(ii) the matrix $\mathbf{A}_h^{-1}\mathbf{B}_h$ has exactly $d-n$ eigenvalues with modulus greater than 1 and $d-n$ eigenvalues with modulus smaller than 1.

Furthermore, there exists an energy $E^{\mathrm{h}}_0 < E^{\mathrm{e}}_0$ such that for all energies $E < E^{\mathrm{h}}_0$

(iii) the matrix $\mathbf{A}_h^{-1}\mathbf{B}_h$ has exactly $2\,(d-n)$ eigenvalues with modulus 1, $d-n$ having a positive complex argument and $d-n$ having a negative complex argument,

(iv) the matrix $\mathbf{A}_h^{-1}\mathbf{B}_h$ has exactly n eigenvalues with modulus greater than 1 and n eigenvalues with modulus smaller than 1.

Remark 5.8. The discrete splitting theorem is needed in order to derive the DTBCs in the following section. Analogously to Thm. 5.1, numerical evidence shows the correctness of Thm. 5.7. Once a proof for the continuous splitting theorem 5.1 has been found, we are confident to be able to derive a proof of Thm. 5.7 as discrete analogon.

By using the identity

$$k_h = \frac{1}{h}\left(\arg(\alpha) - \mathrm{i}\ln|\alpha|\right),$$

it follows

Corollary 5.9. Let n denote the number of positive eigenvalues of $\mathbf{N}$. Then there exists an energy $E^{\mathrm{e}}_{0,h} \in \mathbb{R}$ such that for all energies $E > E^{\mathrm{e}}_{h,0}$

(i) there are exactly n positive and n negative discrete wave vectors (i.e. n right and n left-traveling discrete envelope waves),

(ii) there are exactly $2\,(d-n)$ complex discrete wave vectors, $d-n$ with positive imaginary part (i.e. $d-n$ evanescent discrete envelope waves decaying for $x \to \infty$) and $d-n$ with negative imaginary part (i.e. $d-n$ evanescent discrete envelope waves growing for $x \to \infty$).

Moreover, there exists an energy $E^{\mathrm{h}}_{h,0} < E^{\mathrm{e}}_{h,0}$ such that for all energies $E < E^{\mathrm{h}}_{h,0}$

(iii) there are exactly $d-n$ positive and $d-n$ negative discrete wave vectors (i.e. $d-n$ right and $d-n$ left-traveling discrete envelope waves) and

(iv) there are exactly $2n$ complex discrete wave vectors, n with positive imaginary part (i.e. n evanescent discrete envelope waves decaying for $x \to \infty$) and n with negative imaginary part (i.e. n evanescent discrete envelope waves growing for $x \to \infty$).

Remark 5.10. We already pointed out that in all considered examples the geometric multiplicity of the eigenvalues of $\mathbf{A}_h^{-1}\mathbf{B}_h$ is equal to their algebraic multiplicity and hence, the eigenvectors are linearly independent. In addition, we note that for all considered examples the d discrete amplitudes $\hat{\mathbf{F}}_h(k_h)$ that correspond to the n positive discrete wave vectors and the $d-n$ complex discrete wave vectors with positive imaginary part are linearly independent. Moreover, the d discrete amplitudes $\hat{\mathbf{F}}_h(k_h)$ that are associated with the n negative discrete wave vectors and the $d-n$ complex discrete wave vectors with negative imaginary part are linearly independent.

5.4 Discrete Transparent Boundary Conditions

In order to derive the DTBCs for the general $\mathbf{k}\cdot\mathbf{p}$-model we apply the discrete solution derived in the previous section to the reflection and transmission conditions (5.21), (5.22) and assume that they hold in a small vicinity of the two boundaries, i.e. $j = 0, 1$ and $j = J-1, J$ respectively.

Let us from now on assume that the energy is greater than some lower bound $E^{\mathrm{e}}_{h,0}$ and hence, the number n of positive eigenvalues of $\mathbf{N}$ is equal to the number of purely imaginary, complex conjugate pairs of discrete wave vectors.

Suppose that there is at least one pair of discrete traveling envelope functions, in other words $n \geq 1$. If $n \geq 2$, then we have two or more pairs of traveling envelope functions and hence, the incoming envelope function is not unique. In this case we shall proceed accordingly to the derivation of the TBCs and consider a unitary superposition of all discrete right-traveling envelope functions weighted by the coefficients $\omega_1, \ldots, \omega_n \in \mathbb{C}$.

Let $\hat{k}^+_{h,0,l}$, $l = 1, \ldots, n$, denote the n positive discrete wave vectors and $\hat{k}^-_{h,0,l}$, $l = 1, \ldots, n$, the n negative discrete wave vectors in the left exterior domain. Moreover, the $d-n$ complex discrete wave vectors with positive imaginary part in the left exterior domain are called $\check{k}^+_{h,0,l}$, $l = 1, \ldots, d-n$, and the $d-n$ complex discrete wave vectors with negative imaginary part are denoted by $\check{k}^-_{h,0,l}$, $l = 1, \ldots, d-n$. The discrete wave vectors in the right exterior domain are defined analogously with subscript L instead of 0.

In all considered examples, e.g. the two-band $\mathbf{k}\cdot\mathbf{p}$-model in Chap. 4, we have $\hat{k}^+_{h,l} = -\hat{k}^-_{h,l}$, for $l = 1, \ldots, n$, and $\check{k}^+_{h,l} = -\check{k}^-_{h,l}$, for $l = 1, \ldots, d-n$.

Let $\hat{\mathbf{F}}_{h,0}(k_h)$ denote the amplitude of norm 1 in the left exterior domain that corresponds to the discrete wave vector k_h, i.e. the eigenvector of norm 1 of $\hat{\mathbf{H}}_h(k_h)$ to the energy eigenvalue E. On the other hand, let $\hat{\mathbf{F}}_{h,L}(k_h)$ be the corresponding amplitude in the right exterior domain.

Then we have

$$\begin{aligned}\mathbf{F}_j = \mathbf{F}^{\mathrm{in}}_j + \mathbf{F}^{\mathrm{r}}_j = &\sum_{l=1}^{n} \omega_l \hat{\mathbf{F}}_{h,0}(\hat{k}^+_{h,0,l}) e^{\mathrm{i}\hat{k}^+_{h,0,l} jh} \\ &+ \sum_{l=1}^{n} \hat{r}_{h,l} \hat{\mathbf{F}}_{h,0}(\hat{k}^-_{h,0,l}) e^{\mathrm{i}\hat{k}^-_{h,0,l} jh} + \sum_{l=1}^{d-n} \check{r}_{h,l} \hat{\mathbf{F}}_{h,0}(\check{k}^-_{h,0,l}) e^{\mathrm{i}\check{k}^-_{h,0,l} jh},\end{aligned}$$

at the left boundary, i.e. for $j = 0, 1$, and

$$\mathbf{F}_j = \mathbf{F}^{\mathrm{t}}_j = \sum_{l=1}^{n} \hat{t}_h \hat{\mathbf{F}}_{h,L}(\hat{k}^+_{h,L,l}) e^{\mathrm{i}\hat{k}^+_{h,L,l} jh} + \sum_{l=1}^{d-n} \check{t}_h \hat{\mathbf{F}}_{h,L}(\check{k}^+_{h,L,l}) e^{\mathrm{i}\check{k}^+_{h,L,l} jh},$$

at the right boundary, i.e. for $j = J-1, J$.

Let us introduce

$$\mathbf{P}_{h,0} = \left(\hat{\mathbf{F}}_{h,0}(\hat{k}^-_{h,0,1}) \quad \cdots \quad \hat{\mathbf{F}}_{h,0}(\hat{k}^-_{h,0,n}) \quad \hat{\mathbf{F}}_{h,0}(\check{k}^-_{h,0,1}) \quad \cdots \quad \hat{\mathbf{F}}_{h,0}(\check{k}^-_{h,0,d-n})\right) \in \mathbb{C}^{d\times d},$$

and

$$\mathbf{K}_{h,0} = \operatorname{diag}\left(e^{\mathrm{i}\hat{k}^-_{h,0,1}h}, \ldots, e^{\mathrm{i}\hat{k}^-_{h,0,n}h}, e^{\mathrm{i}\check{k}^-_{h,0,1}h}, \ldots, e^{\mathrm{i}\check{k}^-_{h,0,d-n}h}\right) \in \mathbb{C}^{d\times d},$$

as well as

$$\mathbf{r}_h = (\hat{r}_{h,1}, \ldots, \hat{r}_{h,n}, \check{r}_{h,1}, \ldots, \check{r}_{h,d-n})^{\mathrm{T}} \in \mathbb{C}^d.$$

Then we can rewrite the discrete envelope function $\mathbf{F}_j$ for $j = 0, 1$ in the form

$$\mathbf{P}_{h,0}\mathbf{r}_h = \mathbf{F}_0 - \sum_{l=1}^{n} \omega_l \hat{\mathbf{F}}_{h,0}(\hat{k}^+_{h,0,l}), \tag{5.37a}$$

and

$$\mathbf{P}_{h,0}\mathbf{K}_{h,0}\mathbf{r}_h = \mathbf{F}_1 - \sum_{l=1}^{n} \omega_l \hat{\mathbf{F}}_{h,0}(\hat{k}^+_{h,0,l}) e^{\mathrm{i}\hat{k}^+_{h,0,l}h}. \tag{5.37b}$$

Since the discrete amplitudes

$$\hat{\mathbf{F}}_{h,0}(\hat{k}^-_{h,0,1}), \ldots, \hat{\mathbf{F}}_{h,0}(\hat{k}^-_{h,0,n}), \hat{\mathbf{F}}_{h,0}(\check{k}^-_{h,0,1}), \ldots, \hat{\mathbf{F}}_{h,0}(\check{k}^-_{h,0,d-n})$$

are linearly independent, cf. Remark 5.10, the matrix $\mathbf{P}_{h,0}$ is regular and hence, its inverse $\mathbf{P}^{-1}_{h,0}$ exists. Then the reflection coefficient vector $\mathbf{r}_h$ is given by

$$\mathbf{r}_h = \mathbf{P}^{-1}_{h,0}\left(\mathbf{F}_0 - \sum_{l=1}^{n} \omega_l \hat{\mathbf{F}}_{h,0}(\hat{k}^+_{h,0,l})\right),$$

cf. Eq. (5.37a). Applied to Eq. (5.37b) we get the left DTBC

$$\mathbf{F}_1 - \mathbf{P}_{h,0}\mathbf{K}_{h,0}\mathbf{P}^{-1}_{h,0}\mathbf{F}_0 = \sum_{l=1}^{n}\left(e^{\mathrm{i}\hat{k}^+_{h,0,l}}\mathbb{1} - \mathbf{P}_{h,0}\mathbf{K}_{h,0}\mathbf{P}^{-1}_{h,0}\right)\omega_l \hat{\mathbf{F}}_{h,0}(\hat{k}^+_{h,0,l}), \tag{5.38}$$

compared to the left TBC (5.25).

At the right boundary we proceed analogously. Let us introduce

$$\mathbf{P}_{h,L} = \left(\hat{\mathbf{p}}_1 \cdots \hat{\mathbf{p}}_n \quad \check{\mathbf{p}}_1 \cdots \check{\mathbf{p}}_{d-n}\right) \in \mathbb{C}^{d\times d},$$

with the columns

$$\hat{\mathbf{p}}_l = \hat{\mathbf{F}}_{h,L}(\hat{k}^+_{h,L,l}) e^{\mathrm{i}\hat{k}^+_{h,L,l}hJ},$$

and

$$\check{\mathbf{p}}_l = \hat{\mathbf{F}}_{h,L}(\check{k}^+_{h,L,l}) e^{\mathrm{i}\check{k}^+_{h,L,l}hJ}.$$

Moreover, we introduce

$$\mathbf{K}_{h,L} = \operatorname{diag}\left(e^{-\mathrm{i}\hat{k}^+_{h,L,1}h}, \ldots, e^{-\mathrm{i}\hat{k}^+_{h,L,n}h}, e^{-\mathrm{i}\check{k}^+_{h,L,1}h}, \ldots, e^{-\mathrm{i}\check{k}^+_{h,L,d-n}h}\right) \in \mathbb{C}^{d\times d},$$

as well as

$$\mathbf{t}_h = \left(\hat{t}_{h,1}, \ldots, \hat{t}_{h,n}, \check{t}_{h,1}, \ldots, \check{t}_{h,d-n}\right)^{\mathrm{T}} \in \mathbb{C}^d.$$

Then we can rewrite the discrete envelope function $\mathbf{F}_j$ for $j = J-1, J$ in the form

$$\mathbf{P}_{h,L}\mathbf{t}_h = \mathbf{F}_J, \tag{5.39a}$$

and

$$\mathbf{P}_{h,L}\mathbf{K}_{h,L}\mathbf{t}_h = \mathbf{F}_{J-1}. \tag{5.39b}$$

Since the discrete amplitudes

$$\hat{\mathbf{F}}_{h,L}(\hat{k}^+_{h,L,1}),\ldots,\hat{\mathbf{F}}_{h,L}(\hat{k}^+_{h,L,n}),\hat{\mathbf{F}}_{h,L}(\check{k}^+_{h,L,1}),\ldots,\hat{\mathbf{F}}_{h,L}(\check{k}^+_{h,L,d-n})$$

are linearly independent, cf. Remark 5.10, so are

$$\hat{\mathbf{F}}_{h,L}(\hat{k}^+_{h,L,1})e^{\mathrm{i}\hat{k}^+_{h,L,1}hJ},\ldots,\hat{\mathbf{F}}_{h,L}(\hat{k}^+_{h,L,n})e^{\mathrm{i}\hat{k}^+_{h,L,n}hJ},$$
$$\hat{\mathbf{F}}_{h,L}(\check{k}^+_{h,L,1})e^{\mathrm{i}\check{k}^+_{h,L,1}hJ},\ldots,\hat{\mathbf{F}}_{h,L}(\check{k}^+_{h,L,d-n})e^{\mathrm{i}\check{k}^+_{h,L,d-n}hJ}$$

and hence, the matrix $\mathbf{P}_{h,L}$ is regular and its inverse $\mathbf{P}^{-1}_{h,L}$ exists. Then the transmission coefficient vector $\mathbf{t}_h$ reads

$$\mathbf{t}_h = \mathbf{P}^{-1}_{h,L}\mathbf{F}_J,$$

cf. Eq. (5.39a). Applied to Eq. (5.39b) we get the right DTBC

$$\mathbf{F}_{J-1} - \mathbf{P}_{h,L}\mathbf{K}_{h,L}\mathbf{P}^{-1}_{h,L}\mathbf{F}_J = \mathbf{0}, \tag{5.40}$$

in contrast to the right TBC (5.28).

5.5 Numerical Examples

5.5.1 The Free Scattering State

In our first example, we want to examine the numerical result of an unstrained eight-band $\mathbf{k}\cdot\mathbf{p}$-model of the lowest conduction band and the three top-most valence bands, all doubly degenerate, with $\mathbf{k}_{||} = \mathbf{0}$, in the case of the free scattering state and compare it with the analytical solution, that can be derived from the results in Sec. 5.1.

In this case the 8×8-$\mathbf{k}\cdot\mathbf{p}$-Hamiltonian reduces to

$$\mathbf{H} = \mathbf{H}_0 + \mathbf{H}_\Delta + \mathbf{H}_1\frac{\mathrm{d}}{\mathrm{d}x} + \mathbf{H}_2\frac{\mathrm{d}^2}{\mathrm{d}x^2}, \tag{5.41}$$

where $\mathbf{H}_0$ describes the *band edge profile*, $\mathbf{H}_\Delta$ denotes the *spin orbit coupling*, $\mathbf{H}_1$ contains all *first order couplings*, i.e. the inter-band couplings, and $\mathbf{H}_2$ contains all *second order couplings*, i.e. the intra-band couplings, see [19].

The band edge profile is given by

$$\mathbf{H}_0 = \mathrm{diag}\left(E_\mathrm{c}, E_\mathrm{v}, E_\mathrm{v}, E_\mathrm{v}, E_\mathrm{c}, E_\mathrm{v}, E_\mathrm{v}, E_\mathrm{v}\right), \tag{5.42}$$

where E_c is the conduction band edge and E_v is the valence band edge with the $E_\mathrm{g} = E_\mathrm{c} - E_\mathrm{v}$.

The spin orbit coupling matrix $\mathbf{H}_\Delta$ takes the form

$$\mathbf{H}_\Delta = \begin{pmatrix} \mathbf{G} + \mathrm{i}\mathbf{G}_z & \mathbf{G}_y + \mathrm{i}\mathbf{G}_x \\ -\mathbf{G}_y + \mathrm{i}\mathbf{G}_x & \mathbf{G}_\mathrm{so} - \mathrm{i}\mathbf{G}_z \end{pmatrix}, \tag{5.43}$$

with

$$\mathbf{G}_\mathrm{so} = \frac{\Delta_\mathrm{so}}{3}\,\mathrm{diag}\left(0,-1,-1,-1\right),$$

$$\mathbf{G}_x = \frac{\Delta_\mathrm{so}}{3}\begin{pmatrix} 0 & 0 & 0 & 0 \\ 0 & 0 & 0 & 0 \\ 0 & 0 & 0 & -1 \\ 0 & 0 & 1 & 0 \end{pmatrix},$$

$$\mathbf{G}_y = \frac{\Delta_{\mathrm{so}}}{3}\begin{pmatrix} 0 & 0 & 0 & 0 \\ 0 & 0 & 0 & 1 \\ 0 & 0 & 0 & 0 \\ 0 & -1 & 0 & 0 \end{pmatrix},$$

$$\mathbf{G}_z = \frac{\Delta_{\mathrm{so}}}{3}\begin{pmatrix} 0 & 0 & 0 & 0 \\ 0 & 0 & -1 & 0 \\ 0 & 1 & 0 & 0 \\ 0 & 0 & 0 & 0 \end{pmatrix}.$$

The parameter Δ_{so} denotes the so-called *spin orbit splitting*.

The matrix of first order couplings reads

$$\mathbf{H}_1 = \begin{pmatrix} 0 & 0 & 0 & P_0 & 0 & 0 & 0 & 0 \\ 0 & 0 & 0 & 0 & 0 & 0 & 0 & 0 \\ 0 & 0 & 0 & 0 & 0 & 0 & 0 & 0 \\ -P_0 & 0 & 0 & 0 & 0 & 0 & 0 & 0 \\ 0 & 0 & 0 & 0 & 0 & 0 & 0 & -P_0 \\ 0 & 0 & 0 & 0 & 0 & 0 & 0 & 0 \\ 0 & 0 & 0 & 0 & 0 & 0 & 0 & 0 \\ 0 & 0 & 0 & 0 & P_0 & 0 & 0 & 0 \end{pmatrix} \tag{5.44}$$

while the matrix of second order couplings takes the form

$$\mathbf{H}_2 = -\operatorname{diag}(\alpha, \mu, \mu, \lambda, \alpha, \mu, \mu, \lambda), \tag{5.45}$$

where the coefficients $\alpha, \lambda, \mu \in \mathbb{C}$ are given by

$$\begin{aligned} \alpha =& \frac{\hbar^2}{2m_{\mathrm{c}}} - \frac{P_0^2}{E_{\mathrm{g}}}\frac{E_{\mathrm{g}} + 2\frac{\Delta_{\mathrm{so}}}{3}}{E_{\mathrm{g}} + \Delta_{\mathrm{so}}}, \\ \lambda =& \frac{P_0^2}{E_{\mathrm{g}}} - \frac{\hbar^2}{2m_0}(\gamma_1 + 4\gamma_2), \\ \mu =& -\frac{\hbar^2}{2m_0}(\gamma_1 - 2\gamma_2), \end{aligned}$$

with the effective mass m_{c} of the conduction band and the *Luttinger parameters* γ_1 and γ_2.

Written in the usual notation

$$-\mathbf{N}\frac{\mathrm{d}^2}{\mathrm{d}x^2}\mathbf{F} + \mathrm{i}\mathbf{M}\frac{\mathrm{d}}{\mathrm{d}x}\mathbf{F} + (\mathbf{V} - E\mathbb{1})\mathbf{F} = \mathbf{0}, \tag{5.46}$$

cf. Eq. (5.4), we have

$$\mathbf{N} = -\mathbf{H}_2 = \operatorname{diag}(\alpha, \mu, \mu, \lambda, \alpha, \mu, \mu, \lambda),$$

$$\mathbf{M} = -\mathrm{i}\mathbf{H}_1 = \begin{pmatrix} 0 & 0 & 0 & -\mathrm{i}P_0 & 0 & 0 & 0 & 0 \\ 0 & 0 & 0 & 0 & 0 & 0 & 0 & 0 \\ 0 & 0 & 0 & 0 & 0 & 0 & 0 & 0 \\ \mathrm{i}P_0 & 0 & 0 & 0 & 0 & 0 & 0 & 0 \\ 0 & 0 & 0 & 0 & 0 & 0 & 0 & \mathrm{i}P_0 \\ 0 & 0 & 0 & 0 & 0 & 0 & 0 & 0 \\ 0 & 0 & 0 & 0 & 0 & 0 & 0 & 0 \\ 0 & 0 & 0 & 0 & -\mathrm{i}P_0 & 0 & 0 & 0 \end{pmatrix}$$

and

$$\mathbf{V}=\mathbf{H}_0+\mathbf{H}_\Delta=\begin{pmatrix} E_\mathrm{c} & 0 & 0 & 0 & 0 & 0 & 0 & 0\\ 0 & E_\mathrm{v}-\frac{\Delta_\mathrm{so}}{3} & -\mathrm{i}\frac{\Delta_\mathrm{so}}{3} & 0 & 0 & 0 & 0 & \frac{\Delta_\mathrm{so}}{3}\\ 0 & \mathrm{i}\frac{\Delta_\mathrm{so}}{3} & E_\mathrm{v}-\frac{\Delta_\mathrm{so}}{3} & 0 & 0 & 0 & 0 & -\mathrm{i}\frac{\Delta_\mathrm{so}}{3}\\ 0 & 0 & 0 & E_\mathrm{v}-\frac{\Delta_\mathrm{so}}{3} & 0 & -\frac{\Delta_\mathrm{so}}{3} & \mathrm{i}\frac{\Delta_\mathrm{so}}{3} & 0\\ 0 & 0 & 0 & 0 & E_\mathrm{c} & 0 & 0 & 0\\ 0 & 0 & 0 & -\frac{\Delta_\mathrm{so}}{3} & 0 & E_\mathrm{v}-\frac{\Delta_\mathrm{so}}{3} & \mathrm{i}\frac{\Delta_\mathrm{so}}{3} & 0\\ 0 & 0 & 0 & -\mathrm{i}\frac{\Delta_\mathrm{so}}{3} & 0 & -\mathrm{i}\frac{\Delta_\mathrm{so}}{3} & E_\mathrm{v}-\frac{\Delta_\mathrm{so}}{3} & 0\\ 0 & \frac{\Delta_\mathrm{so}}{3} & \mathrm{i}\frac{\Delta_\mathrm{so}}{3} & 0 & 0 & 0 & 0 & E_\mathrm{v}-\frac{\Delta_\mathrm{so}}{3} \end{pmatrix}.$$

For simplicity, we set $\hbar=m_0=1$ as well as $L=1$. We use the dimensionless version of the parameters as given in [24] that are given by $\alpha=3.32$, $\lambda=-18.77$, $\mu=-3.24$, $P_0=132.744$ and $\Delta_\mathrm{so}=419.07$. According to [24], we set the band edges to $E_\mathrm{c}=905.96$ and $E_\mathrm{v}=0$.

For these settings and a step size $h=1/50$ Fig. 5.1 shows the analytical and discrete dispersion relations. Analogously to the two-band $\mathbf{k}\cdot\mathbf{p}$-model in Chap. 4, the discrete dispersion relation is $2\frac{\pi}{h}$-periodic. But note that in contrast to the discrete dispersion relation of the two-band $\mathbf{k}\cdot\mathbf{p}$-model using the centered FDS, the positive trunk of the discrete dispersion relation for these particular settings is injective in $[0,\pi/h]$. Thus, there does not exist an energy window such that we expect spurious oscillations for all admissible energies outside this window due to the wrong choice of the discrete wave vectors, cf. Sec. 4.3.

Fig. 5.2 shows a comparison of the analytical solution and the numerical solution for a step size $h=1/50$ and an energy $E=1500$. While the norms of the analytical and numerical solutions coincide and are equivalent to one, the phases are plotted in Fig. 5.2(a) and the real parts of the conduction bands are shown in Fig. 5.2(b). The small phase error we can observe in both plots decreases for smaller step sizes. This is demonstrated in Fig. 5.3 where the discrete L^2-error is plotted versus the number of grid points. Recall that the discrete L^2-error is the solution of the nonlinear optimization problem

$$\Delta\mathbf{F}_h^{\min}=\min_{\varphi\in[-\pi,\pi]}\Delta\mathbf{F}_h=\min_{\varphi\in[-\pi,\pi]}\frac{1}{J+1}\sqrt{\sum_{j=0}^{J}\|\mathbf{F}(x_j)-\mathbf{F}_j e^{\mathrm{i}\varphi}\|^2}, \tag{5.47}$$

where $\mathbf{F}(x_j)$ denotes the analytical solution at $x=x_j$ and $\mathbf{F}_j$ the numerical solution using the step size $h=1/J$. The discrete L^2-error in Fig. 5.3 is clearly in $\mathcal{O}(h^2)$ which coincides with the formal order of the standard and centered difference operator we used in order to discretize the general $\mathbf{k}\cdot\mathbf{p}$-model.

5.5.2 The Single Barrier Potential

In our second example we want to analyze the numerical results of the unstrained eight-band $\mathbf{k}\cdot\mathbf{p}$-model with $\mathbf{k}_{||}=\mathbf{0}$ in the case of a single barrier potential. We consider a semiconductor of length L that is split into three parts. Let $0<x_1<x_2<L$, then the three subdomains of the semiconductor are defined by $[0,x_1)$, $[x_1,x_2)$ and $[x_2,L]$. The two outer subdomains have the same physical properties and are denoted by $A=[0,x_1)\cup[x_2,L]$, while the inner subdomain is called $B=[x_1,x_2)$.

We use the same problem as in the previous example, but in the domain B we shall set the band edges to $E_\mathrm{c}^B=1169.33$ and $E_\mathrm{v}^B=-167.60$, see [24]. Due to physical conventions, we shall refer to this band edge profile as *quantum well structure*.

Analogously to the previous chapters, we can compute the analytical solution since the matrices $\mathbf{N}$, $\mathbf{M}$ are constant the matrix $\mathbf{V}$ is piecewise constant. Let us denote the matrix $\mathbf{V}$ in the domain A by $\mathbf{V}_A$ and in the domain B by $\mathbf{V}_B$. Suppose that the energy E is greater than some lower bound E_0^e, cf. Thm. 5.1. Then the number of positive wave vectors is equal to the number n of positive eigenvalues of N.

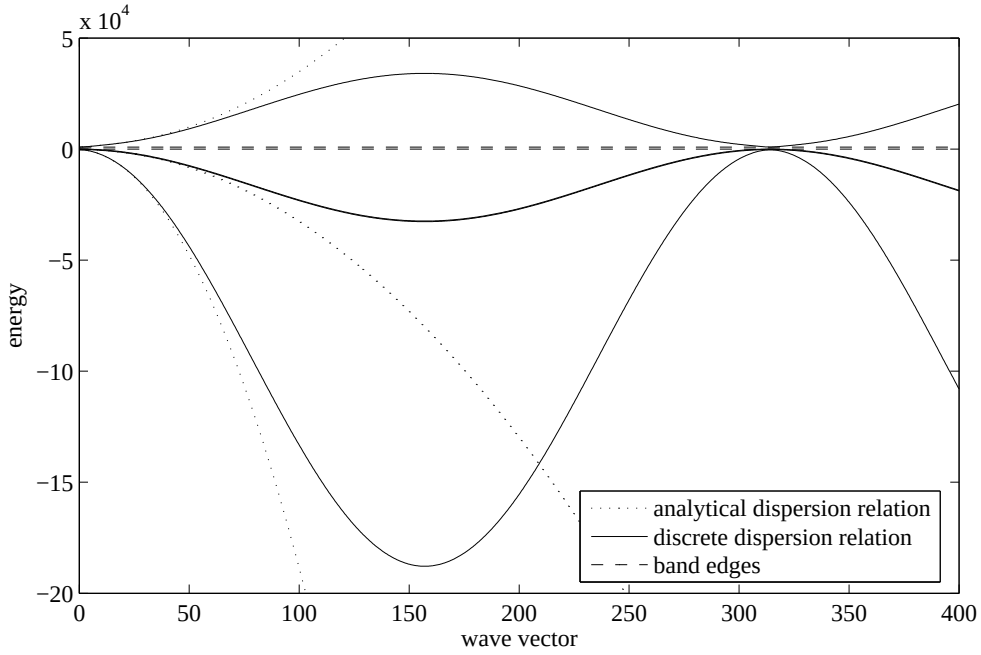

(a) Analytical and discrete dispersion relations.

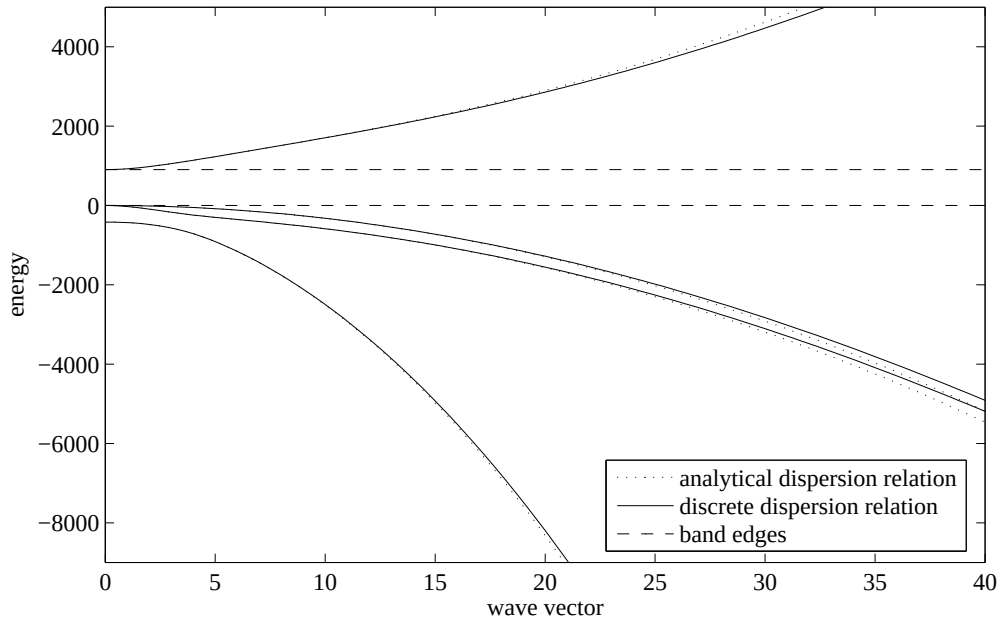

(b) Detail view of (a).

Figure 5.1: Analytical (dotted line) and discrete (solid line) dispersion relations of the unstrained eight-band $\mathbf{k} \cdot \mathbf{p}$-model with $\mathbf{k}_{||} = \mathbf{0}$. The discrete dispersion relation is plotted for a step size $h = 1/50$.

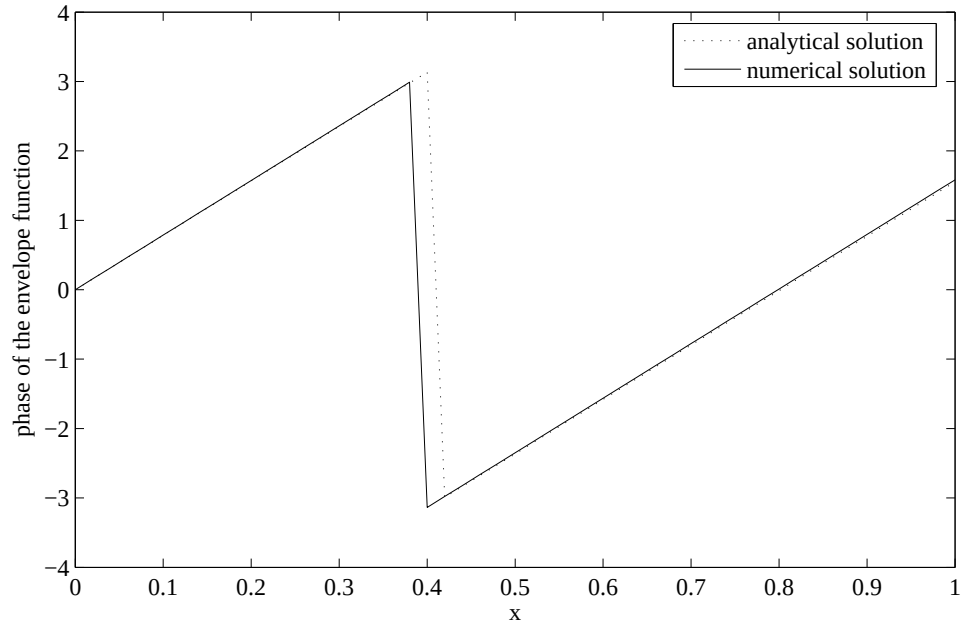

(a) Phases of the analytical and numerical solutions.

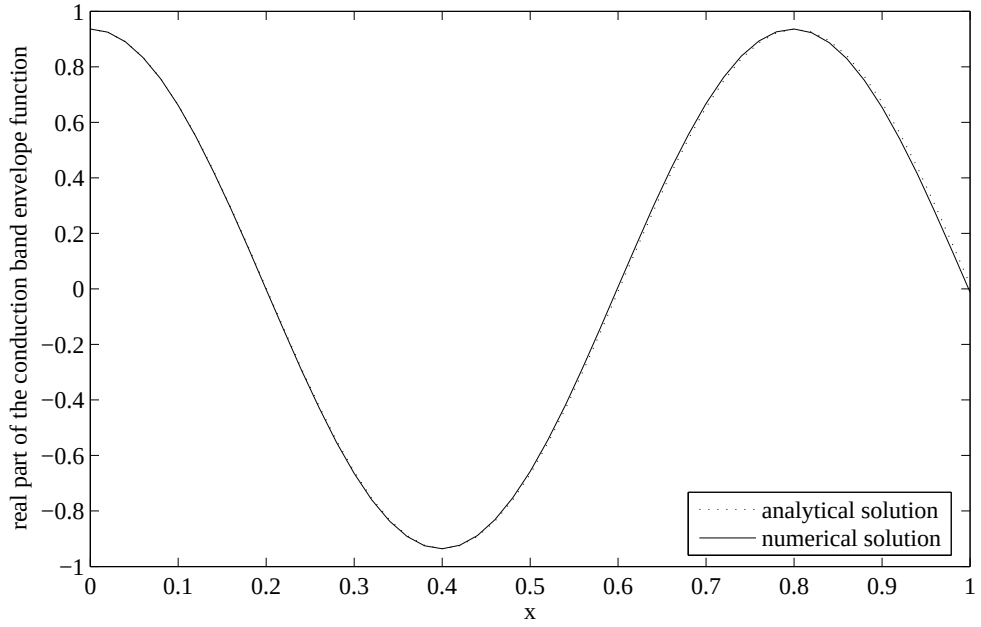

(b) Real part of the conduction band of the analytical and numerical solutions.

Figure 5.2: Comparison of the analytical solution (dotted line) and the numerical solution (solid line) for a step size $h = 1/50$ and an energy $E = 1500$.

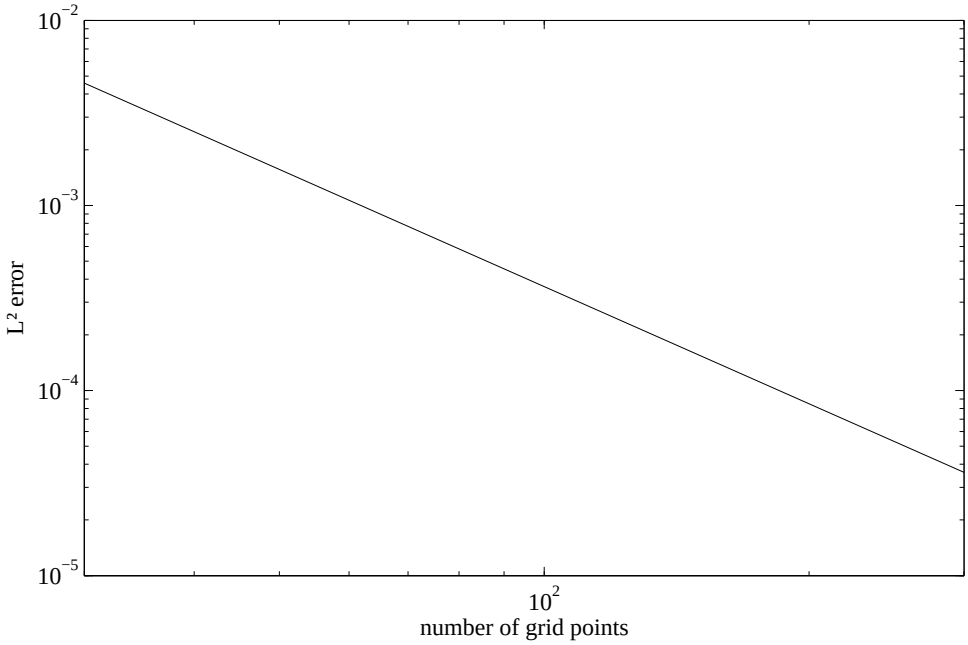

Figure 5.3: L^2-error of the numerical solution for an energy $E = 1500$.

Thus, in each domain the envelope function takes the form

$$\mathbf{F}(x) = \sum_{l=1}^{n} \hat{a}_l \hat{\mathbf{F}}(\hat{k}_l^+) e^{\mathrm{i}\hat{k}_l^+ x} + \sum_{l=1}^{d-n} \check{a}_l \hat{\mathbf{F}}(\check{k}_l^+) e^{\mathrm{i}\check{k}_l^+ x} + \sum_{l=1}^{n} \hat{b}_l \hat{\mathbf{F}}(\hat{k}_l^-) e^{\mathrm{i}\hat{k}_l^- x} + \sum_{l=1}^{d-n} \check{b}_l \hat{\mathbf{F}}(\check{k}_l^-) e^{\mathrm{i}\check{k}_l^- x},$$

with the coefficients $\hat{a}_p, \check{a}_q, \hat{b}_p, \check{b}_q \in \mathbb{C}$, with $p = 1, \ldots, n$ and $q = 1, \ldots, d-n$. Here we used the notation of wave vectors and amplitudes we introduced in Sec. 5.2. Note that the amplitudes are of norm 1. In the sequel we will add a subscript A or B to the amplitudes and wave vectors in order to indicate which domain they belong to.

We consider a unitary superposition of all right-traveling envelope functions in A that enters the semiconductor at $x = 0$. Again we shall multiply these n incoming envelope waves with the coefficients $\omega_1, \ldots, \omega_n$. At $x = x_1$ this superposition of envelope functions is partly reflected. On the other hand, we expect a superposition of transmitted envelope functions in the domain $[x_2, L]$ that leaves the semiconductor at $x = L$. Thus, the envelope function reads

$$\mathbf{F}(x) = \begin{cases} \mathbf{F}_{A_1}(x) & \text{if } x \in [0, x_1), \\ \mathbf{F}_B(x) & \text{if } x \in [x_1, x_2), \\ \mathbf{F}_{A_2}(x) & \text{if } x \in [x_2, L], \end{cases} \tag{5.48}$$

with

$$\begin{aligned}
\mathbf{F}_{A_1}(x) &= \sum_{l=1}^{n} \omega_l \hat{\mathbf{F}}_A(\hat{k}_{A,l}^+) e^{\mathrm{i}\hat{k}_{A,l}^+ x} + \sum_{l=1}^{n} \hat{r}_l \hat{\mathbf{F}}_A(\hat{k}_{A,l}^-) e^{\mathrm{i}\hat{k}_{A,l}^- x} + \sum_{l=1}^{d-n} \check{r}_l \hat{\mathbf{F}}_A(\check{k}_{A,l}^-) e^{\mathrm{i}\check{k}_{A,l}^- x}, \\
\mathbf{F}_B(x) &= \sum_{l=1}^{n} \hat{a}_l \hat{\mathbf{F}}_B(\hat{k}_{B,l}^+) e^{\mathrm{i}\hat{k}_{B,l}^+ x} + \sum_{l=1}^{d-n} \check{a}_l \hat{\mathbf{F}}_B(\check{k}_{B,l}^+) e^{\mathrm{i}\check{k}_{B,l}^+ x} \\
&\quad + \sum_{l=1}^{n} \hat{b}_l \hat{\mathbf{F}}_B(\hat{k}_{B,l}^-) e^{\mathrm{i}\hat{k}_{B,l}^- x} + \sum_{l=1}^{d-n} \check{b}_l \hat{\mathbf{F}}_B(\check{k}_{B,l}^-) e^{\mathrm{i}\check{k}_{B,l}^- x}, \\
\mathbf{F}_{A_2}(x) &= \sum_{l=1}^{n} \hat{t}_l \hat{\mathbf{F}}_A(\hat{k}_{A,l}^+) e^{\mathrm{i}\hat{k}_{A,l}^+ x} + \sum_{l=1}^{d-n} \check{t}_l \hat{\mathbf{F}}_A(\check{k}_{A,l}^+) e^{\mathrm{i}\check{k}_{A,l}^+ x}.
\end{aligned}$$

We know that the solution (5.48) and its derivative are continuous, cf. [24]. In particular they are continuous at $x = x_1$ and $x = x_2$. Hence, we get a system of $4d$ linear equations for the $4d$ unknown coefficients $\hat{r}_p, \check{r}_q, \hat{a}_p, \check{a}_q, \hat{b}_p, \check{b}_q, \hat{t}_p, \check{t}_q \in \mathbb{C}$, with $p = 1, \ldots, n$ and $q = 1, \ldots, d-n$. We have

$$\mathbf{Q}\mathbf{c} = \mathbf{s},$$

with $\mathbf{c}, \mathbf{s} \in \mathbb{C}^{4d}$ given by

$$\mathbf{c} = \left(\hat{r}_1, \ldots, \hat{r}_n, \check{r}_1, \ldots, \check{r}_{d-n}, \hat{a}_1, \ldots, \hat{a}_n, \check{a}_1, \ldots, \check{a}_{d-n}, \hat{b}_1, \ldots, \hat{b}_n, \check{b}_1, \ldots, \check{b}_{d-n}, \hat{t}_1, \ldots, \hat{t}_n, \check{t}_1, \ldots, \check{t}_{d-n}\right)^{\mathrm{T}}$$

and

$$\mathbf{s} = \begin{pmatrix} -\sum_{l=1}^{n} \omega_l \hat{\mathbf{F}}_A(\hat{k}^+_{A,l}) e^{\mathrm{i}\hat{k}^+_{A,l}x_1} \\ \mathbf{0} \\ -\sum_{l=1}^{n} \mathrm{i}\hat{k}^+_{A,l}\omega_l \hat{\mathbf{F}}_A(\hat{k}^+_{A,l}) e^{\mathrm{i}\hat{k}^+_{A,l}x_1} \\ \mathbf{0} \end{pmatrix},$$

and the coefficient matrix

$$\mathbf{Q} = \begin{pmatrix} \mathbf{Q}_{\hat{r}} & \mathbf{Q}_{\check{r}} & \mathbf{Q}_{\hat{a}} & \mathbf{Q}_{\check{a}} & \mathbf{Q}_{\hat{b}} & \mathbf{Q}_{\check{b}} & \mathbf{Q}_{\hat{t}} & \mathbf{Q}_{\check{t}} \end{pmatrix} \in \mathbb{C}^{4d\times 4d},$$

with

$$\mathbf{Q}_{\hat{r}} = \begin{pmatrix} \hat{\mathbf{F}}_A(\hat{k}^-_{A,1}) e^{\mathrm{i}\hat{k}^-_{A,1}x_1} & \cdots & \hat{\mathbf{F}}_A(\hat{k}^-_{A,n}) e^{\mathrm{i}\hat{k}^-_{A,n}x_1} \\ \mathbf{0} & \cdots & \mathbf{0} \\ \mathrm{i}\hat{k}^-_{A,1}\hat{\mathbf{F}}_A(\hat{k}^-_{A,1}) e^{\mathrm{i}\hat{k}^-_{A,1}x_1} & \cdots & \mathrm{i}\hat{k}^-_{A,n}\hat{\mathbf{F}}_A(\hat{k}^-_{A,n}) e^{\mathrm{i}\hat{k}^-_{A,n}x_1} \\ \mathbf{0} & \cdots & \mathbf{0} \end{pmatrix} \in \mathbb{C}^{4d\times n},$$

$$\mathbf{Q}_{\check{r}} = \begin{pmatrix} \hat{\mathbf{F}}_A(\check{k}^-_{A,1}) e^{\mathrm{i}\check{k}^-_{A,1}x_1} & \cdots & \hat{\mathbf{F}}_A(\check{k}^-_{A,d-n}) e^{\mathrm{i}\check{k}^-_{A,d-n}x_1} \\ \mathbf{0} & \cdots & \mathbf{0} \\ \mathrm{i}\check{k}^-_{A,1}\hat{\mathbf{F}}_A(\check{k}^-_{A,1}) e^{\mathrm{i}\check{k}^-_{A,1}x_1} & \cdots & \mathrm{i}\check{k}^-_{A,d-n}\hat{\mathbf{F}}_A(\check{k}^-_{A,d-n}) e^{\mathrm{i}\check{k}^-_{A,d-n}x_1} \\ \mathbf{0} & \cdots & \mathbf{0} \end{pmatrix} \in \mathbb{C}^{4d\times (d-n)},$$

$$\mathbf{Q}_{\hat{a}} = \begin{pmatrix} -\hat{\mathbf{F}}_B(\hat{k}^+_{B,1}) e^{\mathrm{i}\hat{k}^+_{B,1}x_1} & \cdots & -\hat{\mathbf{F}}_B(\hat{k}^+_{B,n}) e^{\mathrm{i}\hat{k}^+_{B,n}x_1} \\ \hat{\mathbf{F}}_B(\hat{k}^+_{B,1}) e^{\mathrm{i}\hat{k}^+_{B,1}x_2} & \cdots & \hat{\mathbf{F}}_B(\hat{k}^+_{B,n}) e^{\mathrm{i}\hat{k}^+_{B,n}x_2} \\ -\mathrm{i}\hat{k}^+_{B,1}\hat{\mathbf{F}}_B(\hat{k}^+_{B,1}) e^{\mathrm{i}\hat{k}^+_{B,1}x_1} & \cdots & -\mathrm{i}\hat{k}^+_{B,n}\hat{\mathbf{F}}_B(\hat{k}^+_{B,n}) e^{\mathrm{i}\hat{k}^+_{B,n}x_1} \\ \mathrm{i}\hat{k}^+_{B,1}\hat{\mathbf{F}}_B(\hat{k}^+_{B,1}) e^{\mathrm{i}\hat{k}^+_{B,1}x_2} & \cdots & \mathrm{i}\hat{k}^+_{B,n}\hat{\mathbf{F}}_B(\hat{k}^+_{B,n}) e^{\mathrm{i}\hat{k}^+_{B,n}x_2} \end{pmatrix} \in \mathbb{C}^{4d\times n},$$

$$\mathbf{Q}_{\check{a}} = \begin{pmatrix} -\hat{\mathbf{F}}_B(\check{k}^+_{B,1}) e^{\mathrm{i}\check{k}^+_{B,1}x_1} & \cdots & -\hat{\mathbf{F}}_B(\check{k}^+_{B,d-n}) e^{\mathrm{i}\check{k}^+_{B,d-n}x_1} \\ \hat{\mathbf{F}}_B(\check{k}^+_{B,1}) e^{\mathrm{i}\check{k}^+_{B,1}x_2} & \cdots & \hat{\mathbf{F}}_B(\check{k}^+_{B,d-n}) e^{\mathrm{i}\check{k}^+_{B,d-n}x_2} \\ -\mathrm{i}\check{k}^+_{B,1}\hat{\mathbf{F}}_B(\check{k}^+_{B,1}) e^{\mathrm{i}\check{k}^+_{B,1}x_1} & \cdots & -\mathrm{i}\check{k}^+_{B,d-n}\hat{\mathbf{F}}_B(\check{k}^+_{B,d-n}) e^{\mathrm{i}\check{k}^+_{B,d-n}x_1} \\ \mathrm{i}\check{k}^+_{B,1}\hat{\mathbf{F}}_B(\check{k}^+_{B,1}) e^{\mathrm{i}\check{k}^+_{B,1}x_2} & \cdots & \mathrm{i}\check{k}^+_{B,d-n}\hat{\mathbf{F}}_B(\check{k}^+_{B,d-n}) e^{\mathrm{i}\check{k}^+_{B,d-n}x_2} \end{pmatrix} \in \mathbb{C}^{4d\times (d-n)},$$

$$\mathbf{Q}_{\hat{b}} = \begin{pmatrix} -\hat{\mathbf{F}}_B(\hat{k}^-_{B,1}) e^{\mathrm{i}\hat{k}^-_{B,1}x_1} & \cdots & -\hat{\mathbf{F}}_B(\hat{k}^-_{B,n}) e^{\mathrm{i}\hat{k}^-_{B,n}x_1} \\ \hat{\mathbf{F}}_B(\hat{k}^-_{B,1}) e^{\mathrm{i}\hat{k}^-_{B,1}x_2} & \cdots & \hat{\mathbf{F}}_B(\hat{k}^-_{B,n}) e^{\mathrm{i}\hat{k}^-_{B,n}x_2} \\ -\mathrm{i}\hat{k}^-_{B,1}\hat{\mathbf{F}}_B(\hat{k}^-_{B,1}) e^{\mathrm{i}\hat{k}^-_{B,1}x_1} & \cdots & -\mathrm{i}\hat{k}^-_{B,n}\hat{\mathbf{F}}_B(\hat{k}^-_{B,n}) e^{\mathrm{i}\hat{k}^-_{B,n}x_1} \\ \mathrm{i}\hat{k}^-_{B,1}\hat{\mathbf{F}}_B(\hat{k}^-_{B,1}) e^{\mathrm{i}\hat{k}^-_{B,1}x_2} & \cdots & \mathrm{i}\hat{k}^-_{B,n}\hat{\mathbf{F}}_B(\hat{k}^-_{B,n}) e^{\mathrm{i}\hat{k}^-_{B,n}x_2} \end{pmatrix} \in \mathbb{C}^{4d\times n},$$

$$\mathbf{Q}_{\check{b}} = \begin{pmatrix} -\hat{\mathbf{F}}_B(\check{k}^-_{B,1})e^{\mathrm{i}\check{k}^-_{B,1}x_1} & \cdots & -\hat{\mathbf{F}}_B(\check{k}^-_{B,d-n})e^{\mathrm{i}\check{k}^-_{B,d-n}x_1} \\ \hat{\mathbf{F}}_B(\check{k}^-_{B,1})e^{\mathrm{i}\check{k}^-_{B,1}x_2} & \cdots & \hat{\mathbf{F}}_B(\check{k}^-_{B,d-n})e^{\mathrm{i}\check{k}^-_{B,d-n}x_2} \\ -\mathrm{i}\check{k}^-_{B,1}\hat{\mathbf{F}}_B(\check{k}^-_{B,1})e^{\mathrm{i}\check{k}^-_{B,1}x_1} & \cdots & -\mathrm{i}\check{k}^-_{B,d-n}\hat{\mathbf{F}}_B(\check{k}^-_{B,d-n})e^{\mathrm{i}\check{k}^-_{B,d-n}x_1} \\ \mathrm{i}\check{k}^-_{B,1}\hat{\mathbf{F}}_B(\check{k}^-_{B,1})e^{\mathrm{i}\check{k}^-_{B,1}x_2} & \cdots & \mathrm{i}\check{k}^-_{B,d-n}\hat{\mathbf{F}}_B(\check{k}^-_{B,d-n})e^{\mathrm{i}\check{k}^-_{B,d-n}x_2} \end{pmatrix} \in \mathbb{C}^{4d\times(d-n)},$$

$$\mathbf{Q}_{\hat{t}} = \begin{pmatrix} \mathbf{0} & \cdots & \mathbf{0} \\ \hat{\mathbf{F}}_A(\hat{k}^+_{A,1})e^{\mathrm{i}\hat{k}^+_{A,1}x_2} & \cdots & \hat{\mathbf{F}}_A(\hat{k}^+_{A,n})e^{\mathrm{i}\hat{k}^+_{A,n}x_2} \\ \mathbf{0} & \cdots & \mathbf{0} \\ \mathrm{i}\hat{k}^+_{A,1}\hat{\mathbf{F}}_A(\hat{k}^+_{A,1})e^{\mathrm{i}\hat{k}^+_{A,1}x_2} & \cdots & \mathrm{i}\hat{k}^+_{A,n}\hat{\mathbf{F}}_A(\hat{k}^+_{A,n})e^{\mathrm{i}\hat{k}^+_{A,n}x_2} \end{pmatrix} \in \mathbb{C}^{4d\times n},$$

$$\mathbf{Q}_{\check{t}} = \begin{pmatrix} \mathbf{0} & \cdots & \mathbf{0} \\ -\hat{\mathbf{F}}_A(\check{k}^+_{A,1})e^{\mathrm{i}\check{k}^+_{A,1}x_2} & \cdots & -\hat{\mathbf{F}}_A(\check{k}^+_{A,d-n})e^{\mathrm{i}\check{k}^+_{A,d-n}x_2} \\ \mathbf{0} & \cdots & \mathbf{0} \\ -\mathrm{i}\check{k}^+_{A,1}\hat{\mathbf{F}}_A(\check{k}^+_{A,1})e^{\mathrm{i}\check{k}^+_{A,1}x_2} & \cdots & -\mathrm{i}\check{k}^+_{A,d-n}\hat{\mathbf{F}}_A(\check{k}^+_{A,d-n})e^{\mathrm{i}\check{k}^+_{A,d-n}x_2} \end{pmatrix} \in \mathbb{C}^{4d\times(d-n)}.$$

Analogously to the single barrier problems in the previous chapters, we do not prove mathematically that the matrix $\mathbf{Q}$ is regular. Instead we shall again point out that a singular matrix $\mathbf{Q}$ implies that the homogeneous case of the system of linear equations has a nonzero solution. Thus, there can exist envelope waves inside the computational domain without the existence of an incoming envelope wave which is a physical contradiction. We note that in our particular example the matrix $\mathbf{Q}$ is in fact regular and hence, the unknown coefficients $\hat{r}_p$, $\check{r}_q$, $\hat{a}_p$, $\check{a}_q$, $\hat{b}_p$, $\check{b}_q$, $\hat{t}_p$, $\check{t}_q$, with $p = 1, \ldots, n$ and $q = 1, \ldots, d-n$ are defined uniquely.

5.5.2.1 Numerical Solutions of the Envelope Functions

In this section we compare the analytical and numerical solutions of the quantum well structure. Fig. 5.4 shows the norms and phases of the analytical and numerical solutions as well as a schematic view of the band edge profile.

As expected, we do not observe any spurious oscillations. Fig. 5.1(b) illustrates that for the chosen energy $E = 1500$ there exists a unique positive discrete wave vector in $[0, \pi/h]$. However, we observe a small phase error. This error decreases for smaller step sizes.

5.5.2.2 The Transmission Coefficient

Now we examine the transmission coefficient of the quantum well structure introduced above. In Fig. 5.5 the analytical and numerical transmission coefficients are plotted against the energy E. As before, the step size $h = 1/150$ is used. Since the curve of the numerical transmission coefficient coincides with the curve of the analytical transmission coefficient for the used level of detail in Fig. 5.5(a), only the analytical transmission coefficient is plotted. We observe that the qualitative behavior of the transmission coefficient of this particular quantum well structure is similar to the behavior of the transmission coefficient of the single barrier examples in the previous chapters. Note that the first resonance is located at $E \approx 1856$.

5.5.2.3 The L^2-Error

Finally, we want to investigate the discrete L^2-error of the numerical scheme. Recall that we have to solve the optimization problem (5.47). Fig. 5.6 shows the discrete L^2-error of the numerical scheme applied to the quantum well structure. In the free scattering state example

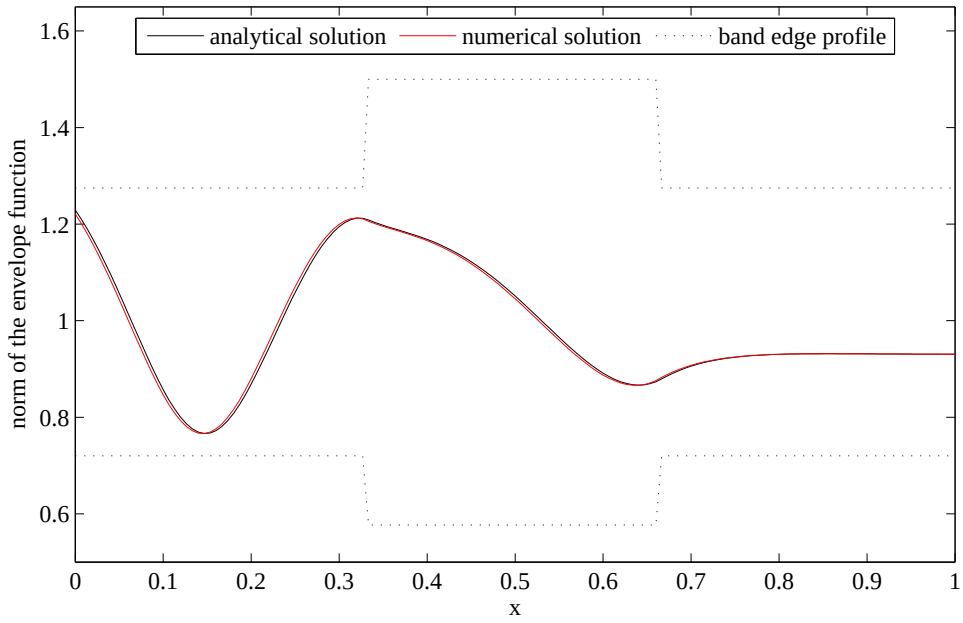

(a) Norm of the analytical and numerical solutions.

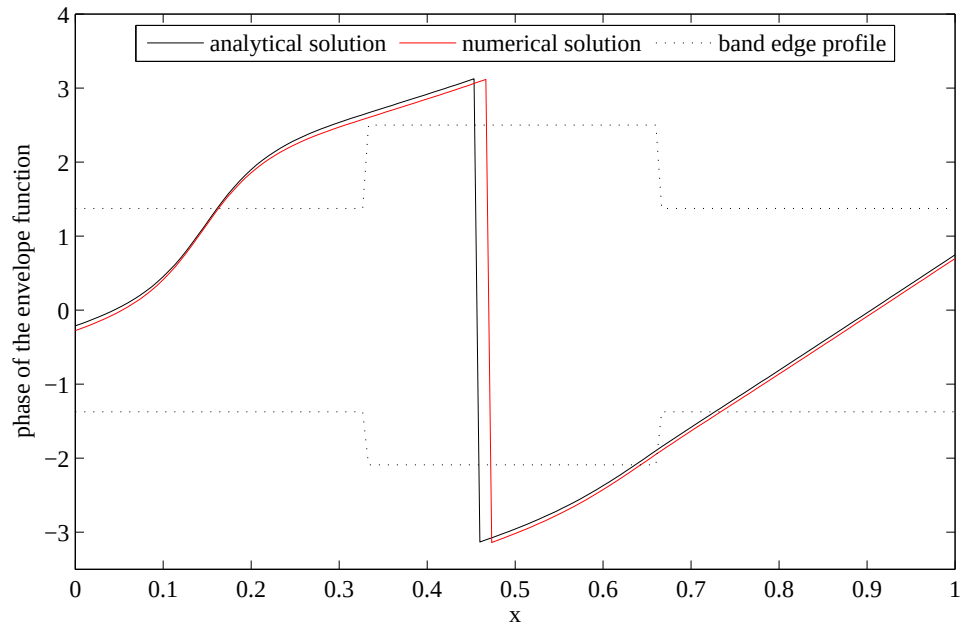

(b) Phases of the analytical and numerical solutions.

Figure 5.4: Comparison of the analytical solution (black) and the numerical solution (red) of the quantum well structure for a step size $h = 1/150$, an energy $E = 1500$. The dotted line indicates schematically the band end profile.

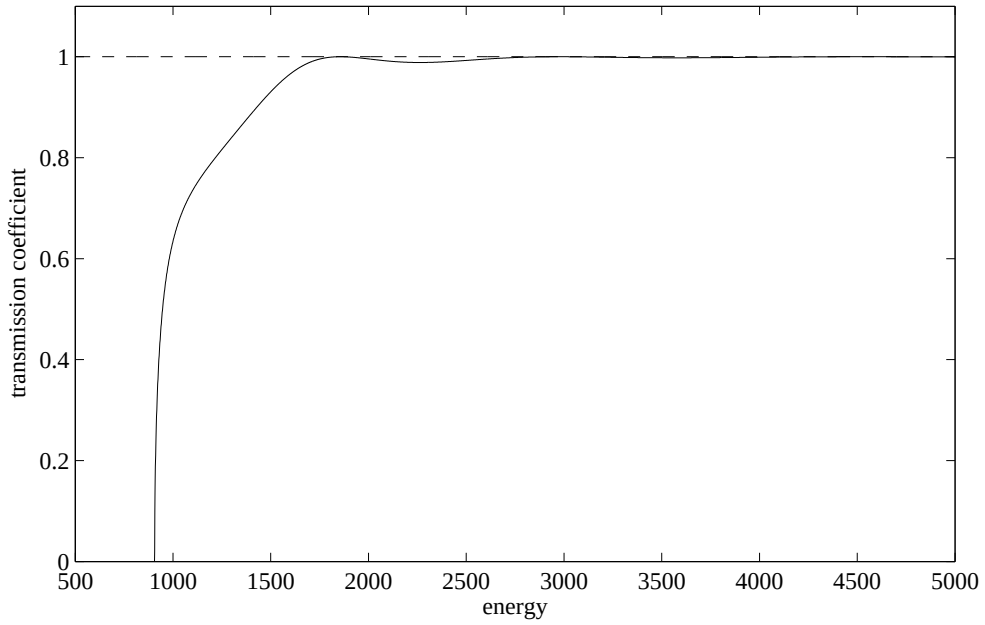

(a) Analytical transmission coefficient.

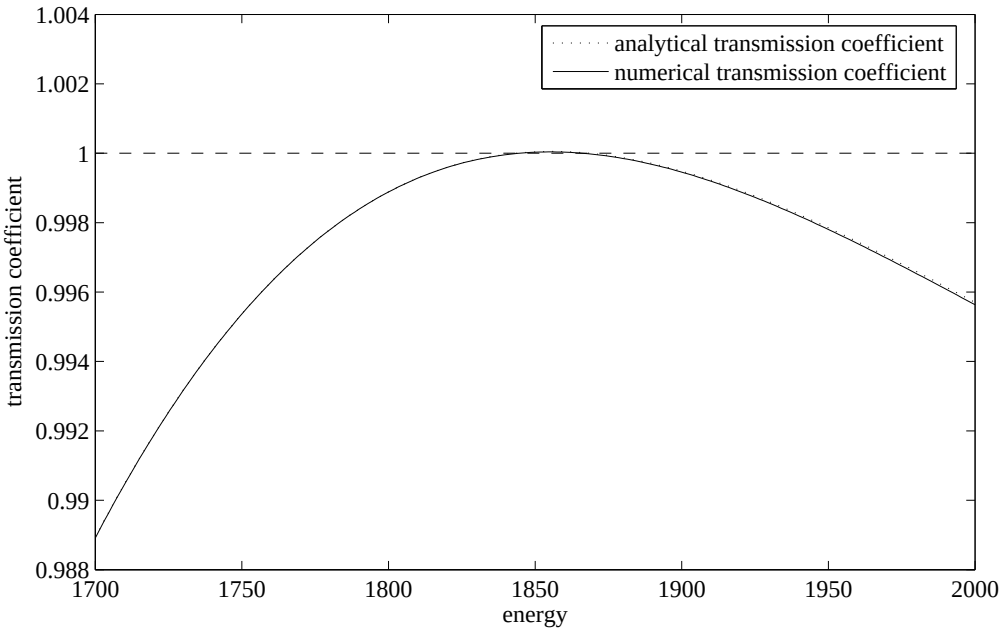

(b) Analytical (dotted line) and numerical (solid line) transmission coefficients near the first resonance at $E \approx 1856$.

Figure 5.5: Analytical and numerical transmission coefficients of the quantum well structure for a step size $h = 1/150$.

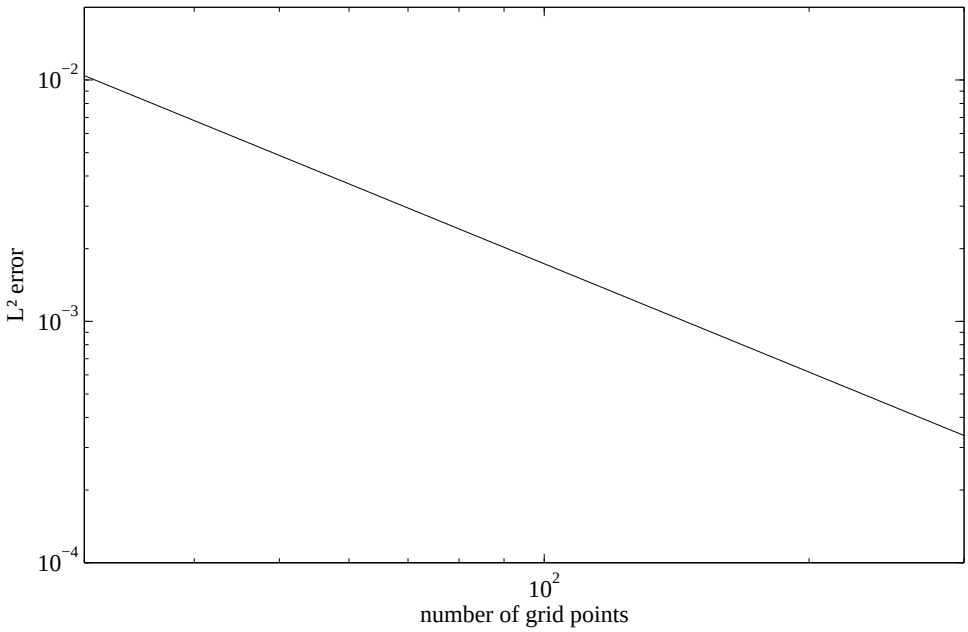

Figure 5.6: L^2-error of the numerical solution of the quantum well structure for an energy $E = 1500$.

the L^2-error decayed like $\mathcal{O}(h^2)$, which confirmed the formal order of the numerical scheme. In the quantum well example, however, the numerical scheme turns out be of order one only. This observation corresponds to the discrete L^2-error of the two-band $\mathbf{k} \cdot \mathbf{p}$-model in the previous chapter. We showed that any numerical scheme only converges in $\mathcal{O}(h)$ if the band edges are not continuous.

5.6 Summary

We introduced the general d-band $\mathbf{k} \cdot \mathbf{p}$-model and analyzed the exterior problem. Numerical evidence showed that the wave vectors of the general $\mathbf{k} \cdot \mathbf{p}$-model can be split into real and complex-valued wave vectors, while the number of positive wave vectors is equal to the number of negative wave vectors and the number of wave vectors with positive imaginary part is equal to the number of wave vectors with negative imaginary part. A general proof of this splitting theorem has not been found and is subject to future work. With the help of the splitting theorem we derived the TBCs of the general $\mathbf{k} \cdot \mathbf{p}$-model.

We used the the standard and centered FDS to transform the continuous problem into a problem on the discrete level. After analyzing the discrete exterior problem and stating the discrete analogon of the splitting theorem, we developed the DTBCs of the general $\mathbf{k} \cdot \mathbf{p}$-model.

A physically realistic example of an eight-band unstrained $\mathbf{k} \cdot \mathbf{p}$-model with $\mathbf{k}_{||}$ was presented. The numerical results were compared with the analytical solutions of the free scattering state and a quantum well structure. It turned out that the numerical scheme when applied to an example with discontinuous band edges is at most of order one.

Chapter 6

Conclusions and Perspectives

We derived DTBCs for stationary multiband effective mass approximations. To do this, we first solved the continuous exterior problem and derived elementary solutions in the exterior domains and defined the TBCs. After discretizing the underlaying BVP and solving the discrete exterior problem, we used the discrete elementary solutions in the exterior domains to derive DTBCs. This fully discrete approach results in reflection-free boundary conditions, while an ad-hoc discretization of the TBCs leads to spurious oscillations of the numerical solution. We tested the numerical schemes and the DTBCs in examples for which an analytical solution can be derived, i.e. for semiconductor nanostructures with piecewise constant band edges.

We extended the study of DTBCs for the scalar Schrödinger equation, i.e. the single-band effective mass approximation, by advanced FDSs, such as the Numerov FDS and the Mickens FDS. We showed the existence and uniqueness of the numerical solutions of the introduced FDSs and their respective DTBCs.

The two-band Kane-model and the two-band $\mathbf{k}\cdot\mathbf{p}$-model with inter-band coupling were introduced as particular examples of multiband effective mass approximations. The discretization of the Kane-model with the help of the centered FDS led to spurious oscillations when applied to non-constant band edges due to a non-injective discrete dispersion relation. We introduced the so-called symmetrized FDS that prevents this error and gives reasonable results for the two-band Kane-model. For the two-band $\mathbf{k}\cdot\mathbf{p}$-model, which is basically the Kane-model with added Laplace-operator, we showed the existence of a so-called energy window of the centered FDS. For all energies inside this window the centered FDS does not yield spurious oscillations as observed for the Kane-model. We showed that the discrete L^2-error of the combined standard and centered FDS, that is formally of order two, decays at most like $\mathcal{O}(h)$ when applied to discontinuous band edges. Therefore, it implies no numerical advantage compared to the combined standard and symmetrized FDS which is formally and numerically of order one.

Finally, we introduced the general d-band $\mathbf{k}\cdot\mathbf{p}$-model. The analysis of the exterior problem gave rise to a splitting theorem that was confirmed numerically. A mathematical proof of the general case of the splitting theorem and its discrete analogon has not been found and will be a topic of future research. We developed the TBCs and the DTBCs of the general $\mathbf{k}\cdot\mathbf{p}$-model and pointed out that they depend on the choice of the elementary solutions in the exterior domain. Since there might exist more than one right-traveling solution in the left exterior domain we have to define coefficients that weight the incoming envelope waves.

The numerical solutions of all multiband examples we examined were unique. However, a general proof of the existence and uniqueness of the analytical and numerical solutions of multiband models needs to be investigated. Note that a general proof of the existence and uniqueness of the analytical solution of the Kane-model is presented.

Another topic of future research is the comparison of the introduced methods to solve multiband effective mass approximations numerically with other methods, such as the transfer matrix method, [36] and [37], as well as the R-matrix method, [42]. In particular, a comparison of these methods is of interest when the analytical solution cannot be derived, such as a quantum

barrier structure with added bias.

Simulations of quantum cascade lasers are currently an extensively discussed topic, [10]. The current density and the optical gain of quantum cascade lasers can be computed when the envelope functions are known. Based on the DTBCs for multiband effective mass approximations, developed in this thesis, we plan to perform a fully discrete analysis of these simulations compared to the approach in [32], where an ad-hoc discretization of the TBCs was used.

Chapter A

Appendix

A.1 Proof that the weak formulation of the two-band k·p-Model can be written in terms of a coercive, sesquilinear and anti-linear form

Before we start to show that the weak formulation of the two-band $\mathbf{k}\cdot\mathbf{p}$-Model can be expressed in terms of a coercive, sesquilinear and anti-linear form, we note that the vector $\mathbf{F}$ of the envelope functions is in the space $\left(L^2(0,L)\right)^2$ with the scalar product

$$\langle \mathbf{F}, \mathbf{G}\rangle = \int_0^1 \mathbf{F}(x)\cdot\mathbf{G}(x)\mathrm{d}x, \qquad \mathbf{F},\mathbf{G}\in\left(L^2(0,L)\right)^2,$$

where the product $\mathbf{F}(x)\cdot\mathbf{G}(x)$ is the standard Hermitian scalar product on $\mathbb{C}^2$ given by

$$\mathbf{F}(x)\cdot\mathbf{G}(x) = F_\mathrm{c}(x)\overline{G_\mathrm{c}(x)} + F_\mathrm{v}(x)\overline{G_\mathrm{v}(x)}.$$

The two-band $\mathbf{k}\cdot\mathbf{p}$-model with inter-band coupling reads

$$\mathbf{HF} = E\mathbf{F}, \tag{A.1}$$

with

$$\mathbf{H} = \begin{pmatrix} -\epsilon\frac{\mathrm{d}^2}{\mathrm{d}x^2} + E_\mathrm{c}(x) & -\mathrm{i}P_0(x)\frac{\mathrm{d}}{\mathrm{d}x} \\ -\mathrm{i}P_0(x)\frac{\mathrm{d}}{\mathrm{d}x} & \epsilon\frac{\mathrm{d}^2}{\mathrm{d}x^2} + E_\mathrm{c}(x) - E_\mathrm{g}(x)\end{pmatrix},$$

cf. Eq. (4.3). In the sequel we will assume that P_0 is constant.

We multiply Eq. (A.1) by an arbitrary function $\mathbf{G}\in\left(L^2(0,L)\right)^2$ and integrate over $(0,L)$ to get

$$\begin{aligned}\int_0^L E\mathbf{F}(x)\cdot\mathbf{G}(x)\mathrm{d}x = &\int_0^L \epsilon\begin{pmatrix}-1 & 0\\ 0 & 1\end{pmatrix}\frac{\mathrm{d}^2}{\mathrm{d}x^2}\mathbf{F}(x)\cdot\mathbf{G}(x)\mathrm{d}x\\ &-\mathrm{i}P_0\int_0^L\begin{pmatrix}0 & 1\\ 1 & 0\end{pmatrix}\frac{\mathrm{d}}{\mathrm{d}x}\mathbf{F}(x)\cdot\mathbf{G}(x)\mathrm{d}x\\ &+\int_0^L\begin{pmatrix}-E_\mathrm{c}(x) & 0\\ 0 & E_\mathrm{c}(x)-E_\mathrm{g}(x)\end{pmatrix}\mathbf{F}(x)\cdot\mathbf{G}(x)\mathrm{d}x.\end{aligned}$$

Integrating by parts gives

$$\begin{aligned}0 =&\epsilon\int_0^L \frac{\mathrm{d}}{\mathrm{d}x}F_\mathrm{c}(x)\frac{\mathrm{d}}{\mathrm{d}x}\overline{G_\mathrm{c}}(x)\mathrm{d}x - \epsilon\frac{\mathrm{d}}{\mathrm{d}x}F_\mathrm{c}(L)\overline{G_\mathrm{c}}(L) + \epsilon\frac{\mathrm{d}}{\mathrm{d}x}F_\mathrm{c}(0)\overline{G_\mathrm{c}}(0)\\ &-\epsilon\int_0^L \frac{\mathrm{d}}{\mathrm{d}x}F_\mathrm{v}(x)\frac{\mathrm{d}}{\mathrm{d}x}\overline{G_\mathrm{v}}(x)\mathrm{d}x + \epsilon\frac{\mathrm{d}}{\mathrm{d}x}F_\mathrm{v}(L)\overline{G_\mathrm{v}}(L) - \epsilon\frac{\mathrm{d}}{\mathrm{d}x}F_\mathrm{v}(0)\overline{G_\mathrm{v}}(0)\\ &-\mathrm{i}P_0\left(\int_0^L \frac{\mathrm{d}}{\mathrm{d}x}F_\mathrm{v}(x)\overline{G_\mathrm{c}}(x) + F_\mathrm{c}(x)\frac{\mathrm{d}}{\mathrm{d}x}\overline{G_\mathrm{v}}(x)\mathrm{d}x + F_\mathrm{c}(L)\overline{G_\mathrm{v}}(L) - F_\mathrm{c}(0)\overline{G_\mathrm{v}}(0)\right)\\ &+\int_0^L \mathbf{F}(x)\cdot\mathbf{G}(x)\mathrm{d}x + \int_0^L \left(E_\mathrm{c}(x) - E - 1\right)\mathbf{F}(x)\cdot\mathbf{G}(x)\mathrm{d}x - \int_0^L E_\mathrm{g}(x)F_\mathrm{c}(x)\overline{G_\mathrm{c}}(x)\mathrm{d}x.\end{aligned} \tag{A.2}$$

Let us introduce

$$\mathbf{D} = \begin{pmatrix}1 & 0\\ 0 & -1\end{pmatrix}.$$

Then we find that

$$\epsilon\frac{\mathrm{d}}{\mathrm{d}x}F_\mathrm{c}(0)\overline{G_\mathrm{c}}(0) - \epsilon\frac{\mathrm{d}}{\mathrm{d}x}F_\mathrm{v}(0)\overline{G_\mathrm{v}}(0) = \epsilon\mathbf{D}\frac{\mathrm{d}}{\mathrm{d}x}\mathbf{F}(0)\cdot\mathbf{G}(0)$$

and

$$-\epsilon\frac{\mathrm{d}}{\mathrm{d}x}F_\mathrm{c}(L)\overline{G_\mathrm{c}}(L) + \epsilon\frac{\mathrm{d}}{\mathrm{d}x}F_\mathrm{v}(L)\overline{G_\mathrm{v}}(L) = -\epsilon\mathbf{D}\frac{\mathrm{d}}{\mathrm{d}x}\mathbf{F}(L)\cdot\mathbf{G}(L).$$

Now we can apply the TBCs (4.34) and (4.37) to Eq. (A.2) and obtain

$$C(\mathbf{F},\mathbf{G}) + S(\mathbf{F},\mathbf{G}) = A(\mathbf{G}), \tag{A.3}$$

with the coercive and sesquilinear form

$$C(\mathbf{F},\mathbf{G}) = \int_0^L \mathbf{F}(x)\cdot\mathbf{G}(x)\mathrm{d}x,$$

the sesquilinear form

$$\begin{aligned}S(\mathbf{F},\mathbf{G}) =&\epsilon\int_0^L \frac{\mathrm{d}}{\mathrm{d}x}F_\mathrm{c}(x)\frac{\mathrm{d}}{\mathrm{d}x}\overline{G_\mathrm{c}}(x)\mathrm{d}x - \epsilon\int_0^L \frac{\mathrm{d}}{\mathrm{d}x}F_\mathrm{v}(x)\frac{\mathrm{d}}{\mathrm{d}x}\overline{G_\mathrm{v}}(x)\mathrm{d}x\\ &+\epsilon\mathbf{D}\mathbf{P}_0\mathbf{K}_0\mathbf{P}_0^{-1}\mathbf{F}(0)\cdot\mathbf{G}(0) - \epsilon\mathbf{D}\mathbf{P}_L\mathbf{K}_L\mathbf{P}_L^{-1}\mathbf{F}(L)\cdot\mathbf{G}(L)\\ &-\mathrm{i}P_0\left(\int_0^L \frac{\mathrm{d}}{\mathrm{d}x}F_\mathrm{v}(x)\overline{G_\mathrm{c}}(x) + F_\mathrm{c}(x)\frac{\mathrm{d}}{\mathrm{d}x}\overline{G_\mathrm{v}}(x)\mathrm{d}x + F_\mathrm{c}(L)\overline{G_\mathrm{v}}(L) - F_\mathrm{c}(0)\overline{G_\mathrm{v}}(0)\right)\\ &+\int_0^L \left(E_\mathrm{c}(x) - E - 1\right)\mathbf{F}(x)\cdot\mathbf{G}(x)\mathrm{d}x - \int_0^L E_\mathrm{g}(x)F_\mathrm{c}(x)\overline{G_\mathrm{c}}(x)\mathrm{d}x,\end{aligned}$$

and the anti-linear form

$$A(\mathbf{G}) = -\epsilon\mathbf{D}\left(\mathrm{i}\hat{k}\mathbb{1} - \mathbf{P}_0\mathbf{K}_0\mathbf{P}_0^{-1}\right)\hat{\mathbf{F}}_0^{\mathrm{e/h}}(\hat{k}_0)\cdot\mathbf{G}(0).$$

According to the Riesz representation theorem, there exist compact operators R_C and R_S such that

$$C(\mathbf{F},\mathbf{G}) = \langle R_C\mathbf{F},\mathbf{G}\rangle,$$

and

$$S(\mathbf{F},\mathbf{G}) = \langle R_S\mathbf{F},\mathbf{G}\rangle.$$

Moreover, there exists a function a_L such that

$$A(\mathbf{G}) = \langle a_L,\mathbf{G}\rangle.$$

Then we can rewrite Eq. (A.3) in the form

$$(R_C + R_S)\,\mathbf{F} = a_L.$$

By applying the Fredholm alternative we can show that this expression has a unique solution if $R_C + R_S$ is injective. This is equivalent to show that the solution of

$$(R_C + R_S)\,\mathbf{F} = 0$$

is identically to zero. To do this, we set the $\mathbf{G} = \mathbf{F}$ and take the imaginary part of Eq. (A.3). By considering the identity

$$-\mathrm{i}P_0 \int_0^L \frac{\mathrm{d}}{\mathrm{d}x} F_\mathrm{v}(x)\overline{F_\mathrm{c}}(x) + F_\mathrm{c}(x)\frac{\mathrm{d}}{\mathrm{d}x}\overline{F_\mathrm{v}}(x)\mathrm{d}x = 2P_0 \int_0^L \mathrm{Im}\left(\frac{\mathrm{d}}{\mathrm{d}x} F_\mathrm{v}(x)\overline{F_\mathrm{c}}(x)\right)\mathrm{d}x \in \mathbb{R},$$

we obtain

$$\begin{aligned} 0 = \mathrm{Im}\left(\epsilon\mathbf{D}\mathbf{P}_0\mathbf{K}_0\mathbf{P}_0^{-1}\mathbf{F}(0)\cdot\mathbf{F}(0) - \epsilon\mathbf{D}\mathbf{P}_L\mathbf{K}_L\mathbf{P}_L^{-1}\mathbf{F}(L)\cdot\mathbf{F}(L)\right) \\ - P_0\,\mathrm{Re}\left(F_\mathrm{c}(L)\overline{F_\mathrm{v}}(L) - F_\mathrm{c}(0)\overline{F_\mathrm{v}}(0)\right), \end{aligned}$$

which implies

$$\begin{aligned} 0 = \mathrm{Re}\left(-\mathrm{i}\epsilon\mathbf{D}\mathbf{P}_0\mathbf{K}_0\mathbf{P}_0^{-1}\mathbf{F}(0)\cdot\mathbf{F}(0) + \mathrm{i}\epsilon\mathbf{D}\mathbf{P}_L\mathbf{K}_L\mathbf{P}_L^{-1}\mathbf{F}(L)\cdot\mathbf{F}(L)\right. \\ \left. + P_0\,\mathrm{Re}\left(\mathbf{A}\mathbf{F}(0)\cdot\mathbf{F}(0) - \mathbf{A}\mathbf{F}(L)\cdot\mathbf{F}(L)\right)\right), \end{aligned}$$

where $\mathbf{A}$ is given by

$$\mathbf{A} = \begin{pmatrix} 0 & 0 \\ 1 & 0 \end{pmatrix}.$$

Let us introduce

$$\mathbf{T}_0 = \mathrm{i}\mathbf{P}_0^\mathrm{T}\mathbf{D}\mathbf{P}_0\mathbf{K}_0 - P_0\mathbf{P}_0^\mathrm{T}\mathbf{A}\mathbf{P}_0$$

and

$$\mathbf{T}_L = \mathrm{i}\mathbf{P}_L^\mathrm{T}\mathbf{D}\mathbf{P}_L\mathbf{K}_L - P_L\mathbf{P}_L^\mathrm{T}\mathbf{A}\mathbf{P}_L.$$

Then we end up with the equation

$$0 = \mathrm{Re}\left(\mathbf{T}_L\mathbf{P}_L^{-1}\mathbf{F}(L)\cdot\mathbf{P}_L^{-1}\mathbf{F}(L) - \mathbf{T}_0\mathbf{P}_0^{-1}\mathbf{F}(0)\cdot\mathbf{P}_0^{-1}\mathbf{F}(0)\right). \tag{A.4}$$

In order to finish the proof and show the uniqueness of the solution one has to find a negative definite matrix $\mathbf{S}_0$ and a positive definite matrix $\mathbf{S}_L$ such that Eq. (A.4) can be written in the form

$$0 = \mathbf{S}_L\mathbf{P}_L^{-1}\mathbf{F}(L)\cdot\mathbf{P}_L^{-1}\mathbf{F}(L) - \mathbf{S}_0\mathbf{P}_0^{-1}\mathbf{F}(0)\cdot\mathbf{P}_0^{-1}\mathbf{F}(0).$$

This implies that $\mathbf{F}(0) = \mathbf{F}(L) = \mathbf{0}$ and hence, by applying the homogeneous TBCs we get $\frac{\mathrm{d}}{\mathrm{d}x}\mathbf{F}(0) = \frac{\mathrm{d}}{\mathrm{d}x}\mathbf{F}(L)\mathbf{0}$. Considering the Cauchy-Lipschitz theorem we showed that $\mathbf{F}$ vanishes everywhere.

Thus, it will be future work to investigate the existence of the matrices $\mathbf{S}_0$ and $\mathbf{S}_L$.

A.2 Proof of Thm. 5.1 for M = 0 and V diagonal

Before we start to prove Thm. 5.1 for $\mathbf{M} = \mathbf{0}$ and $\mathbf{V}$ diagonal we show

Proposition A.1. Let $\mathbf{P} \in \mathbb{C}^{n\times n}$ be regular with the real eigenvalues $p_1, \ldots, p_n \in \mathbb{R}$. Then the matrix

$$\mathbf{Q} = \begin{pmatrix} \mathbf{0} & \mathbb{1} \\ \mathbf{P} & \mathbf{0} \end{pmatrix} \in \mathbb{C}^{2n\times 2n}$$

is regular and its eigenvalues $q_1, \ldots, q_{2n} \in \mathbb{C}$ take the form

$$q_{2m-1} = \sqrt{p_m}, \quad q_{2m} = -\sqrt{p_m},$$

with $m = 1, \ldots, n$.

Proof. According to [39], the determinant of the block matrix

$$\mathbf{A} = \begin{pmatrix} \mathbf{A}_1 & \mathbf{A}_3 \\ \mathbf{A}_2 & \mathbf{A}_4 \end{pmatrix}$$

reads

$$\det \mathbf{A} = \det \left(\mathbf{A}_1 \mathbf{A}_4 - \mathbf{A}_2 \mathbf{A}_3 \right).$$

Hence, the characteristic polynomial of $\mathbf{Q}$ can be written in the form

$$0 = \det \begin{pmatrix} -q\mathbb{1} & \mathbb{1} \\ \mathbf{P} & -q\mathbb{1} \end{pmatrix} = \det \left(q^2\mathbb{1} - \mathbf{P} \right) = -\det \left(\mathbf{P} - q^2\mathbb{1} \right).$$

This implies that all eigenvalues q of $\mathbf{Q}$ satisfy

$$q^2 = p,$$

with some eigenvalue p of $\mathbf{P}$. Thus, the $2n$ eigenvalues of $\mathbf{Q}$ read

$$q_{2m-1} = \sqrt{p_m}, \quad q_{2m} = -\sqrt{p_m},$$

with $m = 1, \ldots, n$. □

If $\mathbf{M} = \mathbf{0}$ and $\mathbf{V} = \operatorname{diag}(v_1, \ldots, v_d)$ the matrix $\mathbf{A}^{-1}\mathbf{B}$ reduces to

$$\mathbf{A}^{-1}\mathbf{B} = \begin{pmatrix} \mathbf{0} & \mathbb{1} \\ \mathbf{N}^{-1}\left(\mathbf{V} - E\mathbb{1}\right) & \mathbf{0} \end{pmatrix}.$$

Since $\mathbf{N}$ and $\mathbf{V}$ are diagonal the eigenvalues of $\mathbf{N}^{-1}\left(\mathbf{V} - E\mathbb{1}\right)$ are

$$\nu_m = \frac{v_m - E}{n_m},$$

with $m = 1, \ldots, d$. Then the eigenvalues of $\mathbf{A}^{-1}\mathbf{B}$ take the form

$$\alpha_{2m-1} = \sqrt{\nu_m} = \sqrt{\frac{v_m - E}{n_m}}, \quad \alpha_{2m} = -\sqrt{\nu_m} = -\sqrt{\frac{v_m - E}{n_m}},$$

with $m = 1, \ldots, n$, cf. Prop. A.1. If $E > E_0^{\mathrm{e}} = \max\{v_1, \ldots, v_d\}$, then

$$\operatorname{sign} \nu_m = -\operatorname{sign} n_m,$$

for $m = 1, \ldots, d$. Hence, the number n of positive eigenvalues of $\mathbf{N}$ is equal to the number of complex conjugate pairs of eigenvalues of $\mathbf{A}^{-1}\mathbf{B}$ while the number of real eigenvalues is $2(d-n)$, with $d-n$ being positive and $d-n$ being negative.

On the other hand, if $E < E_0^{\mathrm{h}} = \min\{v_1, \ldots, v_d\}$, then

$$\operatorname{sign} \nu_m = \operatorname{sign} n_m,$$

for $m = 1, \ldots, d$. Thus, the number $d-n$ of negative eigenvalues of $\mathbf{N}$ is equal to the number of complex conjugate pairs of eigenvalues of $\mathbf{A}^{-1}\mathbf{B}$ while the number of real eigenvalues is $2n$, with n being positive and n being negative.

This finishes the proof of Thm. 5.1 for the case that $\mathbf{M} = \mathbf{0}$ and $\mathbf{V}$ is diagonal.

Bibliography

[1] X. Antoine, A. Arnold, C. Besse, M. Ehrhardt, A. Schädle, *A Review of Transparent and Artificial Boundary Conditions Techniques for Linear and Nonlinear Schrödinger Equations*, Commun. Comput. Phys. **4** (2008), 729–796.

[2] A. Arnold, M. Ehrhardt and I. Sofronov, *Discrete Transparent Boundary Conditions for the Schrödinger Equation: Fast calculation, approximation, and stability*, Commun. Math. Sci. **1** (2003), 501–556.

[3] A. Arnold, *Numerically Absorbing Boundary Conditions for Quantum Evolution Equations*, VLSI Design **6** (1998), 313–319.

[4] A. Arnold, *Mathematical concepts of open quantum boundary conditions*, Trans. Theory Stat. Phys. **30** (2001), 561–584.

[5] U. Bandelow, H.-Chr. Kaiser, Th. Koprucki and J. Rehberg, *Spectral properties of* $\mathbf{k} \cdot \mathbf{p}$ *Schrödinger operators in one space dimension*, Numer. Funct. Anal. Optimization **21** (2000), 379–409.

[6] M. Baro, *One-dimensional open Schrödinger-Poisson systems*, Ph.D. Thesis, Humboldt Universität Berlin, 2005.

[7] G. Bastard, *Wave Mechanics Applied to Semiconductor Heterostructures*, Hasted Press, 1988.

[8] N. Ben Abdallah, P. Degond and P. A. Markowich, *On a one-dimensional Schrödinger-Poisson scattering model*, ZAMP **48** (1997), 135–155.

[9] N. Ben Abdallah, J. Kefi-Ferhane, *Mathematical Analysis of the Two-Band Schrödinger Model* Math. Meth. Appl. Sci. **31** (2008), 1131–1151.

[10] S. Birner, T. Kubis, P. Vogl, *Simulation of quantum cascade lasers - optimizing laser performance*, Photonik International **2** (2008), 60–63.

[11] F. Bloch, *Über die Quantenmechanik der Electronen in Kristallgittern*, Z. Physik **52** (1932), 555-600.

[12] M. G. Burt, *The justification for applying the effective-mass approximation to microstructures*, J. Physics. Condens. Matter **4** (1992), 6651-6690.

[13] M. G. Burt, *Direct derivation of effective-mass equations for microstructures with atomically abrupt boundaries*, Physical Review B **50** (1994), 7518-7525.

[14] M. G. Burt, *Fundamentals of envelope function theory for electronic states and photonic modes in nanostructures*, J. Physics. Condens. Matter **11** (1998), 53-83.

[15] R. Chen, Z. Xu and L. Sun, *Finite-difference scheme to solve Schrödinger equations*, Phys. Review E **47** (1993), 3799–3802.

[16] M. Ehrhardt, *Discrete Artificial Boundary Conditions*, Ph.D. Thesis, Technische Universität Berlin, 2001.

[17] M. Ehrhardt and A. Arnold, *Discrete transparent boundary conditions for the Schrödinger equation*, Rivista di Matematica della Universit a di Parma **6** (2001), 57-108.

[18] S. N. Elaydi, *An Introduction to Difference Equations*, Springer, New York, 1996, 1st ed.

[19] P. Enders and M. Woerner, *Exact* 4×4 *block diagonalization of the eight-band* $\mathbf{k} \cdot \mathbf{p}$ *Hamiltonian matrix for the tetrahedral semiconductors and its application to strained quantum wells*, Semicond. Sci. Technol. **11** (1996), 983–988.

[20] B. A. Foreman, *Effective-mass Hamiltonian and boundary conditions for the valence bands of semiconductor microstructures*, Physical Review B **48** (1993), 4964-4967.

[21] G. Grawert, *Quantenmechanik*, Aula Verlag, Wiesbaden, 1989, 5th ed.

[22] E. O. Kane, *Energy Band Theory*, In W. Paul (ed.), Handbook on Semiconductors, **1**, 193–217. North-Holland, Amsterdam, New York, Oxford, 1982.

[23] J. Kefi, *Analyse mathématique et numérique de modèles quantiques pour les semiconducteurs*, Ph.D. Thesis, Université Toulouse III — Paul Sabatier, 2003.

[24] Th. Koprucki, *Zu* $\mathbf{k} \cdot \mathbf{p}$*-Schrödingeroperatoren*, Ph.D. Thesis, Freie Universität Berlin, 2008.

[25] Th. Koprucki, *Modeling of electronic states in semiconductor nanostructures*, Talk, Leipzig-Berlin-Seminar, Technische Universität Berlin, 2008.

[26] Th. Koprucki, H. C. Kaiser, J. Fuhrmann, *Electronic States in Semiconductor Nanostructures and Upscaling to Semi-Classical Models*, In A. Mielke (ed.), Analysis, Modeling and Simulation of Multiscale Problems, 365–394. Springer Verlag, Heidelberg, 2006.

[27] P. Matus, *Exact difference schemes for time-dependent problems*, Comput. Meth. Appl. Math. **5** (2005), 422–448.

[28] R. E. Mickens, *Difference Equations: Theory and Applications*, Van Nostrand Reinhold, New York, 1990, 2nd ed.

[29] R. E. Mickens, *Novel explicit finite-difference schemes for time–dependent Schrödinger equations*, Comput. Phys. Commun. **63** (1991), 203–208.

[30] R. E. Mickens and I. Ramadhani, *Finite-difference scheme for the numerical solution of the Schrödinger equation*, Phys. Review A **45** (1992), 2074–2075.

[31] R. E. Mickens, *A nonlinear nonstandard finite difference scheme for the linear time-dependent Schrödinger equation*, J. Diff. Eq. Appl. **12** (2006), 313–320.

[32] G. Milovanovic, O. Baumgartner and H. Kosina, *Simulation of Quantum Cascade Lasers using Robin Boundary Conditions*, 9th International Conference on Numerical Simulation of Optoelectronic Devices, Gwangju Institute of Science and Technology, 2009.

[33] C. A. Moyer, *Numerical solution of the stationary state Schrödinger Equation using discrete transparent boundary conditions*, Comput. Sci. Engin. **8** (2006), 32–40.

[34] B. V. Numerov, *A method of extrapolation of perturbations*, Monthly Notices of the Royal Astronomical Society **84** (1924), 592-601.

[35] A. Ostrowski and H. Schneider, *Some Theorems on the Inertia of General Matrices*, J. Math. Anal. Appl. **4** (1962), 72-84.

[36] R. Pérez-Alvarez and H. Rodriguez-Coppola, *Transfer matrix in 1D Schrödinger problems with constant and position-dependent mass*, Phys. Stat. Sol. (b) **145** (1988), 493–500.

[37] R. Pérez-Alvarez, H. Rodriguez-Coppola V. R. Velasco and F. Garcia-Moliner, *A study of the matching problem using transfer matrices*, J. Phys. C: Solid State Phys. **21** (1988), 2197–2206.

[38] F. Schmidt, P. Deuflhard, *Discrete Transparent Boundary Conditions for the Numerical Solution of Fresnel's Equation*, Comput. Math. Appl. **29** (1995), 53–76.

[39] J. R. Silvester, *Determinants of Block Matrices*, Math. Gaz. **501** (2000), 460–467.

[40] T. E. Simos and P.S. Williams, *On finite difference methods for the solution of the Schrödinger equation*, Computers & Chemistry **23** (1999), 513–554.

[41] W. Walter, *Gewöhnliche Differentialgleichungen*, Springer, Heidelberg, 2000, 7th ed.

[42] U. Wulf, J. Kucera, P. N. Racec and E. Sigmund, *Transport through quantum systems in the R-matrix formalism*, Phys. Rev. **58** (1998), 16209–16220.

[43] P. Y. Yu, M. Cardona, *Fundamentals of Semiconductors: Physics and Materials Properties*, Springer, Heidelberg, 2005, 3rd ed.

[44] A. Zisowsky, *Discrete Transparent Boundary Conditions for Systems of Evolution Equations*, Ph.D. Thesis, Technische Universität Berlin, 2003.

[45] A. Zisowsky and M. Ehrhardt, *Discrete Transparent Boundary Conditions for Parabolic Systems*, Math. Comput. Modelling **43** (2006), 294–309.

[46] A. Zisowsky, A. Arnold, M. Ehrhardt and Th. Koprucki, *Discrete Transparent Boundary Conditions for transient* $\mathbf{k} \cdot \mathbf{p}$*-Schrödinger Equations with Application to Quantum-Heterostructures*, J. Appl. Math. Mech. (ZAMM) **85** (2005), 793–805.

Erklärung

Hiermit erkläre ich, dass ich die vorliegende Arbeit selbständig verfasst und keine anderen als die angegebenen Quellen und Hilfsmittel benutzt habe.

Berlin, den 15. September 2009

(Unterschrift)